SCIENTIFIC RESEARCH OF THE SCO COUNTRIES: SYNERGY AND INTEGRATION

上合组织国家的科学研究：协同和一体化

Proceedings of the International Conference

Date: May 25

Beijing, China 2022

上合组织国家的科学研究：协同和一体化国际会议

参与者的英文报告

International Conference “Scientific research of the SCO countries: synergy and integration”

2022年5月25日，中国北京
May 25, 2022. Beijing, PRC

Proceedings of the International Conference
“Scientific research of the SCO countries: synergy and integration”. Part 1 - Reports in English

(May 25, 2022. Beijing, PRC)

ISBN 978-5-905695-82-7

这些会议文集结合了会议的材料 – 研究论文和科学工作者的论文报告。 它考察了职业化人格的技术和社会学问题。一些文章涉及人格职业化研究问题的理论和方法论方法和原则。
作者对所引用的出版物，事实，数字，引用，统计数据，专有名称和其他信息的准确性负责

These Conference Proceedings combine materials of the conference – research papers and thesis reports of scientific workers. They examines tecnical and sociological issues of research issues. Some articles deal with theoretical and methodological approaches and principles of research questions of personality professionalization.

Authors are responsible for the accuracy of cited publications, facts, figures, quotations, statistics, proper names and other information.

ISBN 978-5-905695-82-7

CONTENTS

BIOLOGICAL SCIENCES

EARTH SCIENCES

TECHNICAL SCIENCES

DOI 10.34660/INF.2022.56.45.176

双语环境下语言类大学生俄语语音能力的形成
FORMATION OF PHONETIC COMPETENCE OF LINGUISTIC STUDENTS IN THE CONDITIONS OF BILINGUAL EDUCATION

颜巧燕
Yan Qiaoyan
湖南工学院 湖南省衡阳市

摘要：构建语言环境是俄语教学的重要方面，但是随着当前疫情的蔓延，阻碍了相关学校的语言环境构建，所以有不少学校基于线上技术构建起全新的双语环境。本文基于当前双语环境下俄语大学生语音能力的形成出发，对当前相关教师的双语环境构建问题进行分析，并且基于的问题对线上双语线上双语环境构建的优势进行了分析，最后从培养策略和评价体系两个方面对双语环境下语言类大学生俄语语音能力的培养进行了全面的优化。

关键词：俄语；双语环境；语音能力

一、序言

当前我国国际交流日渐频繁，构建起一套行之有效的交流体系则是国际交流的重要前提。俄罗斯是我国重要的外交伙伴，无论是在官方还是民间都有着紧密的联系，培养优秀的俄语人才也成为了中俄交流的前提之一。随着对俄语教学领域“以学习者为中心”的观念逐渐成为共识，对于双语环境构建的研究也日渐获得关注。我们想要提高语言学习的效果，不能光从教学法的角度切入，而是应该更多地关注到学习者的角度，试图建立有效的学习环境，从而融合教与学之间共同的优势。构建语言环境是俄语教学的重要方面，但是随着当前疫情的蔓延，阻碍了相关学校的语言环境构建，所以有不少学校基于线上技术构建起全新的双语环境。本文基于当前双语环境下俄语大学生语音能力的形成出发，对当前相关教师的双语环境构建问题进行分析，并且给出相应的优化建议，希望能为俄语大学生语音教学提供参考。

二、俄语大学生双语环境构建存在的问题及原因

当前俄语大学生双语环境的构建仍处于探索阶段，如何培养双语环境下俄语大学生语音能力的教学必须要有实证材料作为支撑，而不能基于理论进行空泛的分析。笔者针对当前俄语大学生双语环境的构建问题对相关学生进行了相应的调查，并且对所发现的问题进行了分析。

1. 现状调查

笔者结合了相关文献的研究成果，针对当前疫情环境下俄语大学生的学习

问题进行了调查，主要调查方向为当前缺少线下交际氛围的学下环境下，自身学习是否遇到了相应的问题，其问题主要集中在哪些方面。本次调查问卷共发放50份，收回45份。

2. 问题概述

基于调查结果，不少学生和教师认为当前疫情环境下，俄语大学生现实中的交际策略大大减少，线上教学模式又没能为学习者提供予以弥补的交际环境，主要体现在：

（1）线上教学的模式使得师生关系、生生关系发生了变化

长期以来我们进行的线下课堂教学是以班级为一个整体，师生之间在教室这个空间内面对面进行互动的教学活动。教师既是语言知识的传授者，也是语言技能的训练者，同班同学相互之间既是合作关系，又是竞争关系。可以说，每个人在这个微型社会结构中的角色与职责都是明确的，学生和老师之间、学生和学生之间的联系是更为紧密的，交际也是更为直接的。在课堂之外，学生之间也有私下交流、学习的可能。而网络课堂教学则是以师生之间的线上虚拟互动为主要形式，以网络平台为授课空间来进行的教学活动。现实课堂教学是一种建立在身体体验上的身体化实践，是在客观、真实的现实世界中展开的教学活动。而虚拟课堂教学则是“去身体化”的、剥离了身体参与的符码化活动，是在虚拟的符号世界中开展的教学活动。目前学界已普遍达成共识，相比较录播，直播模式是能够最大程度地弥补师生之间互动短缺的一种授课模式。虽然直播的授课模式能够实现一部分的互动式教学，但这也仅仅是弥补了师生互动的缺陷，却忽视了生生互动的重要性。在实际的教学活动中我们能够发现，学生如果有共同学习俄语的伙伴，相互激励、相互促进，在语言学习过程中并肩作战，无疑对俄语学习是有积极作用的。然而在线上教学模式下，学生只在有限的课堂时间内见面，情感链接还来不及建立。课堂直播一结束，学生之间的联系仿佛立即就被切断了，更不要说在课后还有一起学习的机会。在这样的情况下，学生在俄语口语学习的道路上实际是“孤军奋战”，而没有办法“找到共同学习的伙伴”或者“请求朋友帮助”等，也因此失去了使用交际策略的机会。

（2）课堂交际任务设计不佳导致其积极作用不明显

在课堂教学过程中有一个环节是“小组讨论”，是一种任务型教学，即给出一个交际任务，让学生用所学语言点完成任务。但任务型教学的核心是通过让学生完成任务来进行意义的协商与互动，在专注于内容的同时能够自然习得语言形式，从而提高交际能力根据笔者观察发现，课堂上教师所设计的小组讨论的主题虽然与实际生活比较相关，但仅停留在要求学生用所学语言点完成任务的层面，而缺少对学生使用自身的语言储备完成交际任务的引导，学生的回答也普遍是对教材内容的“依瓢画葫芦”。因此，与课下学生自己自然创设的交际环境不同，“小组讨论”的模拟交际某种程度上是生硬的，比较缺乏情感流动，学生会机械地认为这仅仅是完成一个任务，而不是自主地、为了提高口语而主动开启的对话，也自然而然不会有意识地去构建自身所处的双语环境了。

（3）线上教学模式使得课后作业与活动的形式受到了一定程度的限制

在线下课程中，课后学习任务的形式通常是更为丰富多样的，也会提供更多的俄语活动供学生们选择，而在线上教学时，教师布置课后任务时十分受限，通常只能布置由学生独立完成的作业，缺少了口语交际的互动感。我们知道，课后练习是学生操练口语的一个重要方式，在互动与交际性较强的课后学习任务中，学习者更有机会能够使用社交策略、补偿策略等辅助完成交际的策略。

三、双语环境下语言类大学生俄语语音能力的培养途径

基于上述问题我们可以发现，当前线上双语环境构建的问题集中在线上教学环境构建不成熟，交际任务设计不合理，课后作业活动收到限制三个方面。基于这三个方面的问题，笔者认为应当基于俄语大学生语音能力形成规律构建起全新的双语环境，这样才能更好的促进大学生俄语语音能力的形成。

1.线上双语环境优势分析

（1）丰富了教学途径

线上教学模式应用在俄语教学中，可以通过线上预习、学习资料的查阅等方式，使学生获取更多的学习内容和更加丰富的学习形式，符合现代学生的学习习惯，可以充分调动学生的学习兴趣。教学途径的丰富，在很大程度上解决了俄语课时不足的问题，并且使学生可以通过观看俄语视频、阅读俄语书报、听俄语广播等方式，来丰富俄语教学内容和方法。学生间的讨论也是学生学习途径增加的重要体现，可以有效开阔学生的知识面和视野。浓厚的学习氛围还促使学生使用俄语进行交流与沟通，从而提升语言运用能力。线上应用于学生课后知识的复习和巩固方面，可以使学生通过反复观看教学知识，提升复习效果。

（2）利于学生开展个性化学习

线上教学的应用，使学生获取了更多的交流方式，使学生之间、师生之间可以有更多的交流渠道，特别是增进了师生交流的机会和情感，使教师可以向学生提供更有针对性的指导与建议。学生还可依据自身的兴趣、爱好，进行相关学习资料的自主查阅，进而提升实践学习能力。

2.双语环境下语言类大学生俄语语音能力的培养策略

（1）加强俄语文化背景的融合

双语环境的构建应当充分基于俄中两国的差异性进行分析，在构建双语环境的过程中建立起俄罗斯自身的文化背景，而不是单纯的进行日常用语对话。比如俄语满音体和略音体的应用场合，如元音的极度弱化(пожа[л]ста=пожалуйста)，元音的质变 (дев[ъ]шка=девушка)，辅音的脱落(сонце=солнце) 和音节的脱落 (спокойнночи=спокойнойночи) 在不同场景下的实际应用情况，基于俄罗斯的文化背景和历史典故进行双语环境的构建。

（2）重视语音能力形成规律

线上模式下口语教学确实存在一定的困难，但教师应该积极应对，采取予以弥补的策略。俄语大学生如果对学习者的发音问题不予以重视，则非常容

易引起“语音石化”，这也会导致学习者后续在交际场景中进行操练时困难重重。语音教学的指导思想由音素教学法过渡到语流教学法，但由于语音的教学贯穿在整个基础教学过程中，因此在具体教学实践中往往是以音素教学为基础，再慢慢渗透语流教学。对于俄语大学生来说，教师在进行线上口语教学时应着重强化单音训练。提出俄语大学生语音能力形成的关键并不在其他方面，而在声调和比声调更高的语音层次，因此在学习俄语语音基本结构阶段，声调教学比其他方面教学更为重要一些。基于这一现实，教师在语音教学时要注重语音能力的训练，引导学生进行经常性的练习。

（3）积极开发线上语音教学内容

针对课堂交际活动的开展，教师应明确一个目的，那就是使学生进行意义协商与互动，在专注于内容的同时完成交际任务，从而自然习得语言形式。教师在备课时可以注意增加有意义的交际活动，并且引导学生利用自己的语言储备来进行交际而不仅仅进行语言点的机械训练。交际话题的选择要多以生活交际方面出发，结合学生的兴趣。此举的目的就在于引导学生在线上环境下有意识地多使用交际策略，以此来提高自身的交际能力。例如可以通过有组织的课外活动弥补线上教学的不足，通过电影、读书会、小组话题讨论等多种多样的形式扩展教材内容，扩大操练范围。通过举办文艺节目表演、网上人物采访、语伴对谈等各种课外活动加强生生、师生之间的交流，增进同学们的感情。线上教学模式的短板并非无法克服，只是目前我们对其的重视程度不够，总觉得线上教学模式只是过渡时期的一种替代。但实际上，我们应该抱有这种意识，即对外俄语教学将向线上线下并行的教学模式转型。因此，对于线上教学，需要我们投入更多的人力物力，以求得更优的教学效果。

（4）充分借助阐释讲解工具

线上双鱼环境的构建应当充分利用线上教学优势，通过图片增加画面感和视觉感，学生才能真实地表达出感情。教师在构建双语环境的过程中，应当熟悉学生原有的储备知识及在学习过程中可能遇到的学习困难，在教学过程中他善用阐释讲解工具，有针对性地指导学生学习，用引导性的方式推进其理解。比如学生在朗读《Мне снилась музыка》这首诗时，很难正确地表达出“золотистоголубая”所要表达的感情。通过图片“增加学生的画面感和视觉感”，增加他们对“内含的语义和文化的了解”，这样才能正确地表达出“宗教色彩所隐含的圣洁、空灵和虔诚”，运用画面感来解决学生在诗歌情感表达和语义表达时遇到的困难，使其实现由语音的表象表达向深层语义表达转换。

（5）针对俄语大学生双语交流中的短板进行改正

由于身处疫情的大背景下，俄语大学生没有太多口语交际情境，在口语交际策略的使用上也较为单一。无论是课堂上创设的交际环境还是日常生活中，当交际出现困难时，如果对方会英语，俄语大学生更倾向于利用英语来完成交际任务；如果对方不会英语，不少选择的策略则是重复和利用体态语策略。运用媒介语、体态语等补偿策略从交际的角度来看，是积极主动的应

对策略，但从俄语学习和运用的角度说，则是消极被动的回避策略。因为这虽然解决了暂时的困难，但却背离了学习和交际的最终目的。正因为如此，在建立俄语大学生的双语环境时，要积极避免媒介语和体态语的使用。能够坚持用目的语进行交际而不使用补偿策略当然是最好的，然而这也受到学习者水平的限制。如果对于俄语词汇的积累程度较高，在交际遇到困难时可以变换表达，而如果本身水平就不足以变换俄语表达方式，则只能运用补偿策略来完成交际了。针对这些问题，在构建双语环境的过程中教师不应进行一刀切，而是让学生逐步的减少媒介语、体态语的应用，让学生基于自身的俄语水平组织交流的语言。

3.评价体系优化

（1）确立评价导向

双语环境构建之后的学习成果应当是目标导向，而不是错误导向，具体分为以下两个方面：如何进行（关注每个教学阶段的目标，依据阶段目标进行评价）、有何作用（对学生学习具有导向性）。由教学中的每个阶段目标看到学生的进步，对学生进行引导。学生能够清楚地知道自己在每个学习阶段中的情况，是否达到学习目标，对自己做出正确的判断，能够为其学习提供明确的方向，使其关注自身要学习的重点。

（2）强调语音指标的正确性

双语环境构建之后教师应当强调语音指标的正确性，对单音或语调问题零容忍。教师应当对每一个阶段的语音指标严格把关，在不同的阶段有不同的指标，比如在单音阶段，不允许有单音错误，到某一个子目标的时候也是不允许有错误的。对俄语大学生单音、连读、语速的等的指标进行构建，让结果做到可测量，增强专业性和执行力。

（3）增加学生自我评价环节

在双语环境的交流过程中，教师应当对交流过程进行记录，让学生进行自我评价。学生也可以针对自身的发音问题借助录音工具不断对比、改善自己的发音，真正做到了发现问题并解决问题，并且在操练与复习部分付出了比别人更多的时间，从而使得自己的口语发音准确性和流利度高于其他人。

四、总结

本文基于当前双语环境下俄语大学生语音能力的形成出发，对当前相关教师的双语环境构建问题进行分析，认为当前疫情环境下，俄语大学生双语环境构建存在的问题主要分为线上教学的模式使得师生关系、生生关系发生了变化；课堂交际任务设计不佳导致其积极作用不明显；线上教学模式使得课后作业与活动的形式受到了一定程度的限制三个方面。并且基于这三个方面的问题对线上双语线上双语环境构建的优势进行了分析，认为优势主要集中在丰富了教学途径、利于学生开展个性化学习两点，最后从培养策略和评价体系两个方面对双语环境下语言类大学生俄语语音能力的培养进行了全面的优化。

参考文献：

1. 黄秀坤. 基于汉语作为第二语言教学的留学生语篇建构能力研究[D]. 吉林大学, 2015.

2. ZAVERTAILO KATERYNA（郑紫帆）. 俄语母语者汉语并列连词学习偏误研究[D]. 武汉大学, 2017.

3. 王洪玲. 基于学习动机理论的俄语专业课堂教学策略研究[D]. 哈尔滨师范大学, 2012.

4. 张爽, 王维维, 徐玉敏, 王洋, 侯丽娜. 三语习得中语言迁移理论对俄语教学的影响——以英语(L2)对俄语(L3)名词范畴习得的影响为例[J]. 黑龙江工业学院学报(综合版), 2021, 21(11):144-148.

5. 张丽娜. 苏联及俄罗斯语言策略的演变与俄语状况研究[D]. 黑龙江大学, 2017.

6. 宁琦. 中国俄语教育70年回顾与展望[J]. 上海交通大学学报(哲学社会科学版), 2019, 27(05):76-88.

DOI 10.34660/INF.2022.86.69.177

N.M.卡拉姆津作品中音乐的叙事功能
THE NARRATIVE FUNCTION OF MUSIC IN N.M. KARAMZIN'S WORK

Chen Yangyang
Doctor of Literature, Post-doctor, Sun Yat-sen University, Zhuhai, China
ORCID 0000-0002-2478-3252

摘要：音乐作为卡拉姆津作品的有机组成部分，在故事情节的发展中发挥着重要作用。本文基于卡拉姆津作品中的音乐文本，对音乐的叙事功能进行阐述。卡拉姆津作品中的音乐是多元化的，例如在小说《叶甫盖尼和尤利娅》和戏剧《索菲娅》等作品中音乐的呈现方式就不尽相同。在《一位俄罗斯旅行者的信札》和《莫斯科杂志》中，音乐被认为是一种历史叙事手法。卡拉姆津作品中的音乐通常被作者用来刻画人物，烘托情感，推动情节发展，展示人物内心世界，因此是具有多种功能且相互关联密不可分的。

关键词：卡拉姆津，音乐，叙事功能，感伤主义

Abstract. *Music plays an important role in the development of the storyline as an integral part of N. M. Karamzin's work. Based on the musical texts in Karamzin's works, this article expounds the narrative function of music. The music in Karamzin's works is diversified, in the novel "Evgeniy and Yulia" and in the drama "Sofia", as well as in the author's other works, the music is also presented in different forms. In the "Letters of a Russian Traveler" and "Moscow Journal", music is considered as a historical narrative technique. The music in Karamzin's work is often used by the author to portray characters, express emotions, promote the development of plots, show the inner world of characters, so it is multifunctional and inseparable..*

Keywords: *N.M. Karamzin, music, narrative function, sentimentalism*

Introduction

Musical art develops and evolves within the framework of literary trends. The writers of the era of classicism touch upon music exclusively as the realization of a poetic text and contribute to the development of new musical genres. Sentimentalism introduces music into the narrative, thus creating the theme of music in literature. It is in Karamzin's prose that music first becomes an integral

element of sentimentalism. Already from the first translated stories published in the "Children's Reading magazine", music will be used to create an atmosphere of a sentimental landscape.

I. Sentimental music-making in Karamzin's prose

Starting with the first independent story "Evgeniy and Yulia", Karamzin creates a certain model of sentimental music-making, where music helps to reveal the image of the characters, reflecting their feelings and being included in the general psychological structure of the sentimental story.

An important role is played by the songs that sound in the stories, "Letters of a Russian Traveler" and the drama "Sofia". Whether telling entire stories or hinting at subsequent events, the songs take the music beyond mere sentimental detail.

Music playing of the heroes of the story "Evgeniy and Yulia" simultaneously reveals the inner world of the heroes, creates a sentimental atmosphere, and anticipates subsequent events.

"Evgeniy gave Yulia a lot of notes, a lot of French, Italian, German books. She played the harpsichord and sang beautifully. Klopstockov's song "Willkommen, silberner Mond" (German) (Come to us, silver moon), to which the gentleman Gluck composed the music, she fell in love with him. She could never sing the last stanza without softening her heart, in which Gluk so skillfully matched the tones with the feelings of the great poet. Meek, gentle souls! You alone know the price of these virtuosos, and their immortal works are dedicated to you alone. One tear of yours is their greatest reward. " (Karamzin,1979)

This description of the music-making of the two young heroes of the story "Evgeniy and Yulia" refers to the scene of Charlotte playing the piano for Werther in the novel "The Sorrows of Young Werther" by Johann Wolfgang von Goethe.

"She has one favorite melody, which she divinely plays on the piano – so simply, with such feeling! The very first note of this song heals me from sadness, anxiety, and blues. I easily believe everything that has long been said about the magical power of music. What an artless chant touches me! And how, by the way, she knows how to play it, just when it's time for me to put a bullet in my forehead! The confusion and darkness of my soul dissipate, and I breathe more freely again." (Goethe, 2013)

These two descriptions are united not only by a special sensitivity in the perception of music, but also by a special sentimental atmosphere caused by the intimacy of the performance. It is music in both cases that reveals the image of the characters, expressing their feelings not at the verbal, but at the musical level.

This scene from the story "Evgeniy and Yulia" is remarkable not only atmosphere of music-making, but also by the fact that the reader is given a link to a specific composer and a line from the song is quoted. Friedrich Gottlieb Klopstock's poem "Die frühen Gräber" was indeed set to music by Christoph

Willibald Gluck and was an example of early sentimental poetry. In the story, the song is named after the first line "Come to us, silver month" and at first glance does not cause dissonance with the image of lovers. However, its real name is "Early Tombs". It is possible that Karamzin deliberately did not indicate such a gloomy phrase in the description of the music-making of "meek, gentle souls."

The landscape of the night cemetery, characteristic of the sentimental tradition, and the melancholic mood of the poem foresee the subsequent tragic development of the events of this story. The musical side of the song is also curious. There is some contrast between the text and the choice of musical means. The mood of the song is conveyed through a clear melody and an extremely simple rhythm using fourths and eighths. The song was written in a light key in C major, and this is curious, since in the 17th and 18th centuries, the semantic interpretation of tonalities, which were assigned certain meanings, was widespread. For example, in the description of the composer of the XVII century, M. A. Charpentier in C-dur (C major) is characterized as cheerful and warlike (Medushevsky, 1973). However, Gluck pointed to the nature of the performance, putting the designation affettuoso, which translates as gentle, languid, passionate.

Klopstock's poetry is also mentioned in the novel The Sorrows of Young Werther. “I saw that her eyes filled with tears; she put her hand on mine and said, “Klopstock!” I immediately remembered the magnificent ode that came to her mind and plunged into the stream of sensations that she awakened with her exclamation (Goethe, 2013). A parallel arises not only between references to the poetry of the German poet, but also between the work of Klopstock and Karamzin as a whole. N. V. Gerbel, in the preface to Klopstock's translations, noted that “He <Klopstock> is S.P. was for German poetry what Karamzin later became with his "Poor Lisa" for ours (Gerbel, 1877).

Singing, accompanied by playing the harpsichord, becomes almost the most important characteristic of the heroes in Karamzin's stories, emphasizing their upbringing, education, and sensitivity. These are the already mentioned Evgeniy and Yulia, Sofia from the drama of the same name, the heroes of the Letters of a Russian Traveler.

The heroes of the stories "Liodor" and "Bornholm Island" accompany themselves on the guitar. Playing this instrument adds exoticism to their image. Unlike the harpsichord and violin, the guitar was not as popular in Russia. Jakob Shtelin in "Izvestiya o musik v Rossii" noted that "according to foreign custom, the guitar is intended to accompany the sighs of love under the windows of the beloved" (Shtelin, 1935). It should be noted that there is no purely instrumental music in the stories. Music always appears as an accompaniment to poetic texts. It is logical that in Karamzin we will not meet heroes playing the violin or flute.

II. Music in the plot development

Karamzin creates a world in which music serves not only to create a sentimental atmosphere, but also participates in the movement of the plot, accompanying entire stories of characters or duplicating the main line. This function was noted by T. N. Livanov, defining Karamzin's introduction of music into the structure of sentimental prose as an unconditional innovation, which was later repeated by many sentimentalist writers.

The story of the heroes of "Letters of a Russian Traveler", "Bornholm Island", "Liodora" is told to the reader through music, namely songs. The song anticipates events or is a self-presentation. This technique distinguishes these characters from the general plot, poeticizing their image. In addition, the appeal to the musical component of these songs allows us to expand the usual understanding of the stories.

The interaction of lyrics and music in Karamzin's prose demonstrates the transition of music as a fine art to an expressive one. A. E. Makhov in his work "Lyrics. The Formation of the Idea of Lyrics as a Literary Genus" showed that the formation of lyrics as a separate kind was influenced by music. "The formation of a new idea for poetics about the autonomous 'essence' of lyrics took place in close interaction with musical aesthetics: in fact, the model of a special – inimitable, non-mimetic – expressiveness, which was developed in texts about music, was transferred to the lyrics" (Makhov, 2010). In Karamzin's prose, music, conveying mood and creating an atmosphere, is a means of expression.

In the story "Bornholm Island" the song of a young stranger is the center of the whole work. It is the song that talks about his past and at the same time is the key to the mysterious plot. In addition, the story describes the nature of the performance and the genre: "He sighed, raised his eyes to the sky, lowered them again to the waves of the sea – he moved away from the tree, sat down on the grass, played a sad prelude on his guitar, looking constantly at the sea, and sang in a quiet voice the next song". The song does not reveal the secrets of his past directly, but only hints, presenting some details of the stranger's life. E. I. Osetrov noted that "Karamzin laid the foundation for the reception of a mysterious hint, not only burning like a hellish flame, but also being a game of hide and seek, allowing the reader to guess what is happening – a manner that many then resorted to"(Osetrov, 1985).

It is also important that Karamzin uses the musical term, pointing to the genre of prelude. A prelude is an introduction that precedes a more formalized piece. The mention of this genre in the story only testifies to Karamzin's acquaintance with the European musical tradition.

It should be noted that the stranger's song arouses interest in the hero, becoming the plot of the whole plot. The sad sounds and words of his song echoed in my

ears. "They contain the secret of his heart, – I thought, – but who is he? What laws condemn the love of the unfortunate? What oath removed him from the shores of Bornholm, so dear to him? Will I ever know his story?"(Karamzin, 1984).

Another situation arises in the story "Liodor". It was not finished, the reader is presented with only the beginning of the plot, however, one cannot fail to note the similarity of this beginning with "Bornholm Island", only here a beautiful stranger, and not a stranger, she also sings a song.

As in "Bornholm Island", the stranger's singing is the opening. The song allegorically narrates about imprisonment, and we can make assumptions about the fate of the heroine. Her singing also leaves a mark on the soul of the hero and arouses curiosity. "Never, my dear friends, have I ever felt such pleasure from singing as I did then; the voice (it was female) merged with the tones of the strings, penetrated right into my heart, and poured an indescribable sweetness through all its fibers; my chest languished in ecstasy, and tears flowed from my eyes" (Karamzin, 2007).

The stranger sings the song "La violetta", composed to the lyrics by Gabriello Chiabrera, accompanying herself on the guitar. There is no reference to the composer in the story itself, but there are two well-known musical versions of this song. The first was composed by an unknown 16th century composer and the second by Claudio Monteverdi. It is noteworthy that in the story the translation was not published in its entirety but broke off at the third stanza.

III Music – a sentimental element

Having entrusted the storylines of his characters to the songs, including music in the general psychological structure of his works, Karamzin managed to achieve harmonious unity, taking music beyond the boundaries of a simple sentimental element.

In "Letters of a Russian Traveler" music is described not only in critical reviews. First, the traveler mentions music when describing the national identity of the culture of another country. Such musical impressions are most often cited for comparison with the native culture and cause homesickness in the traveler. "The mountain dwellers had fun below, and sang their simple songs, which, combined with the noise of the wind, brought my soul to despondency. I listened to the melodies and found in them something like our folk songs, which are so touching to me. Sing, my mountain friends, sing, and delight the sorrows of life with the pleasantness of harmony!" (Karamzin, 2007)

This description expresses the position of a "sensitive" person who can appreciate the way of life of rural residents and their relationship with nature. The sentimental traveler quite often turns to "natural people", admires their culture, but soon returns to the "benefits of enlightenment" again, visiting theaters, museums, and universities.

Music is often the motivation for the traveler's sentimental or philosophical reflections. N. D. Kochetkova in her work "Russian Sentimentalism" noted that art for the traveler provides an opportunity for introspection and the most important thing is the circumstances that make a work of art close to him personally.

Individual, one's own perception – that's what becomes the main thing (Kochetkova, 1978). S. E. Pavlovich, noting the musicality of such reasoning, writes that "lyrical digressions are directly related to the general orientation of the 'Letters' and repeat in a concentrated form the main thoughts of the author, scattered in different places of the work" (Pavlovich, 1974).

Such descriptions will not affect the plot or reflect the culture of a particular country, but will reveal the image of the traveler, demonstrating his feelings and knowledge. For example: "Suddenly singing began in the church so pleasant that I forgot to look, listened, and was captivated in the depths of my soul. Beautiful boys, in a white dress, sang in chorus: they seemed to me Angels! What could be more charming than the harmony of human voices? It is the direct organ of the divine soul! Descartes, who wanted to recognize all animals except man as machines, could not listen to nightingales without annoyance; it seemed to him that tender Philomela, touching his soul, refutes his system; and the system, as you know, is dearest of all to the Philosopher! What is it like for a Materialist to listen to human singing? He needs to be deaf or overly stubborn." (Karamzin, 2007)

Repeatedly in the text of "Letters of a Russian Traveler" playing the harpsichord is mentioned. Only young girls play this instrument, demonstrating their talent to the audience: "Sitting at the harpsichord, among a brilliant society, you, beauty, want to be liked and sing like a robin" (Karamzin, 2007). Another description of the harpsichord playing is interesting in that different editions of "Letters of a Russian Traveler" present several versions of the description of young Charlotte's playing. "Good-looking Charlotte was silent for the most part, but her eyes and smiles were eloquent. After dinner, she played the harpsichord, although in the German style, but not without pleasantness"(Karamzin, 2007). In both editions of the "Moscow Journal" and in a separate edition of "Letters of a Russian Traveler" 1797-1801. another characteristic of the girl's game is presented. "After dinner, on the orders of her father, she played the harpsichord, and I would be glad to listen to her until the evening." (Karamzin, 1791)

As in the stories, the songs in "Letters of a Russian Traveler" will be used to present the characters themselves or to explain their feelings and to anticipate future events. The traveler feels longing for his homeland and for his friends, and then he hears a "pleasant, quiet melody", namely the song of a young man who lives in the neighborhood. "My fatherland! All my blood burns with love for you; I am ready to shed it for your benefit; I will die as your most tender son... (Karamzin, 2007)". The young man's song is a continuation of the hero's thoughts,

transferring them to the outer plane. It should be noted that such a technique is close to dramatic art, the opera genre.

The stories "Evgeniy and Yulia", "Bornholm Island" and "Liodor", "Letters of a Russian Traveler" and the drama "Sofia" demonstrate musical diversity. Playing music at the harpsichord, singing songs to the accompaniment of a guitar in stories, the musical culture of different countries, singing, both peasants and nobles in "Letters of a Russian Traveler", Sofia's performance, which creates a sentimental atmosphere and anticipates further events in the drama of the same name.

The presented material can prove Karamzin's attitude to music not as a simple everyday detail, but as an obligatory element of sentimentalism, participating in the construction of a separate plot or creating the tone of the whole direction.

Conclusion

According to the narrative function of music in Karamzin's prose, music creates a general sentimental background, participating in the description, transmission of the landscape, interior. In addition, music is involved in the movement of the plot, telling the whole story of the characters, or duplicating the main line. Music was described by Karamzin in critical reviews and performing various functions, participated in the narrative.

References

[1] Gerbel N. V. German poets in biographies and samples. SPb., 1877.

[2] Goethe I. V. The sufferings of the young Werther. M., 2013.

[3] Karamzin N. M. Bornholm Island / Essays: in 2 vols., 1984.

[4] Karamzin N. M. Evgeny and Yulia // Russian sentimental story. M., 1979.

[5] Karamzin N. M. Liodor // Letters of a Russian traveler. Stories. M., 2007.

[6] Kochetkova N. D. Russian sentimentalism (N. M. Karamzin and his entourage) // Russian Romanticism, L., 1978.

[7] Makhov A. E. Lyrics. Formation of the idea of lyrics as a literary genus // European poetics from antiquity to the Enlightenment: An Encyclopedic guide. M., 2010.

[8] Medushevsky V. V. On the problem of semantic syntax // Soviet music. No. 8. M., 1973.

[9] Osetrov E. I. Three lives of Karamzin. M., 1985.

[10] Shtelin Ya. Ya. News about music in Russia / Per. B.I. Zagursky // Shtelin Ya. Music and ballet in Russia of the XVIII century. L., 1935.

[11] Sokolovsky A. Early tombs // Gerbel N. V. German poets in biographies and samples. SPb., 1877.

DOI 10.34660/INF.2022.97.88.178

BFB疗法对学生非生产性心理压力的矫正
CORRECTION OF NON-PRODUCIVE MENTAL STRESS AMONG STUDENTS USING BFB THERAPY METHODS

Sharapov Alexey Olegovich
Candidate of Psychological Sciences, ***A****ssistant Professor*
Vorotyntseva Darya Alekseevna
Graduate student
Belgorod State University

抽象的。使用生物反馈（BFB）原理的基于硬件的计算机技术是适应不良精神状态心理治疗的优先方法。本研究是关于用BFB疗法矫正紧张焦虑和学生自我调节诱导的问题。可能发生的非生产性精神压力会导致心理情绪反应，降低学生的适应能力。假设：对于自我调节水平较差的学生，非生产性精神压力是其特征。使用 BFB 疗法的方法可以减轻压力并形成有效的自我调节机制。这项研究基于受试者活动和系统方法、暴露前后测试的两个随机组的实验计划，以及确定的结构相关性计数。这项研究已经进行了2年多。研究小组由别尔哥罗德州立大学的 65 名学生组成。我们使用了以下方法：精神紧张评估、情境和个人焦虑的主观评估、«行为自我调节类型»问卷和基于心率的 BFB 训练。 BFB疗法显示了精神紧张和自我调节对生理和心理水平的影响。因此，通过BFB疗法改善自我调节机制可以纠正心理压力水平，提高学生的适应能力和学习活动的有效性。

关键词：使用生物反馈原理的基于硬件的计算机技术、非生产性精神压力、自我调节、学生。

Abstract. *Hardware-based computer techniques using the principles of biological feedback (BFB) is the priority way for psychotherapy of maladaptive mental states. This research is about the problem of tense anxiety correction and students' self-regulation induction with BFB therapy. Non-productive mental stress that may occur actualizes psycho-emotional reactions, reduces students adaptation. Hypothesis: for students with a poor level of self-regulation, an unproductive mental stress is characteristic. Using the methods of BFB therapy it is possible to decrease the tension and to form effective self-regulation mechanisms. This research is based on subject-activity and systemic methods, an experimental plan for two randomized groups tested before and after the exposure, and an ascertaining structural-correlational count. This research had been performing for over 2 years. The study group consisted of 65 students of*

Belgorod State University. We used the following methods: Evaluation of mental tension, Subjective assessment of situational and personal anxiety, «Behavior self-regulation type» questionnaire, and BFB training based on heart rate. BFB therapy showed the influence on physiological and psychological levels of mental tension and self-regulation. Therefore, self-regulation mechanisms improvement by the means of BFB therapy may correct the level of mental stress and increase students adaptation skill and effectiveness of the learning activities.

Keywords: *Hardware-based computer techniques using the principles of biofeedback, non-productive mental stress, self-regulation, students.*

Introduction

The issue of the non-productive neuropsychic stress study in students is related to problems of the educational process optimization. How to master different ways of the effective management of one's own psychophysiological state and psychic processes for the effective training activities?

According to available data, the non-productive stress state, that students have during the academic year, actualizes psycho-affective reactions, that significantly decreases the training activity quality [1-2]. The issue of the neuropsychic stress correction as a condition for the students personality self-regulation formation has been underrepresented in psychological science.

An interest of some foreign and Russian psychologists currently lies in the field of the human self-regulation study. In researches of N.D. Levitov, Y.E. Leonova, L.G. Dikaya, E.P. Il'in et al. a number of crucial patterns and mechanisms concerning the mental states dynamics, functions, structure, phenomenology identification were determined [3-9]. T.N. Nemchin, P. Zil'berman, I.V. Syromyatnikov et al. paid attention to the neuropsychic stress in their works, and also P.K. Anohin, S.S. Besova, S.A. Datchenko, V.V. Kolbanov, E.A. Denisova et al. paid attention to the biofeedback methods. However, a separate study on these categories does not provide a full picture of their influence and connection between them [6-9]. The neuropsychic stress is an alternative personal variable reflecting both dynamic and static personality characteristics (states and features) [10]. It is possible to control the neuropsychic stress through the properly formed self-regulation in a subject. In terms of the systemic-activity approach, self-regulation is a systemic psychophysiological state, which has a certain hierarchy from a physiological level to a psychological level.

Formed self-regulation allows the subject to provide the stability of the organism functional system, its relative sustainability and balance [10-17].

The issue of the research: how does the students self-regulation system change under the influence of formed by means of BFB-therapy neuropsychic stress?

The purpose of the study: the purpose is to justify the BFB-therapy effective-

ness in the psychological correction of the non-productive neuropsychic stress in students with the low self-regulation level.

It is determined that the non-productive stress decreases the organism adaptation in students, leads to somatic disorders, acts as a factor, which prevents the achievement of academic goals, decreases the educational activity quality and success etc. It is empirically confirmed that the lower self-regulation level, the higher neuropsychic stress measure, less developed the need for planning, the achievement of academic goals is decreased, the adequacy of the current life significant internal conditions and external circumstances assessment is complicated. Using the BFB-therapy, it is possible to form the higher self-regulation level, improve the adaptation, the behavior planning level, the educational activity quality.

Materials and methods

The research is based on subject-activity and systemic approaches. The BFB-training (biological feedback method) is choosed as a tool for the personal self-regulation correctionand formation [18-20]. The BFB-therapy method provides an opportunity to scan and differentiate internal sensations, detect signals of one's own organism, which usually are under perception threshold [21-27]. It allows to reduce the psycho-affective stress and anxiety level, promotes the so-called «health intuition» development, creates conditions for the mental and physical well-being maintenance, acting as the stress development prevention. The necessity of taking into account psychological factors when using the BFB method is confirmed in the V.I. Abatova study, where she showed that clinical improvement in observed by her patients has discovered in the absence of significant changes in physiological systems.

Thus, it is possible to make a theoretically founded conclusion that the BFB-training can promote the effective decrease of the non-productive neuropsychic stress in students with the low self-regulation level.

At the stage of the forming experiment the next hypothesis was verified: for students with the low self-regulation level the non-productive neuropsychic stress state is typical. A psychophysiological correction by means of the BFB-therapy will allow to decrease the neuropsychic stress level, raise and form effective self-regulation level.

The research base is «Belgorod State Research University RU «BelSU»». The psychophysiology and neurophysiology training laboratory of the Psychology Faculty at RU «BelSU». The research sample included 65 students of the Psychology Faculty at Teacher-training Institute of RU «BelSU» aged between 18 and 20.

In the study a set of methods was used, the application of which has been determined by the logic of the research at every stage of research tasks: observation, conversation, forming experiment, questionnaires, standardized self-reports.

Subjects were surveyed with the psychodiagnostic techniques battery in the

following sequence:

A technique «The neuropsychic stress assessment» (T.A. Nemchin);

A technique of the situational and personality anxiety subjective assessment (Ch. D. Spielberger and Y.L. Hanin);

A questionnarie «The behavior self-regulation style» (V.I. Morosanova).

The study was conducted in several successive stages and included stated (including the structural and correlated research) and forming experiments. The outline of the study is experimental for two randomized groups with testing before and after the influence. The non-productive neuropsychic stress correction with the BFB-therapy (a training on the heart rate) has been carried out during 3 months, classes lasting 30-35 minutes have been conducted 4 times a week with each separate subject.

For the experimental influence effectiveness assessment during the work we compared a degree of a change in the self-regulation parameters, that happened in an experimental group in comparison with a control group. The significance of the conducted research results and received conclusions was verified using the qualitative data analysis methods, the Mann–Whitney U nonparametric test and the Fisher φ*-test. The statistical processing of the obtained data was conducted using SPSS Statistics 21 suite.

Results

As a result of the preliminary testing, three groups of subjects were identified: a group of students with the high self-regulation level (23,1%) a group of students with the average self-regulation level (46,1%); a group of students with the low self-regulation level (30,8%). In students of the last group the need for the conscious programming and planning of their behavior is not formed.

At the stated experiment stage the sample of subjects was divided into groups: 1 – a group of students with the weak neuropsychic stress (20% of the sample); 2 – a group of students with the moderate neuropsychic stress (49,2% of the sample); 3 – a group of students with the excessive neuropsychic stress (30,8% of the sample). In the third group subjects has the significant non-productive neuropsychic stress.

As the results of the structural and correlated research, significant correlations between the neuropsychic stress level and parameters were identified: «planning» (r_s =-0,465; p <0,05), programming (r_s =-0,426; p <0,05), assessment of results (r_s=-0,612; p <0,01), independence (r_s =-0,384; p <0,05) and general self-regulation level (r_s =-0,501; p <0,01).

The lower self-regulation level, the higher neuropsychic stress measure, the worse a need for planning is developed, academic goals are rarely attained, the assessment of significant internal conditions and external circumstances is more inadequate. The stronger discomfort state is experienced, the less a need for con-

scious programming and planning of one's own behavior is formed. In students with the high neuropsychic stress level difficulties are more likely to occur in determining the purpose and the program of actions appropriate to a current situation, they do not always observe a change of the situation, that can lead to failures. The stronger discomfort and anxiety state is experienced, the less a need for conscious programming and planning of one's own behavior is formed.

Thus, the less self-regulation level, the higher neuropsychic stress measure.

At the final stage 20 students (30,8% of the sample) with the low self-regulation level took part in the experiment: 10 subjects constituted an experimental group, 10 subjects constituted a control group.

As a result of the psychological correction with the BFB-therapy, we were able to detect significant improvement of initial measures. The presence of differences between the heart rate at the first class and the heart rate at the last class ($U=5,0$; $p<0,01$) in the experimental group students confirms that used by us program, based on the heart rate decrease, works efficiently.

Table 1.

Heart rate in the the experimental group students (score)

№ of a student	Heart rate at the first class	Heart rate at the last class
1	83,78	67,22
2	79,81	61,14
3	72,33	56,68
4	73,18	59,34
5	76,17	68,29
6	79,02	67,84
7	70,93	65,14
8	69,01	59,34
9	80,71	71,04
10	67,43	63,12

The neuropsychic stress level in the experimental group subjects after influence has significantly decreased in comparison with the experimental group parameters before influence, and, accordingly, the control group parameters.

During the results of the experimental group (EG) members comparison on the neuropsychic stress intensity, measured before and after experimental influence, significant differences were detected on this parameter ($U = 23,5$; $p<0,05$). We have empirically confirmed the tendency of the discomfort, anxiety and neuropsychic stress state decrease in subjects of an experimental group.

Discussion

A problem of the neuropsychic stress is topical because of continuously developing scientific and technological progress and the increasing pressure on the cognitive and emotional personality sphere of students. The non-productive neuropsychic stress state, occurring during the hard training activity, leads to the development of several psycho-affective reactions, which decrease adaptive capacities of an organism and promote the development of somatic disorders. The individual self-regulation formation level is a significant predictor of the productivity of different types of professional activity.

The BFB-therapy use, that has direct influence on the physiological level and mediated influence on psychological level of the neuropsychic stress and self-regulation, is justified.

The BFB-therapy is an effective method of the self-regulation formation and the neuropsychic stress level decrease.

The hypotheses put forward at the beginning of the study, has completely proved.

The BFB-therapy has direct influence on the physiological level and mediated influence on psychological level of the neuropsychic stress and self-regulation.

References

1. Kireyeva N.N., Kotova Ye.Ye. Osobennosti samoregulyatsii studentov vuzov kak indikatora uspeshnosti obucheniya v situatsii informatsionnoy nagruzki [Features of self-regulation of University students as an indicator of learning success in the situation of information load] Izvestiya YUFU. Tekhnicheskiye nauki. [News SFU. Technical science (Russia)], 2008, no.6. pp. 93-96. (in Russ)

2. Bolotova A.K., Puretsky M.M. Concepts of Self/Regulation: A Historical Retrospective Cultural Historical Psychology [CulturalHistorical Psychology (Russia)], 2015, vol. 11, no. 3. pp. 64—74. Doi: 10.17759/chp.2015110306 (in Russ)

3. Didur M.D. Voprosy pravovogo i normativnogo regulirovaniya primeneniya tekhnologii biologicheskoy obratnoy svyazi v sistemakh zdravookhraneniya, obrazovaniya i sotsial'noy zashchity [Issues of legal and regulatory regulation of biofeedback technology application in health, education and social protection systems] SPGMU im. Akad. I.P. Pavlova, kafedra Fizicheskikh metodov lecheniya i sportivnoy meditsiny. – Saint Petersburg., 2004. pp. 13-26. (in Russ)

4. Abatova V.I. Individualizatsiya psikhologicheskoy korrektsii i terapii metodom biologicheski obratnoy svyazi (BOS) [Individualization of psychological correction and therapy by biofeedback (BOS)] Vestnik VSO Akademii. [Bulletin of the Vso Academy (Russia)], 2017, no. 7. pp. 18-31 (in Russ)

5. Dikaya L.G. Psikhologicheskaya samoregulyatsiya funktsional'nogo sostoyaniya cheloveka (sistemno-deyatel'nostnyy podkhod) [Psychological self-regulation of human functional state (system-activity approach)] Moscow: Institut psikhologii RAN [Institut psikhologii of the Russian Academy of Sciences (Russia)], 2003. 318 p. (in Russ)

6. Kolbanov V.V. Samoregulyatsiya na osnove biologicheskoy obratnoy svyazi kak sredstvo povysheniya psikho-emotsional'noy ustoychivosti cheloveka [Self-regulation on the basis of biofeedback as a means of increasing psycho-emotional stability of a person] Valeologiya. [Valeologiya (Russia)], 2002, no. 1. pp. 27-31. (in Russ)

7. Kovaleva M.E., Bulygina V.G. Physiological characteristics of regulation of emotional responses among specialists of extreme profile. Psychology and law psyandlaw.ru [Psychology and law (Russia)], 2017, vol. 7, no. 1. pp. 53-67. Doi: 10.17759/psylaw.2017070105 (in Russ)

8. Prokhorov A.O. Samoregulyatsiya psikhicheskikh sostoyaniy: fenomenologiya, mekhanizmy, zakonomernosti [Self-regulation of mental States: phenomenology, mechanisms, regularities)]. – Moscow.: PER SE, 2005. 352 p. (in Russ)

9. Sorokina L.V., Korolev S.A., Dolmatova T.V. Effektivnost' ispol'zovaniya BOS-treninga v korrektsii funktsional'nogo sostoyaniya sotsial'no dezadaptirovannykh podrostkov [The effectiveness of biofeedback training in the correction of the functional state of socially maladapted] Perspektivy nauki. [Perspectives of science (Russia)], 2017, no. 2 (53). pp. 190-193. (in Russ)

10. Rasskazova E.I., Migunova Y.M. Positive and negative priming as a factor of bodily sensations in the healthy controls (on the sensations in head and neck). Eksperimental'nakya psikhologiya [Experimental psychology (Russia)], 2018, vol. 11, no. 3. pp. 94—107. Doi:10.17759/exppsy.2017100207 (in Russ)

11. deCharms R.C., Maeda F., Glover G.H. [et al.] Control over brain activation and pain learned by using real-time functional MRI Proc. Natl. Acad. Sci. U.S.A., 2005, no. 102 (51). pp. 18-31.

12. Durand V.M.,Barlow D.Abnormal psychology: an integrative approach. Wadsworth Cengage Learning, 2009. 311 p.

13. Gruzelier J.H. EEG-neurofeedback for optimising performance. i: A review of cognitive and affective outcome in healthy participants. Neuroscience & Biobehavioral Reviews, 2014, no. 44. pp. 124-141.

14. Hammond D.C. Neurofeedback treatment of depression and anxiety. Journal of Adult Development, 2005, no. 12. pp. 131–137.

15. Hwang H.J., Kwon K., Im C.H. Neurofeedback-based motor imagery training for brain–computer interface (bci) Journal of neuroscience methods, 2009, no. 179.pp. 150-156.

16. Kamiya J. Conscious Control of Brain Waves Psychology Today, 1968, no. 1. pp. 56-60.

17.Miller N.E. Editorial: Biofeedback: evaluation of a new technicN. Engl J. Med, 1974, no. 290 (12).pp. 684.

18.Zotev V., Phillips R., Yuan H., Misaki M. & Bodurka J. Self-regulation of human brain activity using simultaneous real-time fmri and EEG neurofeedback NeuroImage, 2014, no. 85 (3).pp. 985-995.

19.Zuberer A., Brandeis D. & Drechsler R. Are treatment effects of neurofeedback training in children with adhd related to the successful regulation of brain activity? A review on the learning of regulation of brain activity and a contribution to the discussion on specificity Frontiers in human neuroscience, 2015, no 9.pp. 135.

20.Bazanova O., Vernon D. Interpreting EEG alpha activity Neuroscience & Biobehavioral Reviews, 2014, no. 44. pp. 94-110.

21.Moore N.C. A review of EEG biofeedback treatment of anxiety disorders. Clin Electroencephalgr, 2000, no. 31(1). pp. 1-6.

Neuper C., Pfurtscheller G. Neurofeedback training for bci control. In Brain-Computer Interfaces, 2009. pp. 65-78.

22.Sterman M.B. Suppression of seizures in an epileptic following sensorimotor EEG feedback training Electroencephalography and Clinical Neurophysiology, 1972,no. 33(1). pp. 89-95.

23.Sterman M.B. Basic concepts and clinical findings in the treatment of seizure disorders with EEG operant conditioning. Clin Electroencephalgr, 2000, no. 31(1). pp. 45-55.

24.Strehl U. What learning theories can teach us in designing neurofeedback treatments Frontiers in human neuroscience, 2014, no. 8. 894. p.

25.Striefel S. The Case for Clinical Practice Guidelines for Neurofeedback and General Biofeedback. S. Striefel Biofeedback, 2008, no. 36 (4). pp. 121-125.

26.Tan G. [et al.]. Meta-analysis of EEG biofeedback in treating epilepsy. Clinical EEG and Neuroscience, 2009, no. 40. pp. 173–179.

27.Vernon D., Frick A. & Gruzelier J. Neurofeedback as a treatment for adhd: A methodological review with implications for future research. Journal of Neurotherapy, 2004, no. 8. pp. 53-82.

DOI 10.34660/INF.2022.80.70.179

三岁以下儿童严重合并颅脑损伤急性期每搏输出量昼夜节律
CIRCADIAN RHYTHM OF STROKE VOLUME IN THE ACUTE PERIOD OF SEVERE CONCOMITANT TRAUMATIC BRAIN INJURY IN CHILDREN UNDER THE AGE OF THREE YEARS

Muhitdinova Hura Nuritdinovna
Doctor of Medical Sciences, Full Professor
Center for the Development of Professional Qualifications of Medical Workers
Babajanova Zumrad Umarovna
Candidate of Medical Sciences, Head of the Department of Pediatrics
Republican Scientific Center for Emergency Medical Aid
Bardibekov Nurlan Bahodir ogli
Clinical resident
Republican Scientific Center for Emergency Medical Aid

抽象的。 在 SCTBI 后的第一天，在所有儿童组中，都有增加心脏每搏输出量的趋势。 在 ICU 的重症监护期间，第 1 组的 CO 昼夜节律中速没有显着变化。在第 2 组，第 5-15 天和第 3 组，在第 14-19 天，指标有降低的趋势 . 第 1 天 CO 昼夜节律幅度最高，第 1 组为 8 ml，第 2 组为 16 ml，第 3 组为 12 ml，这是由于创伤性休克、输液导致血流动力学不稳定所致 治疗。 强化治疗的充分性表现为心输出量每日波动幅度的降低。 在第 3 组最严重的儿童中发现婴儿期使用 SCTBI 的 CO 昼夜节律最明显和最长时间的倒置。

关键词：昼夜节律，每搏输出量，严重合并颅脑损伤，儿童

Abstract. *On the first day after SCTBI, in all groups of children, there was a tendency to increase the stroke volume of the heart. During intensive care in the ICU, no significant changes in the CO circadian rhythm mesor were detected in group 1. In group 2, on days 5-15 and in groups 3, on days 14-19, there was a tendency to decrease the indicator. The highest values of the amplitude of the circadian rhythm of CO in the first day, which amounted to 8 ml in group 1, 16 ml in group 2, and 12 ml in group 3, were due to hemodynamic instability due to traumatic shock, infusion therapy. The adequacy of intensive therapy was expressed in a decrease in the amplitude of daily fluctuations in cardiac output. The most pronounced and prolonged inversion of the CO circadian rhythm with SCTBI in infancy was found in the most severe children of group 3.*

Keywords: *circadian rhythm, stroke volume, severe concomitant traumatic brain injury, children*

Relevance

The main goal of emergency care for children with SCTBI is to restore, maintain vital functions, and prevent secondary brain damage. With the development or increase of hemodynamic instability with a decrease in blood pressure against the background of ongoing infusion therapy, adrenomimetics are used in parallel (dopamine 4% 3 - 5 mcg/kg per minute, if necessary, the dose is increased to 10 mcg/kg or more in 1 minute; and if ineffective - in combination - adrenaline or mezaton at an age dose. With the development and growth of dislocation symptoms, hyperosmolar solutions are used. Use 3% NaCl solution in dextran at a dose of 0.1–1.0 g/kg/hour or 15% mannitol solution at an initial dose of 1 g/kg for 20 minutes, when the body is subjected to extreme exposure, there is an increase in heart rate of 3 or more times compared to normal. The heart rate changes under the chronotropic influence that the sympathetic and vagus nerves have on the sinoatrial node of the heart. In parallel with chronotropic changes in cardiac activity, inotropic influences can be exerted on the myocardium. [1-4]. Due to the lack of information on hemodynamic disorders in infants, we tried to assess the changes in stroke volume at the age of up to 3 years in the acute period of severe concomitant traumatic brain injury.

Purpose of the work

To study and identify the features of the circadian rhythm of stroke volume in children with severe concomitant traumatic brain injury in children under the age of three years.

Material and research methods

A detailed analysis of reliably significant deviations, intergroup differences in the studied hemodynamic parameters was carried out. The results were obtained by monitoring with hourly recording of body temperature, systolic (SBP), diastolic (DBP) blood pressure. Impact volume (IV), Calculation of the stroke volume index was carried out according to the formula: CO=PBP*50/MBP.

The research data were processed by the method of variation statistics using the Excel program by calculating the arithmetic mean values (M) and the errors of the means (m). To assess the significance of differences between the two values, Student's parametric test (t) was used. The relationship between the dynamics of the studied indicators was determined by the method of pair correlations. The critical level of significance in this case was taken equal to 0.05.

Of the 18 children (tab. 1) diagnosed with severe concomitant traumatic brain injury (SCTBI), admitted to the Republican Center for Emergency Medical Care in infancy, 7 patients received intensive care in the ICU for 5.9±1.3 days, 6 patients for 14±1.7 days, 7 children for 31.2±5.3 days, which served as the basis for the creation of randomized groups according to the severity of the condition. The difference is significant ($p<0.05$).

Table 1.

Characteristics of SCTBI patients admitted before the age of 3 years

Groups	Num. of days in ICU	Num. of pat.	Gender Male	Age	RTA	Catatrauma	Traum. shock of 2 deg.	Operated on admission	Number of days in hospital
1	5,9±1,3	7	4.	20,8±7,8	71% (5)	29% (2)	71% (5)	71% (5)	15,2±7
2	14±1,7	6	4	23,1±4,7	50% (3)	50% (3)	83% (5)	66% (4)	20±4
3	31,2±5,3	5	3	18,2±4,6	80% (4)	20% (1)	100% (5)	100% (5)	37,4±5,3

In group 1, the frequency of closed craniocerebral injury (CCCI) (71%), concussion (28%) prevailed, the number of operations on the first day after injury was 71%. In the 2nd more severe group, the number of open craniocerebral injury (OCCI) prevailed - 66%, the incidence of severe brain injury (SBI) - 50%, fracture of the parietotemporal bone with the transition to the base of the skull 48%, severe traumatic shock was observed in all patients. In the most severe group 3, 100% of the severity of the condition at admission was due to CCCI, SBI, subarachnoid hemorrhage (SAH), traumatic shock. In group 1, out of 5.9±1.3 days spent in the ICU, only 1 patient out of 7 was on ALV for 3 days in CMV mode, followed by extubation upon restoration of spontaneous breathing. In groups 2 and 3, all patients were transferred to ALV upon admission according to indications. Subsequently, out of 14.6 ±1.7 days spent in the ICU, the average ALV in CMV mode in group 2 was carried out for 6.8±2.2 days, SIMV 1.75±0.8, CPAP in 1 patient - 1 day, the duration of spontaneous breathing was 7±1.6 days. In group 3, ALV in the CMV regimen was performed for three patients for 17±3 days, SIMV 9.5±4.6 days, CPAP 2.5±1.5 days, spontaneous breathing 34±9.5 days.

Results and its discussion

The phase structure of the CO circadian rhythm in the acute period of SCTBI in infancy was studied and assessed. Tab. 1 shows changes in the mesor index of the circadian rhythm of stroke volume by groups.

Table 1.

Dynamics of the CO circadian rhythm mesor in the acute period of SCTBI in children under 3 years old, in ml

Days	Group 1	Group 2	Group 3
1	27.0±2.7	30.0±3.2	30.5±3.5
2	26.4±1.8	31.0±2.0	27.1±2.0
3	27.5±1.5	30.9±1.3	25.9±1.7

4	29.6±3.0	27.6±2.7	26.7±2.0
5	25.8±1.6	25.0±1.3	26.2±1.4
6	25.6±2.5	25.0±1.6	29.6±2.1
7	26.5±2.3	26.1±1.5	27.8±2.1
8		24.4±1.9	26.7±1.4
9		27.3±1.5	28.0±1.2
10		27.1±1.8	28.2±1.6
11		27.6±2.5	30.3±1.3
12		27.3±0.8	23.8±1.5
13		28.3±1.9	28.0±2.7
14		26.1±1.6	27.5±1.9
15		25.2±1.9	25.6±2.5
16			27.6±1.5
17			27.7±2.0
18			26.1±2.2
19			26.4±1.8
20			31.4±1.3
21			28.8±2.0
22			26.9±2.4
23			27.3±1.8
24			30.3±2.5
25			28.8±1.5
26			29.5±2.5
27			27.5±2.0
28			27.8±1.8
29			30.2±2.8
30			29.7±2.4

As shown in Table 1 and fig. 1, on the first day after SCTBI, in all groups of children, there was a tendency to increase stroke volume, but there was no relationship with the severity of the injury. In group 1, during intensive care in the ICU, no significant changes in the mesor of the circadian rhythm CO were detected. In groups 2 on days 5-15 and in groups 3 on days 14-19, there was a tendency to decrease the indicator. The tendency to increase cardiac output in the first 3 days was due not only to the compensatory mechanism aimed at adequate

supply of oxygen, metabolites, macroergic ingredients for increased needs of vital organs, tissue structures under conditions of a severe stress response of the child's body to SCTBI. Another factor that led to an increase in CO predominantly in 1 day was the amount of infusion therapy aimed at compensating for acute losses caused by trauma, recovering from shock, and restoring the perfusion abilities of vital organs and systems. The third factor affecting cardiac output was the transfer to ALV, when in groups 2 and 3 all patients were transferred to ALV upon admission and were on prolonged respiratory support as indicated.

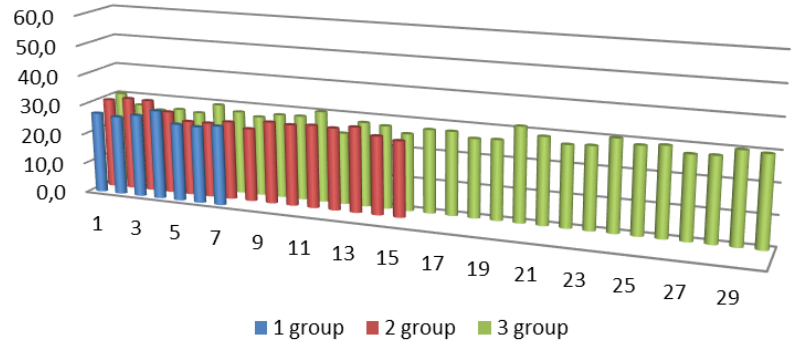

Figure 1. *Dynamics of the mesor of the circadian rhythm of the stroke volume up to 3 years, ml*

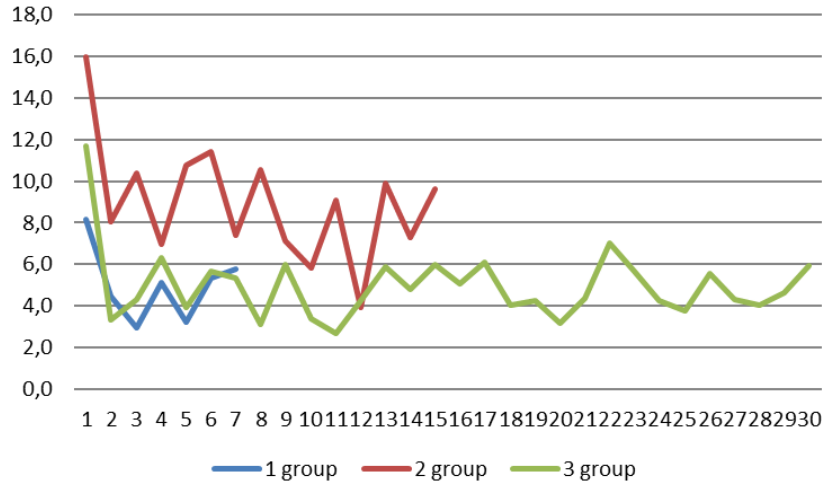

Figure 2. *Dynamics of the amplitude of daily fluctuations in CO, ml*

The highest indicators of the amplitude of the circadian rhythm of CO in the first day, which amounted to 8 ml in group 1, 16 ml in group 2, and 12 ml in group 3, were due to hemodynamic instability due to traumatic shock, corrective infusion therapy aimed at compensating for losses, the introduction of solutions in order to restore central and peripheral hemodynamics. The adequacy of intensive therapy was expressed in a decrease in the amplitude of cardiac output fluctuations on the second day in patients in the 1st group up to 3 ml, in the second - up to 8 ml, in the third group up to 3 ml (fig. 2). In subsequent days, changes in the amplitude of daily fluctuations in CO were within 3-6 ml in groups 1 and 3 of children, in groups 2 – 7-11 ml per day.

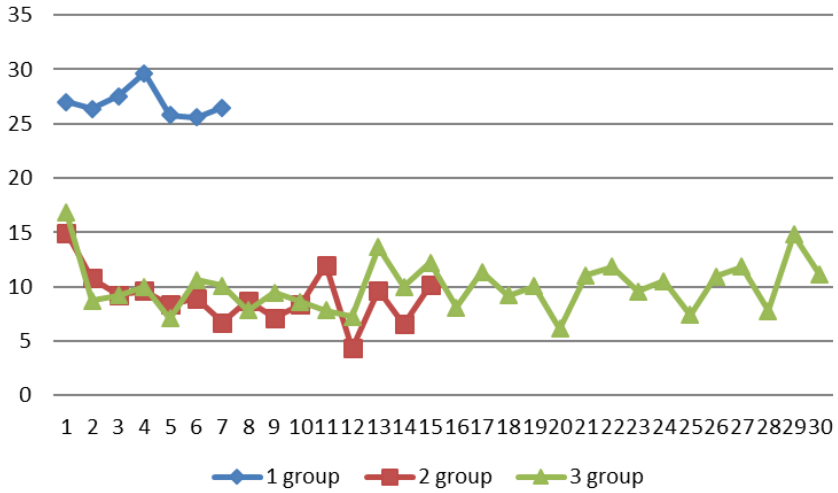

Figure 3. *The range of daily fluctuations in stroke volume in the acute period of SCTBI up to 3 years*

The most significant indicator of the range of daily CO fluctuations in group 1 draws attention - 25-30 ml/day (fig. 3), while in groups 2 and 3 daily CO fluctuations ranged from 5-10 ml in the first two weeks. In the following days, there was a trend towards an increase in daily CO changes up to 12-15 ml in injured children of the 3rd group. The latter corresponded to the more severe condition of children on ALV due to the greater degree of STBI predominant brain damage. Instability of CO in group 1 may be evidence of insufficient stress-limiting, sedative therapy due to the lack of hardware respiratory support to prevent drug-induced centrogenous respiratory failure in conditions of a lesser degree of traumatic brain damage.

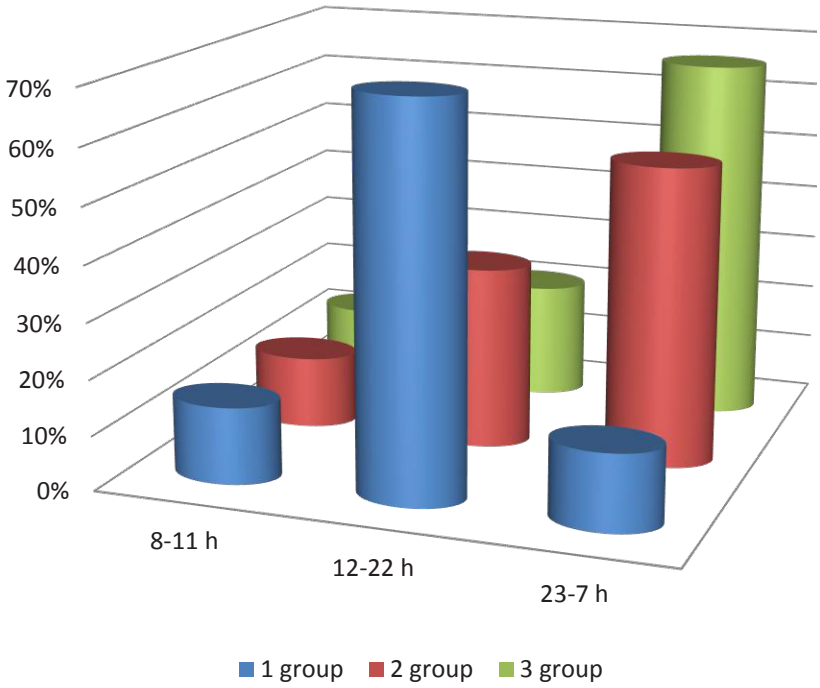

Figure 4. *Duration of CO acrophase shifts*

The longest shift in the peak of the acrophase of the CO circadian rhythm to the night hours was found in children of the 3rd group, that is, the inversion continued for 20 days (out of 30), amounting to 66%. In group 2, the inversion of the circadian rhythm CO continued for 8 days out of 15, which amounted to 54%; in group 1, only 14% (fig. 4). That is, the most pronounced and prolonged destructuring of the CO circadian rhythm in infancy was found in the heaviest children of the 3rd group. Taking into account the increased functional load on the myocardium due to the increased risk of acute functional failure of cardiac function at night in group 3, it seems appropriate to emphasize drug maintenance of myocardial function also at night in children of group 3. In group 1, a moderate shift in the peak of the acrophase of the circadian rhythm CO during the daytime prevailed against the background of the most pronounced changes in CO (fig. 3).

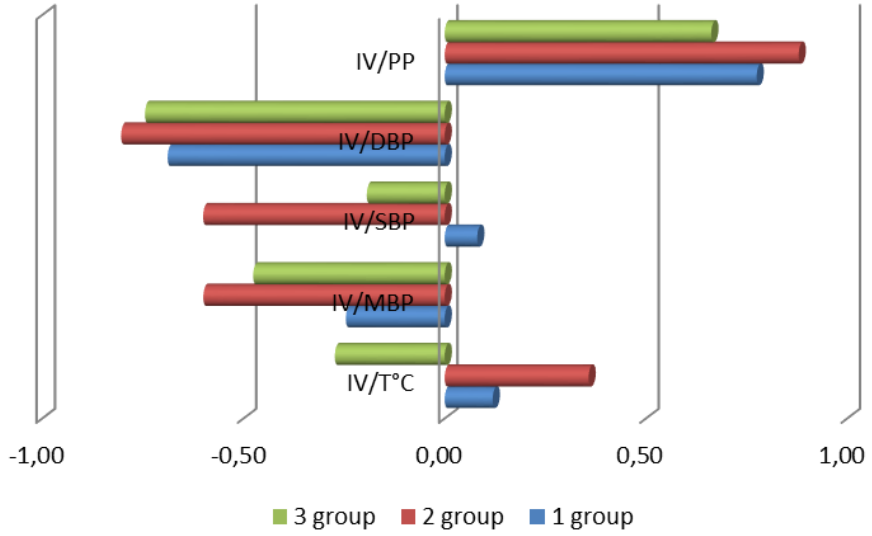

Figure 5. *CO correlations up to 3 years*

A direct correlation between CO and PBP dynamics was found in all injured children. The tendency to decrease DBP with an increase in CO found in all young children can be interpreted as a physiological compensatory response of peripheral vessels to an increase in cardiac output, formed in connection with infusion and drug correction. In group 2, there was a tendency to form an inverse correlation between CO indicators and SBP, CO, and MBP.

Conclusions

On the first day after SCTBI, in all groups of children, there was a tendency to increase the stroke volume of the heart. During intensive care in the ICU, no significant changes in the CO circadian rhythm mesor were detected in group 1. In group 2, on days 5-15 and in groups 3, on days 14-19, there was a tendency to decrease in the indicator. The highest values of the amplitude of the circadian rhythm of CO in the first day, which amounted to 8 ml in group 1, 16 ml in group 2, and 12 ml in group 3, were due to hemodynamic instability due to traumatic shock, corrective infusion therapy. The adequacy of intensive therapy was expressed in a decrease in the amplitude of cardiac output fluctuations. The most pronounced and prolonged inversion of the CO circadian rhythm with SCTBI in infancy was found in the most severe children of group 3.

References

1. https://vbgi.ru/cough/sochetannaya-cherepno-mozgovaya-travma-sochetannaya-cherepno-mozgovaya-i/

2. https://yazdorovdi.ru/udarnyj-obem-serdca-normy-u-vzroslyh-i-detej.html

3. https://ymkababy.ru/good-to-know/sochetannaya-cherepno-mozgovaya-travma-sochetannaya-cherepno-mozgovaya.html

4. https://zakon.today/pediatriya_1044/intensivnaya-terapiya-detey-cherepno-mozgovoy-90572.html

DOI 10.34660/INF.2022.42.54.180

西伯利亚第二成熟期女性从 COVID-19 康复、患有冠心病的每月北欧式步行周期中的身体表现以改善健康为导向

PHYSICAL PERFORMANCE IN THE MONTHLY CYCLE OF NORDIC WALKING OF A HEALTH-IMPROVING ORIENTATION IN WOMEN OF THE SECOND PERIOD OF MATURE AGE IN SIBERIA, RECOVERED FROM COVID-19, SUFFERING FROM CORONARY HEART DISEASE

Boyarskaya Larisa Aleksandrovna
Candidate of Medical Sciences, Associate Professor
Tyumen State Medical University, Tyumen
Prokopyev Nikolay Yakovlevich
Doctor of Medical Sciences, Full Professor
Tyumen State University, Tyumen
Ananyev Vladimir Nikolaevich
Doctor of Medical Sciences, Full Professor
Institute of Biomedical Problems, RAS, Moscow
Gurtovoy Elisey Sergeevich
Tyumen State Medical University, Tyumen

目的。 在西西伯利亚南部患有 Covid-19、患有冠心病 (CHD) 的第二个成熟年龄期的女性中，在每月一次的北欧式步行 (NW) 周期中，研究身体表现指标 (PP) 。 材料与方法。 在门诊对 10 名患有 Covid-19 并患有冠心病 (CHD) 的第二成熟年龄 (42.4±2.7 岁) 女性进行了门诊检查。 在俄罗斯秋明市的 FGBUZ ZSMC FMBA 森林公园区有一个月的时间，女性经常练习 NW。 PP的水平根据Rufier方法控制。 结果。 一个月内每天进行 60 分钟的 NW 训练不仅有助于提高 FR 水平，还有助于改善生活质量。

关键词：女性，越野行走，体能。

Purpose. *In women of the second period of mature age in the south of Western Siberia, who had Covid-19, suffering from coronary heart disease (CHD), in the monthly cycle of Nordic walking (NW), to study indicators of physical performance (PP). Material and methods. 10 women of the second period of mature age (42.4±2.7 years) who had Covid-19 and suffered from coronary heart disease (CHD) were examined on an outpatient basis. For a month in the forest park zone of the FGBUZ ZSMC FMBA of Russia in the city of Tyumen, women*

regularly practiced NW. The level of PP was controlled according to the Rufier method. Results. Daily 60-minute NW sessions for a month contributed not only to an increase in the level of FR, but also to an improvement in the quality of life.

Keywords: *women, Nordic walking, physical performance.*

Relevance

In recent years, Nordic walking (NW) has become increasingly popular in various countries of the world, which is associated with its availability in terms of not only increasing physical activity, but also as an effective means of healing and saving health [3, 6, 10]. Walking itself is an adequate axial load for the spinal column and joints of the lower limb, and this load is 2.5 times less than when running [13]. In addition, there are very few medical contraindications for NW, which makes it popular and attractive for various age groups of the population [2, 15, 17].

The undoubted advantages of NW include the fact that it allows you to increase the oxygen transport function of the body, thereby improving the functionality of the cardiorespiratory system [11, 12, 19, 20, 21, 22, 23, 24].

The importance and relevance of NW contributed to the emergence of NW learning technologies [1, 18] and the publication of textbooks and guidelines for its application [7, 9,https://elibrary.ru/author_items.asp?refid=459197456&-fam=%D0%9B%D0%B8%D0%BD%D0%B4%D0%B1%D0%B5%D1%80%D0%B3&init=%D0%90+%D0%9D 14]. Prospects for the use of NW [4] are outlined.

The problem of our study is the lack of information in the scientific and methodological literature on the indicators of the functional state of central hemodynamics and PP in women of the second period of adulthood who had Covid-19, suffering from CHD, living in the south of Western Siberia in the monthly cycle of NW classes.

Purpose: in women of the second period of adulthood, living in the south of Western Siberia, who had Covid-19, suffering from CHD, to study the PP indicators in the monthly cycle of Nordic walking for health purposes.

To achieve the goal of the study, the following tasks were set:

1. In second-adult women who have had Covid-19 and are suffering from CHD, test baseline PP using the Ruffier method at the start of NW training.

2. Compare the initial PP indicators and their change in the course of monthly NW health-improving classes.

Material and methods

10 women of the second period of mature age (42.4±2.7 years) were examined. Conduct a questionnaire to determine the influence of inactive lifestyle factors associated with a number of cumulative factors - professional activity, the consequences of the Covid-19 pandemic, the severity of CHD, emotional and psycho-

logical mood.

The content of the classes was NW aimed primarily at improving PP and functional status. During the month-long period of NW health-improving classes, we built the structure of the classes in such a way that each of the women was fluent in the skills of controlling the heart rate (HR, beats/min) before classes, during the main part of the classes and after it. Particular attention was paid to the emotional and psychological mood during the entire monthly cycle of the wellness NW.

When assessing PP, we used the standard Rufier test, which is simple to use and easy to interpret, and which has found wide application both in the practice of physical education and clinical medicine [5, 8, 16].

The Rufier index (RI) was calculated using the formula:

$RI = (4 \times (P1 + P2 + P3) - 200)/10$

In our study, the result was evaluated by the value of the index: less than 3 – good performance; 3-6 – medium; 7-9 – satisfactory; 10-14 – bad.

The principles of voluntariness, the rights and freedoms of the individual, guaranteed by Articles 21 and 22 of the Constitution of the Russian Federation, as well as the Order of the Ministry of Health and Social Development of Russia №774n dated August 31, 2010 "On the Council on Ethics", were observed. The study was conducted in compliance with the ethical standards set forth in the Declaration of Helsinki and the Directives of the European Community (8/609EC) and the informed written consent of the women.

Results and discussion.

In studying the functional state of the body of women involved in NW, we proceeded from the fact that the most important thing during exercise is the control of blood circulation. It is the indicators of central hemodynamics that, firstly, are of primary importance for resolving the issue of admission to NW classes. Secondly, about the "dose" of physical activity that can be offered to a woman suffering from CHD during NW.

We consider the most important condition for NW classes to be the correct approach to the process of adaptation of a woman's body to physical activity, which develops on the basis of the interaction of regulatory functional systems. At the same time, violations of adaptive processes can contribute to functional and organic changes in the body. We believe that even minor deviations in the functioning of the female body, especially the second period of adulthood, as a result of excessive physical activity when walking, can cause serious changes in the state of health.

It should be noted that NW women practiced daily for a month for 60 minutes. As a self-control, heart rate was calculated before, during and after the end of NW. When conducting the study, we proceeded from the fact that if in a state of physiological rest lasting 5 minutes, the heart rate of a woman exceeded 90 beats/min

or was less than 60 beats/min, then we recommended NW either not to carry out, or to walk, but only at slow pace (up to 70 steps per minute).

The results of individual testing of PP women of the second period of adulthood according to the Rufier test at the initial and final stages of NW classes are shown in table 1.

Table 1.

Dynamics of PP indicators according to the Rufier test of women of the second period of mature age involved in NW

Subject number	Rufier index values (before and after a monthly NW session)	PP level
1	Before exercises – 5.8	average
	After exercises – 5.6	average
2	Before exercises – 10.9	bad
	After exercises – 9.7	satisfactory
3	Before exercises – 5.9	average
	After exercises – 5.5	average
4	Before exercises – 7.6	satisfactory
	After exercises – 7.1	satisfactory
5	Before exercises – 2.8	good
	After exercises – 2.7	good
6	Before exercises – 10.6	bad
	After exercises – 9.8	satisfactory
7	Before exercises – 6.6	average
	After exercises – 6.2	average
8	Before exercises – 7.4	satisfactory
	After exercises – 6.8	average
9	Before exercises – 10.5	bad
	After exercises – 9.6	satisfactory
10	Before exercises – 4.3	average
	After exercises – 4.1	average
M±m	Before exercises – 7.24±0.21	satisfactory
	After exercises – 6.71±0.14	satisfactory

The results of the study show that the individual values of the Rufier index ranged from 2.2 to 10.9. The monthly cycle of NW classes indicated that the women's PP improved significantly ($p<0.05$) (fig. 1).

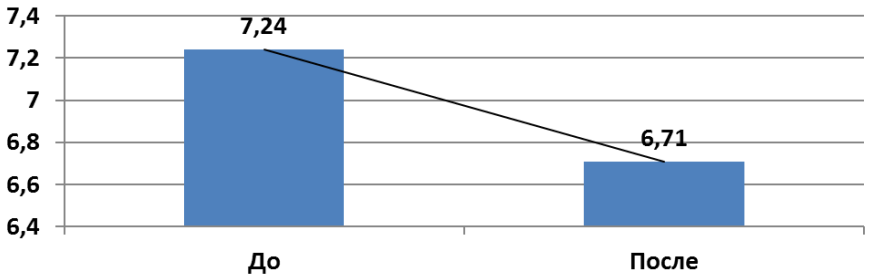

Figure 1. *Dynamics of the Rufier index in women of the second period of adulthood who had Covid-19, suffering from coronary heart disease before and after 30 days of Nordic walking*

It can be concluded that in absolute terms, all women after 30 days of regular Nordic walking classes had a significant ($p<0.05$) increase in PP, which in absolute terms amounted to 0.53 units. At the final stage of training, the average level of PP was obtained in 5 people, the transition from bad PP to satisfactory performance was detected in 3 women, and in 4 women it remained at the same average level. Only 1 woman had a good PP level. We also note that all women note a significant improvement in their emotional and psychological state, an increase in self-confidence, an improvement in the quality of sleep, albeit insignificant, but a decrease in body weight. Keeping a self-control diary developed by us, women note a decrease in HR by 2.8±0.34 beats/min, a decrease in SBP by 4.6±0.67 mmHg and a decrease in body weight by 1.7±0.29 kg.

Conclusions.

1. When assessing human PP, the Rufier test belongs to the category of informative, it is easy to perform, therefore it can be used in clinical practice to assess PP in patients with diseases of the circulatory system.

2. Regular dosed physical activity in the form of NW in women of the second period of adulthood suffering from coronary heart disease after suffering Covid-19 not only increases their PP level, but also improves their emotional and psychological mood, body weight correction and central hemodynamics.

Conflict of interest. The authors declare no conflict of interest.

Research transparency. The study was not sponsored. The authors are solely responsible for providing the final version of the manuscript for publication.

Declaration of financial and other relationships. The authors were involved in the development of the topic, study design, and writing of the manuscript. The final version of the manuscript was agreed and approved by all authors. The authors did not receive a fee for the study.

References

1. Alekseeva N.V. Teaching technology for Nordic walking as a component of a healthy lifestyle / N.V. Alekseev. // Bulletin of A.S. Pushkin Leningrad State University – 2013. – V. 3. – № 4. – P. 111–115.

2. Borisova V.V. Nordic walking as a means of improving the motor fitness of high school students / V.V. Borisova. //Bulletin of the Tula University (TIEI). – 2016. – V. 1. – № 7. – P. 34-37.

3. Venediktova I.A. Nordic walking as a means of restoring and strengthening the health of medical students with medical limitations / I.A. Venediktova, A.A. Burkland. // Promising directions in the field of physical culture, sports and tourism: materials of the VII All-Russian scientific-practical conference. (Nizhnevartovsk, March 17-18 2017), 2017. – P. 59-62.

4. Evdokimov V.A. Prospects for the use of Nordic walking in the classes of a special medical group / V.A. Evdokimov //Theory and practice of innovative technologies in the agro-industrial complex Materials of the scientific and educational-methodical conference of scientific and pedagogical workers and post-graduate students of VSAU. Voronezh, March 10-20, 2017. – P. 135-137.

5. Ivko I.A. Comparison of the growth rates of indicators of the morphofunctional state and physical fitness of young and mature women at the initial stage of health-improving aerobics classes / Ivko I.A., Pozdeeva E.A. //Man. Sport. Medicine. 2016. V. 16. № 4. P. 5-17.

6. Kiryakina T.V. Nordic walking as a means of health saving for middle-aged and elderly people / T.V. Kiryakina. //New Science: Experience, Traditions, Innovations. – 2017. – V. 2. – № 4. – P. 49-52.

7. Kolodiy N.G. Nordic walking: guidelines / N.G. Kolodiy, L.A. Sharenkov. // Northern State Medical University. Arkhangelsk, 2017. – 19 P.

8. Levchuk E.A. Changes in the functional state of the cardiovascular system of women 40-45 years old under the influence of fitness products and nutritional factors / Levchuk E.A., Uchasov D.S. // Notes of a scientist. 2021. № 9-1. P. 109-112.

9. Lindberg A.N. Nordic walking and jogging against diseases. Practical course of natural movement. / A.N. Lindberg. – SPb: Vector, 2014. – 160 P.

10. Lysikov V.I. Nordic walking - as a means of improving the physical condition of a person / V.I. Lysikov, Yu.I. Boyko. // Physical culture and sports in modern society: materials of the All-Russian scientific-practical conference dedicated to the 50th anniversary of the formation of the Far Eastern State Academy of Physical Culture. EUnder the editorship of S. S. Dobrovolsky. – 2017. – P. 140-142.

11. Mayornikova S.A. Nordic walking in the physical rehabilitation of elderly women with stage II hypertension / S.A. Mayornikova, S.A. Tkachenko, L.A. Sharapova. // Therapeutic physical culture: achievements and development prospects: materials of the V All-Russian scientific-practical conference with international participation. – 2016. – P. 167-172.

12. Martynenko N.A. The use of Nordic walking in the rehabilitation of patients with arterial hypertension / N.A. Martynenko, N.V. Mishchenko. //New Science: Experience, Traditions, Innovations. – 2015. – № 1. – P. 5-10.

13. Nikitina T.V. Nordic walking in the sanatorium rehabilitation of patients with osteoarthrosis of large limb joints / T.V. Nikitina, E.A. Kurnyavkina, V.A. Drobyshev. // Medicine and education in Siberia. – 2015. – № 6. – P. 55.

14. Poletaeva A. Nordic walking. Health in an easy step. / A. Poletaeva. – SPb: Peter, 2016. – 150 P.

15. Nordic walking in the complex of measures to improve the quality of life of elderly and senile people / O.B. Krysyuk, V.V. Deineko, R.K. Kantemirova, Yu.A. Sukhonos, V.A. Arutyunov // Successes of gerontology. 2020. V. 33. № 3. P. 590-594.

16. Skrygin S.V. Rufier index – universal indicator of cardiovascular system performance in the process of physical education / S.V. Skrygin. //Electronic scientific journal. – 2016. – № 2 (5). – P. 551-554.

17. Fedyakin A.A. Features of the health-improving and training impact of Nordic Walking on the human body / A.A. Fedyakin. // Bulletin of the Adyghe State University. – 2012. – № 2 (97). – P. 231-236.

18. Shcherbinina N.P. Technique and rules of Nordic walking. Goals of Nordic walking / N.P. Shcherbinina, N.V. Abdullova, S.A. Aldarova //International Journal of the Humanities and Natural Sciences. 2022. № 3-2 (66). P. 246-248.

19. Latosik E. Physiological Responses Associated with Nordic-walking training in Systolic Hypertensive Postmenopausal Women / E. Latosik, I.Z. Zubrzycki, Z. Ossowski. // J Hum Kinet. – 2014. – Nov 12. – № 43. – P. 185-190.

20. Church T.S. Field testing of physiological responses associated with Nordic Walking / T.S. Church, C.P. Earnest, G.M. Morss. //Res Q Exerc Sport. 2002 Sep; 73(3): 296-300.

21. Hansen E.A. Energy expenditure and comfort during Nordic walking with different pole lengths. / E.A. Hansen, G. Smith. //J Strength Cond Res, 2009; 23(4): 1187-1194.

22.Efficacy of Nordic Walking in Obesity Management. / H. Figard-Fabre, N. Fabre, A. Leonardi, F. Schena. //Int J Sports Med, 2011; 32(6): 407-414.

23.Mikalacki M. Effect of nordic walking on functional ability and blood pressure in elderly women. / M. Mikalacki, N. Cokorilo, R. Katic. //Coll Antropol, 2011; 35(3): 889-894.

24.Physiological responses to Nordic walking, walking and jogging. / T. Schiffer, A. Knicker, U. Hoffman, B. Harwig, W. Hollmann, H.K. Struder. //Eur J Appl Physiol, 2006; 98(1): 56-61.

DOI 10.34660/INF.2022.38.36.181

合并感染：艾滋病毒、肺结核
CO-INFECTION: HIV, TUBERCULOSIS

Azovtseva Olga Vladimirovna
Doctor of Medical Sciences, Associate Professor
Yaroslav-the-Wise Novgorod State University

抽象的。 近年来，俄罗斯已经看到艾滋病毒流行的性质向合并症的发展方向发生了变化。 结核病是 HIV 感染者最常见的继发性疾病。 在这项工作的过程中，发现合并感染的临床形式和表现取决于免疫抑制水平。 抗逆转录病毒治疗的较晚开始以及药物和/或酒精的使用会对疾病的进程及其结果产生负面影响。

关键词：HIV 感染、合并感染、结核病、慢性病毒性丙型肝炎、表现、结果。

Abstract. *In recent years, Russia has seen a change in the nature of the HIV epidemic towards the development of comorbid diseases. Tuberculosis is the most common secondary disease in HIV-infected patients. In the course of this work, it was revealed that the clinical forms and manifestations of coinfection depend on the level of immunosuppression. Late initiation of antiretroviral therapy, as well as the use of drugs and/or alcohol, negatively affects the course of the disease and its outcome.*

Keywords: *HIV infection, coinfection, tuberculosis, chronic viral hepatitis C, manifestations, outcome.*

In recent years, the Russian Federation has seen a change in the nature of the HIV epidemic towards the development of comorbid diseases [1-3]. The most common and severe association with HIV-infection is tuberculosis (TB). If we do not influence the situation of coinfection at the moment, we will annually observe an increase in the number of coinfected patients and note a high mortality rate in this group of patients.

In the last decade, the Russian Federation has recorded a decrease in the incidence of TB, while the number of people living with HIV is increasing every year. As a result, there is an annual increase in the incidence and prevalence of coinfection, which indicates a significant role of HIV in the spread of TB.

In this work, a retrospective clinical and epidemiological analysis of cases of coinfection (n=137) was carried out. The average age of the patients was 37.4±0.71 years, among the observed men predominated - 69.3%. In terms of social status,

the following dominated: unemployed - 88.4% of persons; users of psychoactive substances - 61.3%; alcohol - 70.8%, as well as persons previously in prison - 45.9%. In the observed patients in 77.4% of cases, the presence of chronic viral hepatitis was recorded, in the structure of which hepatitis C dominated (87.6%).

The work revealed that the degree of immunosuppression in HIV-infected patients affects the development of TB and aggravates the course of co-infection (table 1). In addition, a high level of immunosuppression (less than 200 cells/μl) leads to the development of severe and generalized TB (table 1).

Table 1.

Clinical forms of tuberculosis process depending on the degree of immunosuppression

Level of CD4-lymphocytes (cell/μl)	Generalized TB (n=64)	TB of the chest (n=73)
199 and below	65.7	47.9
200-349	18.7	19.2
350-499	6.25	19.2
500 or more	9.37	13.7

Among the generalized forms of TB in coinfected patients, TB of the lymph nodes (75%), genitourinary system (29.7%), brain and its membranes (23.5%), spleen (14.1%), musculoskeletal apparatus (14.1%), intestines (12.5%) and liver (9.4%).

The high proportion of involvement of the organs of the lymphoid system in the tuberculous process indicates the predominance of the lymphogenous distribution of MBT over the hematogenous one. In coinfected patients, peripheral (34.4%), intraperitoneal (23.4%) and retroperitoneal (17.2%) lymph nodes were most frequently affected.

Two-thirds of co-infected patients (66%) had a long history of HIV infection (5 years or more). At the same time, 61% of co-infected patients, despite the long history of HIV infection, did not take specific antiretroviral therapy (Figure 1), which indicates low adherence to therapy, as well as low adherence to dispensary and, as a result, low coverage of TB chemoprophylaxis in HIV-infected people.

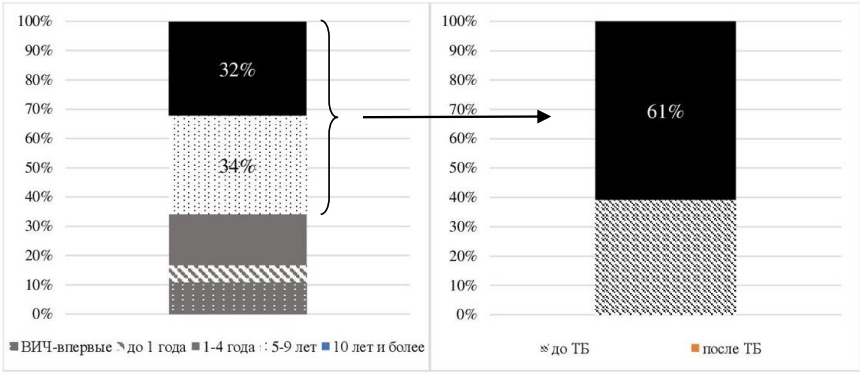

Figure 1. *Duration of HIV infection and timing of antiretroviral therapy (n=137)*

Mortality in the group of patients with generalized TB (14.1%) was higher than mortality in the group of patients with pulmonary TB (1.37%). However, the addition of antiretroviral therapy to anti-tuberculosis therapy in the generalized TB group reduced mortality by 8 times (mortality on ART - 1.56%, mortality without ART - 12.5%).

The proportion of drug-resistant TB was 56.2%. The presented work did not reveal the effect of drug-resistant TB on the form of tuberculous inflammation and the rate of death. Perhaps this is a feature of this group of observations.

Conclusions

The socio-epidemic situation of HIV infection has a significant impact on the incidence and prevalence of coinfection. Among co-infected patients with a high frequency there were: users of drugs (61.3%) and alcohol (70.8%), as well as persons with experience of being in penitentiary institutions (45.9%). Clinical forms and manifestations of TB in coinfected patients depend on the level of CD4-lymphocytes. Patients with severe immunosuppression have an increased risk of developing extrapulmonary forms of TB (65.7% vs. 47.9%). The leading clinical form of TB was generalized TB, which most often occurred with lesions of the lymph nodes (75%), the brain and its membranes (23.5%), the genitourinary system (29.7%), the spleen (14.1%), intestines (12.5%), liver (9.4%).

In co-infected patients, ART, in 56.8% of cases, was started after the detection of the tuberculosis process, despite the fact that these patients had a long period of infection with the human immunodeficiency virus. This fact indicates a late start of ART.

The lethality in the group of patients with generalized TB was higher than the lethality in the group of patients with pulmonary TB, joining anti-tuberculosis

therapy with ART reduces the lethality by 8 times even in the group of patients with generalized TB.

The most common comorbidities in co-infected patients are CH. In the etiological structure, CHC prevails both in the monoform (87.6%).

References

1. Belyakov N. A., Rassokhin V. V., Trofimova T. N., Stepanova E. V., Panteleev A. M., Leonova O. N., Buzunova S. A., Konovalova N. V., Milichkina A. M., Totolyan A. A. Comorbid and severe forms of HIV infection. HIV infection and immunosuppression. 2016; V.8. 3: 9–25. https://doi.org/10.22328/2077-9828-2016-8-3-9-25

2. Belyakov N. A., Rassokhin V. V. Comorbid conditions in HIV infection. Part II. Secondary and concomitant infections. SPb.: Baltic medical educational center. 2019; 252 P.

3. Leonova O. N., Stepanova E. V., Belyakov N. A. Severe and comorbid conditions in patients with HIV infection: an analysis of adverse outcomes. HIV infection and immunosuppression. 2017; V.9. 1: 55–64. https://doi.org/10.22328/2077-9828-2017-9-1-55-64.

DOI 10.34660/INF.2022.32.54.182

一种修复缺失的临床牙冠的新方法
A NOVEL WAY OF RESTORING THE MISSING CLINICAL CROWN OF THE TOOTH

Nesterov Alexander Michailovich
Doctor of Medical Sciences, Full Professor,
Head of the department of prosthetic treatment
Sadykov Mukatdes Ibragimovich
Doctor of Medical Sciences, Full Professor
Sagirov Marsel Ramilevich
Candidate of Medical Sciences, Assistant
Samara State Medical University

抽象的。

文章介绍了临床牙冠完全破坏患者的修复治疗新方法。

该研究的目的是描述用于修复缺失的临床牙冠的装置，并评估其在体内和体外的有效性。

材料和方法。在研究期间，我们治疗了 70 名牙冠完全破坏的患者。我们在体内研究的治疗效果。我们使用了有针对性的 X 线摄影、咬合造影和 OHIP-14 RU 指数对患者的生活质量进行评估。此外，我们还在体外研究了 10 个本装置样品和 10 个传统金属陶瓷冠样品的陶瓷涂层的抗断裂性。

结果。由于修复治疗，1个月后靶向X线片，所有患者都有良好的结果，在咬合造影期间，10%的患者检测到侧面咬合的轻微过早接触，通过选择性研磨消除。 1个月后对患者的生活质量进行评估，95%的患者生活质量良好，5%的患者生活质量不满意。

体外研究表明，新型器械陶瓷涂层的安全性是传统器械样品的 2.4 倍。

结论。修复缺失的临床冠的新方法在临床实践中显示出良好的效果。此外，它具有比传统设备更高的抗断裂性。

关键词：临床牙冠全毁，金属陶瓷冠，抗折性。

Abstract.

The article describes a new method of prosthetic treatment of patients with total destruction of the clinical crown of the tooth.

The aim of the research is a description of the device for restoring the missing clinical crown of teeth and evaluate it's effectiveness in vivo and in vitro.

Materials and methods. *During the research, we have treated 70 patients with*

total destruction of the crown. Effectiveness of the treatment we studied in vivo. We have used targeted radiography, occlusiography and assessment of the quality of life of patients with the OHIP-14 RU index. In addition, we have explored fracture resistance of ceramic coatings for 10 samples of the proposed device and 10 samples of traditional metal-ceramic crown in vitro.

Results. *As a result of prosthetic treatment, after 1 month on targeted radiographs, all patients have a favorable outcome, during occlusiography, minor premature contacts in lateral occlusion were detected in 10% of patients, which were eliminated by selective grinding. During the assessment of the quality of life of patients after 1 month, 95% of patients had a good level of quality of life, 5% had an unsatisfactory level of quality of life.*

In vitro studies have shown that the safety of the ceramic coating of novel device is 2.4 times higher than in the samples of a traditional device.

Conclusions. *The novel way of restoring the missing clinical crown has shown a good result in clinical practice. In addition, it has a higher fracture resistance than traditional device.*

Keywords: *total destruction of the clinical crown of the tooth, metal-ceramic crown, fracture resistance.*

Introduction

Today, the problem of restoring teeth with a total destroyed clinical crown is an urgent problem. [1, 2, 3]. Prevalence of total destruction of the clinical crown among patients can reach 17,7 % [4,5,6]. The combination of this pathology with a low clinical crown of teeth is difficult to treat [7]. Restoration of such teeth has a great preventive importance, becouse it allows to prevent the development of morphological changes in the dentition, as well as the overload of others teeth [8]. For restoration dentists usually use metal pinlays with coating them by the crowns [9]. But, using of this construction has drawbacks and complications, which are observed from 10 to 18.03% of cases [10].

The aim of the research is a description of the device for restoring the missing clinical crown of teeth and evaluate it's effectiveness in vivo and in vitro.

Materials and Methods.

During the in vivo study, we have treated 70 patients with the total destruction of a clinical crown of tooth. Patients have been aged 20-69 years (42 women and 28 men). 26 people from the research group had low clinical crowns of teeth. Informed consent from the participants was recorded. Institutional ethical clearance was obtained for the study.

For the treatment we used the device for restoring of the destroyed clinical crown of teeth, which was proposed by the authors. The device consists of a metal pinlay, covered by ceramics for the restoration of the shape and the size of the tooth (Fig.1).

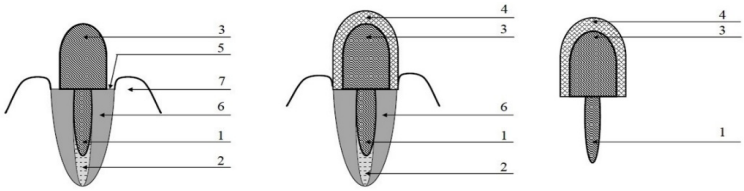

Figure 1. *Schematic image of the device for restoring the missing clinical crown of tooth: 1-pin; 2-filling material in the root canal of the tooth; 3-pinlay; 4-ceramic lining; 5-subgingival part of the root of the tooth; 6-root of the tooth; 7-gum*

These constructions were made for all patients with total destruction of the clinical crown of tooth.

For the objective assessment of the effectiveness of the treatment we used sighting X-ray, occlusiography, assessment of the quality of life of patients by the OHIP-14 RU index.

For sighting X-ray, we used radiovisiograph "X genus DS" at the 3' dental clinic in Samara (Russian Federation). The studies have been conducted before the start of prosthetic treatment and 1 year after the fixation of the crown. During the research, we reviewed the presence of inflammation, the condition of the periodontal gap, the quality of the filling of the root canal, the location of the pin in the root canal, and the adhesion of the insert with ceramics to the tooth tissues.

Computerized real-time occlusal analysis system Tekscan has been used to analyze and equilibrate forces. The research has been conducted before the start of prosthetic treatment and 1 mounth after the fixation of the crown.

The quality of life of patients was assessed using the OHIP-14 RU index, which contains 14 questions reflecting the impact of fixed prosthetics on the patient's daily life. The answers were scored on a five-point scoring system: 1 - never; 2 - almost never; 3 - rarely; 4 - usually; 5 - very often, after which the points were summed up and the number of points was assessed according to the index: 14-28 points - a good level of quality of life after prosthetic treatment, 28 - 56 points - satisfactory, 57-70 - an unsatisfactory level of quality of life. The studies were carried out 1 month after prosthetic treatment.

To analyze the fracture resistance of ceramic coating in vitro, we conducted a compression test on the devices. For this, we made cobalt-chromium samples to the average size of the tooth (premolars) after their preparation for metal-ceramic crowns. The first group of samples (the new device) was covered with ceramics by firing it directly on samples (1.5 mm thick), and the second group of samples (the traditional device) was covered by crowns with a ceramic thickness of 1.5 mm and a metal cap 0.4 mm (Fig. 2).

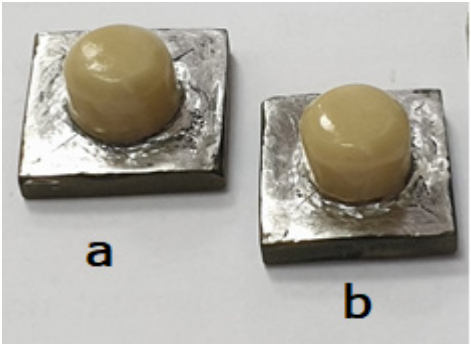

Figure 3. *Photo of finished samples with ceramic coating structures: a-sample of a new device; b-sample of a traditional device*

We made 20 samples (10 in each group). The samples were tested for compression in the vertical direction until the beginning of partial destruction of ceramics using. For that we used the apparatus "Instron 5988" (Fig. 3). The research was carried out on the basis of the Department of Mechanics in laboratory No. 12 of Samara State Technical University (Samara, Russian Federation).

Figure 3. *Test machine Instron 5988 before the experiment*

After the prosthetic treatment, we watched for the patients for 1 year. Statistical processing of the obtained digital data was carried out using the program IBM SPSS Statistiics 25 IMAGO 5.0 - license No. 5725 - A54.

Results

One year after the prosthetic treatment, we performed X-ray analysis. On the X-ray images we didn't find any chronic inflammation, bone tissue had clear fine-mesh pattern, bone trabeculae were evenly traced in all areas (Fig. 4).

Figure 4. *X-ray image of the tooth, one year after prosthetic treatment*

Occlusal equilibration guided by Tekscan brought about significant harmony in distribution of forces in preprosthetic phase. In preprosthetic phase, close to 60% of patients had no equilibrium in the distribution of occlusal force (Tab. 1). Among these patients, 90% showed greater occlusal load on intact half of the arch. Paired t-test conducted between the right–left balance of force after equilibration in the preprosthetic phase and 1 mounth after prosthetic treatment showed significant differences in 70% of patients. Out of these, in 43% of patients, the occlusal load was increased on half of the arch rehabilitated with FPD. In the remaining 54% of patients, it was unanticipated to find that the occlusal load was increased on the intact half of the arch, compared to the rehabilitated side.

The DT was significantly high when quadrant with missing tooth was on non-working side. After prosthetic treatment, DT in general was seen to increase. The amount of increase was significantly high when prosthesis was on nonworking side.

Table 1.

Mean relative force distribution on each quadrant (percentage) during four stages

Treatment phase	Quadrant	Percentage force ± SD		t	p
		Before equilibration	After equilibration		
Preprosthetic	Intact side	43,70±14,82	48,10±4,36	2,292	0,0032*
	Side of missing tooth	56,30±14,82	51,90±4,36	2,292	0,0032*
Postprosthetic	Intact side	47,65±16,58	50,40±5,23	0,964	0,347
	Side of missing tooth	52,35±16,58	49.60±5,23	0,964	0,347

p≤0,05 significant difference, SD: standard deviation

Assessment of the quality of life of patients in 1 month after prosthetic treatment with a new device showed the following results. 64 patients had a good level of quality of life, the average score was 23.0 ± 2.5. An unsatisfactory level of quality of life was identified in 2 patients, the score was 62,3± 1.7.

Laboratory studies showed the following results: in the first group of samples, the ceramics began to fracture at an average load of 10.86 ± 0.56 KN at a press displacement speed of 0.50 mm / min. Sample test diagram (Fig. 5).

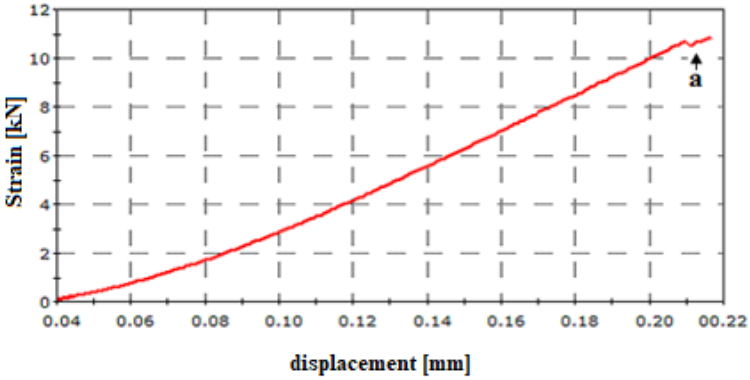

Figure 5. *Diagram of the research of the strength of a ceramic coating on a sample of a new device: a-the moment of destruction of the ceramic*

In the 2-nd group of samples covered with metal-ceramic crowns, the ceramic covering began to fracture under the pressure of the apparatus press at 4.96 ± 0.32 KN at a press displacement speed of 0.50 mm / min. Sample test diagram (Fig. 6).

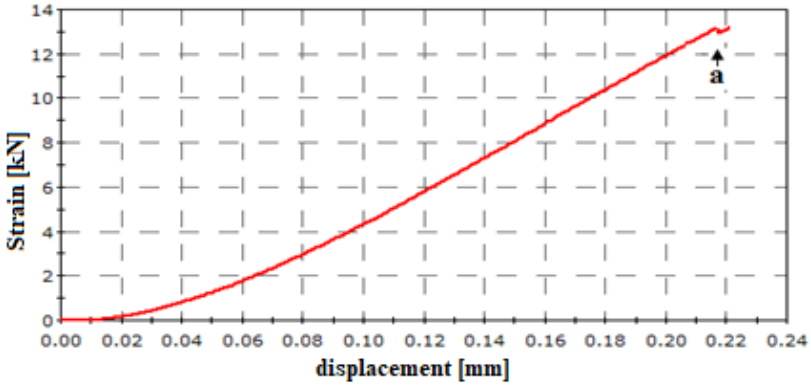

Figure 6. *Diagram of the research of the strength of a ceramic coating on a sample of a traditional device: a-the moment of destruction of the ceramic*

The tests of the samples showed that the safety of the ceramic coating on the samples of new device is 2.4 times higher than in the samples with the metal-ceramic crowns of the traditional device.

Conclusion

As a result of prosthetic treatment of 70 patients with total destruction of the clinical crown of tooth using the new device, we can conclude that the developed new design makes it possible to qualitatively and fully achieve the restoration of the clinical crown of tooth in a short time, while the strength of the ceramic coating of the new design is much higher. So, the novel way of restoring the missing clinical crown has shown a good result in clinical practice. In addition, it has a higher fracture resistance than traditional device.

References

1. Venatovskaya NV., Pudovkina EA., Suetenkov DE. Prosthetics of defects in hard tissues of teeth and dentition as prevention of dental anomalies in children: from necessity to possibility. Saratov scientific medical journal. 2011; 24(1):226-230.

2. Khaikin MB, Nesterov AM, Chigarina SE, Sadykov MI, Sagirov MR. Integral assessment of the quality of life in patients with chronic generalized periodontitis and medium periodontosis. Problems of Dentistry. 2020; - 16(4): 90-96.

3. Kojaev MF, Vorobyova MV, Nevzorov AYu. Effectiveness of the use of tabs for defects in hard dental tissues. Bulletin of medical Internet conferences. 2016; 6: 1091-1093.

4. Nesterov AM, Sadykov MI, Sagirov MR. Analysis of prosthetic treatment of patients with stump pinlays with artificial crowns according to archival materials of a large dental clinic. The scientific heritage. 2021. 76(1):17-20.

5. Kainose K, Nakajima M, Foxton R. Stress distribution in root filled teeth restored with various post and core techniques: effect of post length and crown height. International Endodontic Journal. 2015; 71(4):1023– 1032.

6. Abdulrazzak SS, Sulaiman E, Atiya BK, Jamaludin M. Effect of ferrule height and glass fibre post length on fracture resistance and failure mode of endodontically treated teeth. Australian Endodontic Journal. 2014; 17(4):P.81–86.

7. Kalay TS, Yildirim T, Ulker M. Effects of different cusp coverage restorations on the fracture resistance of endodontically treated maxillary premolars. J Prosthet Dent. 2016; 116(1):404–410.

8. Lazari PC, De Carvalho MA, Del Bel Cury A.A, Magne P. Survival of extensively damaged endodontically treated incisors restored with different types of posts-and-core foundation restoration material. Journal of Prosthetic Dentistry. 2018; 119(5): 769-776.

9. Shuman I. Excellence in class II direct composite restorations. Dent. Today. 2007; 26(4);102- 105.

10. Von Stein-Lausnitz M, Bruhnke M. Direct restoration of endodontically treated maxillary central incisors: post or no post at all? Clin. Oral Investig. 2018; 23(1): 381-389.

DOI 10.34660/INF.2022.39.79.183

矿工肺组织形态学变化作为尘肺病早期诊断的标志物
MORPHOLOGICAL CHANGES IN THE PULMONARY HISTIONE IN MINERS AS MARKERS OF EARLY DIAGNOSIS OF PNEUMOCONIOSIS

Bondarev Oleg Ivanovich
Candidate of Medical Sciences, Associate Professor
NSIFTPh-Branch Campus of the FSBEI FPE RMACPE MOH Russia
Novokuznetsk, Russia

抽象的。 对30名在尘土飞扬的条件下工作0.5-30年（16.4±2.0）的矿工进行了肺组织病理学研究，这些矿工根据定期体检结果被认为是健康的，并在人为灾难中死亡。 萎缩性支气管病、间质性肺组织、胸膜、支气管、动脉平滑肌细胞肥大和血管周围硬化的显着硬化变化的发展证明，作为一个疾病学单位，在检查的患者中存在尘肺病（炭疽病），没有症状 与形态系统性变化。 研究结果表明，需要改进评估工人健康状况的方法，以及呼吸器官粉尘病理学的疾病诊断标准。

关键词：矿工，职业病理学，尘肺病，肺动脉高压，全身性疾病。

Abstract. *Pathomorphological studies of the lung tissue of 30 miners who worked in dusty conditions from 0.5 to 30 years (16.4±2.0), who were considered healthy according to the results of periodic medical examinations and died in a man-made disaster, were carried out. The development in each case of atrophic bronchopathy, pronounced sclerotic changes in interstitial lung tissue, pleura, bronchi, arterial smooth muscle cell hypertrophy and perivascular sclerosis testified to the existence of pneumoconiosis (anthracosis) in the examined patients as a nosological unit that proceeded without symptoms with morphological systemic changes. The results of the study indicate the need to improve methods for assessing the health status of workers, as well as criteria for nosological diagnosis of dust pathology of the respiratory organs.*

Keywords: *miners, occupational pathology, pneumoconiosis, pulmonary hypertension, systemic disease.*

Relevance of the problem

Coal mining for today's period of development of any technological process is the most complex and time-consuming professional process. One of the main risk factors in the work of coal industry workers is damage to organs and tissues

in miners. The literature contains a lot of scientific data on functional and morphological disorders of numerous organs and systems in coal industry workers. However, almost all of them are devoted to clinical changes in the stage of organ damage. There are practically no pathomorphological works related to early preclinical changes [1–2].

Occupational diseases caused by exposure to the dust factor in mining enterprises have been known for a long time. In Russian literature, indications of lung diseases from inhalation of dust in miners are found in the works of M.V. Lomonosov "The first foundations of metallurgy or ore affairs" (1763).

At the enterprises of the mining industry, due to the specific features of the technology of underground and open pit mining, workers are simultaneously affected by a variety of adverse factors in the production environment (dust, noise, vibration, unfavorable microclimate, etc.). The depth and severity of pathological changes largely depend on the climatic, geographical and mining conditions at enterprises located in Russia.

Until recently, it was believed that pulmonary fibrosis could only develop as a result of exposure to dust containing free silicon dioxide (SiO2). However, at the present stage it has been proven that pneumoconiosis can also develop under the influence of dust containing silicon dioxide not in a free state, but also in a state associated with other elements (asbestos, talc, olevin, nepheline and other silicates), as well as under the influence of dust, completely free of silicon dioxide, such as pure coal dust. Taking into account the ability of these dusts to cause occupational diseases of "dust etiology" – pneumoconiosis and dust bronchitis – the name "aerosols of a predominantly fibrogenic type of action" was assigned to them [3].

Previous scientific ideas about bronchopulmonary pathology with increased dust load are outdated views on pneumoconiosis (PC) as an isolated pathology, mainly of the lungs, the bronchi and vessels of the pulmonary circulation (PCL) remain outside the pathology. Clinically, this is manifested by extremely late radiologically detected changes in PC in the late work periods of work in mines [4].

Purpose of the work

Determination of morphological criteria for PC lesions of the pulmonary histion, which are evidence of an early pre-radiological stage of PC development.

Material, methods and object of study

The material of the study is lung sections obtained during 30 forensic medical examinations of a group of miners (X) who died while working in a mine during a man-made disaster. All the dead underwent medical examinations according to the regulations of Order № 90 of March 14, 1996 [5] and were found fit for work.

The age of the dead was in the range of 23-64 (39.3±2.1) years, the duration of the harmful experience was 0.5-30 (16.4±2.0) years. None of the dead was registered at the dispensary for occupational lung pathology.

The professions of the dead belonged to the main professions of the coal mining industry: a sinker, a stope miner, an underground miner, an underground electrician, a mining machine operator, and a site foreman. According to the sanitary and hygienic characteristics of the workplaces of miners examined at the CPP, at the workplaces of the listed and other main professions of the coal mining industry at all mines of Kuzbass, the level of dust content with coal-rock dust exceeds the maximum allowable concentration from several to several tens of times, that is, it belonged to the third class hazard 1-4 degree (class 3.1-3.4 according to the "Guidelines for the hygienic assessment of factors of the working environment and the labor process. Criteria and classification of working conditions. Guidelines R.2.2.2006-05."- Moscow, 2006. - 205 p.). The control group (CG) was formed from 20 cases of forensic medical examinations of young men in Novokuznetsk who died in a road accident, were under the age of 25 years and did not have any organ pathology according to the results of an autopsy study.

Object of study: morphometric and histological characteristics of the lung histion, as well as intertissue correlations of these structures. Preparation of tissue samples for histological examination was standard.

Morphometric measurements of the linear dimensions of structures and areas were carried out on a Nikon Eclipse E 200 microscope with a Nikon digital sight-Fi 1 (Japan) digital video camera using a computer program from West Medica HandelsgmbH - Bio Vision 4.0. Statistical processing of the results was carried out using the Student's t-test for paired measurements; comparison of the distribution of the frequency of cases in groups of observations – by the value of χ^2. To identify the relationship between the indicators, a correlation analysis was performed.

Research results:

The studies included bronchi of all calibers: with an outer diameter of up to 500 μ (terminal bronchioles), from 500 to 1500 μ (intralobular bronchi), from 1500 to 3500 μ (lobular bronchi), from 3500 to 5000μ (lobular and partially already subsegmental bronchi) and over 5000μ (subsegmental and segmental bronchi). The number of cases of the examined bronchi (n) depending on their outer diameters indicated above was 10-41-12-18-53 in CG and 5-10-30-17-23 in MG. The difference in incidence rates in bronchial caliber between CG and MG was statistically significant ($\chi2$=30,67; d.f. = 4; p<0,001) due to the greater proportion of smaller caliber bronchi in MG. However, as will be seen from the results of the study, this difference was not of fundamental importance. In total, 85 bronchi samples (mean diameter – 4263±323 μ) were examined in CG and 134 bronchi samples (mean diameter – 3712±234 μ).

The following were measured in the bronchi: inner diameter (Dinnb); epithelial layer thickness (Tel); basal membrane thickness (Tbm); own plate thickness (Top); thickness of the layer of smooth muscle cells (Tlsmc); thickness of bronchi-

al glands (Tbg); wall thickness (Tw); thickness of peribronchial sclerosis (Tpbs); area of the inner lumen of the bronchi (Sinlb); area of the epithelial layer (Setl); length of the bronchus wall, on which Setl is measured (Sbw) was based; area of bronchial glands (Sbg); area of the layer of smooth muscle cells (Slsmc); bronchial wall area (Sbw). Calculation was determined: the outer diameter of the bronchi (Dob) according to the formula: Dob = Dinnb + 2×Tw; the degree of provision of the epithelial layer with bronchial glands (Setl/Sbg) according to the formula: Setl/Sbg = Setl: Sbg; relative density of the epithelial layer of the bronchial wall, that is, the area of the mucosa per 1 mm of the length of the bronchial wall directly under the epithelial layer (Setl/Lbw), according to the formula: Setl/Lbw\u003d Setl×1000: Lbw (as an indicator of the degree of folding of the bronchial mucosa) ; the relative thickness of the bronchus wall, the so-called Kernogan index (IKb), according to the formula: IKb \u003d (2×Tw):Dob. The Kernogan index assessed the change in the thickness of the bronchial wall, not associated with a change in its caliber, and formed a certain idea of the degree of bronchial obstruction.

Quantitative indicators are given in Table 1. The average values of the area of the epithelial layer per 1 mm of the length of the bronchial wall were expressed as numbers in CG - 108479±6753 μ^2, and in MG - 25507±1299 μ^2. The calculated data indicated a statistically significant relative predominance of the area of the bronchial glands over the area of the epithelium for the bronchi in MG due to a decrease in the severity of the epithelial layer and an increase in the size of the bronchial glands. Peribronchial sclerosis was a phenomenon found only in MG.

Table 1.

Number of measurements and values of indicators of bronchial wall structures in CG and MG

Bronchial structures	Number of measurements and values of structure indicators (μ) in:				t (p)
	CG		MG		
	n	M±m	n	M±m	
Tel	841	49.11±0.67	1382	34.05±0.81	14.36 (<0.001)
Tbm	687	9.19±0.14	856	23.58±0.45	13.11 (<0.001)
Top	699	45.73±1.01	769	107.7±2.07	26.85 (<0.001)
Tbg	570	145.8±5.06	647	235.2±7.22	10.14 (<0.001)
Sbg	570	0.129±0.01	647	0.412±0.021	13.38 (<0.001)
Tlsmc	820	42.41±0.92	1377	86.57±2.22	18.40 (<0.001)
Tw	850	151.7±0.92	1405	193.4±2.22	8.05 (<0.001)
IKb (%)	850	7.12±054	1405	10.42±0.36	5.08 (<0.001)
Tpbs			577	51.48±1.27	

Conclusion: according to bronchial morphometry, it follows that in miners, the main changes in the bronchi are atrophy of the mucosa; development of bronchial sclerosis; thickening of the basement membrane and the lamina propria of the bronchial wall; hypertrophy of the bronchial glands; hypertrophy of smooth muscle cells. The nature of the changes corresponded to the concept of primary atrophic bronchopathy. Intertissue correlations were revealed for smooth muscle tissue and mesenchymal structure acting as a stroma capable of collagen synthesis and providing stromal-parenchymal interactions.

In the respiratory tissue, the number and size of macrophages (MF) and coniophages (CP), thickness of interalveolar septa (IAS), areas of MF and CP, dust zoning, dust granuloma size, and pleural thickness (Tplv) were determined. Respiratory structures in MG contained coal dust accumulations visible in any histological specimen at 20x magnification or more. In CG, accumulations of coal dust were completely absent. Based on this, the fact of dustiness of the lung tissue was significant.

The ranges of areas of accumulations of dust particles lay between 188145-491099 μ^2, averaging 158200 μ^2, which, when determining their diameter as spherical formations, corresponded to an average of 0.3-0.4 mm. The sizes of dust particles were beyond the resolution of radiography, as well as the methods of radiation diagnostics.

There were CPs in the alveolar lumens, their enlarged size and loading with dust particles indicated coniotic inflammation. Areas MF fluctuated in CG from 120.4 μ^2 to 324.4 μ^2, averaging 171, μ^2, in MG from 174.9 to 552.1 μ^2, averaging 374.6 μ^2.

IAS in MG were significantly thickened: 20.12±0.24 μ vs. 8.73±0.19 μ in CG ($p<0.001$). Thickening of the IAS was total and was significantly realized through collagenization caused by PC. With specific stains for connective tissue in the accumulations of coal dust, layers of connective tissue were determined, as well as histioid elements, which made it possible to interpret these accumulations of dust as PC granulomas. The proliferation of cellular elements indicated the dynamics of PC formations. Based on the above, we can talk about pathomorphological evidence of MS progression due to an increase in the prevalence of nodular formations, which are little available by conventional research methods during PMO.

In all examined sections of the MG lungs, there was widespread sclerosis, which involved the IAS, peribronchial and perivascular tissue, and the pleura. Sclerosis was characterized by a powerful development of collagen fibers of various thicknesses and orientations, between which were visible in a small amount of histiocytic and lymphoid cells, single plasma cells and dust accumulation. Morphological evidence of damage not only to the lungs, but also to the diffuse development of anthracosilicosis, was a thickening of the pleura with massive ac-

cumulations of dust in it. The dust was arranged linearly along the entire length of the tissue section. The thickness of the pleura in MG was 140.51±5.36 μm versus 33.74±1.98 μm in CG ($p<0.01$).

Conclusion: in the respiratory tissue of the miners, diffuse dusting of the lungs with coal-rock dust, a massive macrophage reaction, the formation of granulomas, pulmonary fibrosis, thickening of the IAS with collagenization were observed; development of zones of interstitial fibrosis.

In the study of the hamodynamic constant, arterioles and precapillaries were included - ≤100 μ, small arteries of the muscular type >100-≤1000 μ and arteries of medium caliber belonging to vessels of the elastic type - >1000 μ. The number of examined arteries (n) depending on their outer diameters indicated above was 5-42-3 in CG and 8-139-8 in MG. In total, arteries were examined in CG 50 samples (391.1±47.1 μ) and in MG -155 samples (418.4±23.4 μ). Elements of the pulmonary arteries were studied similarly to bronchial structures. They determined: the inner diameter of the artery (Dinna), the thickness of the arterial endothelium (Tena), the thickness of the layer of smooth muscle cells of the artery (Tsmcl), the thickness of periarterial sclerosis (Tps), the area of the internal lumen of the artery (Sinla). Calculation was determined: arterial wall thickness (Taw) according to the formula: Taw= Tena+Tsmcl; outer diameter of the artery (Douta) according to the formula: Douta = Dinna+2×Taw; relative wall thickness of the artery, the so-called Kernogan index (IKa), according to the formula: IKa = (2×Taw): Douta.

Quantitative indicators of the listed morphological structures of the arteries were determined in the arteries of each caliber, but the size of the article allows only average data to be given (table 2).

Table 2.

Number of measurements and values of indices of arterial wall structures in CG and MG

Artery structures	Frequency of measurements and values of arterial structures (μ) in:				t (p)
	CG		MG		
	n	M±m	n	M±m	
Tena	665	2.74±0.04	1272	3.91±0.08	12.95 (<0.001)
Tsmcl	694	13.69±0.49	1301	42.10±0.61	36.56 (<0.001)
Taw	898	15.62±0.41	1938	39.45±0.57	34.06 (<0.001)
IKa (%)	898	9.52±0.14	1938	21.60±0.27	39.11 (<0.001)
Tps			1740	54.03±1.28	

The data obtained indicated a significant thickening of the endothelial layer in MG. It was not accompanied by inflammation and is a consequence of coniotic endotheliosis. Thickening of the muscle layer in the arteries of all calibers associated with SMC hypertrophy. SMC hypertrophy in the group of miners led to 1.5-3-fold thickening of the vascular wall in the arteries of each caliber.

Thickening of the endothelial, smooth muscle layers and the vascular wall as a whole in the MG, reducing the lumen of the vessel, created the preconditions for an increase in vascular resistance. Perivascular sclerosis was a phenomenon found only in miners. Periarterial sclerosis was diffuse and did not contain signs of inflammation. To identify the patterns of intertissue interactions, a correlation analysis of the sizes of the morphological structures of arteries was used, since from the above tables they found a direct proportional relationship with their caliber. The factor determining the size of the arterial lumen in CG was the thickness of the endothelium ($r = 0.38$), while in MG it was the thickness of the SMC layer ($r = 0.22$). SMC hypertrophy of the arteries was interpreted not from the standpoint of "compensation", because there was nothing to compensate, but as a reaction to coniotic inflammation triggered by circulating pro- and anti-inflammatory mediators.

Conclusions:

1. The presence of macrophage inflammation, granulomas, fibrosis, and pleural lesions in the lungs clearly indicated the formation of anthracosilicosis in miners who were considered healthy according to the results of PMT.

2. Atrophic bronchopathy in miners without signs of inflammation serves as reliable morphological criteria for the PC process.

3. Endothelial changes, as well as hypertrophy of arterial smooth muscle cells in the lungs, are among the initial manifestations of the PC process leading to vascular resistance with further development of pulmonary hypertension.

4. Peribronchial sclerosis is a manifestation of the PC process.

5. Hemodynamic and/or histological evidence of PCL vascular involvement in association with atrophic bronchopathy may be considered diagnostic criteria for early PCL.

References

1. Karenov R.S. Priorities of the strategy of industrial and innovative development of the mining industry in Kazakhstan. — Astana: KazUEFMT Publishing House, 2010. — 539 P.

2. Plakitkina L.S. Intensification of the innovation process in the Russian coal industry // Mining industry. — 2011. — № 3(97). — P. 4–11.

3. Chebotarev A.G. Dust factor and pathology of the respiratory organs of employees of mining enterprises // Journal "Mining Industry" №3 2012, P. 24

4. Classification of pneumoconiosis. Guidelines № 95/235. – M., 1996. – 28 P.

5. Order № 90 of March 14, 1996. On the procedure for conducting preliminary and periodic medical examinations of workers and medical regulations for admission to the profession. – Moscow, 1996. – 122 P.

DOI 10.34660/INF.2022.71.21.184

贝加尔湖西南部土壤和植物中的天然铀和钍
NATURAL URANIUM AND THORIUM IN THE SOILS AND PLANTS OF SOUTH-WESTERN BAIKAL REGION

Shvetsov Sergey Georgievich
Candidate of Biological Sciences
Voronin Viktor Ivanovich
Doctor of Biological Sciences
Siberian Institute of Plant Physiology and Biochemistry of the Siberian Branch of the Russian Academy of Sciences

抽象的。 测定了贝加尔湖西南部森林生态系统土壤和木材中铀和钍的含量。与沉积岩（分别为 1.1 和 2.2 mg/kg）相比，与岩浆岩成因相关的土壤含有更多的铀（5.2 mg/kg）和钍（15.0 mg/kg）。 松灰中这些元素的含量在风化岩浆岩产物上形成的植物群落中也较高——0.21mg/kg（铀）和0.43mg/kg（钍）。 在沉积岩上，这些数字明显较低——分别为 0.082 和 0.141 mg/kg。 相对于钍，植物和土壤样品中的铀含量始终高于成土岩石中的含量，这表明与钍相比，所研究的生态系统中铀的生物地球化学活性更高。

关键词：土壤中铀和钍含量，木材，森林生态系统，贝加尔湖地区

Abstract. *The content of uranium and thorium in the soils and wood of the forest ecosystems of the south-western Baikal region was determined. Soils genetically associated with magmatic rocks contained more uranium (5.2 mg/kg) and thorium (15.0 mg/kg) compared to sedimentary rocks (1.1 and 2.2 mg/kg, respectively). The content of these elements in pine ash was also higher in phytocenosis formed on the products of weathering magmatic rocks - 0.21mg/kg (uranium) and 0.43 mg/kg (thorium). On sedimentary rocks, these figures were significantly lower - 0.082 and 0.141 mg/kg, respectively. The amount of uranium, relative to thorium, in plant and soil samples has always been higher than in soil-forming rock, which indicates a higher biogeochemical activity of uranium in the ecosystems studied, compared to thorium.*

Keywords: *uranium and thorium content in soil, wood, forest ecosystems, Baikal region*

The ecological importance and industrial use of heavy natural radionuclides supports interest in the study of uranium and thorium as part of various biogeo-

systems of Baikal region (Pribaikalye). Information on the content of uranium and thorium in the environment of the region is contained in a number of publications [4, 5, 6, 8, 9, 13]. Some articles looked at patterns of distribution of these elements between soil and plants in natural ecosystems [10, 12].

The objects of this study were the forest ecosystems located in a meridional direction 20-50 km south of the city of Irkutsk. There are a marked changes in geological, geomorphological and soil conditions at this distance. The study area is a foothill of The Eastern Sayan with hilly-wavy (gently rugged) relief (rounded and flat tops, shallow hollows). Near Irkutsk there are Jurassic sedimentary rocks, which are then replaced by Cambrian sedimentary rocks, followed by intrusive and metamorphic rocks of proterozoic and archaic age. The change of rocks is accompanied by an overall increase in the altitude of the territory from about 500 m to 1000. The increase in height causes, in turn, a decrease in the average annual temperature and the associated increase in humidity [1].

Soil cover and vegetation naturally change due to these geographical factors. Thus, with the increase in the distance from Irkutsk in pine forests increases the share of larch, fir and cedar. Gray forest soils are consistently replaced by sod-podzolic soils, sod carbonate soils, forest sod soils, podzolic soils and burozems [11]. The main purpose of this work was to study the specifics of uranium and thorium distribution between plants and soils of forest ecosystems in the area. The study identified soil types, measured uranium and thorium content in soil and in pine wood, and analyzed the data.

Gross uranium and thorium content were measured in soil samples (average sample by layers of A-B and separately - in shallow-earth layer C). The moving form of elements in the soil was estimated by their content in 1 M HCl extract from the soil. Plant samples were presented by pine wood, taken from trunks at an altitude of 1.2 m. Soil and wood samples were incandescent in a muffel oven at 550 C, then dissolved in nitric acid. The resulting solution was extracted by tributylphosphate, the extract was divided into fractions with the help of ion exchange resin, then determined the mass of uranium and thorium by their radioactivity. All experiments and measurements were carried out 3-4 times. The data are presented in tables 1 and 2 as averages; table 3 shows the results of calculating the ratio of some indicators to each other. The relative confidence interval was 17-20% at 95.5% probability level.

The classification of Russia soils (2004) was used to determine the type of soils [3, 7]. The following soils were identified in the study area: a burozem typical (BT), a burozem typical medium carbonate (BC), a podzolic noncarbonate (PN), a turf-podbur illuvalic-iron (PI), a sod-podzolic typical (SP) and a turf-eluvozem glay (EG). These soils were formed on products of weathering proterozoic granitoids (PN, PI, EG), cambrian dolomitic limestones (PC), jurassic sandstones (BT and SP).

Content of uranium and thorium in soils was different and depended on the type of soil. The amount of these elements in plants (pine wood) was similar to their content in soil on which these plants grew (table 1 and 2)., and SP

Gross uranium content in the soil decreased in the range of PN>PI>EG>BT>SP>BC, varying from 5.2 mg/kg in PN to 1.1 mg/kg in PC (table 1). The soil amount of uranium depended on its content in the soil-forming rock, which varied from 4.7 mg/l in PN to 1.3 mg/kg in BC. It can be seen that this dependence was not strictly linear, probably due to differences in the features of migration and accumulation of uranium in different types of soils.

Table 1.

Uranium content in samples of soil, soil-forming rock and ash of pine wood, mg/kg

Indicator	Podzolic noncarbonate	Turf-podburilluvalic-iron	Turf-eluvozem glay	Sod-podzolic typical	Burozem typical carbonate	Burozem typical
	PN	PI	EG	SP	BC	BT
Gross uranium in the soil	5,23	5,14	3,84	1,94	1,13	1,97
Moving uranium in the soil*	0,135	0,156	0,102	0,072	0,068	0,082
Gross uranium in soil-forming rock	4,70	3,30	3,80	1,82	1,31	1,13
Moving uranium in soil-forming rock*	0,136	0,111	0,115	0,068	0,058	0,055
Uranium in the ash of trees	0,126	0,210	0,120	0,124	0,082	0,124
Coefficient of gross uranium absorption	0,024	0,041	0,031	0,064	0,073	0,063
Coefficient of moving uranium absorption	0,93	1,35	1,07	1,72	0,68	1,51

Note: * – HCl (1 M) extract from the soil (1:10).

The content of movable uranium (soluble at 0.1 M HCl) in the soil was much less than its gross amount, varying from 0.156 mg/kg in PI to 0.068 mg/kg in SP (table 1). Direct proportionality between gross and mobile forms of uranium was also not observed. For example, the content of gross uranium exceeded its content in mobile form in PI by 38.7 times, and in SP - only 16.9 times (table 3).

The highest quantity of uranium (0.210 mg/kg of ash) in pine trunks was associated with PI, and the lowest (0.082 mg/kg of ash) - with BC, according the change of uranium content in the soil and soil-forming rock (table 1).

The absorption rate of gross uranium (the ratio of uranium concentration in plant ash to its gross concentration in the soil - $K_{GU} = U_P/U_G$) was highest (0.073) on BC, and the lowest (0.024) - on PN (table. 1). However, in order to assess the absorption of uranium by plants, it is preferable to use its mobile form in calculations, considering it as a direct source. In this way of calculating, the uranium absorption rate (K_{MU}) ranges from 0.93 per PN to 1.72 per SP. (table 1).

You can see that the maximum K_{GU} was more than the minimum 3 times, and in the case of K_{MU} - less than 2 times. These data show the unequal availability of uranium for plants on different soil types.

Table 2.

Thorium content in soil, soil-forming and pine wood samples, mg/kg.

Indicator	Podzolic noncarbonate	Turf-podbur illuvalic-iron	Turf-eluvozem glay	Sod-podzolic typical	Burozem typical carbonate	Burozem typical
	PN	PI	EG	SP	BC	BT
Gross thorium the soil	14,98	14,64	10,68	4,69	2,20	4,95
Moving thorium in the soil*	0,207	0,334	0,213	0,117	0,085	0,097
Gross thorium in soil-forming rock	17,3	11,8	9,80	4,09	1,48	3,03
Moving thorium in soil-forming rock*	0,260	0,230	0,220	0,082	0,091	0,107
Thorium in the ash of trees	0,261	0,425	0,255	0,245	0,131	0,222
Coefficient of gross thorium absorption	0,0174	0,0290	0,0238	0,0522	0,0594	0,0701
Coefficient of moving thorium absorption	1,26	1,27	1,20	2,82	1,65	3,81

Note: * – HCl (1 M) extract from the soil (1:10).

Gross thorium content in the soil was not the same in different types of soils, it varied from 15.0 mg/kg in SP to 2.2 mg/kg in BC (table 2). As well as the content of uranium, the content of thorium decreased in the number of PN>PI>EG>BT>SP>BC. This dependence was determined, in general, by the

content of this element in the soil-forming rock - from 17.3 mg/kg in PN (products of weathering proterozoic granitoids), to 1.48 mg/kg in BC, (products of weathering dolomitized limestone).

The content of mobile thorium (soluble at 0.1 M HCl) varied similarly to the change of gross uranium from 0.334 mg/kg in PI to 0.085 mg/kg in SP (table 2). At the same time, the quantity of mobile thorium was 72.8 times less than the gross amount in PN, and only 27.5 times less in BC. The same relations for soil-forming rocks were 66.5 in PN and 16.3 in BC (table 3). It is likely that these differences are due to the cumulative effects of soil formation factors.

Table 3.

Some indicators of the relative distribution (relation of concentrations) of uranium and thorium in the soil

The relate of	Podzolic noncarbonate	Turf-podburilluvalic-iron	Turf-eluvo-zem glay	Sod-podzolic typical	Burozem typical carbonate	Burozem typical
	PN	PI	EG	SP	BC	BT
gross uranium to movable uranium in the soil	38,74	32,95	34,29	26,94	16,93	24,02
gross uranium to movable uranium in soil-forming rock	34,56	29,73	33,04	26,76	22,59	20,55
gross thorium to movable thorium in the soil	72,37	43,83	54,93	53,91	27,85	54,40
gross thorium to movable thorium in the soil-forming rock	66,54	51,30	44,55	49,88	16,26	28,32
gross thorium to movable thorium in the soil-forming rock	2,86	2,85	3,05	2,42	1,48	2,51
gross thorium to gross uranium in the soil-forming rock	3,68	3,58	2,58	2,25	1,13	2,68
thorium to uranium in plant ash	2,07	2,02	2,13	1,98	1,59	2,80
movable thorium in the soil to the movable uranium in the soil	1,53	2,14	2,09	1,21	1,31	1,11

The thorium content in pine wood was highest on PI (0.425 mg/kg of ash) and the smallest (0.131 mg/kg ash) on SP, reflecting a direct dependence on thorium content in the soil and soil-forming rock (table 2). Table 2 also shows that the ratio of thorium concentration in ash plants to its gross content in the soil (the coefficient absorption of gross thorium K_{GTh}) was highest (0.0701) on BT, and the lowest (0.0174) on the SP. The coefficient absorption of mobile thorium (K_{MTh}) was the highest (2.1) on the SP, and the lowest (1.2) on EG. You can see that the maximum K_{GTh} was more than the minimum 4 times, and in the case of K_{MTh} - less than 2 times. As with uranium, these data show different accessibility of thorium for plants on different soil types. It should be noted that comparing the results of these methods of calculating uranium and thorium absorption rates does not show the particular advantages of one method over another, but only increases the number of possible interpretations.

In tables 1 and 2, you can see that the highest value of uranium in the soil exceeded the lowest value of 4.6 times, and the soil-forming rock - 4.2 times; for the thorium these relations were 4.6 and 11.7, respectively. These data show significant differences in the migration of uranium and thorium accumulation, both at the soil level and at the soil type level.

A convenient indicator of the specific state of uranium and thorium in the ecosystem is the ratio of uranium and thorium concentrations (thorium-uranium ratio – Th/U) in the interacting components of these system (see table 3). Th/U in the soil layer varied from 3.5 (EG) to 1.5 (BC), with an average value of 2.5, and in soil-forming rock - from 3.7 (PN) to 1.1 (BC), with an average value of 2.7, which reflects a slight enrichment of soils in the area uranium relative to thorium. The average Th/U in acid extraction from the soil was noticeably lower (1.6), which is comparable to the same rate in plant ash (1.9). This can serve as an indirect confirmation that acid extract from soil adequately represents a pool of available for plants forms of uranium and thorium.

Thus, the soils and plants in the study area differed significantly in the content of uranium and thorium, which, most of all, was determined by the content of these elements in soil-forming rocks. Soils formed on magmatic rocks and plants that grew on them contained more uranium and thorium compared to sedimentary rocks. The soils studied also differed in the content of forms of uranium and thorium available to plants, which influenced the accumulation of these elements by plants. Thorium-uranium ratio of concentrations in soil and plants showed the relative enrichment of these objects with uranium, compared to thorium.

References

1. Атлас. Иркутская область: экологические условия развития. М. – Иркутск, 2004 – 90 с. [Atlas. Irkutsk region: environmental conditions of development. M. – Irkutsk, 2004 – 90 p., (in Russian)].

2. Белов А.В. Карта растительности юга Восточной Сибири. Принципы и методы составления // Геоботаническое картографирование. – Л., 1973. – С. 16–30. [Belov A.V. Map of vegetation of the south of Eastern Siberia. Principles and methods of compilation // Geobotanical mapping. – Leningrad, 1973. pp. 16–30, (in Russian)].

3. Воробьева Г.А., Куклина С.Л. и др. Почвоведение: типология почв и их диагностика: учебно- методическое пособие. Иркутск: Издательство ИГУ, 2017. – 237 с. [Vorobyova G.A., Kuklina S.L. et al. Soil science: soil typology and their diagnostics: educational and methodical manual. Irkutsk: Publishing House of ISU, 2017. – 237 p., (in Russian)].

4. Гребенщикова В.И., Китаев Н.А., Лустенберг Э.Е., Медведев А.И., Ломоносов И.С., Карчевский А.Н. Распределение радиоактивных элементов в окружающей среде Прибайкалья (Сообщение 1. Уран) // Сибирский экологический журнал, 2009. .№ 1. С. 17-28. [Grebenshchikova V.I., Kitaev N.A., Lustenberg E.E., Medvedev A.I., Lomonosov I.S., Karchevsky A.N. Distribution of radioactive elements in the environment of the Baikal region (Message 1. Uranus) // Siberian Ecological Journal, 2009. .№ 1. pp. 17-28, (in Russian)].

5. Гребенщикова В.И., Китаев Н.А., Лустенберг Э.Е., Медведев А.И., Ломоносов И.С., Карчевский А.Н. Распределение радиоактивных элементов в окружающей среде Прибайкалья (Сообщение 2. Торий и цезий-137) // Сибирский экологический журнал, 2010. № 3. С. 493-503. [Grebenshchikova V.I., Kitaev N.A., Lustenberg E.E., Medvedev A.I., Lomonosov I.S., Karchevsky A.N. Distribution of radioactive elements in the environment of the Baikal region (Message 2. Thorium and cesium-137) // Siberian Ecological Journal, 2010. № 3. pp. 493-503, (in Russian)].

6. Гребенщикова В.И., Грицко П.П., Кузнецов П. В., Дорошков А. А. Уран и торий в почвенном покрове Иркутско-Ангарской промышленной зоны (Прибайкалье) // Известия Томского политехнического университета. Инжиниринг георесурсов. 2017. Т. 328. № 7. С. 93–104. [Grebenshchikova V.I., Gritsko P.P., Kuznetsov P. V., Doroshkov A. A. Uranium and thorium in the soil cover of the Irkutsk-Angarsk industrial zone (Pribaikalye) // News of Tomsk polytechnical university. Georesources engineering. 2017. T. 328. № 7. pp. 93–104, (in Russian)].

7. Классификация и диагностика почв России / Авторы и составители Л.Л. Шишов, В.Д. Тонконогов, И.И. Лебедева, М.И Герасимова – Смоленск: Ойкумена, 2004.- 324 с. [Classification and diagnostics of russian soils / Authors and compilers L.L. Shishov, V.D. Tonkonogov, I.I. Lebedeva, M.I. Gerasimova – Smolensk: Oikumena, 2004.- 324 p., (in Russian)].

8. Кузнецов П.В., Гребенщикова В.И. Распределение урана и тория в некоторых почвах Иркутской области // Материалы III международной конференции "Радиоактивность и радиоактивные элементы в среде обитания человека", Томск, 23 – 27 июня 2009 г. – С. 302– 306. [Kuznetsov P.V., Grebenshchikova V.I. Distribution of uranium and thorium in some soils of the Irkutsk region // Materials of the III International Conference "Radioactivity and Radioactive Elements in the Human Environment", Tomsk, June 23 – 27, 2009 – pp. 302 – 306, (in Russian)].

9. Кузнецов П.В., Айсуева Т.С. Уран и торий в почвах р. Куды (Иркутская область) // Материалы V Международной конференции, г. Томск, 13–16 сентября 2016 г. [Kuznetsov P.V., Aisueva T.S. Uranium and thorium in the soils of the Kuda river (Irkutsk region) // Materials of the V International Conference, Tomsk, September 13–16, 2016, pp. 250-254, (in Russian)].

10.Швецов С.Г., Воронин В.И. Распределение урана и тория в почве и растениях Восточной Сибири (Иркутская область) // Журнал СФУ. Серия Биология 2019, Изд-во СФУ (Красноярск), Т. 12 № 1, С. 86-100. [Shvetsov S.G., Voronin V.I. Distribution of uranium and thorium in the soil and plants of Eastern Siberia (Irkutsk region) // Journal of SibFU. Series Biology 2019, Publishing House of SibFU (Krasnoyarsk), Vol. 12 No 1, pp. 86-100, (in Russian)].

11.Швецов С. Г., Мартынова Н. А. Типология почв лесных экосистем юго-запад Прибайкалья // Фундаментальные основы развития науки и образования / Под общ. редакцией Г. Ю. Гуляева. – Пенза, 2018. – С. 216–226. [Shvetsov S. G., Martynova N. A. Soil typology of forest ecosystems on south-west of the Baikal region // Fundamentals for development of science and education / Penza, 2018. – pp. 216–226, (in Russian)].

12.Швецов С. Г., Воронин В. И. Содержание урана и тория в почвах и растениях лесных экосистем Олхинского плато // Фундаментальные и прикладные научные исследования, актуальные вопросы, достижения и инновации: Сборник статей XIII Международной научно-практической конференции (в 2-х частях, Ч. 1) (Пенза, 15 ноября 2018 г.). – Пенза : МЦНС «Наука и Просвещение», 2018. – С. 296–301. [Shvetsov S. G., Voronin V. I. Content of uranium and thorium in soils and plants of forest ecosystems on Olkha plateau // Fundamental and applied scientific research, actual issues, achievements and innovations: Collection of articles of the XIII International Scientific and Practical Conference (in 2 parts, Part 1) (Penza, November 15, 2018). – Penza : ICNS « Science and Education», 2018. – pp. 296–301, (in Russian)].

13.Швецов С.Г. Почвы Олхинского плато (Иркутская область) и содержание в них природных урана и тория //«Евразийское Научное Объединение», № 5 (51), Май, 2019, С. 580-583. [Shvetsov S.G. Content of natural uranium and thorium in soils of the Olkha Plateau (Irkutsk Region) //«Eurasian Scientific Association», No 5 (51), May, 2019, pp. 580-583, (in Russian)].

DOI 10.34660/INF.2022.87.65.185

Emar 湾地衣
LICHENOINDICATION OF EMAR BAY

Agibalova Anna Alekseevna
Senior Lecturer
Zenkina Victoria Gennadievna
Candidate of Medical Sciences, Associate Professor, Head of the Department
Ustimenko Oksana Anatolyevna
Candidate of Medical Sciences, Associate Professor
Pacific State Medical University

抽象的。 远东地衣植物区系的特点是多样性增加，这在很大程度上与该地区的生物气候特征有关。 地衣指示是评估地区大气污染状况的一种相当有效的方法。 研究了位于埃马尔湾地区符拉迪沃斯托克郊区的FGBOU VDC“海洋”森林带的一部分。 获得的地衣植物状况结果显示了沿海地区大气纯度的高指数。

关键词：地衣； 地衣指示；投影覆盖区，埃马尔湾； 字段容差等级。

Abstract. *The lichen flora of the Far East is characterized by an increased diversity, which is associated to a greater extent with the bioclimatic features of the territory. Lichen indication is a fairly effective method for assessing the state of atmospheric pollution of territories. A section of the forest belt in FGBOU VDC "Ocean" located in the suburban area of Vladivostok in the area of Emar Bay was studied. The obtained results of the state of lichen flora show a high index of the purity of the atmosphere of the coastal territory.*

Keywords: *lichens; lichen indication; projective cover area, Emar Bay; classes of field tolerance.*

At present, the assessment of the quality of soil, water and air is of great importance for humans. A special environmental problem is observed in the air pollution of large cities, caused by the anthropogenic factor. This is due to the regular release of pollutants by industrial enterprises and vehicles that adversely affect the well-being and health of people [3, 1]. Also, air pollution leads to a decrease in the thickness of the ozone layer and the formation of ozone holes. It is known that a 1% decrease in the thickness of the ozone layer increases the intensity of

UV radiation on the Earth's surface by 2%, which increases the incidence of skin cancer in humans by 3-5% [2]. In addition, air pollution leads to an increase in air humidity, an increase in the amount of fog and clouding of the atmosphere - a greenhouse effect is formed.

In turn, it is necessary to determine both the actual and the possible future degree of environmental pollution. For this, there are 2 approaches: physicochemical and biological. The latter includes the direction of biological monitoring, which studies environmental pollution, based on the reaction of biological objects to pollutants. It includes the observation, assessment and forecast of changes caused by anthropogenic impact. Lichens are one of the main objects of global biological monitoring. The absorption of pollutants from rainwater and the atmosphere is most pronounced in these widespread symbiotic organisms, with high climate tolerance. Lichens, composed of fungus and algae, and receiving minerals and moisture from the air, precipitation, dew and fog, are highly sensitive to air pollution. Therefore, with intensive urbanization, lichen indication can be effectively used to indicate the purity of the atmosphere [4, 5]. This method has a number of advantages over instrumental methods, it is cheaper and makes it possible to assess the state of the environment over a long period of time.

Lichens, which have high tolerance to abiotic environmental factors, easily adapt to the conditions of the substrate, and are the first to develop substrate places where other plants cannot exist. Rocky surfaces represent a special niche for living organisms, and epilithic lichens are the first settlers on them [8]. It is known that all lichens grow very slowly. But in good ecological conditions, the growth of thallus can reach several mm per year. Dead and functioning thalli of epilithic symbionts, together with dust and sand, create conditions for soil formation. Epiphytic lichens, occupying their ecological niche, settle on trees and shrubs. Being an indispensable component of all forest ecosystems, they react to atmospheric pollution earlier and stronger than higher plants.

Purpose of the study

To analyze the lichen flora and assess the level of air pollution in the Emar Bay using the lichen indication method.

Materials and methods

The material for this study was the monitoring data of rock habitats of epilithic lichens of the coastal zone and epiphytic lichens of test sites in the forest zone of Emar Bay. The work was carried out according to the method of A.S. Bogolyubov, M.V. Kravchenko "Assessment of air pollution by lichen indication" ("Ecosystem", 2001) with a quantitative approach. The selected test rock surfaces of the coastal zone, partly related to supralittoral (rock No. 1, No. 2, No. 3, No. 4), ranging in size from 40 to 60 m2, had the same distance from the sea and were characterized by similar environmental conditions in relation to abiotic factors.

The total projective cover for epilithic lichens of all species was determined at a height of 150 cm, in total, in relation to the rock habitats covered with symbionts to the total rock surface using the “palette method”.

The condition of the epiphytic lichen flora of the forest zone (with model trees: Mongolian oak, linden, birch, maple) was assessed on selected and planted test plots No. 1, No. 2, No. 3 with a size of 400 m2. The structure, composition of phytocenoses and ecological conditions of the sites were similar. The projective cover was determined for epiphytic lichens of all species in total in relation to the part of the trunk covered with organisms to its total surface by the method of "linear intersections".

Results and discussions

The epilithic lichen cover of the study area is typical of the eastern coast of the Muravyov-Amursky Peninsula [6]. It was formed in the process of evolution due to the adaptation of coastal algae and fungi to rocky habitats. The symbiont thalli clearly have a well-defined fruiting body and growth zone (in scale forms, it is clearly visible along the edge of the thallus, while in foliose forms it is at the top). Lobes near parts of the thallus without signs of deformation and significant color change [7]. The average value of the projective cover on rock surfaces No. 1, No. 2, No. 3, No. 4 is in the range of 35.09% - 67.95% (Fig. 1).

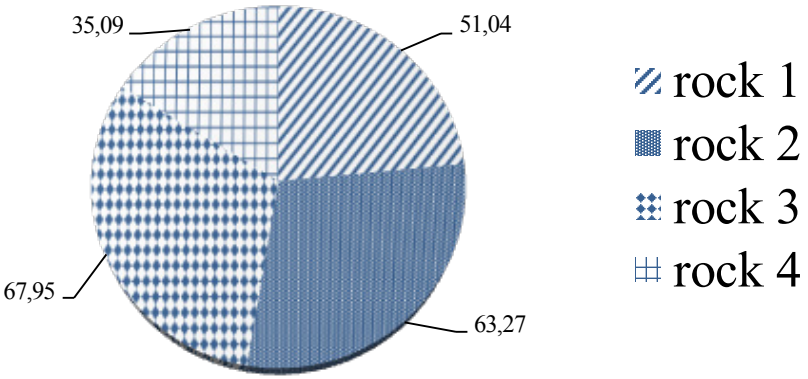

Figure 1. *Average projective cover, %.*

On a 10-point scale, the assessment of the projective cover is from 6 to 9 points, which corresponds to a high air purity index. In terms of field tolerance classes, the studied area with symbiotic organisms belongs to class I - II (Trass Kh.Kh., 1985, for the territory of the Far East), i.e. to landscapes without tangible anthropogenic influence (often) and anthropogenically slightly modified habitats (rarely).

As proof of the high value of the projective cover of lichens and the index of cleanliness of the atmosphere, the IAQ indicator - the index of field tolerance - (Index of Atmosphere Quality, Truss H.Kh., 1985). Since the IAQ, like the field tolerance index, correlates with the concentration of SO2 in the air, we find that the concentration of SO_2 for the studied area is less than 0,014 mg/m^3 and defines it as a normal conditional zone.

The taxonomic characteristics of the leading families of the studied epilithic lichen flora are quite diverse (Fig. 2). The most common are representatives of the families Parmeliaceae and Physciaceae (26.9%, 21.4%), the least - Ramalinaceae (2.9%). Lichens, whose belonging to the family is not defined, make up 14%. The names of taxa are given in accordance with the electronic resource CABI Bioscience Databases [9].

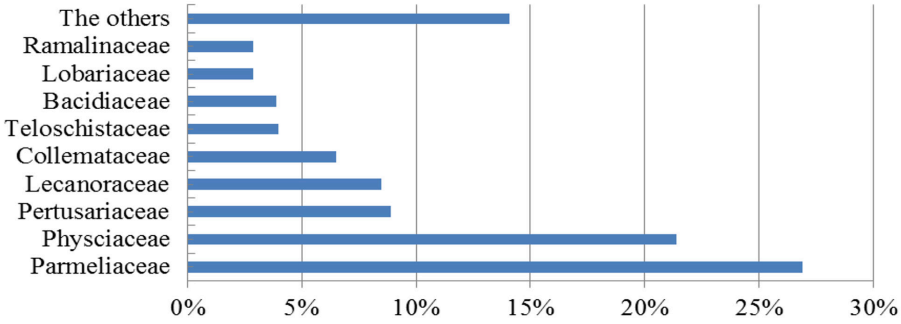

Figure 2. *Taxonomic characteristics of the leading families*

When determining the vital state of epiphytic lichens in test plots No. 1, No. 2, No. 3, it was noted that their thalli have well-defined fruiting bodies. The lobes of the thallus are not wrinkled and show no signs of discoloration, which is a sign of the absence of oppression. At intersection points (method of "linear intersections"), lichens are found over the entire visible height on all trees. The average value of the projective cover on the test plots No. 1, No. 2, No. 3 is 35.54%, 35.54% and 72.34%, respectively. On the test plots under study, the projective cover rating on a 10-point scale was from 8 to 10 points, which indicates a high index of atmospheric purity. A significant value of the projective cover of site No. 3 (72.34%) can be explained by its greater proximity to the sea than sites No. 1, No. 2. According to the classification of H.Kh. According to the field tolerance index, the lichen communities of the forest zone belong to classes I-II, which corresponds to natural and rarely anthropogenically modified habitats.

Conclusions

The average value of the projective cover, the assessment of lichen communities according to the classes of field tolerance, and taxonomic diversity correspond to a high index of atmospheric purity in the coastal area of Emar Bay. This is the result of favorable conditions for the life of epilithic and epiphytic lichens: coastal areas are remote from central roads, there is no pronounced anthropogenic impact, and there is significant air circulation due to the wind rose. The thalli of organisms do not experience a shortage of assimilation nutrition due to the lack of shading. The studied area of the forest belt and the coastal area in FGBOU VDC "Ocean", located in the suburban area of Vladivostok in the area of Emar Bay, corresponds to a high index of atmospheric purity. The purity of the air basin is a significant advantage of this area, because. The federal state budgetary educational institution All-Russian Children's Center "Ocean" annually accepts more than 13,000 children aged 11-17 years, implementing additional education programs.

References

1. Astafieva O.O., Gladysheva O.V. Study of the degree of atmospheric air pollution in the Gryazinsky district of the Lipetsk region by the method of lichen indication // Trends in the development of science and education. 2021. No. 70-1. pp. 80-83.

2. Byazrov L.G. Lichens in ecological monitoring. M.: Scientific world, 2002. 336 p.

3. Gaydysh I.S., Tarasova V.N., Markovskaya E.F. Lichenoindication of the state of the air environment in the city of Kostomuksha (Republic of Karelia) // Fundamental research. 2013. No. 10-10. pp. 2212-2218.

4. Zhyromskaya O.F., Zhyromsky S.V., Kashkovsky V.A. Study of atmospheric air pollution by lichen indication // Scientific horizons. 2021. No. 4 (44). pp. 73-80.

5. Panchenko L.S. Lichen indication as a particular method of bioindication // Actual science. 2020. No. 12 (41). pp. 13-15.

6. Rodnikova I.M., Skirina I.F. Lichenoindication of anthropogenic impact on the islands of Peter the Great Bay (Sea of Japan) // Geography and Natural Resources. 2014. No. 4. S. 42-48.

7. Skirina I.F. New locations of protected lichens in the south of the Russian Far East // Turczaninowia. 2013. V. 16, No. 2. S. 084-087.

8. Sonina A.V. Species diversity of epilithic lichens in the north-west of Russia Epiphytic lichens of Primorsky Krai and their use in environmental monitoring // Fundamental research. 2014. No. 3. S. 505-509.

9. CABI Bioscience Databases [Electronic resource]. Access mode: http://www.speciesfungorum.org/ (Accessed 11/21/2013).

DOI 10.34660/INF.2022.87.65.185

角叉菜胶的镉结合特性
THE CADMIUM-BINDING PROPERTIES OF THE CARRAGEENANS

Khozhaenko Elena Vladimirovna
Candidate of Biological Sciences, Associate Professor
Far Eastern Federal University
Kovalev Valeri Vladimirovich
Candidate of Biological Sciences, Senior Research Officer
A.V. Zhirmunsky National Scientific Center of Marine Biology, Far Eastern Branch, Russian Academy of Sciences
Podkorytova Elena Alekseevna
Candidate of Biological Sciences, Research Officer
A.V. Zhirmunsky National Scientific Center of Marine Biology, Far Eastern Branch, Russian Academy of Sciences
Kondrateva Galina Konstantinovna
Candidate of Pharmaceutical Sciences, Associate Professor
Far Eastern Federal University

抽象的。 角叉菜胶 – 是源自红藻的天然多糖。 它们最重要的生物学特性之一是结合金属离子的能力。 这一特性使我们可以将角叉菜胶视为预防慢性重金属中毒的功能性食品。 已经研究了各种类型的角叉菜胶的镉结合活性。 根据实验结果，发现κ–和ι–角叉菜胶有效地结合镉离子，而在ι–角叉菜胶中观察到最高活性。

Abstract. *Carrageenans - are natural polysaccharides derived from red algae. One of their most important biological properties is the ability to bind metal ions. This property allows us to consider carrageenans as functional foods for the prevention of chronic heavy metal poisoning. The cadmium-binding activity of various types of carrageenans has been studied. According to the results of the experiment, it was found that* κ- *and* ι-*carrageenans effectively bind cadmium ions, while the highest activity was observed in* ι-*carrageenan.*

Introduction

Cadmium as a pollutant is widely distributed in the environment, as it is actively used in nuclear power, electronic and radio engineering industries, in the production of batteries and in other industries. Cadmium enters the environment

with non-ferrous metallurgy waste and in the production of mineral fertilizers [7]. Cadmium accumulates in plants and animals and enters the human body after eating contaminated foods (seafood, fish, vegetables, water) [9]. Smokers suffer from chronic cadmium poisoning, getting through the respiratory tract, cadmium is absorbed much better than it comes with food and water. Cadmium has a long half-life of 25–30 years. It is known that prolonged exposure to cadmium leads to the development of lung cancer, breast cancer, prostate cancer, and pancreas cancer [1]. Cadmium is a risk factor for the development of osteoporosis, cardiomyopathy, hypertension, pulmonary emphysema, and nephropathy [1,8]. Excess intake of cadmium into the body must be correlated with the use of enterosorbents; in severe cases, chelation therapy in combination with hemodialysis is necessary. In mild cases and for the prevention of cadmium intoxication, it is enough to eat functional foods that help remove heavy metal ions from the human body, such as pectins, alginates and carrageenans.

In the group of dietary fibers, sulfated polysaccharides of seaweeds - carrageenans are of particular value. Natural carrageenans and their low molecular weight derivatives exhibit anticoagulant, antitumor, antiviral activity, hypolipidemic and immunostimulating properties [2,5,6,10]. Carrageenans are sulfated galactans consisting of D units of galactose and its derivatives, the residues of which are connected by regularly alternating β(1→4)- and α(1→3)-glycosidic bonds. Carrageenans differ in 3,6-anhydrogalactose content, location and number of sulfate groups (Fig. 1). The ability of carrageenans to form gels in aqueous solutions is one of the most important physicochemical properties of these polysaccharides, due to which they are used in the food industry, medicine and pharmacy. The purpose of this work was to quantify the ability of carrageenans of three types (κ–,ι–, λ–) to bind and remove toxic cadmium ions from the body.

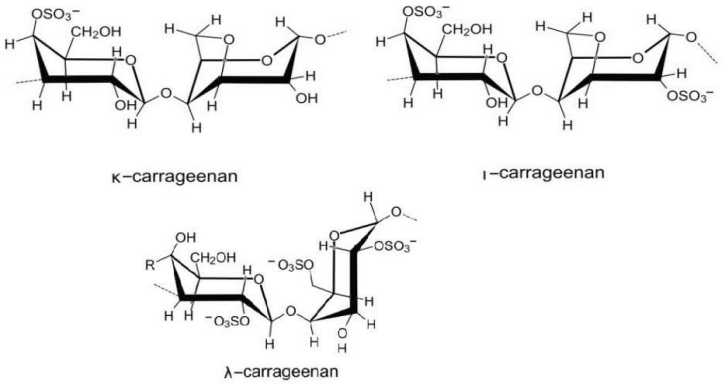

Figure 1. *Chemical structure of various types of carrageenans*

Materials and methods

Samples of κ–, ι–, λ– carrageenans manufactured by Merck (China) were chosen as objects for the study. κ– and ι– carrageenan have a gelling ability, and λ– carrageenan belongs to a non-cutting type. The ability of carrageenans to bind cadmium ions in vitro at pH 2.0–6.0 was determined by the method described by us earlier [3]. The sorption activity of carrageenans in relation to cadmium ions was determined by the formula:

$$Q = \frac{V\,(C_i - C_e)}{m}$$

where Q – the amount of cadmium ions bound by carrageenan, mg/g; V – the total volume of the reaction mixture, l; C_i - initial concentration of cadmium ions in solution, mg/l; C_e – the equilibrium concentration of cadmium ions in solution, mg/ml; m – the mass of carrageenans, g.

The study of kinetics was carried out according to the method described by us earlier for lead and yttrium ions, the calculation of quantitative indicators was carried out according to the above formula.

Results and discussion

Graphs of the cadmium ion binding kinetics were built as follows: the maximum established binding activity of carrageenans to cadmium ions at pH 4.0 was taken as 100%, and the amount of cadmium ion binding measured every 10 minutes was expressed as a percentage of the maximum sorption capacity (activity). As a result of the experiments, it was found that containing three sulfate groups in its structure, but not having anhydrogalactose units, λ-carrageenan does not have a binding activity with respect to cadmium ions. It has been established that λ-carrageenan is not capable of forming an ordered gel structure with an optimal spatial arrangement of sulfate and hydroxyl groups in the presence of a divalent cation. For samples of κ- and ι-carrageenan, it takes 60 minutes and 90 minutes, respectively, to achieve sorption equilibrium (fig. 1).

Based on the obtained experimental data on the binding of cadmium ions by carrageenan samples, sorption equilibrium isotherms were constructed (Fig. 2-3). The shape of the obtained curves made it possible to attribute them to the class of Langmuir isotherms. Therefore, to determine the affinity coefficients of sorbents for strontium and cerium ions, as well as to find the maximum sorption capacity of the studied carrageenans, we used the Langmuir sorption model [4].

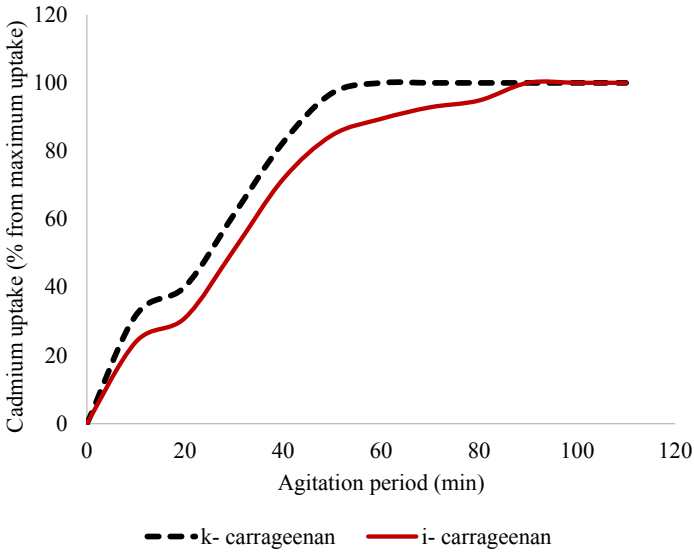

Figure 1. *Effect of agitation period on the yttrium binding activity of carrageenans at pH 4.0: a) κ- carrageenan; b) ι-carrageenan*

According to the results of experiments, it was found that the sorption activity of κ- and, ι-carrageenans slightly depends on the pH of the medium, so the maximum sorption of cadmium ions in two carrageenans was at pH 4.0, it exceeded the sorption capacity at pH 6.0 and 2.0, on average, 1.6-2.1 times. The sorption minimum was at pH 2.0 (tab. 1.) At the same time, the sorption activity of ι-carrageenan exceeded the activity of κ-carrageenan, on average, by 15%, which suggests that with an increase in the number of sulfate groups in the carrageenan molecule, their sorption activity increases. The stability of cerium and strontium complexes with c ι- and κ-carrageenans at low pH values can be associated with the stabilization of these complexes due to additional donor-acceptor bonds of the cation with oxygen atoms of the galactopyranose ring and water molecules included in the structure of the complexes.

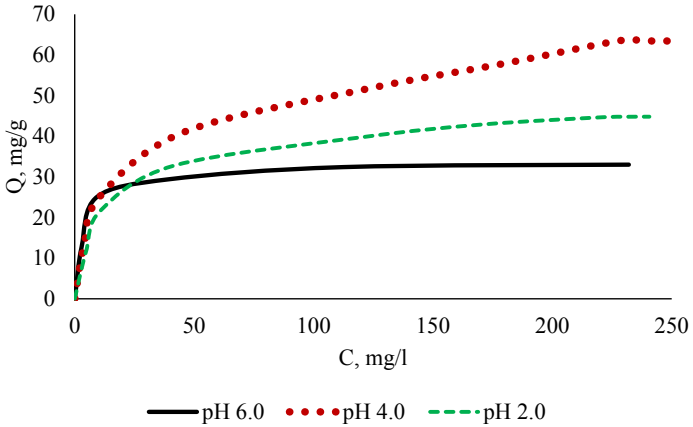

Figure 2. *Cadmium binding activity of κ-carrageenan under various pH values of solution*

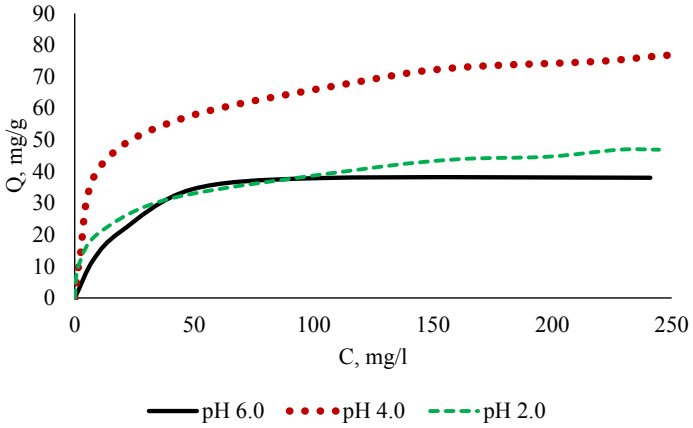

Figure 3. *Cadmium binding activity of ι-carrageenan under various pH values of solution*

Table 1.

Langmuir isotherm constants and correlation coefficients of cadmium binding capacity of carrageenans

	κ- carrageenan			**ι- carrageenan**		
	pH 2.0	**pH 4.0**	**pH 6.0**	**pH 2.0**	**pH 4.0**	**pH 6.0**
Qmax, mg/g	47,62± 1,90	68,49± 2,74	33,67± 1,01	49,02± 1,22	80,0± 2,56	40,82± 1,84
b, l/mg	0,0660 ± 0,0026	0,0504 ± 0,0018	0,2129 ± 0,0096	0,0906 ± 0,0037	0,0967 ± 0,0035	0,0559 ± 0,0017
R^2	0,9987	0,9928	0,9999	0,9957	0,9986	0,9969

Conclusions:

ι- and κ-carrageenans are characterized by the ability to firmly and effectively bind cadmium ions. The sorption activity of carrageenans depends on their structure, including the presence of sulfate groups. ι-carrageenan is the most effective binding polysaccharide for toxic cadmium ions and can be recommended for food as a functional food for the prevention of chronic cadmium intoxication.

References

1. Genchi G, Sinicropi MS, Lauria G, Carocci A, Catalano A. The Effects of Cadmium Toxicity. International Journal of Environmental Research and Public Health. 2020; 17(11):3782.

2. Ha HT, Cuong DX, Thuy LH, Thuan PT, Tuyen DTT, Mo VT, Dong DH. Carrageenan of Red Algae Eucheuma gelatinae: Extraction, Antioxidant Activity, Rheology Characteristics, and Physicochemistry Characterization. Molecules. 2022; 27(4):1268. https://doi.org/10.3390/molecules27041268

3. Khotimchenko YS, Khozhaenko EV, Khotimchenko MY, Kolenchenko EA, Kovalev VV. Carrageenans as a New Source of Drugs with Metal Binding Properties. Marine Drugs. 2010; 8(4):1106–1121.

4. Khotimchenko M, Makarova K, Khozhaenko E, Kovalev V. Lead-binding capacity of calcium pectates with different molecular weight. International Journal of Biological Macromolecules. 2017; 97:526-535.

5. Khotimchenko M, Tiasto V, Kalitnik A, Begun M, Khotimchenko R, Leonteva E, Bryukhovetskiy I, Khotimchenko Y. Antitumor potential of carrageenans from marine red algae. Carbohydrate Polymers. 2020; 246:116568.

6. Nečas, J., & Bartošíková, L. Carrageenan: a review. Veterinarni Medicina, 2018; 58:187-205.

7. Ngoc NTM, Chuyen NV, Thao NTT, et al. Chromium, Cadmium, Lead, and Arsenic Concentrations in Water, Vegetables, and Seafood Consumed in a Coastal Area in Northern Vietnam. Environ Health Insights. 2020; 14:1178630220921410.

8. Rafati Rahimzadeh M, Rafati Rahimzadeh M, Kazemi S, Moghadamnia AA. Cadmium toxicity and treatment: An update. Caspian J Intern Med. 2017; 8(3):135-145.

9. Tamele IJ, Vázquez Loureiro P. Lead, Mercury and Cadmium in Fish and Shellfish from the Indian Ocean and Red Sea (African Countries): Public Health Challenges. Journal of Marine Science and Engineering. 2020; 8(5):344. https://doi.org/10.3390/jmse8050344

10. Wei Q, Fu G, Wang K, Yang Q, Zhao J, Wang Y, Ji K, Song S. Advances in Research on Antiviral Activities of Sulfated Polysaccharides from Seaweeds. Pharmaceuticals. 2022; 15(5):581.

DOI 10.34660/INF.2022.90.22.187

气候变化导致俄罗斯联邦某些地区的自然重点区域发生变化
TRANSFORMATION OF THE NATURAL FOCUS AREAS IN CERTAIN REGIONS OF THE RUSSIAN FEDERATION CAUSED BY CLIMATIC CHANGE

Malkova Irina Leonidovna
Candidate of Geographical Sciences, Associate Professor
Rubtsova Irina Yurievna
Candidate of Geographical Sciences, Associate Professor
Semakina Alsu Valeryevna
Candidate of Geographical Sciences; Head of the Department
Udmurt State University

The problem of the tick-borne infections: tick-borne viral encephalitis (TBE), ixodic tick-born borreliosis (Lime disease) stays acute for the majority of the RF regions. These infections make up 36% of all natural-focal diseases [16]. As an exception, in 2019 tick-borne infections were surpassed by hemorrhagic fever with renal syndrome. Social and economic losses incurred from the spreading of the tick-born infections have amounted to 2.107 billion rubles.

The areas of tick-born zooanthroponoses largely coincide with main carriers habitats (fig. 1) – ixodid ticks (*Parasitiformes*, *Ixodidae*) *Ixodes ricinus* (European part) and *I. persulcatus (some places in the European part, Ural region, Siberia, Far East)*. In Siberia and Far East, the virus might be spread through *I. pavlovskyi* tick species.

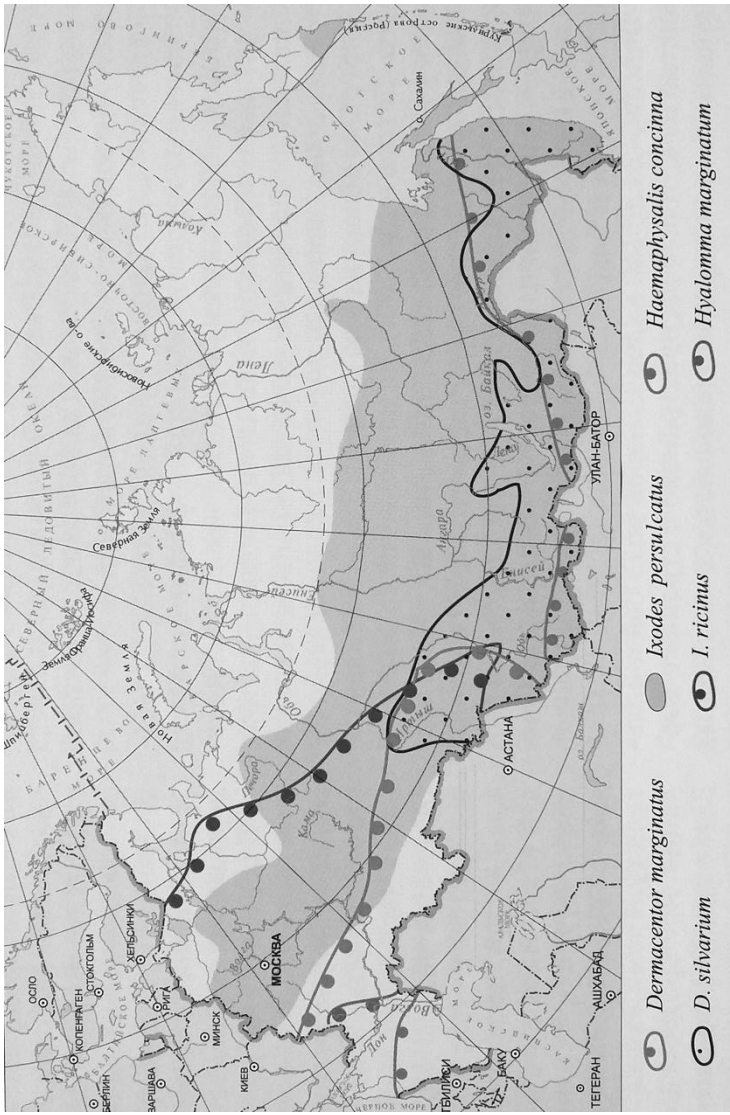

Figure 1. *Ticks habitats on the territory of the Russian Federation [11]*

Conditioned by climate change, the natural focal areas of tick-borne zooanthroponoses are subject to major transformation. The rise of winter temperatures, the increase of precipitation, especially in summer, the prolonged period of warm weather in most cases have had boosting effect on the habitats and the population of taiga ticks. The original habitat of Ixodes persulcatus on the RF territory (from 42° to 62° north latitude) is shifting to more continental north-eastern regions [1, 6, 7, 10, 18, 19]. Some researchers predict Ixodes ricinus habitat expansion in Europe by 2040-2060, and by the end of the 21st century the northern boundary of this species habitat can reach 70° north latitude [20].

According to Instructional Guidelines 2.1.10.0057-12. 2.1.10. "Influence of environmental and living conditions on public welfare. Assessment of risk and damage generated by climate change impact such as surges in infection and death rates in high-risk groups of population" (issued by Rospotrebnadzor on 17.01.2012) collection of data on tick-borne infections has to include: number of people affected by tick bites, number of people with TBE and Lime borreliosis, ticks density index, data on TBE-infected ticks. The present article analyses the tendencies in certain RF regions for these groups of indicators.

The epidemiological situation in last decades is characterized by considerable increase in the number of people who suffered from tick bites. Health-seeking encounter cases after tick bites have risen from 396,000 in 2013 to 580,000 in 2019[16]. The biggest increase was registered in Tomsk oblast (from 1,413.90 to 2,097.2 per 100,000 people), Kaliningrad oblast (by 56%), and Krasoyarsky krai (by 49.5%). The rate in the Altai Republic, Kostromaskaya, Vologodskaya, Kirovskaya, Tyumenskaya, Kemerovskaya oblasts, and the Udmurt Republic is 3-5 times higher (395.34 per 100,000 people) than the average rate in the Russian Federation.

The number of health-seeking encounters after tick bites has significantly increased recently in north-eastern regions of the Udmurt Republic (Vyatka-Kama southern taiga province) despite of dispersed population. In 2019 the rate in these regions was over 3,000 cases per 100,000 people. On the east this territory borders with Elovsky, Ochersky, and Vereshchaginsky regions of the Perm krai with one of highest tick bites rates (over 1,000).

Many regions register the extended period of ticks' activity due to early start of the cycle and late diapause. Thus, in Sverdlovskaya oblast the cycle has extended from 177 days in 2004 to 219 days (from the end of March to the beginning of November) [4], in Udmurtia – from 160 to 220 days [9].

The TBE rate in the last quarter of the 20th century had increased 9-fold and reached 10,000 cases a year. By 2020 the decline of TBE infection rate was observed in all RF regions endemic to this disease. The indicators in the regions most badly affected by the infection – Tomsk oblast and the Altai Republic – are still

5 times higher compared to RF average (1.21 per 100,000 people) [16] despite of overall 2-fold decrease. The situation stays critically acute in Krasnoyarsky krai, Kirov oblast, and the Tyva Republic where despite the overall downward trend the TBE infection rate keeps within 8.92-14.64 cases per 100,000 people for the last 10 years. On the territory of Sverdlovskaya oblast the TBE dynamics since 1990s is characterized by up and down cycles with overall reducing trend at 3.5% annual rate [4].

Many research papers link changes in TBE infection rate to global warming. In Arkhangelskaya oblast the average annual temperature was registered at +0.7° C in 1960-1989. From 2000 to 2009 the readings surged to +2.0°C. Within the same period the human TBE infection rate also increased. The correlation of these two indicators between 1990 and 2009 kept at 0.71 [10] in the central parts of Arkhangelskaya oblast. Whereas the infection rate has reduced 2 times in Russia in recent years, in Arkhangelskaya oblast it has risen 3 times [8].

In Irkutsk oblast the February temperature rose by 6°C and the frostless season extended from 90-100 to 120-130 days. According to observation data in 1956-2003 the number of ixodic ticks increased 57.5 times and the infection rate 40.2 times [5]. Further rise of average annual temperature to +3.86°C resulted in considerable decrease of these numbers [12].

Similarly, in the Udmurt Republic the human infection rate has plummeted in the last 15 years: TBE – by almost 5 times, tick-borne borreliosis – by almost 7 times [15]. Alongside the upsurge in annual temperatures (fig. 2), the annual average precipitation has risen from 501 to 650 mm, the depth of snow cover has increased 1.5 times, and the depth of soil freezing has reduced within the last 50 years [9, 10].

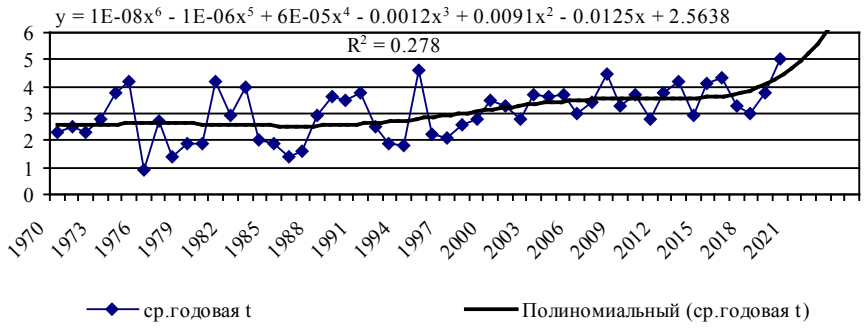

Figure 2. *Long-term changes of average annual temperature on the territory of the Izhevsk city, C and trend line*

In the period from 1954 to 1964 the first surge of tick-borne infection rates was registered (fig. 3). The most alarming situation was characteristic for central and southern regions of the republic (fig. 4). The period of low TBE infection rate (from 1965 to 1986) was determined not only by the predictable trend in the development of the natural epidemic, but by the extensive anti-tick treatment of the territory. The climax of the second wave of the infection rate falls onto 1990s. The sharp fall of indicators in 1994-1995 within the same decade coincides with the period of low average annual temperatures (fig. 2).

It should be noted that starting from late 1990s the infection rates in north-east regions surpass those in south-west 2 to 5 times [2]. Thus, in 2018 TBE rate in Kez region (the north-eastmost region) was 24.4. per 100,00 people which is 7 times higher than average in the republic; the Lime borreliosis rate was 58.8 per 100,000 people – 9 times above average.

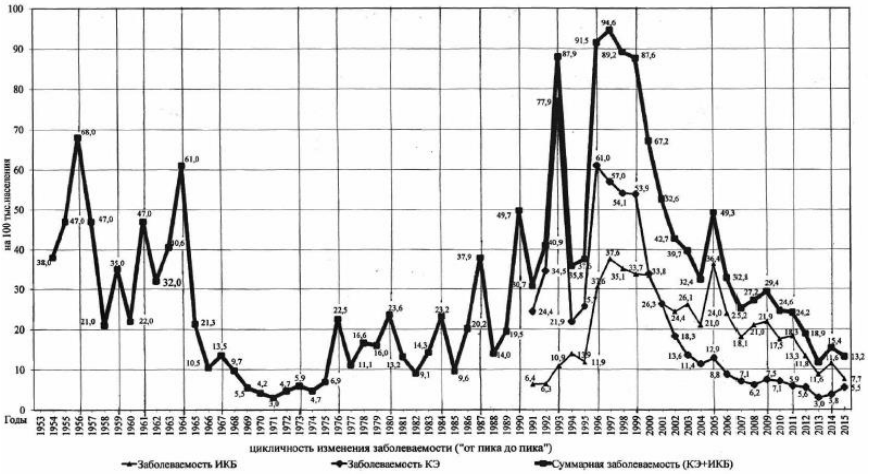

Figure 3. *Tick-born encephalitis (TBE) and ixodic tick-borne borreliosis (Lime disease) infection rates among the population of the Udmurt Republic [3]*

In Perm krai the proportion of the tick-borne infection in the structure of the natural-focus diseases reduced from 68.9% in 2011 to 51.4% in 2020. In 2020 TBE cases were 8.5 times less frequent compared to average long-term rates in 2016-2020 (7.15 per 100,000 people). Lime borreliosis rates reduced 3.6 times compared to 2019 (2.03 per 100,000 people) and were registered lower than the RF average for the first time [13].

Data collected in Perm krai shows that the long-term infection dynamics has cyclic character. The total duration of the TBE cycle is 33-34 years and consists

of 13-14 yearly phase of increased epidemic activity and 19-20 yearly phase of decreased activity (fig. 5)[13]. The first phases of increased (1960-1968) and decreased (1970-1989) TBE infection rates did not much differ in temperature conditions: air temperature was around 2.1-2.2°C (fig. 4). Next phases of the epidemiological process were accompanied by temperature rises. However, the downturn phases (2003-2008 and 2017-2020) match the highest temperature readings (3.5°C and 3.3°C correspondingly). This proves complex correlation between temperature factor and ticks activity. In 2005 the southern regions of Perm krai (Chastinskiy, Elovskiy, Bardymskiy, Uinskiy, Suksunskiy, Kishertskiy, B-Sosnovskiy) registered some of the highest TBE rates at 13.8 to 40.0 cases per 100,000 people. In 2020 the western Ocherskiy and Sivinskiy regions, as well as north-eastern Cherdynskiy and Krasnovisherskiy regions entered the "leaders" chart. For many years the highest rates are observed in Ocherskiy region (TBE – from 51.8 (2005) to 8.68 (2020), Lime borreliosis – 26.04 per 100,000 people) which borders Kez region of the Udmurt Republic on north-east.

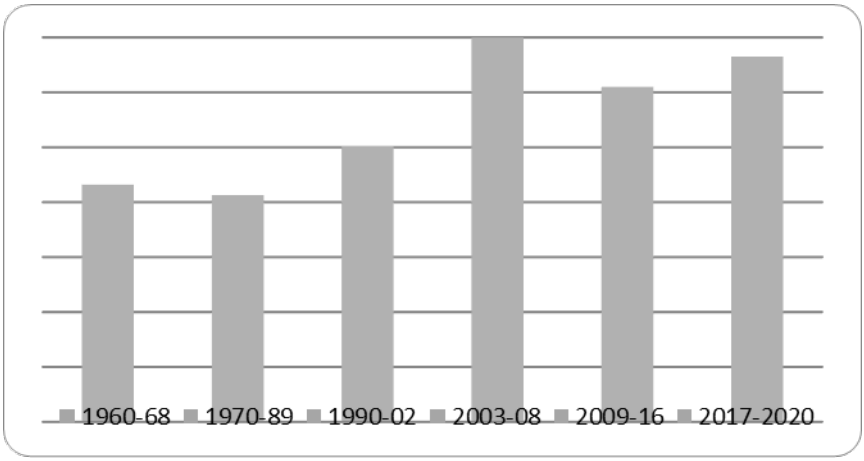

Figure 4. *Dynamics of tick-born zooanthroponosis rates and average annual air temperatures on the territory of Perm krai (based on [13] and http://www.pogodaiklimat.ru/history/28224.htm)*

The average TBE rate by landscape-climatic subzones of Perm krai has changed from 2.7 (middle taiga) to 11.3 (south taiga) per 100,000 people in the last 5 years which can be explained by difference in ticks abundance. In Kirov oblast 89% of cases are registered in south taiga nature zone, 8.5% - in middle taiga zone, and 2.5% - in coniferous-broad-leaved forests zone [17].

In many regions the tick-born zooanthroponosis infection rate has fallen from

the beginning of 2000s, although the ticks density has increased. For example, in urban forest and parkland zones of Izhevsk city the average ticks density in the period of mass activity has increased 2-fold: from 11.1 ticks per flag/km in 2001 to 24.2 in 2013. According to the data provided by Hygiene and Epidemiology Center the highest ticks density on the territory of central Udmurtia was registered in 2015: 67.8 ticks per flag/km in May, 54.7 ticks per flag/km in June. In 2018 the number of ticks collected per flag in May-June was 1.5 times lower; however, ticks density considerably grew in July-September. Ticks density also greatly increased in the period of mass activity for south taiga landscapes: from 3.3 to 27.5 ticks per flag/hour [9]. That said, ticks density readings in taiga zone of Udmurtia stay 4.5 times lower than in sub-taiga zone.

Data collected on permanent observation points in Sverdlovskaya oblast from 2002 to 2012 indicates that ticks density reduced more than 3 times (fig. 7). The most pronounced reduction of ticks density from 14.3 to 0.4 per flag/km is characteristic of aspen-birch forests sub-zone. As regards forest zone, the maximum readings were fixed in 2002-2009 with sharp decline to 0.4-0.8 ticks per flag/km in 2012. In recent years the highest ticks density (6.6-26.7 ticks per flag/km) was registered in north forest-steppe sub-zone. Hence, based on ixodic ticks density monitoring data collected between 1990-2012 the south-west regions of Sverdlovskaya oblast is the area of the most serious epidemiological concern [4]. In 2019 ticks density varied from a single specimen to 90 ticks per flag/km (in 2018 – up to 180 specimens per flag/km) and matched the long-term annual average level (1.3 ticks per flag/km) [14].

In Sverdlovskaya oblast the ticks density reduction results in fewer number of virus-carrying ticks. The number of TBE-infectious specimens collected from tick-bitten population decreased from 32.4% in 1990 to 4.4.% in 2019. As for ticks collected at field stations the indicators for the same period dropped 34 times (to 1%). On the territory of the Udmurt Republic the rate of TBE infectious ticks fell from 21% (2021) to 3.2% (2018). Number of Lime borreliosis positive ticks reached 55-67% in 2010-2013, since 2014 this index has remained at 30-40%.

In recent years the clinical pattern of tick-borne infections has changed as well. In some regions (Udmurtia, Perm krai) the number of cases of febrile TBE - a relatively less acute form of the disease - is growing, and severe TBE forms are being registered much less often. On the contrary, in Baikal region the number of sever (focal) cases surged from 5% to 11% in course of 25 years. Among clinical forms of Lime borreliosis the number of erythema-free cases has considerably increased (from 0% to 50%).

To sum up, evidence from many regions confirms the supposition that the virulence of the tick-borne encephalitis grows from south-west to north-east corresponding the more severe winter conditions climate pattern. The colder winters

are, the more hazardous the virus strain is, and the more acute the disease. The severity of the tick encephalitis form increases parallel to climate conditions severity. That means, warmer summer conditions lead to increase of ticks activity, expansion of their habitat, and more bites. However, warmer winters result in less severe forms of the disease due to more ticks carrying less virulent encephalitis virus. This, in turn, reduces the human infection rates due to light cases, oftentimes not registered, or the disease does not develop altogether.

The changes in hydrothermal conditions reflect upon the dynamics of all components of tick-borne zooanthroponosis parasitic system affecting the severity of epidemiological situation in natural focus areas both directly and indirectly. The spatial transformation of the natural focuses is confirmed by all three indicator groups of ixodic ticks activity: human tick-borne zooanthroponosis infection rate, number of registered tick bites, and ticks territorial density. Tendency towards climate warming is accompanied by TBE and lime borreliosis infection rates increase on the southern boundaries of the diseases environments, whereas southern parts of same environments may have unfavorable for ixodic ticks habitats which results in lower infection rates on such territories. It is predicted that relapsing borreliosis fevers carried by argasid ticks inhabiting Central Asian countries may also spread in RF.

References

1. Алексеев А. Н. 2006. Влияние глобального изменения климата на кровососущих эктопаразитов и передаваемых ими возбудителей болезней. Вестник РАМН. № 3. С. 21-25.

2. Атлас Удмуртской Республики / под общей ред. И. И. Рысина. – Изд. 2-е, доп. и перераб. – М.: Феория; Ижевск: Удмуртия, 2020. – 288 с.

3. Динамика заболеваемости клещевыми инфекциями в Удмуртской Республике в последние 25 лет / Э. Т. Садыкова, Г. И. Мельникова, Л. Ф. Молчанова, Т. Т. Садыков // Здоровье, демография, экология финно-угорских народов. – 2016. – № 2. – С. 22–27.

4. Есюнина М.М. Современные тенденции заболеваемости клещевым вирусным энцефалитом в условиях различных тактик иммунизации и усовершенствование эпидемиологического надзора и контроля Диссертация на соискание ученой степени кандидата медицинских наук Екатеринбург, 2015. 153 с.

5. Злобин В. И. Клещевой энцефалит в Российской Федерации: современное состояние проблемы и стратегия профилактики. Вопросы вирусологии. – 2005. – №3. С. 26–31.

6. Злобин В. И., Данчинова Г. А., Сунцова О. В., Бадуева Л. Б. Климат как один из факторов, влияющих на уровень заболеваемости клещевым энцефалитом. В кн.: Изменение климата и здоровье России в XXI веке. 2004- М.: Издательское товарищество «АдамантЪ». -С. 121-124.

7. Коротков Ю. С. Экология таёжного клеща (Ixodes persulcatus Schultze, 1930) в условиях изменения климата Евразии: автореф. дис. _ д-ра биол. наук. - М., 2009. – 46с.

8. Котцов В.М., Гришина Е.А., Бузинов Р.В., Гудков А.Б. Эпидемиологические особенности клещевого вирусного энцефалита и его профилактика в Архангельской области // Экология человека. № 8, 2010. С. 3—8.

9. Малькова И.Л., Рубцова И.Ю. Медико-географическая оценка природных условий Удмуртии: монография. - Ижевск. Издательский центр «Удмуртский университет», 2016. – 212с.

10. Малькова И.Л., Рубцова И.Ю. Трансформация природного очага клещевых инфекций как следствие изменения климата (на примере Удмуртии) // «Глобальные климатические изменения: региональные эффекты, модели, прогнозы». Воронеж: Издательство «Цифровая полиграфия», 2019. Том 2. С. 355-358.

11. Медико-географический атлас России «Природноочаговые болезни» / под ред. С.М. Малхазовой. – М.: Географический факультет МГУ, 2015 – 20с.

12. Мельникова О.В., Вершинин Е.А., Корзун В.М., Сидорова Е.А., Андаев Е.И. Особенности территориального распределения заболеваемости клещевым энцефалитом среди жителей г. Иркутска // Бюллетень ВСНЦ СО РАМН. № 2(84), 2012. С. 104—109.

13. О состоянии санитарно-эпидемиологического благополучия в Пермском крае в 2020 году: Государственный доклад – П.: Управление Роспотребнадзора по Пермскому краю, ФБУЗ «Центр гигиены и эпидемиологии в Пермском крае», 2021. — 260 с.

14. О состоянии санитарно-эпидемиологического благополучия в Свердловской области в 2019 году: Государственный доклад – Управление Федеральной службы по надзору в сфере защиты прав потребителей и благополучия человека по Свердловской области, 2020.–254 с.

15. О состоянии санитарно-эпидемиологического благополучия в Удмуртской Республике в 2020 году: Государственный доклад – Управление Федеральной службы по надзору в сфере защиты прав потребителей и благополучия человека по Удмуртской Республике, 2021.186 с.

16. О состоянии санитарно-эпидемиологического благополучия населения в Российской Федерации в 2019 году: Государственный доклад – Федеральная служба по надзору в сфере защиты прав потребителей и благополучия человека, 2020.– 299 с.

17. Оборин М.С., Артамонова О.А. Анализ географических закономерностей распространения клещевого энцефалита и Лайм-боррелиоза на территории России // Вестник Алтайского государственного аграрного университета № 1 (135), 2016. С. 87-92.

18. Попов И. О. Климатически обусловленные изменения аутэкологических ареалов иксодовых клещей Ixodes ricinus и Ixodes persulcatus на территории России и стран ближнего зарубежья: автореферат диссертации на соискание ученой степени кандидата биологических наук.– Москва, 2016. – 22 с.

19. Ревич Б.А., Малеев В.В. Изменения климата и здоровье населения России: Анализ ситуации и прогнозные оценки. – М.: ЛЕНАНД, 2011. – 208 с.

20. Semenza, J. C. Vector-borne diseases and climate change: A European perspective / J. C. Semenza, J. E. Suk // FEMS Microbiology Letters. – 2018. – Vol. 365. – No 2. – P. 1–9.

DOI 10.34660/INF.2022.86.88.188

电动巴士充电器的双向转换器仿真
SIMULATION OF A BIDIRECTIONAL CONVERTER FOR AN ELECTRIC BUS CHARGER

Vorobyov Alexander Alfeevich
Doctor of Technical Sciences, Professor

Sychugov Anton Nikolaevich
Postgraduate

Wang Meilun
Master's degree Student

Wang Peng
Master's degree Student

Emperor Alexander I St. Petersburg State Transport University

抽象的。 本文讨论了为电动巴士充电器建模双向转换器的主要方法。 DC-DC 降压-升压电源转换器是一种有前途的为电动巴士电池供电的拓扑结构

关键词：DC-DC Buck-Boost 功率转换器，电动总线，仿真。

Abstract. *The article discusses the main approaches to modeling a bidirectional converter for an electric bus charger. A promising topology for powering a battery for an electric bus is the DC-DC Buck-Boost Power Converter*

Keywords: *DC-DC Buck-Boost Power Converter, electric bus, simulation.*

One of the ways to improve the environmental component of modern megacities is the organization of the operation of urban electric transport, which uses batteries or an energy-efficient electric drive to power it.

Electric buses use several types of energy storage devices. The first electric buses used batteries. The charge accumulated in them made it possible to work in parallel with the internal combustion engine, unloading it at times of peak loads.

The advent of lithium-ion batteries on the market has expanded the possibilities of electric vehicles, since the capacity of these batteries is much larger.

For example, KAMAZ uses lithium batteries for its electric buses.

The main indicators of a battery using lithium titanate are:

- capacity — 40 A/h;
- energy intensity — 17.6 kW/h;

• number of charge-discharge cycles at 50% DOD, not less than — not less than 15 thousand;
• maximum continuous charge/discharge current - 120 A;
• maximum voltage (charging) - 512 V;
• drive usage range according to SOC — 5-95% (DOD 90%);
• climatic design and placement category according to GOST 15150-69 - U2;
• operating temperature range without heating -30…+40oC;
• operating temperature range with heating -40…+40oC;
• shell protection according to GOST 14254-96 - IP65;
- explosion and fire safety.

An alternative to batteries is a capacitive storage based on modules of electrochemical capacitors - supercapacitors. This is a new technology that has already proven itself well and has great prospects.

Lithium-ion batteries are actively used, but now it is clear that they have a smaller resource, supercapacitors. A typical battery life of a modern bus with forwarding office is 6 years, while the life of the bus itself (body, mechanism) is at least 10-12 years. During the operation of the electric bus, the consumer must change the powerful battery at least once. And supercapacitors do not require replacement during the entire life of the bus.

Advantages of a capacitor type drive:
• high specific weight and volume power;
• resistance to overvoltage and overcharging without failure
- safety in operation;
- low level of self-discharge;
- wide operating temperature range,
• maintenance is not required during operation;
• high reliability of products, confirmed by many years of bench tests and operation by consumers.

Battery discharge model

To study the operating modes of the traction battery, several computer models have been developed. One of the models allows you to explore the process of battery discharge (Figure 1).

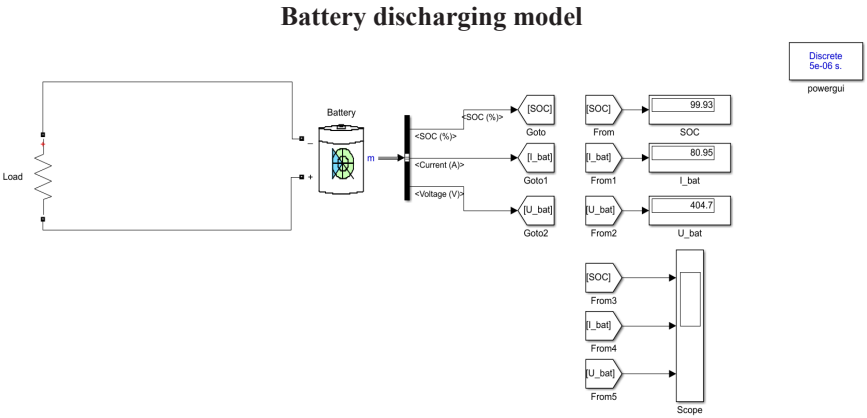

Figure 1. *Model for the study of battery discharge processes*

The following characteristics are adopted in the model (Figure 2).

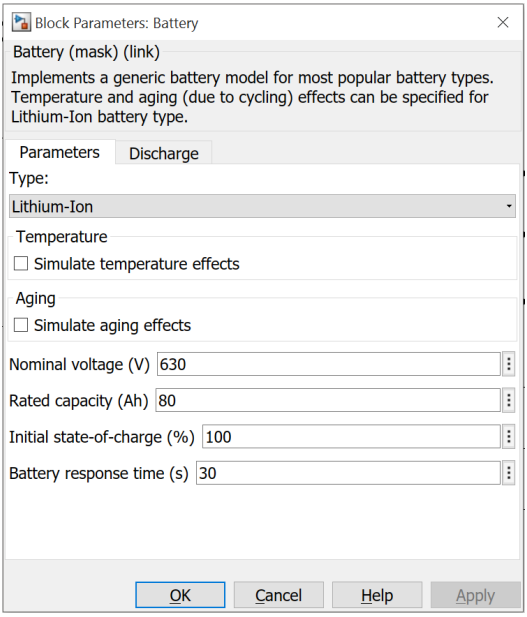

Figure 2. *Battery parameters PP800-705*

The discharge characteristics of the battery are shown in Figure 3.

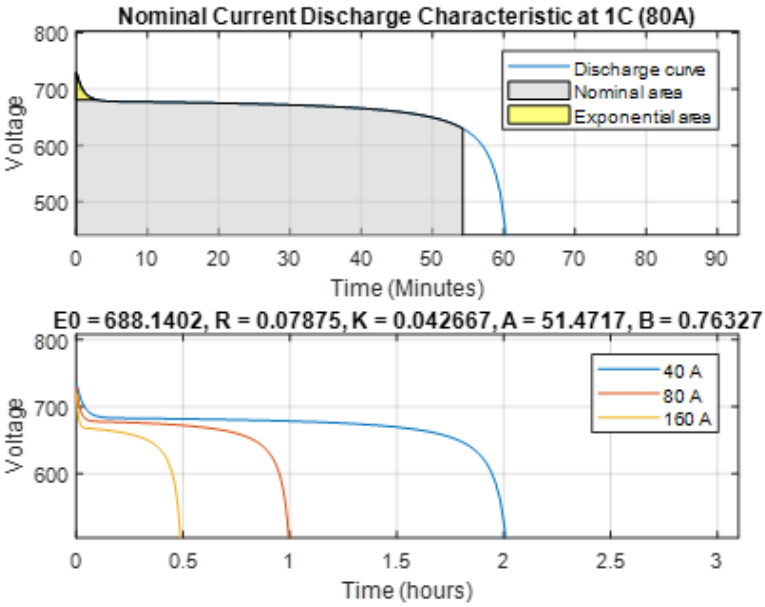

Figure 3. *Discharge characteristics of the PP800-705 battery*

Battery charge model

Similarly, a model was compiled to study the charging characteristics of the battery (Figure 4).

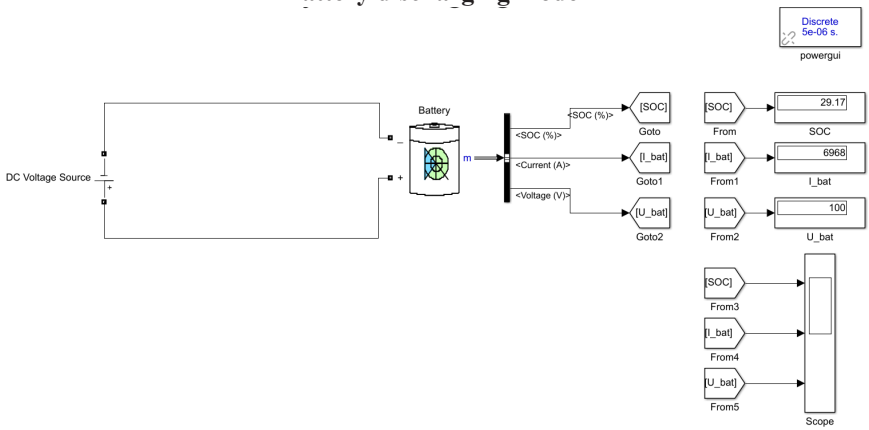

Figure 4. *Model for the study of battery discharge processes*

The process of charging the battery requires mandatory control of the current and voltage of the battery. Therefore, this model must include an electronic converter.

A promising topology for powering a battery for an electric bus is the DC-DC Buck-Boost Power Converter. The circuit contains four transistors operating synchronously in pairs. The control algorithm proposed here is based on combined feedback (CF) and data communication activities. Also, such parameters of the operation of the control system as the possibility of rejecting disturbances were studied.

A diagram showing the functionality of the DC-DC Power converter is shown in Figure 5. Such energy converters are needed in a huge number of electrical devices, which, on the one hand, is an incentive for this project, and on the other hand, also explains why everyone on this topic there is still a lot of research going on. The converters currently on the market have achieved very high efficiencies, but the main goal of this project is to take the never-ending quest for even higher efficiencies a step further by using a new converter topology and modern control methods along with the appropriate selection topology.

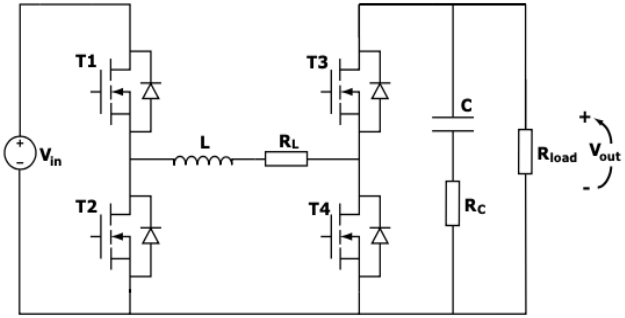

Figure 5.5. *DC-DC Power Converter Topology*

Consider Figure 5, which shows the circuit topology used for this project. It can be divided into two separate voltage conversion stages: increasing "boost" and decreasing "buck".

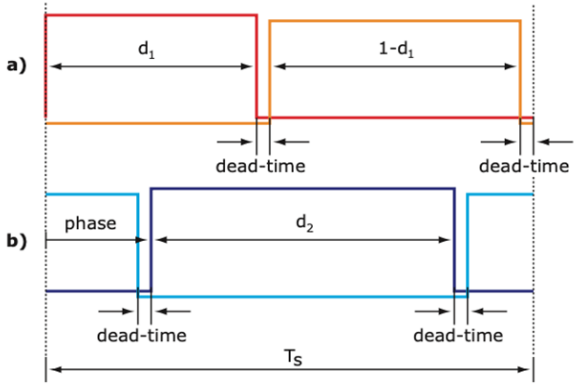

Figure 6. *Converter operation algorithm*

Control signals received for a certain selection (d1,d2,φ); (a) depict the signals sent to the first pair of transistors (T1 and T2), while (b) shows the signals sent to T3 and T4.

Duty cycle (d1 and d2) and phase are important variables influencing circuit behavior because they are actually variables that will be controlled to achieve the desired voltage output. Two surfaces showing how the vout/vin coefficient behaves with respect to the variables (d1 , d2 , φ) at steady state are shown in Figures 6 a) and b).

It is important to note that in order to avoid the appearance of both transistors (which would lead to a short circuit), short periods of time are introduced between switching, during which both transistors turn off; these are the so-called dead-time. This way of working is called synchronous.

The time during which T1 turns on (and therefore T2 turns off) is referred to as d1. Since all switches operate in a cyclic manner (as is usually the case in power converter designs), d1 is actually a fraction of the time during the cycle that T1 operates. To give an example, d1 = 0.2 means that T1 is at 20% of the time of the entire cycle, and is commonly referred to as the T1 duty cycle. So, unless a small idle time is chosen, 1 d1 is the amount of time that T2 is on (i.e. T2's "duty cycle"). The same principle applies to the second stage, when the period of time during which the T3 passes is denoted as d2 (and therefore 1 d2 is the time during which T4 passes).

To study the electromagnetic processes occurring in the system "power source - converter - battery" during battery charging, a computer model has been developed. Since the process of charging the battery is being studied, therefore the model contains only the "buck-leg" (Figure 7).

Battery discharging model
with biderectionak dc/dc converter

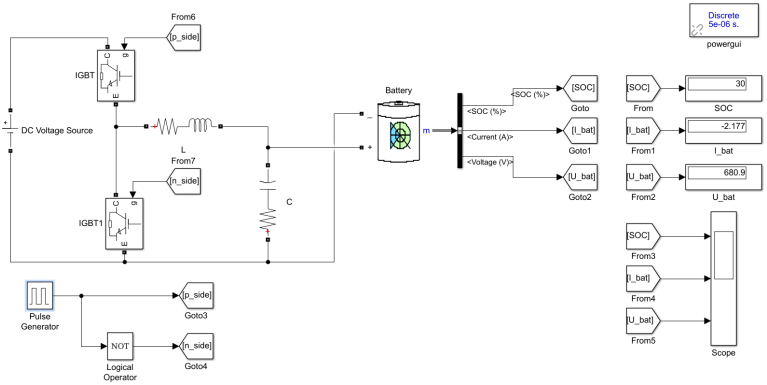

Figure 7. *Model for studying battery charging processes with DC-DC Buck-Boost Power Converter*

Since the internal resistance of the battery is negligible, and the charging process requires very strict control of the charging current and voltage level, this model turns out to be inconvenient, since it requires setting the duty cycle for the control pulse generator.

Battery discharging model with biderectionak dc/dc converter
with PID-controller

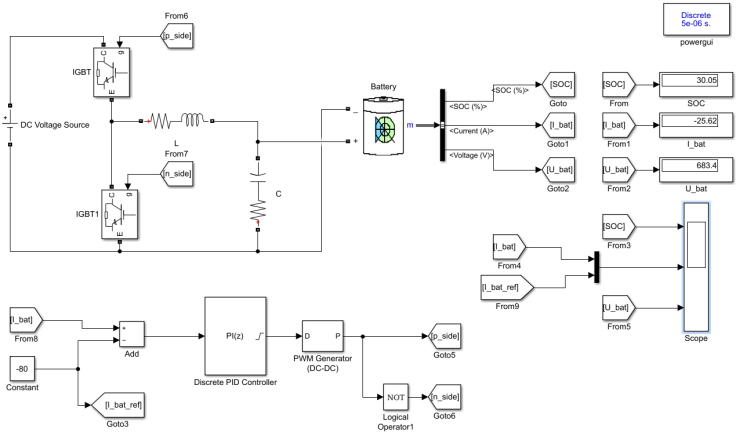

Figure 8. *Model for studying battery charging processes with a DC-DC Buck-Boost Power Converter with a PID controller*

Since the internal resistance of the battery is negligible, and the charging process requires very strict control of the charging current and voltage level, this model turns out to be inconvenient, since it requires setting the duty cycle for the control pulse generator.

The coefficients of the PI controller (Figure 9) are chosen in such a way as to provide an aperiodic process when the charging current setting changes. With the specified settings, the regulation time is not more than 0.05 seconds, the aperiodic transient process and the regulation error are not more than 2A (Figure 10).

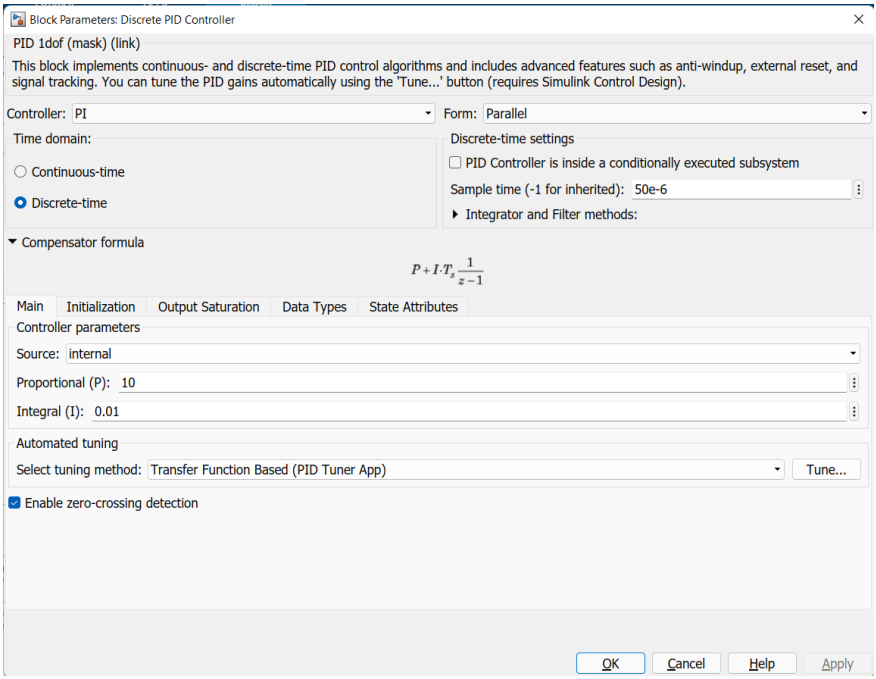

Figure 9. *PI-controller settings*

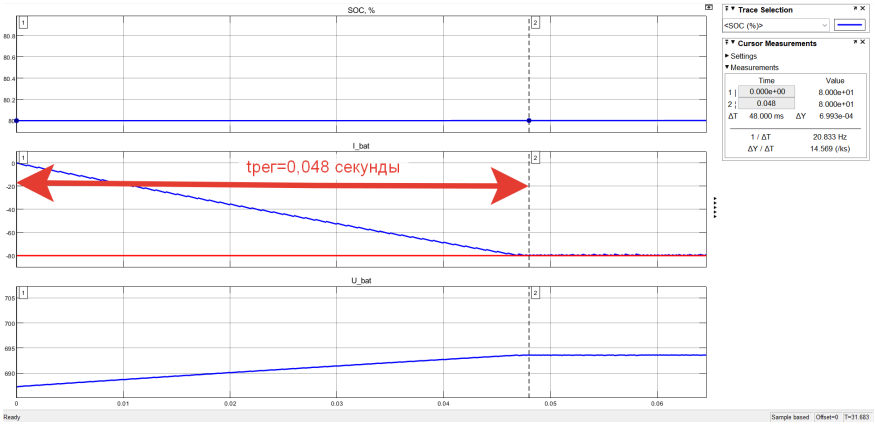

Figure 10. *Transient process with parameters: SOC=80%, charging current 80 A.*

Figure 11 shows the process of charging a battery with an initial level of SOC=80%. To demonstrate the speed and quality of regulation, the process of charging with a current of 0.5C, 1C, 2C is simulated, which corresponds to 40A, 80A and 160A.

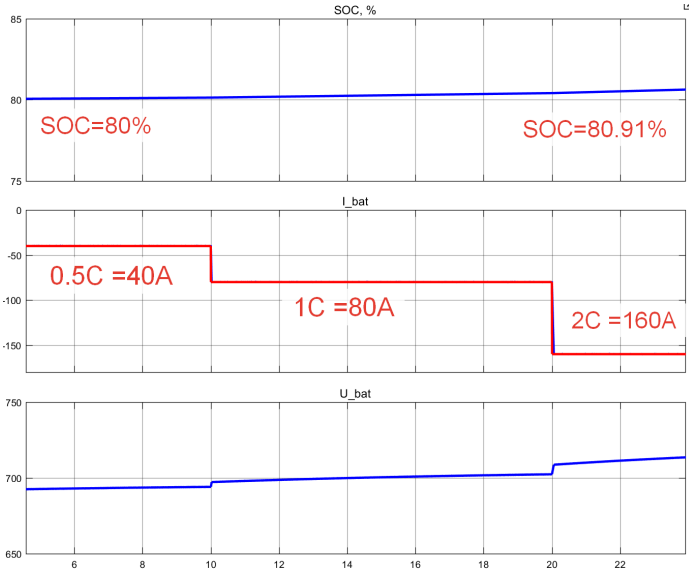

Figure 5.11. *Current Charging Process 0.5C, 1C, 2C*

References

1. Yevstafiev, A.M. Hybrid traction drive systems [Text] / A.M. Evstafiev, I.Yu. Evstafiev // In the collection: Intelligent systems in transport collection of materials of the V International Scientific and Practical Conference. – St. Petersburg, PGUPS, 2015. – P. 363-366.

2. Evstafiev, A.M. Innovative control systems for electric rolling stock [Text] / A.M. Yevstafiev, T.S. Titova // Railway transport. 2017. No. 11. P. 54-59.

3. Yevstafiev, A.M. On the use of supercapacitors [Text] / A.M. Evstafiev // Railway transport. – 2010. – No. 2 – P. 31-32.

4. Yevstafiev, A.M. Improving the energy efficiency of a hybrid locomotive [Text] / A.M. Evstafiev // Electronics and electrical equipment of transport. – 2015. No. 2. P. 6-10.

5. Evstafiev, A.M. Application of capacitive storage on electric rolling stock [Text] / A.M. Evstafiev // Abstracts of the Fifth International Symposium "Electrification, innovative technologies, high-speed and high-speed railway transport Eltrans'2009". – St. Petersburg, PGUPS, 2009. – P. 537-545.

5. Yevstafiev, A.M. Application of supercapacitors on electric rolling stock [Text] / A.M. Evstafiev // Electronics and electrical equipment of transport. – 2009. – No. 1. – P. 16-19.

6. On the use of traction batteries at autonomous substations of urban electric transport / T. P. Satsuk, V. A. Sharyakov, O. L. Sharyakova [et al.] // Elektrotekhnika. – 2021. – No. 10. – P. 32-36. – EDN ZRRYDB.

DOI 10.34660/INF.2022.59.74.189

富含真菌 Eurotium cristatum 代谢物的葡萄酒饮料
WINE DRINK ENRICHED WITH METABOLITES OF THE FUNGUS EUROTIUM CRISTATUM

Nesterov Egor Dmitrievich
Moscow State University of Food Production
Tuchkova Svetlana Nikolaevna
Moscow State University of Food Production
Skorodumov Alexander Sergeevich
General Director
"Bavar+" LLC

抽象的。 今天，葡萄酒饮料在葡萄制成的酒精产品市场中占据越来越大的份额，这就是为什么需要发明富含生物活性成分的葡萄酒饮料。 研究携带大量此类化合物的成分是目前最紧迫的任务之一，因为它将使我们能够提供一种对人体有用的传统葡萄酒饮料的替代品。 这些化合物的来源是菌丝真菌 Eurotium cristatum 的培养物，其代谢物具有广泛的功能特性。

关键词：葡萄酒饮料，Eurotium cristatum，功能性，提取物

Abstract. *Today, wine drinks occupy an increasing part of the market segment of alcoholic products made from grapes, which is why there is a need to invent wine drinks enriched with biologically active components. The study of ingredients that carry a large number of such compounds is currently one of the most urgent tasks, since it will allow us to present an alternative to traditional wine drinks that is useful for the human body. The source of such compounds is the culture of mycelial fungus Eurotium cristatum, the metabolites of which have a wide range of functional properties.*

Keywords: *wine drink, Eurotium cristatum, functionality, extracts*

Introduction

The category of wine drinks includes not only flavored wines with distinctive organoleptic properties, but also drinks with a certain functional potential. The increased content of biologically active substances (BAS) in such drinks is achieved due to the introduction of aromatic raw materials, medicinal plants, beekeeping products, fruit and berry raw materials and some other ingredients into the formulations.

Such drinks include vermouth, fruit, honey wines, etc.

One of the promising sources of BAS is the post-fermented Chinese Hei Cha tea, which is obtained by microbial fermentation with E. cristatum mycelial fungus. The metabolites of this fungus accumulate in the biomass of the fermented raw material during microbial fermentation, have many pharmacological and physiological properties, and significantly affect the flavor profile of the product. Modern medical studies have shown that the metabolites of this culture have an antimicrobial effect, an antioxidant effect, prevent the development of diseases such as diabetes and obesity, prevent the development of thrombosis, and have a cardioprotective, hepatoprotective, oncoprotective effect. [1, 2, 3, 4] Therefore, the study of the possibilities of creating new functional drinks, including wine ones, is an urgent task for the food industry. The purpose of this study was to use the fungus E. cristatum in the formulation of wine drinks.

Materials and methods of research

Vietnamese black fine fermented tea ("Mai" company)

Wine material table ordinary white varieties "Muscat" of 2021 harvest.

E. cristatum fungus culture previously isolated from Fujian tea produced in Anhua province, China, identified by morphological and molecular genetic features as Eurotium cristatum, anam. Asperqillus cristatus, №INA 01267

Malt wort, unhopped, with a solids content of 8%.

Extracts of water wormwood, lemon, orange, peppermint.

Organoleptic parameters were determined according to GOST ISO 3972-2005 [5]

Cultivation was carried out for 5 days at a temperature of 30 °C with constant stirring and aeration.

Tea leaves with a moisture content of 80% and grape pulp weighing 50 g for each sample were sterilized at a temperature of 121 °C for 30 minutes, inoculated with a culture of E. cristatum grown on malt wort at a dosage of 1 × 102 CFU/g of leaf dry matter. Fermentation was carried out for 14 days at a temperature of 30 °C. Culture growth was monitored visually by the presence of golden colonies.

Drying was carried out at a temperature of 56 °C and the obtained samples were stored.

Tea extractivity was determined by infusing a sample of 5 g of dry tea with water at a temperature of 90 °C for 15 minutes. The dry matter content in the extract was determined pycnometrically.

The content of phenolic substances was determined with the Folin-Ciocalteu reagent [6]

The redox potential was determined using an ORP meter ORP-200.

Results and discussion

To obtain extracts containing metabolites of the fungus E.cristatum, black tea was inoculated with a suspension of the fungus, cultured for 14 days at a temperature of 30 ℃. The resulting tea was dried at 56 ℃ for 72 hours. Extractivity, content of phenolic compounds and redox potential were determined in dried tea. The results obtained are shown in table 1.

Table 1.

Comparison of physical and chemical parameters of tea before and after fermentation

	Phenolic compounds, %	**ORP**	**Extract, %**
Tea fermented	21.6	93	0.398
Tea unfermented	10.4	46	0.098

Organoleptic evaluation showed that after fermentation, the tea has a pronounced fruity, floral bouquet with earthy notes. The increase in the yield of the extract also affected the organoleptic.

To determine the optimal fermentation time, the dynamics of changes in the yield of extract and organoleptics was studied for 14 days. Samples were taken every 48 hours, the extract yield and organoleptic properties were determined. The results obtained are presented in table 2 and table 3.

Table 2.

Dynamics of changes in the extract yield

	Day 2	**Day 4**	**Day 6**	**Day 8**	**Day 14**
Extract yield, %	0.257	0.427	0.321	0.103	0.398

Table 3.

Dynamics of organoleptic changes

	Control	**Day 2**	**Day 6**	**Day 8**	**Day 14**
Intensity	3	5	6	8	9
Brightness	2	5	4	7	8
Astringency	2	1	1	1	1
Completeness	1	3	3	8	9
Fruitiness	0	3	5	5	6
Woodiness	7	0	1	1	1
Earthiness	-	3	2	1	2

As can be seen from the data obtained, fermentation has a significant impact on the yield of extractives and changes in organoleptics. On the 6th day, a significant increase in the yield of extractives was noted, a decrease by 8 and an increase by 14, which is associated with the growth stages of the filamentous fungus.

At the next stage, the influence of microbial fermentation on the quality indicators of grape pulp was studied, since they are close in organoleptic to the wine material and their introduction into the wine material will positively affect the quality of the drink.

Table 4.

Comparison of the chemical composition of black tea and grape pulp

	Black tea	**Grape pulp**
Total content of phenolic compounds, mg of gallic acid 100 g of feedstock	554	874
Total content of flavonoids, mg of catechin 100 g of feedstock	1280	267
Mass fraction of sugars, %	0.0093	16.36

As can be seen from the table, tea and grape pulp are characterized by a high content of phenolic compounds, flavonoids; grape pulp has an increased content of sugars. Based on this, it can be concluded that the microbial fermentation of grape pulp by the fungus E. cristatum will have a similar character due to similar indicators.

Grape pulp weighing 50 g was sterilized at a temperature of 121 ℃ for 30 minutes, inoculated with a culture of E. cristatum grown on malt wort at a dosage of 1×10^2 CFU/g of pulp. Fermentation was carried out for 14 days at a temperature of 30 ℃. Culture growth was monitored visually by the presence of golden colonies.

On the 4th day, active growth was observed, the mass appearance of light golden colonies.

The fermented pulp was dried at 56 ℃ for 12 hours.

The dried pulp was extracted with a wine-alcohol mixture and infused for 21 days. Alcoholic infusion was filtered and added to the wine material. The characteristics of the infusion are presented in table 5.

Table 5.

Organoleptic properties of fermented pulp infusion

	Appearance	**Colour**	**Taste**	**Aroma**
Alcoholic infusion of fermented grape pulp	Transparent	Amber with glitter	Soft, grapey, floral	Dried fruit

At the next stage, recipes for wine drinks were developed. Extracts of wormwood, lemon, orange and peppermint were introduced as additional sources of biologically active substances. Biochemical composition, organoleptic and biologically active [7, 8, 9, 10] properties are shown in Table 6.

Table 6.

Characteristics of the developed formulations

Sample number	Colour	Taste	Aroma	Functional orientation	Volume fraction of extracts, cm^3/dm^3
1	Golden, glittery	Pronounced citrus, with a slight bitterness	Wormwood-orange, harmonious	Antioxidant, antimicrobial, soothing	10
2	Golden, glittery	Too bitter, weak citrus	Bright wormwood, pungent menthol	Antimicrobial, soothing	14
3	Golden, glittery	Harmonious citrus-herbaceous	Lemon-orange, fresh, menthol	Antioxidant, antimicrobial, soothing	11
4	Golden, glittery	Spicy citrus	Pronounced orange	Antioxidant, antimicrobial,	12

A tasting assessment was carried out. Samples № 1 and № 3 showed the best results.

The obtained results showed the possibility of creating a wine drink enriched with E. cristatum metabolites with high organoleptic characteristics.

References

1. Peng, Y., Xiong, Z., Li, J., Huang, J. A., Teng, C., Gong, Y., & Liu, Z. (2014). Water extract of the fungi from Fuzhuan brick tea improves the beneficial function on inhibiting fat deposition. International Journal of Food Sciences and Nutrition, 65(5), 610-614.

2. Chen, G., Wang, M., Xie, M., Wan, P., Chen, D., Hu, B., ... & Liu, Z. (2018). Evaluation of chemical property, cytotoxicity and antioxidant activity in vitro and in vivo of polysaccharides from Fuzhuan brick teas. International journal of biological macromolecules, 116, 120-127.

3. Li, P., Zhu, X., Xiao, M., Su, Y., Yu, S., Tang, J., ... & Cai, X. (2022). Rapid Isolation and Hypoglycemic Activity of Secondary Metabolites of Eurotium cristatum by High-Speed Countercurrent Chromatography. Journal of Chromatographic Science.

4. Xiao, Y., Li, M., Wu, Y., Zhong, K., & Gao, H. (2020). Structural characteristics and hypolipidemic activity of theabrownins from dark tea fermented by single species Eurotium cristatum PW-1. Biomolecules, 10(2), 204.

5. GOST R ISO 3972-2005 Organoleptic analysis. Methodology. Method for the study of taste sensitivity from December 29, 2005 - docs.cntd.ru

6. Nikolaeva, T. N., Lapshin, P. V., & Zagoskina, N. V. (2021). METHOD FOR DETERMINING THE TOTAL CONTENT OF PHENOLIC COMPOUNDS IN PLANT EXTRACTS WITH THE FOLIN-DENIS REAGENT AND THE FOLIN-CHOCALTEU REACTIVE: MODIFICATION AND COMPARISON. Chemistry of plant raw materials, (2), 291-299.

7. Sokolova, A. V., Ivanchenko, O. B., & Khabibullin, R. E. (2016). Use of natural antioxidants as micronutrients in foods. Bulletin of Kazan Technological University, 19(24), 157-159.

8. Sokolova, A. V., & Ivanchenko, O. B. (2017). DETERMINATION OF ANTIOXIDANT ACTIVITY OF CITRUS FRUIT PEEL. In SPbPU Science Week (pp. 85-87).

9. Khanina, M. A., & Khanina, M. G. (2018). Wormwood of Siberia and the Far East (chemical composition, taxonomy, biological activity).

10. Uranov, I. O., & Zainutdinov, D. R. (2017). Study of the antioxidant activity of plant raw materials of peppermint, introduced in the Astrakhan Oblast. In TECHNOCONGRESS (pp. 13-14).

DOI 10.34660/INF.2022.69.62.190
UDC 627.8:624.145.4

秋明州卡拉苏尔河流域径流形成过程

PROCESSES OF RUNOFF FORMATION IN THE KARASUL RIVER WATERSHED, TYUMEN OBLAST

Fomicheva Nyailya Nikolaevna
Candidate of Technical Sciences, Associate Professor
Himich Danil Vladislavovich
GTP undergraduate
Siberian State University of Water Transport, Novosibirsk, Russia

抽象的。 本文介绍了秋明州卡拉苏尔河洪水水位线中积雪供应份额的评估数据，并给出了最大径流的统计计算。

关键词：最大径流，最大流量曲线，积雪量，洪水过程线。

Abstract. *The article presents data on the assessment of the share of snow supply in the flood hydrograph of the Karasul River in the Tyumen Oblast, and statistical calculations of the maximum runoff are also given.*

Keywords: *maximum runoff, curves for maximum discharges, snow reserves, flood hydrograph.*

The Karasul River is the left tributary of the Ishim River and flows through the Tyumen Oblast. The length of the river is 128 km; the catchment area is 2660 km2. Belongs to the category of small rivers. According to the water regime, the Karasul River belongs to the rivers with a pronounced spring flood. The peak of the flood is observed in April, the water stays on the floodplain for about 7 days. The thickness of the snow cover varies from 0.2÷0.3 m in open areas to 0.5÷0.8 m in forested areas.

The purpose of the presented work is to estimate the share of snow supply in the flood hydrograph. To solve this problem, it is necessary: to collect data on snow reserves; to analyze the conditions for the formation of a hydrograph in the alignment of the Strekhnino gauging station.

A reasonable forecast of water discharges of small rivers in the spring can be based on the prediction of snowmelt. The processes of runoff formation in the watershed are thus based on models of the formation of snowmelt runoff [1, 2, 3].

The discharge of small rivers during the flood period can be determined by the intensity of snowmelt and water yield of river basins. At the same time, the ele-

ments of the water balance are calculated separately for the field and forest parts [3]. The source material includes a set of hydrometeorological data: snow cover; precipitation; air temperature, etc., as well as the flow rate in the outlet section.

The general water balance equation for the flood period can be written as

$$y = x - p, \tag{1}$$

where y – runoff; x – precipitation; p – losses.

The calculation of the intensity of snowmelt h_c was proposed by V. D. Komarov [4]. Under the conditions of a homogeneous basin and based on the linear relationship between snow reserves at the beginning of snowmelt and the sum of positive air temperatures for this period, we obtain:

$$h_c = \begin{cases} \alpha t \\ 0 \text{ при } t \le 0 \end{cases} \tag{2}$$

Popov E.G. Proposes to determine the intensity of snowmelt per day as a sum separately for daytime and nighttime hours [3].

To assess the share of snow supply in the formation of the hydrograph of the Karasul River near the Strekhnino water station, it seems necessary to perform a statistical assessment of the observational data, as a result of which to obtain probabilistic characteristics of the runoff.

The data of characteristic costs for a 33-year series [5] were processed. The average annual flow rate is 2.9 m³/s; in an average year in terms of water content, the river brings 91.47 million m³.

Having the highest measured water discharges in the river in each year, it is possible to perform a statistical analysis of a series of maximum discharges. As a result, the runoff rate is $Q_0^{\max} = 51,51$ m³/s, and the temporal variability of the maximum discharges according to the coefficient of variation is

$$C_\upsilon = \sqrt{\frac{\sum (k_i - 1)^2}{n}} = 0,66. \tag{3}$$

At the same time, an estimate of the root-mean-square errors of calculating the norm and coefficient of variation was obtained:

$$\delta_{Q_{\max}} = \frac{100 C_\upsilon}{\sqrt{n}}; \tag{4}$$

$$\delta_{C_\upsilon} = \frac{100}{4C_\upsilon^2 + n} \sqrt{\frac{n\left(1 + C_\upsilon^2\right)}{2}}; \tag{5}$$

$$\delta_{Q_{\max}} = 11,32\%; \quad \delta_{C_\upsilon} = 13,71\%.$$

The selection of the asymmetry coefficient showed that for the studied series $C_s = 2C_\upsilon$. Costs of different probability of exceeding in the design range:

$$Q_{0,5\%} = 185\,\text{m}^3/\text{s};\ \ Q_{1\%} = 167\,\text{m}^3/\text{s};\ Q_{5\%} = 122\,\text{m}^3/\text{s}.$$

Curves of security of the maximum expenses are resulted on fig. 1.

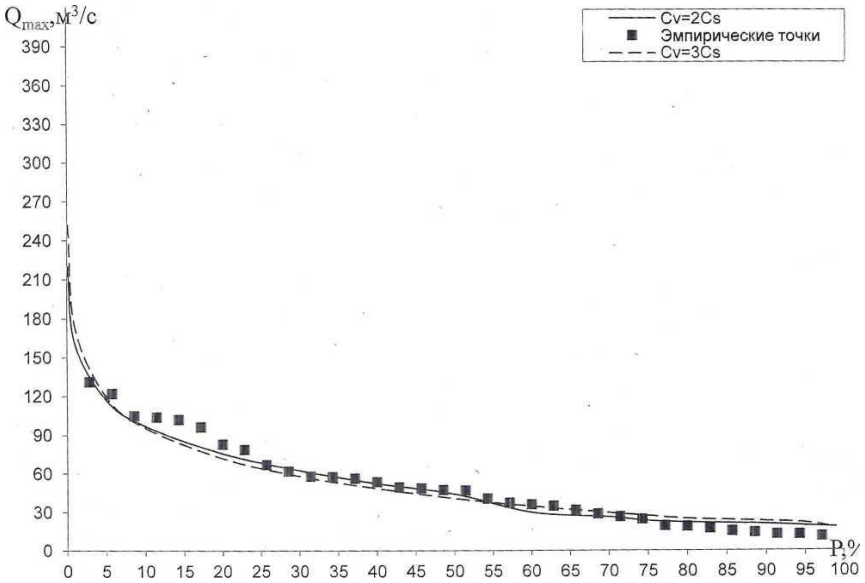

Figure 1. *Theoretical curves and empirical data of maximum discharges in the Karasul river – g/s Strekhnino*

To determine the share of snow nutrition, it is necessary to determine the moisture reserves in the snow cover. The stable snow cover decreases in duration from north to south. The thickness is (0.16÷0.31) m in open areas; (0.5÷0.8) m – on forested [5].

The volume of snow reserves in the watershed is determined by the formula

$$W_c = F \cdot h_c, \qquad (6)$$

where F – the area covered with snow can vary from 0 to 100%. The calculations are shown in table 1.

Table 1.

The volume of snow reserves in the territory of the Karasul river basin. F = 2660 km2

h_s, m	0.16	0.31	0.5	0.8
$W_s \cdot 10^6$, m^3	425.6	824.6	1330.0	2128.0
$W_{\text{water in the snow}} \cdot 10^6$, m^3	46.8	90.7	146.3	234.08

When determining the water reserves in the snow cover, the average value of the snow density was taken. It is known that this characteristic depends on many factors.

The volume of flood runoff at the estimated supply is shown in table 2.

Table 2.

Flood flow volume of the Karasul River

Q_{max}, m^3/s	185.0	167.0	122.0	51.0
$W_n \cdot 10^6$, m^3	479.5	432.8	316.2	132.2

Note: the flood period is assumed to be 1 month.

Analysis of the obtained results allows us to estimate: the share of snow reserves in the basin, which affects the formation of the hydrograph.

So, for example, at a flow rate that was formed once in 200 years, the share of snow supply in the volume of floods can be up to 50%. And for runoff with a frequency of 1 time in 20 years, this value will be up to 80%.

Conclusions:

1. The collection of data on the snow reserves of the studied basin was carried out.
2. Statistical calculations of the probabilities of exceeding the maximum runoff were made.
3. An estimate of the proportion of snow reserves in the study area involved in the formation of spring flood runoff is given.

References

1. Motovilov Yu. G., Gel'fan A.N. Models of Runoff Formation in the Problems of Hydrology of River Basins. – M.: IWP RAS, 2018. – 296 P.

2. Kuchment L.S. River runoff (genesis, modeling, prediction). – M., 2008. – 394 P.

3. Methods for calculating and predicting floods for a cascade of reservoirs and river systems. Edited by E. G. Popova, Leningrad, Gidrometizdat, 1977. 129 P.

4. Komarov V. D., Makarova T. T., Sinegub E. S. Calculation of the flood hydrograph of small lowland rivers based on data on the intensity of snowmelt. – "Op. Hydrometeorological Center", 1969, iss. 37, P. 3-30.

4. The official website of the monitoring of water bodies "AIS GMVO" (electronic resource). – Access: https://gmvo.skniivh.ru.

DOI 10.34660/INF.2022.54.19.191

基于运行状态估计的水力发电机控制
HYDROELECTRIC GENERATOR CONTROL BASED ON THE ESTIMATE OF ITS OPERATING STATE

Lyubanova Anna Sholomovna
Candidate of Physics and Mathematics, Associate Professor
Matorin Michael Andreevich
Student of master's course
Siberian federal university

抽象的。 我们基于控制水轮发电机的数学模型和 SimInTech 程序中的过程模拟建模结果讨论液压单元控制的基本原理。 决策规则基于使用模糊逻辑技术对液压单元的运行状态进行评估，以评估运行状态。

关键词：水轮发电机 运行状态 预防控制 决策规则 模糊逻辑

Abstract. *We discuss the basic principles of hydraulic unit control based on mathematical model of controlling a hydroelectric generator and the results of simulation modeling of the process in the SimInTech program. Decision-making rules are based on the assessment of the operational state of the hydraulic unit using a fuzzy logic technique for assessing the operating state.*

Keywords: *hydroelectric generator, operating state, preventive control, decision-making rules, fuzzy logic*

Introduction

A modern hydroelectric power plant is the system of hydraulic structures and equipment for the conversion of the water flow power into the electrical energy. A significant advantage of the hydroelectric power plants is their ability to reach full power in a short time. The control of operation modes calls for the estimation of the hydroelectric generator operate reliability. This task is multipurpose. Therefore the management of hydroelectric power plants receives much attention.

Management in hydroelectric power plants is fully automated. Automation ensures more efficient use of energy resources by maintaining the specified operation mode with higher accuracy, choosing the optimal number of operating units and more practical load distribution between hydroelectric stations. The efficiency of using energetic resources can also be increased by the decision time reduction. Automation makes it possible to avoid the light running of supplementary equip-

ment and decrease energy consumption for own needs. Automatic continuous in time monitoring of the state of the working equipment and hydraulic structures allows to detect any deviations from the normal mode in a short time. Such control makes it possible to involve the backup mechanisms, send warning signals for the employee and, if necessary, completely disable the equipment.

At present time all studies on the automation of hydroelectric power plants can be devided on three groups. The first group is concerned with the development of the cellular strategy in the management of hydroelectric stations operate reliability [1]. The second group includes the methods of operating state analysis and decision making in the case of damage or accident in hydroelectric station. In [2, 3], a method of formalizing the information on the operating state is proposed for the hydroelectric generator. The method is based on the fuzzy intervals for the operating state parameters. The third group joins metogological and software tools concerning with the systems of hydroelectric generator control [4].

This work is devoted to the control of the hydroelectric units with analysis of their operational state. Purpose of this work is to develop computer simulator of hydroelectric unit control with based on the base of the operational state assessment in two states – manual and automatic. Manual mode is intended to familiarize oneself with the principle of the hydroelectric generator state adjustment. Automatic mode is designed as a simulator of automatic regulation of the hydroelectric generator state.

In this work we discuss the basic principles of hydraulic unit control based on mathematical model of controlling a hydroelectric generator and the results of simulation modeling of the process in the SimInTech program. Decision-making rules are based on the assessment of the operational state of the hydraulic unit using a fuzzy logic technique for assessing operational reliability [2, 13].

Simulation of operational reliability

A simulation model of the hydraulic unit control was built, taking into account its operational state in the environment of dynamic simulation of technical systems SimInTech [5]. Several main reliability parameters were chosen as control parameters: transformer oil temperature increase, turbine bearing lubrication consumption, generator symmetrical overloads, etc.

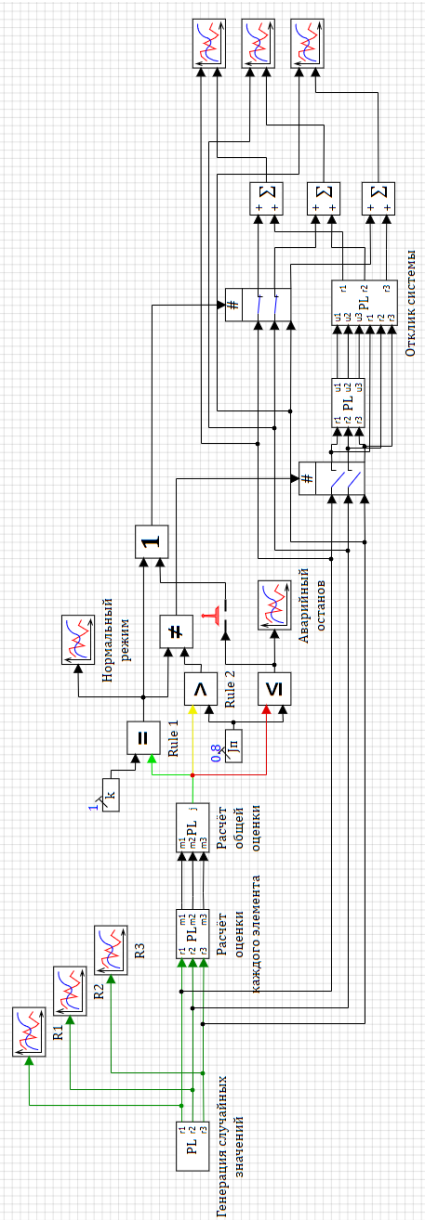

Figure 1. *The simulation model of the hydraulic unit control*

On the preliminary version of the control appearance, the hydroelectric generator state control window is presented. It includes switches for automatic and manual operation of the hydro generator, as well as several data and switches that will work in real time.

During the operation of the hydrogenerator in manual mode, the operator needs to monitor the output data of the hydro generator in real time in order to respond in time to any dangerous situation and make an appropriate decision.

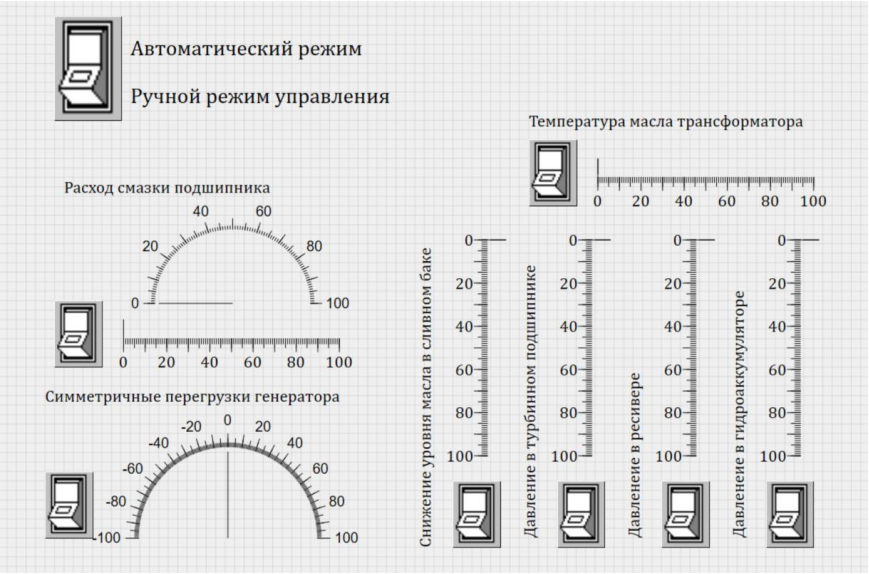

Figure 2. *The window of simulator*

If the operator does not have time to adjust one or another parameter for some time, the system stops abnormally and it is reported that a breakdown has occurred. In automatic mode, in real time, the data is adjusted automatically when the parameter values deviate from the normal mode within acceptable limits.

Each parameter has its own rank (degree of importance). This rank determines the time during which the value of the parameter can be at the boundaries of its allowable range. The higher the rank of the parameter, the less time this parameter can be in the "emergency" mode.

Data were selected for work, using the example of a real hydroelectric power station.

Initial data for several parameters were used to carry out simulation experiments. The preventive control threshold is assumed to be 0.8. In the first experi-

ment, the system generated 13 different values before it went into emergency stop mode. The graphs show that, for example, the temperature on the eighth stroke turned out to be in the preventive control zone.

Since, at certain intervals and at the slightest shift in values from normal, preventive control took place, it is necessary to compare the graphs of the initial and corrected values. In the following figure, graphs are presented in comparison, where the initial data are marked in red, and corrected during preventive management in green.

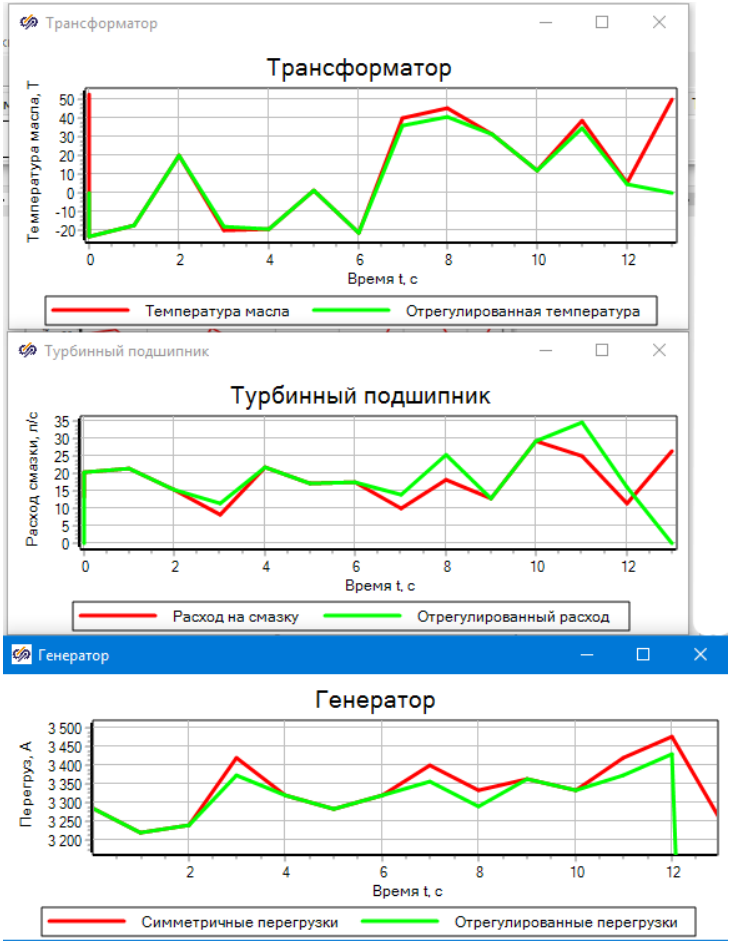

Figure 3. *The results of control simulation*

According to these graphs, it is seen that the adjusted values (from top to the bottom: the transformer, the turbine bearing, generator) became more smoothed (green lines) in comparison with the initial values (red lines), since the preventive control changed the values of the state parameters if the system was on the border of an unstable state.

References

1. Lifar A. S. Otsenka kompleksnoq strategii upravleniya ekspluatatsiey ob'ektov gidroenergiticheskoy otrasly / A. S. Lifar, A. E. Brom // Omskii nauchnii vestnik, 2020. № 1. P. 17 − 21.

2. Sekretarev Yu. A. Osnovniye printsipy i modeli preventivnogo upravleniya gidroagregatami s uchotom ikh ekspluatatsionnogo sostoyaniya / Yu. A. Sekretarev, A. A. Zhdanovich // Journal Sibirskogo Federalnogo Universiteta. Seriya Seriya "Technicheskiye nauki", 2010. № 3. P. 322 − 334.

3. Sekretarev Yu. A. Issledovaniye parametrov ekspluatatsionnoy nadezhnosti gidroagregata s pomoshch'yu teorii necetkikh mnozhestv / Yu. A. Sekretarev, A. A. Zhdanovich // Nauchnii vestnik NGTU, 2010. № 1(38). P. 145 −158.

4. Patent RU 2399787 C1 Russian Federation, MPK F03B 15/08 (2006.01). Sposob adaptivnogo upravleniya skorost'yu vrashcheniya rotora povorotno-lopastnoy turbini / A. S. Goltsov, A. A. Silayev; zayavitel i patentoobladatel Volgogradskii gosudarstvennii tekhnicheskii universitet. − № 2009100458/06; Submitted 11.01.09; Published. 20.09.09, bulletin № 26. − 8p.

5. Matorin M. A. Razrabotka skhemy upravleniya gidroagregatom na osnove otsenki yego ekspluatatsionnogo sostoyaniya / M. A. Matorin, A. Sh. Lyubanova // Visshaya shkola: nauchniye issledovaniya. Materiali Mezhvuzovskogo mezhdunarodnogo kongressa (Moskva, 13 maya 2021 g.). – Moskva: Izdatelstvo Infinity, 2021. P. 149 − 160.

DOI 10.34660/INF.2022.34.51.192

精益生产方法和工具在各行业的实际应用
PRACTICAL APPLICATION OF LEAN PRODUCTION METHODS AND TOOLS IN VARIOUS INDUSTRIES

Fedotova Irina Yurievna
Candidate of Technical Sciences Associate Professor
Blagorodnova Evgeniya Vyacheslavovna
Master
Samara State Technical University

注解。 在分析制造企业的基础上，思考和分析了应用精益制造的实践。 突出精益生产的主要方法。 制定了该方法的实施特点。

关键词：精益制造，生产力，竞争力，损失，方法。

Annotation. *The practice of applying lean manufacturing based on the analysis of manufacturing enterprises is considered and analyzed. The main methods of lean production are highlighted. The features of the implementation of the method are formulated.*

Keywords: *lean manufacturing, productivity, competitiveness, losses, methods.*

Currently, the Russian industry is rich in a large number of competitive industries: oil and gas production, processing of precious stones and metals, aircraft construction, nuclear industry, production of weapons and military equipment, electrical engineering, pulp and paper industry, mechanical engineering, etc.

Today, modern conditions are such that the survival of an enterprise (its sustainable development in the market of goods and services) is determined by the level of competitiveness, which directly depends on the level of price and the level of product quality.

"High" quality goods are in demand on international markets. Goods of "low" quality, in most cases, are not purchased even at the lowest prices.

It is known that lean manufacturing is aimed at reducing the losses that exist at every workplace, regardless of the field of activity, and not reducing costs, which can lead to a decrease in product quality.

Translated from English, "lean" means "lean, fat-free, slim". "Lean Production" ("Lean Manufacturing") is literally "production without fat", production where there are no excesses and losses. In the Russian version, the term Lin was

translated as "lean manufacturing", "lean manufacturing" or simply "Lin" [1].

Lin's ideology implies the organization of lean production, optimization of business processes with maximum orientation to the market and taking into account the motivation of each employee. Lean manufacturing is a broad management concept aimed at eliminating losses and optimizing business processes. Lean production management is maximally focused on identifying the needs of the market and creating maximum value for the client with minimal expenditure of resources: human effort, equipment, time, production space, etc. This approach (from the stage of product development, production and to interaction with suppliers and customers) allows to improve the quality of products and services, to ensure the growth of labor productivity and the level of motivation of personnel, which ultimately affects the growth of the competitiveness of the enterprise.

Let's consider and analyze the procedure for applying lean production methods and tools in practice in various industries.

Gazprom Transgaz Samara LLC

A few years ago, Gazprom Transgaz Tomsk LLC began to apply the concept of lean production, as well as its inherent methods and tools. The realization of the possibility of effective application of this concept in the gas transportation industry, the creation of safe and comfortable conditions at every workplace, visibility in monitoring the availability and maintenance of tools in working condition – all these factors are the goal of the introduction of "Lean Production".

In the process of phased application of the new approach , the following tasks were solved:

• the theoretical aspects of the concept of "lean production" are studied, as well as the experience of domestic and foreign enterprises is analyzed;

• increased level of responsibility, change of approach and attitude of the worker when maintaining his workplace;

• improved visibility during control, ensuring the safety and maintenance of tools in working condition;

• reduced time to select the necessary tool.

Adequate approaches and smart use of appropriate methods can allow any company, regardless of its geographical location, to benefit from Kaizen [2].

A huge step forward was made in Primorsky LPUMG to improve the workplaces of the company's divisions, sorting and visualization of production documentation.

The creation of integrated teams allowed not only to perform tasks faster, but also to extract economic benefits from this through the competent allocation of human resources. For example, earlier the cost of painting the RRS object was 42763.6 rubles. After the introduction of the integrated team, the costs for one

object became significantly lower – 24562.1 rubles. Thus, the economic benefit of servicing a complex team of one object amounted to 18201.5 rubles. Considering that in the area of responsibility of the Primorsky LPUMG, 22 RRS are serviced, the cumulative economic effect reaches 400,433.0 rubles [2].

To improve the safety of working conditions, measures were carried out at the production base of the branch: the ways of movement of vehicles and people were marked, an automatic briefing system was set up through the GGS – for employees and visitors of the enterprise passing through the turnstile (at the checkpoint).

The results of the implementation of the "5S" system continue to bring benefits and benefits in the production activities of the Primorsky LPUMG LLC Gazprom Transgaz Tomsk.

CJSC "AKOM"

The introduction of lean manufacturing has not spared the company CJSC "AKOM" - the domestic leader in the production and sale of batteries in Russia.

Improvements in optimization have made it possible to use materials more efficiently. The documented standardization of all improvements does not allow you to roll back to the initial level.

In order to reduce problems with product quality, technologists and craftsmen were trained in methods for identifying the causes of marriage directly at the place of their occurrence, identifying the root cause. The "point lesson" technique has been developed and introduced into production. Devices that prevent the occurrence of the defect "reversal of the battery case in transport" have been put into operation. The procedure of actions in the SRT is standardized [3].

In the course of bringing the repair box premises to the 5C standard, all unnecessary items were isolated, all equipment, walls were painted, and the floor covering was replaced. Developed, manufactured and installed equipment for working with large-sized nodes. Only the items necessary for repair were left in the room. All racks and fixtures have been identified.

In parallel with the work on the main goals, an analysis of opportunities for improving the environmental aspect of the company's work was carried out.

The result of the introduction of "Lean Production" is a significant increase in the number of offers from staff, reducing or eliminating deficiencies in their workplaces; solving some of the issues of emergency equipment downtime.

JSC "ZMZ"

Over the past couple of years, the growth rate in one of the leading industries in Russia – mechanical engineering has significantly decreased. There are several main problems in this area: low quality of products, worn-out funds, low sales volumes, lack of funds to upgrade equipment.

In 2011, the company in JSC "ZMZ" began the gradual introduction of lean manufacturing elements.

As a result of using such a tool as 5S, visual control (identification of production losses by an employee), special marking of equipment, disciplinary standards appeared at the enterprise.

The implemented Kaizen system at JSC ZMZ is implemented as follows: proposals for improvements are submitted by production personnel and are aimed at improving the quality of products and work performed, improving occupational safety, improving workplace organization and working conditions, reducing costs and increasing labor productivity.

In 2011, a section was formed to implement proposals for improvements. During the implementation period, 23376 such proposals were submitted, of which 18747 were implemented.

The company has recently started using lean manufacturing technologies, but today we can talk about the first results.

As a result of the use of lean manufacturing tools:

• the profitability of the enterprise increased from 1.9% to 11.7%;

• the number of engines rejected at consumer car factories decreased by 7 times;

• the share of losses from internal defects in the total volume of manufactured products has decreased by almost 5 times;

• the number of submitted innovation proposals has increased 3 times;

• the average wage level has increased significantly [4].

Lean manufacturing tools are a set of rules and methods that have been recognized as effective in many companies around the world. One of them is the "Kaizen" system, the "Kanban" method, Just in Time, the 5C method. There are also auxiliary techniques that are used in various combinations and serve to improve the work of personnel and the effective exchange of information between employees (mapping of the production process, visualization), for product quality control (Ishikawa diagram, the "five why" method, etc.), for standardization of the work of the enterprise, etc.

Lean manufacturing is, without exaggeration, the main thing to learn from the Japanese in the field of management. Every manager should know this method regardless of the industry, because the basis of the method is to fight losses, and who can guarantee that there are no inefficient processes, operations or actions in his company? [1]

References

1. Vumek James P., Jones Daniel T. Lean manufacturing. How to get rid of losses and achieve prosperity of your company. -M.,: Alpina Business Books, 2013.

2. Interregional trade union organization "Gazprom Trade Union".

URL: https://xn--80afnaylbafcido5b6k .xn--p1ai/orgs/gazprom_transgaz_tomsk_profsoyuz/events/1808 (accessed 02.05.2022).

3. Practical application of lean production tools at the production enterprise of JSC "AKOM".

URL: https://up-pro.ru/library/production_management/lean/akom-praktika / (accessed 14.10.2021).

4. Methodological materials for the site "Career" of the International Youth Camp "Baikal 2020" "FUNDAMENTALS of LEAN PRODUCTION", June 28 – July 5, 2020. p.31.

DOI 10.34660/INF.2022.88.81.193

牵引变压器理论与研究
THEORY AND RESEARCH OF TRACTION TRANSFORMERS

Zhang Qiyan
Master's degree Student
Vasiliev Vitaly Alekseevich
Candidate of Technical Sciences, Associate Professor
Emperor Alexander I St. Petersburg State Transport University

抽象的。 改变供电系统直接供电，使其安全稳定不影响电气

由于标准化运营的快速发展，高速公路需要一个功能更完善、铁路系统性能正常的系统。

因此，适用于铁路微机继电保护装置非常重要。

本文的主要工作是研制电气化铁路变位保护装置并进行相关原理研究。

关键词：电气化铁路牵引变压器的保护

Abstract. *Change the direct power supply to the power supply system, making it safe and stable to affect electrical*

Due to the rapid development of standardized operations, expressways require a system with better functions and normal performance of the railway system.

Therefore, it is very important to be suitable for the microcomputer protection relay device of the railway.

The main work of this article is to develop a change protection device for electrified railways and conduct related principle studies.

Keywords: *protection of the transformer of electrified railway traction*

1. Traction transformer protection principle

1.1. Structure of the traction power supply system

The power of the electrified railway is obtained from the public power grid. The structure of the traction power supply system is ordinary. The railway is introduced from the three-phase AC power from the public power grid to the traction substation, and the substation voltage is reduced to 27.5 kV. To get electrical energy from the traction network. The power supply traction system is mainly composed of two parts of the traction substation (including the opening and closing department, the breaking center and the automatic transformer, etc.) and the traction network (including the feed wire, contact network, network, iron circuit,

optimization, etc.). D.).

There are many traction substations on the electrification railway. Each traction substation is fed from the traction network on both sides of the substation. On each side - single-phase electricity. Limited range.

The thaw substation includes separation partition (SP) in the power system, office opening and closing (SSP) and automatic transformer (ATP). The main functions of the section is to implement parallel power up and down parallel power supply, over -zone power supply, and two-way power supply. All commutators can be switched on and closer. The main task of the transformer is to install automatic installation of transformers. The use of an automatic transformer can increase the supply voltage by 50KV, which can expand the power supply distance, reduce the number of traction transformers, reduce construction investment in construction investment

The traction network includes a feeder, a contact network, a track loop and a reverse flow line. Its main task is to connect the circuit to give thermal power to draw the traction substation. The traction supply line is a wire between the traction and the contact network of the traction substation. Its task is to bring power from the traction substation to the contact network;

Set up, power supply in the power locomotive in travel; rails are both carriers driven by locomotives, and there is a wire wire: the task of the return line is the flow back to the traction substation. The current circulation chain is; Current flows from the traction substation, the feed line line flows into the contact network, and flows back to the traction substation by electric locomotive, railway and return lines.

Place.

1.2 Characteristics of power supplies

There is a big difference between power systems and public energy systems. It is specially reflected in the following aspects

1. The social power system is a three-phase AC system, and the power system is a single-phase AC system:

2. Because the lifting system is a single-phase load of the catering system. After decomposing in accordance with the symmetrical components method, most of the negative order is obtained. The existence of a serial weight will adversely affect the protection of the first side relay. Countermeasures to affect negative sequence components:

(1) Transformer with a variety of wiring methods: impedance balance transformation can accommodate the power system

Three-phase electrical power becomes two-phase electricity having a difference of 90°. The advantage of vertical balance conversion is that when the balance balance secondary load is equal to or equal to one side. The three-phase current on

one side is equal and symmetrical, and the negative order current is not included.

(2) Wiring method using the rotation stage: the total negative sequence component is lowered by the maximum rotation.

(3) Trying to avoid relay protection based on the negative order principle, replacing other principles.

3. Due to the input and use of a large number of electrical equipment and the rapid change in traction load and large amplitude, the power supply system can easily produce a large number of harmonics and have a high sealant profile. Improved harmonics and harmonics of the ingegovstream will be unfavorable. Influence of relay protection characteristics: when the higher harmonic content is very good, the measurement current

The actual value is very large, and the impedance measurement will be less than the actual value, so it is easy to enter the protected area, resulting in a distance protection error; exciting operation is easier to defend. Harmonic countermeasures:

(1) installation filter equipment in the traction substation, electric vehicle, relay protection device, minimizing

principles in the system.

(2) Measurement of higher harmonics at the installation device, the harmonics must be exhausted by two harmonic and harmonic suppression.

2. Electrical equipment of traction substations

2.1 Traction substation

The traction substation consists of two independent sources of medium voltage AC, converts AC power into DC power and takes on the function of providing DC traction power for electric trains.

Main wiring on the medium voltage side

Two sets of traction rectifiers are connected to two buses, respectively.

If the voltages of the two bus sections of the traction substation are symmetrical or slightly different, two sets of traction rectifiers are connected to the two bus sections, respectively, and one set of traction rectifiers is 12-pulse rectifier. When the voltage of the two busbars of the traction substation is unbalanced, it is easy to cause the output load of the two sets of traction rectifiers to be unbalanced. Balancing reactors are installed on the output side of the two traction rectifier units to ensure that the output load of the two traction rectifier units is matched.

Practice has proven that the operation of this form of wiring is not ideal, and the error in the supply voltage will lead to difficulties in choosing a traction rectifier unit.

Two sets of traction rectifiers are connected to one busbar.

In order to balance the output load of the two sets of traction rectifiers, the two sets of traction rectifiers are connected to the same medium voltage bus segment,

forming an equivalent 24-pulse rectifier, which is useful for harmonic control. When one group of traction rectifiers fails due to a fault, the other group of traction rectifiers can continue to operate under the condition of a tolerable overload.

(1) Single bus wiring

The single busbar on the medium voltage side of the traction substation is not segmented. Two power supplies are inserted into the busbar, and a medium voltage network structure diagram is created according to the actual conditions and needs of the project

(2) Segment wiring with single busbar

The medium voltage side of the traction substation uses a segmented single busbar connection, and a segmented circuit breaker is also provided. One input power source is introduced into each section of the busbars, and a sectional switch or an emergency connection switch is installed on the medium voltage bus of the traction substation in accordance with the medium voltage network structure diagram

(3) Three segment bus wiring

Install two sections of the input power bus and one section of the working bus of the traction rectifier unit. Two input power buses are respectively connected to I-section and m-section buses, and two sets of traction rectifier units are connected to the working bus of the traction rectifier unit. Two sections of the input power busbar and one section of the working busbar of the traction-rectifier unit are respectively segmented by automatic switches, and automatic shutdown of the two input power sources is carried out through a segment switch

References

1. City rail transit power supply. Southwest University JiaOtong Pressing, 2007.

2. Relay Protection Fund.: Beijing Jiaotong University Press, 2010.

3. Design Principle and Application of Urban Rail Transit Power Supply System, Southwest University Press of Jiaotong University 2008.

DOI 10.34660/INF.2022.21.17.194

电力机车电气设备诊断技术创新
TECHNOLOGICAL INNOVATION IN THE DIAGNOSIS OF ELECTRICAL EQUIPMENT OF AN ELECTRIC LOCOMOTIVE

Li Kexin
Master's degree Student
Fu Peisong
Master's degree Student
Tsaplin Aleksey Evgenevich
Candidate of Technical Sciences, Associate Professor
Zelenchenko Alexey Petrovich
Candidate of Technical Sciences
Emperor Alexander I St. Petersburg State Transport University

抽象的。 本文展示了电气参数和物理特性在诊断电气设备故障的技术方法中的绝对相关性。 确定电气列车电气设备故障诊断技术方法的选用方法和手段。
关键词：电气和机械零件，电动机车车辆，技术诊断。

Abstract. *The article shows the absolute correlation of electrical parameters and physical properties in a technical approach to diagnosing electrical equipment failures. Determine the chosen method and means of the technological method for diagnosing malfunctions of the electrical equipment of the electric train.*
Keywords: *Electrical and mechanical parts, electric rolling stock, technical diagnostics.*

The introduction of diagnostics on the railway transport allows you to significantly reduce the operating costs for the maintenance and repair of rolling stock, choose a rational repair system, taking into account the actual technical condition of components and assemblies of equipment, increase the reliability of rolling stock in operation.

The system of technical diagnostics of locomotives uses methods, means, systems and technological methods of diagnostics based on a number of concepts and definitions established by state standards. Diagnosis is the process of establishing signs that characterize the technical condition of an object - a locomotive, a diesel train, etc., as well as any element, according to external signs or parameters with a

certain accuracy in indicating the location, type and causes of the defect, if any. A statistical or instrumental diagnostic method is used, based on physical, mechanical, chemical and other phenomena that form the basis of information about the state of the object. Diagnostic tools are measuring instruments, consoles, stands and other technical devices. The sequence and methods of applying the methods and means of diagnosing constitute the technology of diagnosing. Technical diagnostic system - a set of objects, methods and means, as well as performers, which allows diagnosing according to the rules established by the relevant documentation. It is an obligatory component of the system of preventive maintenance of locomotives.

Diagnosis is the process of establishing signs that characterize the technical condition of an object - a locomotive, a diesel train, etc., as well as any element, according to external signs or parameters with a certain accuracy in indicating the location, type and causes of the defect, if any. A statistical or instrumental diagnostic method is used, based on physical, mechanical, chemical and other phenomena that form the basis of information about the state of the object. Diagnostic tools are measuring instruments, consoles, stands and other technical devices. The sequence and methods of applying the methods and means of diagnosing constitute the technology of diagnosing [1].

Technical diagnostic system - a set of objects, methods and means, as well as performers, which allows diagnosing according to the rules established by the relevant documentation. It is an obligatory component of the system of preventive maintenance of locomotives.

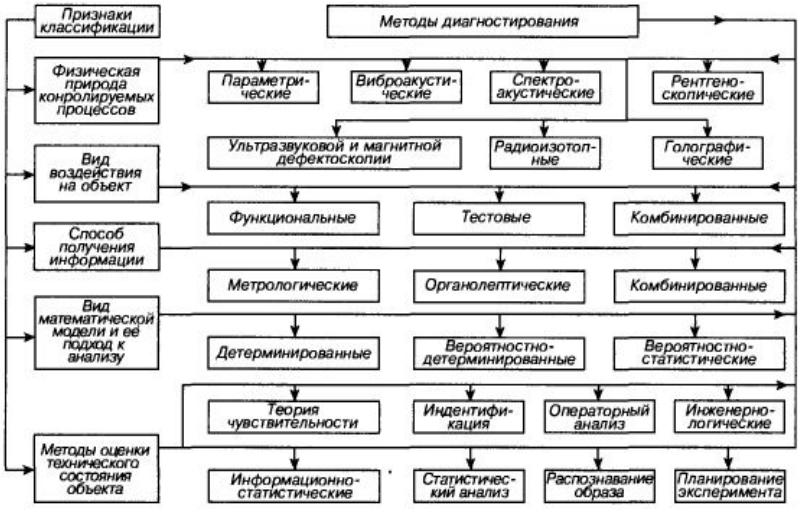

Figure 1. *Classification of diagnostic methods*

Innovations in the diagnosis of electrical equipment.

Through the application of high technology and digital theory, the development of artificial intelligence technology provides an opportunity for the development of monitoring and diagnostics. Its monitoring and diagnostic content is relatively larger, the most important of which are signal detection, signal processing and feature extraction, state recognition and classification, trend prediction, and so on. During the actual monitoring period, the general condition of the equipment system is used as the main basis for assessing the condition. In the process of fault diagnosis, the classification of the condition is to identify the abnormal phenomenon in the equipment, conduct in-depth investigation and analysis of the fault problem, find out the root cause of the fault, and then ensure certain diagnostic basis.

Determination of the state of electrical equipment

During the operation of electrical equipment, it is easily affected by various factors such as electricity, heat, machinery and the environment, so it is subject to a decrease in performance, resulting in equipment failure. In order to effectively avoid economic losses and social consequences caused by failures, it is necessary to control the operating conditions of power equipment. By applying condition monitoring technology and fault diagnosis technology, the operating status of electrical equipment can be fully and clearly understood. When abnormal information occurs, data can be detected and warned as soon as possible so that it can be dealt with in time.

CSE construction technique

Purpose

Assessment of the technical condition of locomotive asynchronous traction motors (ATM) with a squirrel-cage rotor using neural network technologies.

Methods

Intelligent methods are used to monitor and diagnose the state of ATM locomotives based on expert systems.

Results

It is shown that the use of the artificial intelligence method in the diagnosis of locomotives is a powerful tool that can provide reliable results. Expert systems for monitoring and controlling the ATM of locomotives have been developed to recognize the situation, make a diagnosis, formulate a solution, give a recommendation, which consist of a knowledge base, an inference mechanism and an explanation subsystem. The failures of ATM with a squirrel-cage rotor are analyzed.

The main stages of the methodology for constructing an artificial neural network model include: data analysis at the initial stage of setting the problem and choosing the CSE architecture; data transformation to build a more efficient CSE tuning procedure; choice of CSE architecture for ATM; choice of CSE structure; selection of CSE training algorithm for ATM locomotives; testing and training of

CSE; analysis of the accuracy of the neural network solution for ATM; making a decision on the technical condition of ATM locomotives based on the results obtained.

Here are some of the functions performed:

Figure 2 shows the data preprocessing scheme, where the F11 block performs the functions of data filtering, the F12 block normalizes the measured on-board parameters of the locomotive ATM, and F13 visualizes the measured on-board parameters of the locomotive ATM.

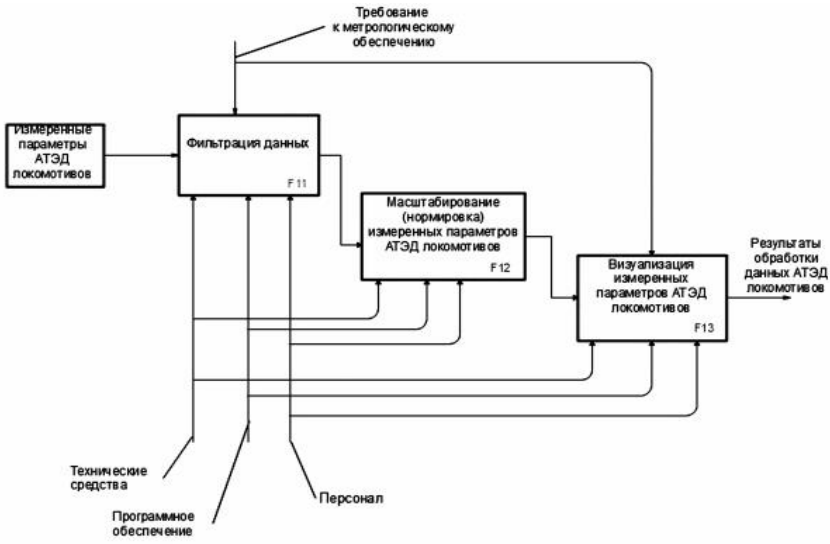

Figure 2. *Structure of data preprocessing*

Figure 3 shows the scheme of statistical data processing from the database (DB) of ATM tests in the form of a hierarchy of diagrams. On it, the blocks perform the following functions: block F21 analyzes the static characteristics of the sample; block F22 performs a correlation analysis of the sample; block F23 removes anomalous values from the sample, “filters” and removes explicit measurement errors [2].

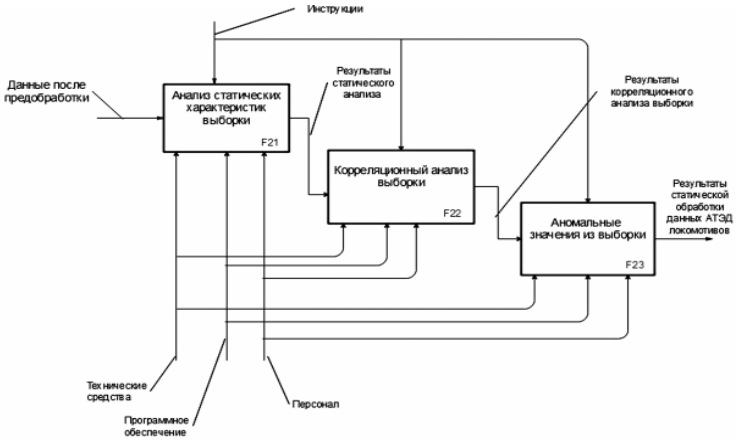

Figure 3. *Statistical processing of data from the test database*

Application of infrared detection technology for real-time monitoring of electrical equipment

Infrared monitoring technology is used to conduct continuous, non-contact detection of power equipment and intuitively find the location of equipment failure.

Performing infrared detection and diagnosis of live line equipment, from the use of infrared point pyrometers, infrared thermal television to modern uncooled focal plane infrared thermal imaging camera, found and solved many problems, such as poor contact, poor insulation, insulation aging. Such phenomena, as well as other defects in design, construction and operation, are a reliable guarantee for the safe operation of the electrical network. In connection with the spread of maintenance of power equipment, infrared monitoring of power lines is becoming increasingly important.

Real case scenario

Due to the large load of the 110kV line, the large B phase side of tower 44 is stressed, and the parallel groove clamps have poor contact and generate heat. The highest temperature in Area02 is 155.0 °C, the highest temperature in Area01 is 50.2 °C, and the highest temperature in Area03 is 33.8 °C. After checking the line when the power is off, it was found that the phase B parallel groove clamp was seriously damaged, and figure 4.8 shows the infrared image of the detection.

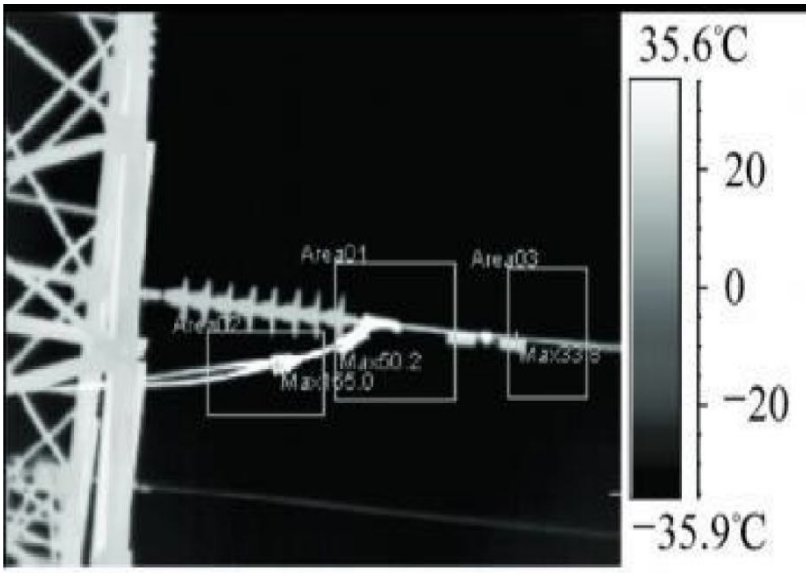

Figure 4. *.Infrared detection image*

Table 1.
Device detecting data

Camera model	**DL700C**
camera serial number	22700CA0104
extended lens	Without extension lead
job code	-20.00/2000
specific emissivity	1.00
distance	10/M
ambient temperature	22.3
humidity	0.7

Online monitoring and diagnostic methods for electrical equipment

Online monitoring refers to the continuous automatic assessment of the state of the electrical equipment of the equipment under test using the appropriate equipment and instruments, when the equipment under test is not turned off and is in normal mode. The electrical equipment detection unit saves the data in the database in the form of graphs and reports through the fieldbus connection, the electrical equipment online monitoring system can fulfill the role of online monitoring of lightning arresters, reactors and other devices in substations.

Offline inspection refers to manual inspection of the production status through various inspection methods such as daily inspection, inspection and diagnostics. Timely collection of data on the condition of the equipment and an accurate assessment of its operating conditions are important benchmarks for future diagnostics and maintenance. The main purpose of an offline inspection is to analyze existing or possible failures, the purpose of online monitoring is to determine the condition of the equipment and the conditions for its future operation, as well as the implementation of maintenance plans before failures occur.

Application of new technical equipment

1. Application of modern sensor technologies in the monitoring of electrical equipment.

The general basis of modern testing technology is mainly based on the acquisition, transmission and processing of signals, the definition of which is the first step in its measurement and monitoring. In the context of the constant development of science and technology, new measurement and measurement technologies have been fully introduced and applied in the testing process of electrical equipment, which further extended the measurement range of traditional electrical equipment such as fiber optic sensors. Noise monitoring technology and technology, as well as infrared monitoring technology, have improved the measurement accuracy to a certain extent, thus contributing to the development of electrical equipment monitoring and diagnostic technology.

2. Application of signal processing technology in the diagnostics of electrical equipment.

Through signal processing, useful signals can be added, signal characteristics can be extracted, and from them it can be known whether there is a malfunction, and then malfunction diagnosis can be performed. It provides a framework for developing appropriate signal processing techniques in diagnostics and other fields such as time domain analysis, wavelet analysis, wavelet packet analysis, and other signal processing and extraction techniques.

3. Application of diagnostic methods

In the actual diagnostic process, its description and other aspects cannot be achieved by traditional mathematical methods, but for the analysis of artificial intelligence technology, since it mimics the human task processing process well, it is easy to apply in this field and refer to human characteristics. Taking artificial intelligence technologies such as expert systems, artificial neural networks and genetic algorithms as examples, the analysis of these artificial intelligence technologies has certain advantages and disadvantages, and it is not isolated. For better diagnosis and good outcome, many cases should be combined with each other [3].

References

1. Biryukov I.V., Savoskin A.N., Burchak G.P. Mechanical part of traction rolling stock. M.: Transport, 1992 – 440 p.

2. Zelenchenko A.P., Rolle I.A., Tsaplin A.E. Technical diagnostics of electric rolling stock: textbook. – St. Petersburg: PGUPS, 2015 – 60 p.

3. Non-destructive testing and diagnostics. Handbook, ed. Klyueva V.V. – M.: Mashinostroenie, 2005 – 656 p.

DOI 10.34660/INF.2022.76.49.195

交流电力机车的主要电气设备
THE MAIN ELECTRICAL EQUIPMENT OF THE AC ELECTRIC LOCOMOTIVE

Rolle Igor Alexandrovich
Candidate of Technical Sciences, Associate Professor
Chu Mingjing
Master's degree Student
Xi Faxiang
Master's degree Student
Emperor Alexander I St. Petersburg State Transport University

抽象的。 学士“交流电力机车的主要电气设备”主题的工作包括引言、七个章节、结论和参考文献。

引言解释了所选主题的相关性，并定义了本科生研究的目标、目的和对象。 交流电力机车的主要电气设备，给出主要技术特性，描述电力机车牵引电机的设计和工作原理。 给出主要技术特点，简要说明1）受电弓，2）牵引变压器，3）主开关，4）高速开关，5）电空接触器的用途和装置。 描述了牵引和电制动模式下电力机车整流器和整流-逆变器的运行原理和控制算法。

关键词：电力设备受电弓，牵引变压器。

Abstract. *Bachelor's work on the topic "The main electrical equipment of an AC electric locomotive" includes an introduction, seven chapters, conclusions and a references.*

The introduction explains the relevance of the selected topics, and defines the goals, objectives and objects of undergraduate research. The main electrical equipment of an AC electric locomotive, to give the main technical characteristics, a description of the design and principle of operation of the traction motor of an electric locomotive. give the main technical characteristics, a brief description of the purpose and device of 1) pantograph, 2) traction transformer, 3) main switch, 4) high-speed switch, 5) electro-pneumatic contactors. give a description of the principles of operation and control algorithms for rectifier and rectifier-inverter converters of electric locomotives in the mode of traction and electric braking.

Keywords: *electrical equipment pantograph, traction transformer.*

Traction electric machines

The traction motor is the main motor that controls the vehicle's axis of motion and is used to accelerate and decelerate the vehicle.

There are many types of traction motors, such as DC traction motors, pulse traction motors, single-phase switch traction motors, AC rotating asynchronous traction motors, AC synchronous traction motors, and AC linear traction motors.

The traction motor is one of the important components of an electric locomotive. It is mounted on a trolley under the body. The gear at the end of the traction motor rotor shaft engages with the gear on the wheelset shaft. When an electric locomotive is in a state of traction, the traction machine converts electrical energy into mechanical energy, which turns the wheelset and makes the locomotive move.

Figure 1. *traction motor NB-514B. General view*

The technical characteristics of the NB-514B and NB-514E traction motors are presented in the table.

Table.

The technical characteristics of the NB-514B and NB-514E traction motors are presented

Наименование показателя	Значение	
Номинальный режим работы	часовой	продолжительный
Номинальная мощность, kW(кВт)	820	765
Номинальное напряжение, V(В)	1000	
Номинальный ток якоря, A(A)	870	810
Номинальная частота вращения, r/min(об/мин)	920	940
КПД, %	94,55	94,7
Расход вентилирующего воздуха при полном напоре 620 Ра(Па), не менее, m^3/min($м^3$/мин)	70	
Класс изоляции: якорь/остов	F/F	
Сопротивление обмоток постоянному току при температуре плюс 20 °С, Ом: - якоря - главных полюсов (без шунта) - компенсационной и добавочных полюсов	 0,0112±0,000560 0,0069±0,000345 0,0125±0,000625	
Масса двигателя НБ-514Б (без зубчатой передачи), kg(кг)	4300	
Масса двигателя НБ-514Е (без зубчатой передачи), kg(кг)	4350	

The traction motor is designed for axial support: it is a six-pole compensation motor, operating in traction mode as a series excitation motor and in electric regenerative braking mode as an independently controlled excitation generator, as well as an independent system ventilation. Cooling air is supplied to the traction motor from the manifold side through the vent hole. Cooling air exits the RB-514E tractor from the opposite side of the current collector through a special chassis through an electric locomotive, and from the NB-514E tractor through a window in the bearing cover, and two hatches in the core are closed with a mesh. According to figure 1, the NB-514B traction motor consists of an axial bearing 1 of the engine, and according to figure 2, it consists of an iron core 1, wire 2, bearing shields 3 and 5 and armature 4. NB-514E traction motor (different from the traction motor NB-514B design of the axial part of the motor in accordance with Fig. 1a and the corresponding parts of the iron core 1 and bearing cover 5 on the side opposite the current collector in accordance with Fig. 2a. (casting). In order to protect the axial bearings of the motor from dust and moisture, the axle with the bearing is closed according to the cover 1 of figure Ta through the linkage 1 The motor is connected to the shaft, the space pressed into the cover 1 is 9 m24x2, and four bolts M36x2 (ten bolts) are used to screw four to B. According to figure 1a, there is a hole in the cover B, which is plugged 2 Closed, used to clean the middle part of the shaft and the axial journal of the motor.

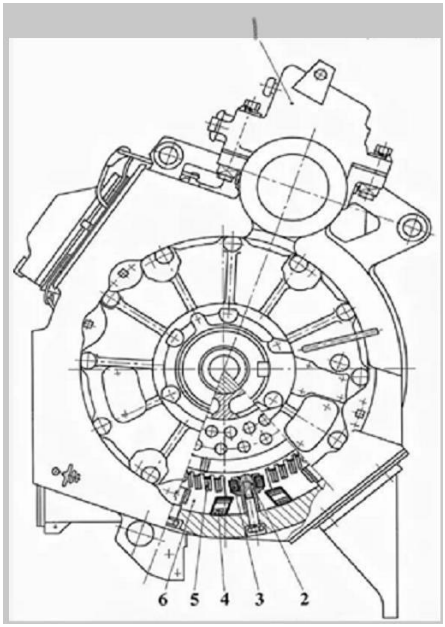

Figure 2. *traction motor NB-514E.*

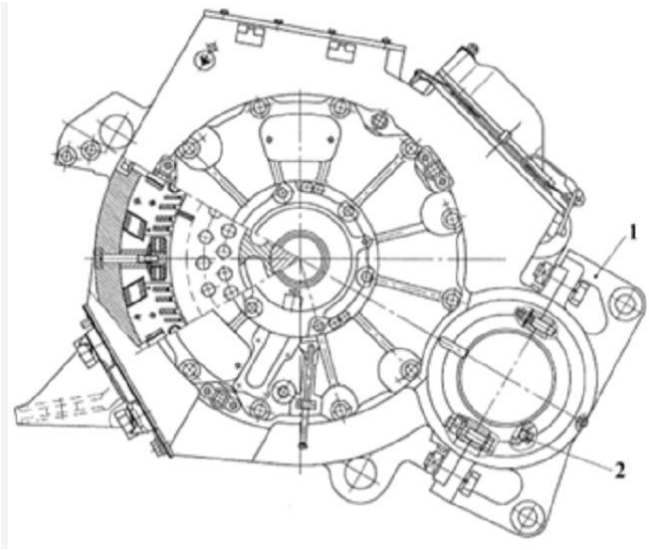

Figure 3. *Traction engine NB-514E1*

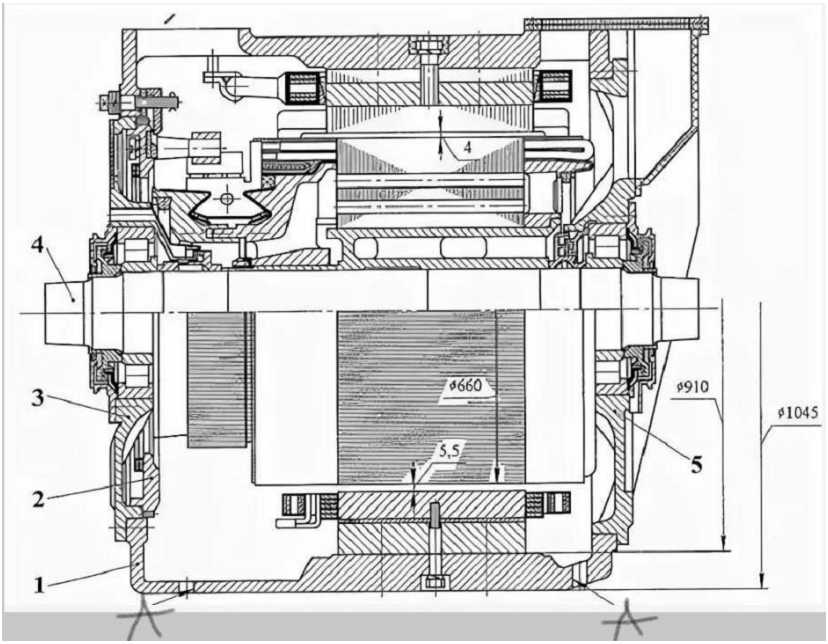

Figure 4. *Longitudinal section of the NB-514B traction motor*

Traction motor operation

The current passing through the armature winding interacts with the flux of the main magnetic pole, creating an electromagnetic moment that causes the armature to rotate.

The magnetic current is generated by the compensation winding of the additional pole and the winding current, which improves the potential conditions on the collector and facilitates the switching process.

The traction (power) transformer ODCE-5000/25AM-02 (Fig. 6) is designed to convert the voltage of the 25 kV contact network to the supply voltage of the traction motor circuits and auxiliary needs of the electric locomotive. The technical data of the transformer are as follows:

Rated power of the network winding, kV-A 4 777
Rated voltage of the mains winding, V..... 25000
Rated voltage of traction windings, V:
al-xl; a2-x2 1230
2-xI; 4-x2..... 615
1-x1; 3-x2.....••..... 922.5
Rated current of traction windings, A..... 1 750

Hourly current of traction windings, A 1 900
Rated voltage of excitation windings ab-a7; a7-x4, B. . . 180
Rated current of the excitation winding, A..... 720
Rated voltage of auxiliary windings, V:
a3-x3.....641
a4-x3 410
a5-x3..... 231
Rated current of auxiliary winding, A..... 520
The same for redundancy, A ..... I 400
Total losses, kW 84
Efficiency, %.....•..... 98.3
Air consumption for cooling, m3/s-..... 5.5
Weight, kg .'..... 7 800

The transformer consists of the following main units: a two-rod magnetic circuit, a winding, a tank and a cooling system. The cores of the magnetic circuit have a stepped shape in cross section and are made of sheets of cold-rolled electrical steel with a thickness of 0.35 mm. The windings are wound on cylinders and secured with cardboard spacers and rails. The axial tie of the windings is made using a spring lever device (clamp).

Each traction winding (Fig. 7) consists of three parts located only on the pole of the pole wire. The position of the winding is concentric. The first heart is a 2-x1 (4-x2) bi-directional spiral winding. The spirals on each pole are connected in parallel. Secondly, in the center is a continuous network winding. Thirdly, the outer center is equipped with 2-1 (4-3) and 1-A1 (3-A2) traction coils.), track winding and your own needs.

Tank 4 (see Fig. 6) is filled with transformer oil. Steel plugs 3 are installed in the lower part of the tank, closing the holes in the places where the threaded stops are installed for fastening the active part. Rubber is used to seal the apron 5 with the floor of the electric locomotive. Two beam-chambers 14 are elements of the frame suspension of the tank. They increase the rigidity of the tank and are also used as air ducts for the cooling system. The transformer is supported by four forged conical cups and the cooling system consists of eight sections of radiators 2 and an electric pump 1. The radiator sections are blown with air from the ventilation system of the electric locomotive. Expander 10 is designed to compensate for temperature fluctuations in the oil level in the tank. The part of the expander above the oil surface is filled with air, which communicates with the atmosphere through the hole in the plug 8. The hole closed by the plug 9 is intended for topping up the oil. The tank is drained and filled with oil through the valve 12.

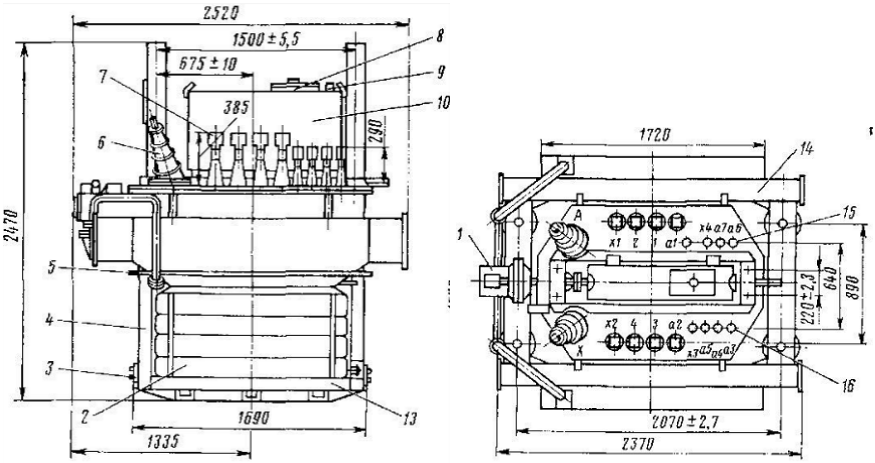

Figure 6. *Traction transformer ODCE-5000 / 25A*

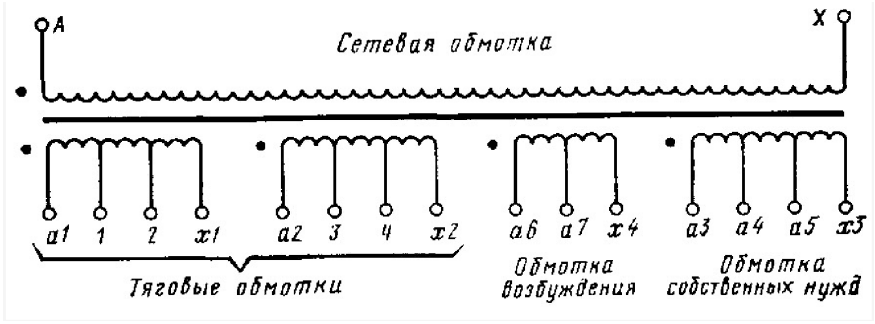

Figure 7. *Transformer winding diagram*

A plug 13 is provided for taking an oil sample. Inputs are installed on the tank cover: two 6 network windings, eight 7 traction windings, three 15 excitation windings and four 16 auxiliary windings. Connection of inputs with taps is made by dampers made of flexible copper conductors. All bushings are detachable and allow the replacement of insulators without lifting the withdrawable part.

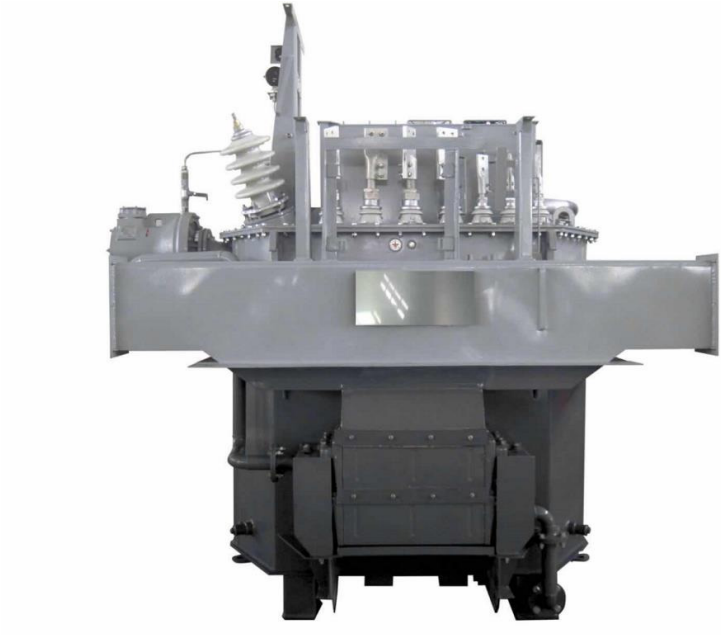

Figure 8. *This Traction Transformers*

For rail vehicles, the traction transformer is one of the most important devices and the main part of the whole electrical traction system, ensuring the stable operation of locomotives, high-speed rail and other rail vehicles. Traction transformers have often been used for railroad traction over the past century and are considered the best choice for traditional traction systems.

Transformer principle and analysis: A transformer is an electrical installation for transmitting electrical energy or signal from one circuit to another using the principle of electromagnetic induction, is an important element in the transmission of electrical energy or signal.

1.Automated control systems for electromotive composition. Part 1//ed. L.A. Baranova and A.N. Savoskina // M.: SEI Educational and Methodical Center for Education in Railway Transport, 2013, - 400 p.

2. Yakushev A.Ya. Automated electric rolling stock control systems, Textbook// M.: SEI Educational and Methodical Center for Education in Railway Transport, 2016, - 301 p.

DOI 10.34660/INF.2022.97.78.196

异步电动机磁场定向精度研究
RESEARCH OF THE ORIENTATION ACCURACY OF THE MAGNETIC FIELD OF AN ASYNCHRONOUS MOTOR

Wang Helin
Master's degree Student
Vikulov Ilya Pavlovich
Candidate of Technical Sciences, Associate Professor
Emperor Alexander I St. Petersburg State Transport University

抽象的。 任何电机控制算法的本质都是准确快速地推导出所需的转矩（包括稳态转矩控制和瞬态转矩响应速度）。 无论采用哪种方法，计算中都会用到电机参数，尤其是间接矢量控制，在运行过程中参数可能会在 50% 到 100% 之间变化，尤其是当电机进入弱磁场时，必须确定或调整。

关键词：感应电机，矢量控制，转子磁路，坐标系d，q

Abstract. *The essence of any motor control algorithm is to accurately and quickly derive the required torque (both steady state torque control and transient torque response speed). Whichever method is used, motor parameters are used in the calculations, especially for indirect vector control, where parameters may vary from 50% to 100% during operation, especially when the motor enters a weak magnetic field, and must be determined or adjusted.*

Keywords: *Induction motor, vector control, rotor magnetic circuit, coordinate system d,q*

Rotor Field Orientation Control (FOC), one of the high performance control algorithms, is widely used in many industrial applications due to its accuracy in torque control and fast dynamic response, to the extent that many high-power electric locomotives use this control strategy.

1. Basic principle of vector control

The block diagram of the indirect vector control circuit is shown in Figure 1, which mainly includes voltage and current command calculation, slip frequency calculation, PID controller, and SVPWM module.

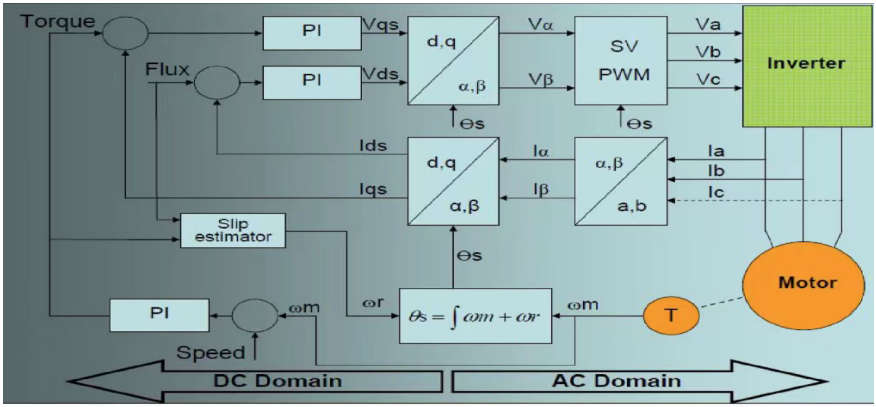

Figure 1. *Block diagram of the principle of vector control*

At the core of controlling the synthetic current vector by means of a synthetic voltage vector, which in turn controls the rotating magnetic field so that it always rotates a certain angle ahead of the rotor field, is current control. The input three-phase currents are coordinate-transformed to obtain iα and iβ,iα and iβ and the motor rotor angle are used as input for the park transformation to obtain id and iq, separate PID-control of these two current components, speed feedback as external loop, current control as an inner loop, Formation of tandem PID-control. Adjustable PID output Uq and Ud, after performing the inverse transformation of the park to obtain Uα and Uβ. It is used as an input for SVPWM, and the algorithm generates three sets of PWM control signals to control a three-phase inverter bridge and thus control a motor.

2. Rotor time constants and errors of load and orientation angle

In vector control, there are many factors that can lead to incorrect orientation of the rotor field, such as changing parameters due to changes in motor temperature, operating frequency, operating conditions, eddy current effects, etc.

The analysis of the inaccurate orientation of the magnetic field is based on the vector control circuit in Figure 1, where the magnetic circuit is controlled by an open loop control system with direct control of the d-axis excitation current.

When this happens, the deviation between the calculated shaft angle and the actual rotor magnetic circuit angle can be estimated, as shown in Figure 2.

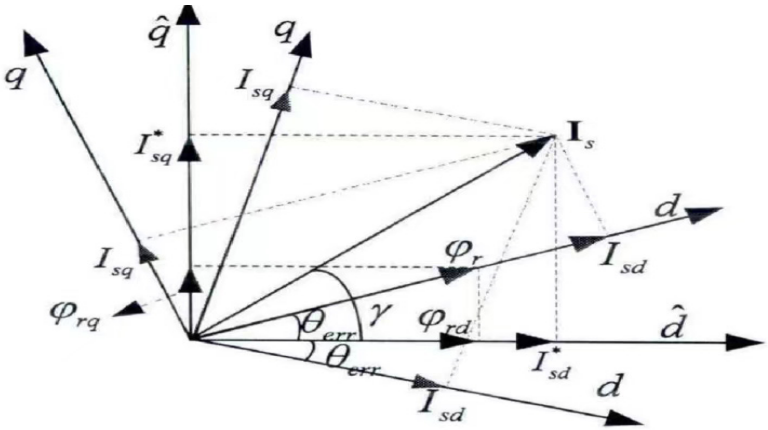

Figure 2. *Schematic diagram of the current of the coordinate axis dq with inaccurate orientation of the magnetic field*

In vector control, due to the setting of the current controller, the current is always able to follow the set value, so that even in case of inaccurate orientation, the current vector of the traction motor does not change with the same current command on the d,q axis, that is, the essence of this situation is to redistribute current along the d,q axis, as can be seen from Figure 2, when the actual angle of the magnetic circuit exceeds the observed angle, the actual d axis current increases and the q axis current decreases, and vice versa, the actual d axis current decreases and the q axis current increases.

Since the traction motor slip adds directly to itself, if the motor speed is accurately measured, the following relationship can be obtained:

$$\omega^*_{sl} = \frac{I^*_{sq}}{\hat{T}_r I^*_{sd}} = \omega_{sl} = \frac{I_{sq}}{T_r I_{sd}} \tag{1}$$

Mark* - Represents the value of the command

Tr-rotor time constant

ˆ is an estimate

According to equation 1 and fig. 2, orientation angle error can be defined as:

$$\theta_{err} = \arctan\left[\frac{I_{sq}}{I_{sd}}\right] - \arctan\left[\frac{I^*_{sq}}{I^*_{sd}}\right] = \arctan\left[\frac{T_r I^*_{sq}}{\hat{T}_r I^*_{sd}}\right] - \arctan\left[\frac{I^*_{sq}}{I^*_{sd}}\right] \tag{2}$$

In accordance with the parameters of an asynchronous traction motor of an electric locomotive, using Matlab, it is possible to construct a three-dimensional diagram of the change in the angular error with the rotor time constant and the ratio of current commands along the d, q axes, as shown in Figure 3.

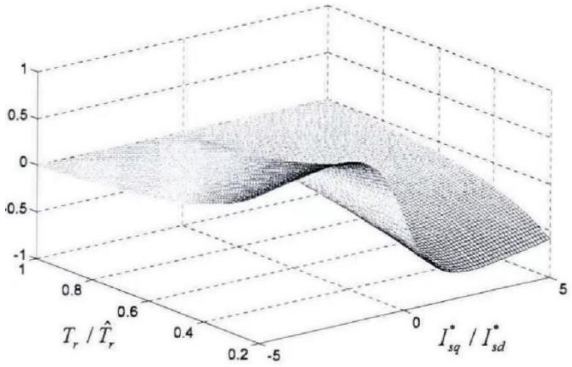

change range(0.2,1)

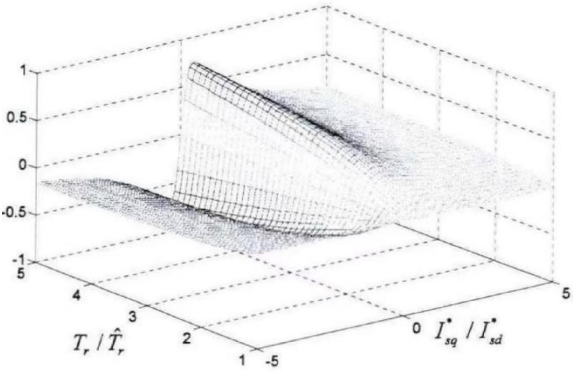

change range(1.5)

Figure 3. *Change of the angular error with the sum of the rotor time constants and* $\frac{I_{sq}^*}{I_{sd}^*}$

It can be seen from Figure 3 that the orientation angle error is related not only to the rotor time constant, but also to the load state of the traction motor. Under the same load conditions, the larger the calculated deviation of the rotor time constant,

the larger the angular error. In the thrust state, if the calculated time constant of the rotor is less than the actual value, the angular error defined by formula 1 is a positive value, that is, the actual flux angle leads the calculated angle, otherwise the calculated angle leads the actual flux angle, the control of the angular error in the dynamic state is completely is opposite to the error in the traction state.

Figure 4 shows the projection of the same stress vector on the d, q axes in different coordinate systems under traction conditions.

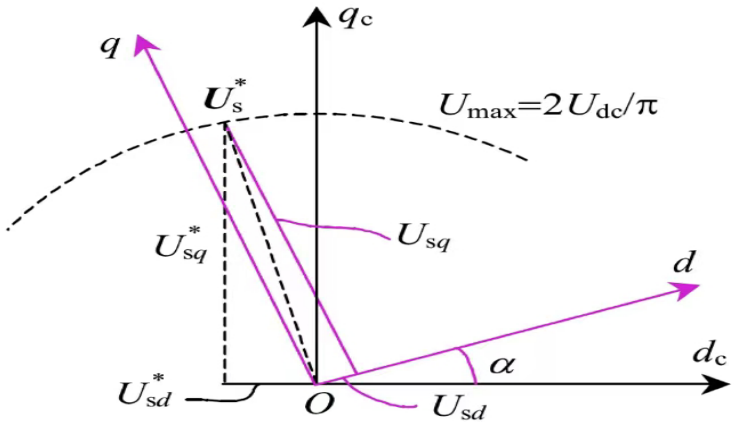

Figure 4. *Vector diagram of the electric locomotive voltage in the traction state*

The voltages on the d and q axes of the motor are determined by the current components of the q and d axes Isq and Isd respectively, and the current is easily obtained by measurement, so current can be used instead of voltage, using the error between the actual current value and the set value to achieve the shi'shi angle of orientation.

Conclusion

There are three key factors in providing conditions for vector control of induction motors.

1. Precise orientation of the rotor field.
2. fast bringing the motor current to the command current.
3. Precise control of the amplitude of the magnetic circuit.

References

1. Feng Xiaoyun, AC Electric Traction Drive and Control, Beijing: Higher Education Press, 2009.-39 p.

2. Zhou Zhigan, Research of the vector control system of an asynchronous motor. North Jiaotong University, 2003.-125p.

3. Vikkon. Railway Traction Inverter Digital Control Research, School of Electrical Engineering, Beijing Jiaotong University, 2012-72p.

4. Development of models of elements and systems of an automated electric drive in the Matlab environment: a tutorial / V.B. Terekhin - Seversk: STI NRNU MEPhI, 2017. -511 p.

5. Tikhmenev B. N., Kuchumov V. A. Alternating current electric locomotives with thyristor converters. – M.: Transport, 1988. – 311 p.

6. Asynchronous traction drive of locomotives: textbook. Allowance / A.A. Andryushchenko, Yu.V. Babkov, A.A. Zarifyan and others; ed. A.A. Zarifyan. – M.: FSBEI <<Training and methodological center for education in railway transport>>, 2013. – 413 p.

DOI 10.34660/INF.2022.64.81.197

电力机车车辆控制系统分类研究
STUDIES ON THE CLASSIFICATION OF CONTROL SYSTEMS FOR THE ROLLING STOCK OF ELECTRIC LOCOMOTIVES

Du Peidong
Master's degree Student
Volodin Anatoly Alexandrovich
Candidate of Technical Sciences, Associate Professor
Emperor Alexander I St. Petersburg State Transport University

抽象的。电力机车车辆由驾驶员和地面交通控制系统通过控制系统控制。控制系统是列车控制的神经中枢。控制系统必须满足列车运行过程中的各种基本要求，完成对主电路、辅助电路、电子电路和微机系统的控制。

电力机车和电动车组的控制系统大致包括：带触点的电气控制子系统、电子控制子系统、微机控制子系统和列车通信网络系统。这些控制子系统各有特点，相互关联，甚至无法区分。带触点的电气控制系统是电力机车和电动车组控制系统的主要控制元件。尽管长期以来人们认为带触点的电气控制技术落后且操作不便，但即使是当今世界上最现代化的列车，仍然支持结构基本相同的电气控制系统。电子控制系统基本上是由电路组成的控制装置，与计算机系统不同。自1980年代开始使用的机车微机控制系统，是电力机车和电动车组控制技术的革命性变革。这导致了微机控制、列车通信网络，甚至最新的无线通信技术的发展，这些技术是当今列车控制系统的发展趋势。本文通过对变流器类型的分析，对电力机车控制系统进行了区分。

关键词：电力机车车辆（ERS）；控制系统（CS）；变流器。

Abstract. *Electric locomotive vehicles are controlled by the driver and the ground traffic control system through the control system. The control system is the nerve center of the train control. The control system must meet various basic requirements during the operation of the train, and complete the control of the main circuit, auxiliary circuit, electronic circuit and microcomputer system.*

Roughly speaking, the control systems of electric locomotives and groups of electric vehicles include: electrical control subsystems with contacts, electronic control subsystems, microcomputer control subsystems and train communication network systems. These control subsystems have their own characteristics, are interconnected and even indistinguishable. Electrical control system with contacts is the main control element of the control system of electric locomotives and

groups of electric vehicles. Although electrical control with contacts has long been considered technologically backward and inconvenient to operate, even the most modern trains in the world today still support an electrical control system with basically the same structure. An electronic control system is basically a control device composed of circuits Shenzi, which are different from the computer system. The microcomputer control system of the locomotive, used since the 1980s, is a revolutionary change in the control technology of electric locomotives and groups of electric vehicles. This has resulted in the development of microcomputer control, the train communication network, and even the latest wireless communication technologies, which today are the development trend of the train control system. This article makes a distinction in the control system of electric locomotives by analyzing the types of converters.

Keywords: *Electric rolling stock (ERS); Control system (CS); converter.*

1 ERS control systems

Management is the impact on the object, aimed at achieving the goal. The purpose of train control is to move it from the initial to the final station within the time interval established by the schedule while ensuring traffic safety and minimizing energy consumption. To do this, the speed of the train V must change in a certain way depending on the distance traveled.

1.1 Functions of the ERS control system

The set goal will be achieved if the locomotive realizes the traction force Fk, sufficient to overcome the resistance force W to train movement and to create the required train acceleration dV/dt.

If it is necessary to reduce the speed of the train ($dV/dt < 0$), it will be necessary to create a braking force B directed against the speed vector V.

The locomotive's ability to implement traction and braking forces is determined by its traction and braking characteristics, which are the dependences Fk(V) and B(V) and have limitations on the forces Fk and B, determined by the parameters of the locomotive.

The task of ERS control is reduced to the creation of certain modes of operation of traction motors (TM), which provide the required values of the traction force Fk (or braking force B) at given speeds V.

The mode of operation of the TM is determined by the voltage at its terminals id, the excitation current Iv, and for an alternating current TM it is also determined by the frequency fd.

The set of devices designed to change the operating mode of the TM is called the ERS control system (ERS CS).

Figure 1.1 shows the elements of an electric railway (ER) involved in the conversion of electrical energy into mechanical energy of the movement of the train,

as well as the information links between these elements necessary to control the train.

The first main function of the ERS control system is to regulate the mode of operation of the TM in order to ensure the movement of trains in accordance with the schedule. The ER power supply system provides power supply to the EPS pantograph. It is known that the capital costs for the construction of the power supply system and the annual energy losses in it can be reduced by using a higher nominal voltage of the contact network. However, in this case, it becomes impossible to directly power the traction motors from the contact network, since the voltage on the TM should not exceed 1500 V, and the optimal parameters of the TM are achieved at Ud = 700–1000 V. Therefore, the second main function of the control system of the ERS is to convert the voltage of the contact network Uc and kind current in it, characterized by the frequency of the contact network fc, into voltage and type of current, suitable for TM (Ud and fd).

In addition, the ERS control system must perform the following additional functions: limiting the speed of movement, traction forces and electric braking in accordance with the ERS parameters and traffic safety requirements; — protection of electrical equipment from damage and dangerous modes; provision of air cooling of electrical equipment and supply of compressed air for pneumatic drives; — ERS control automation.

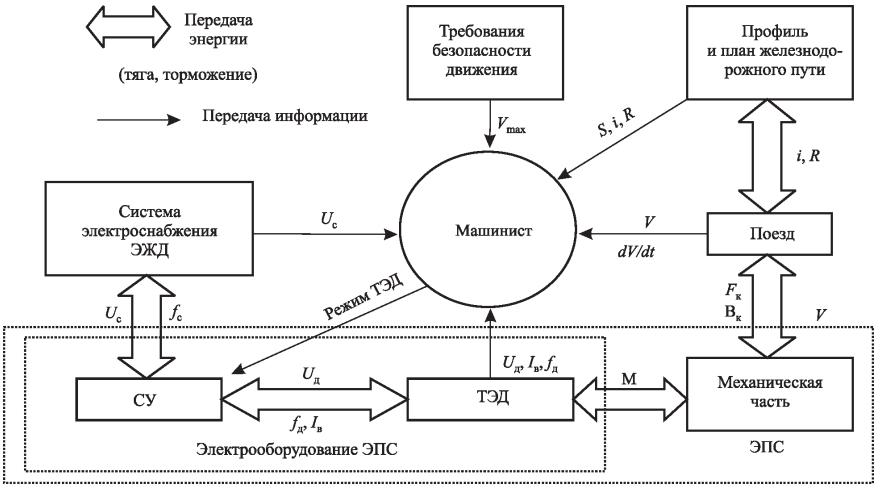

Figure 1.1. *Energy and information links between elements electric railway*

To perform the main and additional functions of the ERS control system in accordance with the conditions of train movement, it is necessary to switch the

operating modes of the ERS control system. These switchings are carried out by the driver, who in his actions must take into account the operating modes of the TED (UR, ІД, ІВ) and power supply systems (Uc), train traffic conditions (V, dV / dt, i, S), as well as traffic safety requirements.

Conclusions: ERS CS is designed to regulate the mode of operation of the TM. The requirements for the levels of nominal voltages of the contact network and TM are contradictory. ERS CS must reconcile this contradiction. ERS CS should be selected based on an assessment of the total capital costs for the power supply system, TM and other electrical equipment of the ERS, as well as operating costs for all elements of the ER

2 Classification of ERS control systems by types of converters

Classification of ERS control systems by types of converters, this classification is shown in Figure 2.1

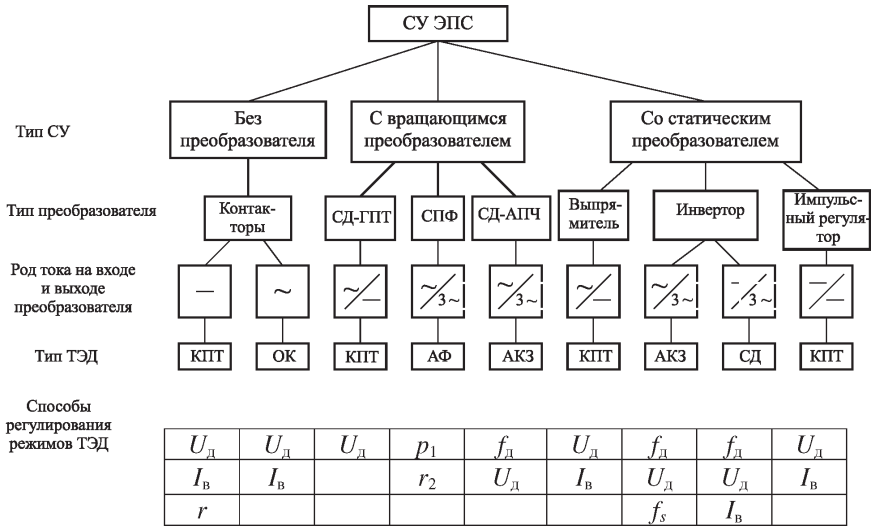

Figure 2.1. *Classification of ERS by types of converters*

2.1 ERS CS without converters

Historically, the first electric locomotives had the simplest control systems without converters. Such control systems provide for step-by-step voltage regulation at the TM Sd by changing the TM groupings, controlling the excitation current Iv and turning on the starting resistors r (for DC ERS) or switching the number of turns of the transformer windings (for AC ERS). Collector DC TM (CDT) and single-phase collector (SPK) are used.

The advantages of control systems without converters are their simplicity and low cost, the disadvantages are significant losses in starting resistors, stepwise regulation of traction force, complexity of the design of collector TMs and limitation of their switching power. Until 1960, the ER of Europe used ERS control systems without converters, with the exception of single experimental electric locomotives. Now, due to the development of converting technology, this type of EPS control system, although it has lost its monopoly position, is still the most common control system on a DC ER.

2.2 ERS CS with static converters

The history of ERS CS with static converters begins in 1936, when an experimental section of the Hellental railway was launched in Germany in the Black Forest near Freiburg, the contact network of which was powered by a voltage of 20 kV 50 Hz. The site had rises up to 55%. Four electric locomotives manufactured by different companies worked at this site, including two electric locomotives with a direct current TM and multi-anode mercury rectifiers.

In 1938, an experimental electric locomotive OR-22 was manufactured by the Dynamo plant and its testing began on an experimental Ring VNIIZhT near Moscow.

In the first post-war years in the USA, France and the USSR, electric locomotives with first-generation static converters were built and tested, on which single-anode mercury rectifiers were used. Their disadvantages: cumbersome design; the difficulty of ensuring the tightness of devices in the conditions of vibration of the rolling stock; the need to maintain the temperature of the rectifiers within a narrow range of 35–40 °C, which required the use of water cooling; mercury contamination of an electric locomotive when the rectifier case is burnt.

At the same time, CS with mercury rectifiers had significant advantages compared to rotating converters: a significantly smaller mass of electrical equipment per unit of TM power, and a higher efficiency factor (EF). These advantages were convincingly confirmed in 1955, when the joint operation of electric locomotives of various types began on the Valenciennes-Thionville (France) heavy-duty line. The second generation of static converters appeared in Europe in 1958-1959 and four years later - in the USSR. Silicon diodes were used as rectifiers. This made it possible to replace water cooling with air cooling, reduce the weight and dimensions of the rectifier, simplify its maintenance, and increase efficiency and reliability.

The voltage on the TM of electric locomotives of the first and second generations was regulated by changing the number of turns of the transformer winding using contactors. The advantages of the second generation converters turned out to be so significant that, as they entered the overhaul on all electric locomotives of the first generation, mercury rectifiers were replaced by silicon ones. The third genera-

tion of static converters was distinguished by the use of controlled semiconductor devices - silicon thyristors. This made it possible to abandon the use of contactors and switch to contactless regulation. In addition, it became possible to regenerate on electric locomotives with static converters, as well as to use brushless TMs. The fourth generation is characterized by the use of fully controlled GTO thyristors (Gate turn off thyristor - lockable thyristor), which ensured a further reduction in weight and size converters, especially noticeable on electric locomotives with asynchronous TMs. Now the fifth generation is being born, characterized by the use of power semiconductor devices IGBT (Insulated Gate Bipolar Transistor - an insulated gate bipolar transistor) and IGCT (Integrated Gate Commutated Thyristor - a lockable thyristor with an integrated control unit). Disadvantages of static converters: a significant decrease in the power factor with deep phase regulation in traction and recuperation modes; distortion of the shape of the current curve consumed from the contact network, and the need to compensate for reactive power at higher harmonics.

In the future, the most common systems will be considered in detail: direct current without converters and alternating current with static converters, as well as promising systems with brushless traction motors and pulsed DC voltage regulation.

2.3 ERS CS with rotary transducers

Back in the first half of the 20th century, electric locomotives with rotary converters were used in the USA and Hungary. The first such electric locomotives had a synchronous single-phase-to-three-phase voltage converter (STC) and an asynchronous traction motor with a phase rotor (AP). Regulation was carried out by switching the number of TM poles and a starting resistor in the rotor circuit. These electric locomotives had a group traction transmission with a connecting rod-crank mechanism similar to a locomotive. The number of such electric locomotives did not exceed two or three dozen.

In 1947-1955. In the USA, France and Hungary, a variety of electric locomotives with rotating converters appear that have collector DC TMs (CDC) or asynchronous TDs with a squirrel-cage rotor (SCR). The speed control was carried out by changing the voltage and frequency of the traction motors.

Such control systems had many advantages: the possibility of using TM with optimal parameters, regardless of the magnitude of the voltage and type of current in the contact network; smooth regulation of speed and traction force; the sinusoidal form of the current consumed from the contact network, and the ability to control the power factor due to the use of a converter with a synchronous motor (SM). However, ERS with rotating converters are characterized by two very serious drawbacks: a significant mass of electrical equipment per unit of TM power. Taking into account the limitation of the load from the wheels on the rails

according to the track design, such electric locomotives can have a power of no more than 400 - 500 kW per driving axle; relatively low efficiency of an electric locomotive, due to three to five times the conversion of energy. After 1955, such electric locomotives were no longer produced.

References

1. Usov V.A. Control systems for electric rolling stock. Textbook of methodics. Yekaterinburg, 1994.

2. Rotanov N.A., Zakharchenko D.D., Plaks A.V., Nekrasov V.I., Inkov Yu.M. Design of control systems for electric rolling stock. M.: Transport, 1986.

3. Tikhmenev B.N., Trakhtman L.M. Rolling stock of electric railways. M.: Transport, 1980.

4. Tishchenko A.I. Handbook of electric rolling stock, diesel locomotives and diesel trains, T.II.M.: Transport, 1976.

DOI 10.34660/INF.2022.92.27.198

“O’Z-ELR” 系列电力机车牵引变压器计算机模型参数的确定和充分性评估
DETERMINATION OF PARAMETERS AND ASSESSMENT OF THE ADEQUACY OF THE COMPUTER MODEL OF THE TRACTION TRANSFORMER OF ELECTRIC LOCOMOTIVES OF THE “O’Z-ELR” SERIES

Samandarov Rakhmatjon Nizamaddin ugli
Master’s degree Student

Valiyev Akhrorjon Alkhamjon ugli
Master’s degree Student

Normuradov Khusnutdin Shukhrat ugli
Master’s degree Student

Volodin Anatoly Alexandrovich
Candidate of Technical Sciences, Associate Professor
Emperor Alexander I St. Petersburg State Transport University

注解。 本文考虑了用于 O’Z-ELR 系列电力机车的牵引变压器的计算机模型。 此外，牵引变压器的参数采用解析法确定。 本文评估了牵引变压器计算机模型的充分性。

关键词：电力机车“O’Z-ELR”，牵引变压器，多绕组变压器，计算机模型，建模。

Annotation. *The article considers a computer model of a traction transformer for electric locomotives of the O'Z-ELR series. In addition, the parameters of the traction transformer are determined by the analytical method. The paper assesses the adequacy of a computer model of a traction transformer.*

Keywords: *Electric locomotive "O'Z-ELR", traction transformer, multi-winding transformer, computer model, modeling.*

Modern AC electric locomotives of the O'Z-EL and O'Z-ELR series equipped with single-phase traction transformers model JQFP-10160/25 with a capacity of 9000 kVA. The diagram and designations of the transformer windings are shown in Figure 1.

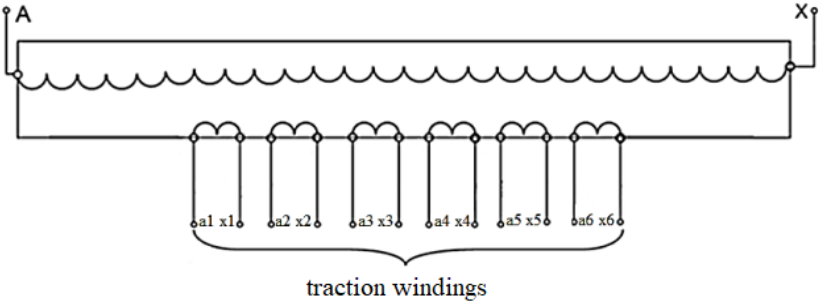

Figure 1. *Winding diagram of JQFP-10160/25 traction transformer*

The computer model of the traction transformer is formed on the basis of the functional block of the Simulink library - Multi-Winding Transformer, shown in Figure 2.

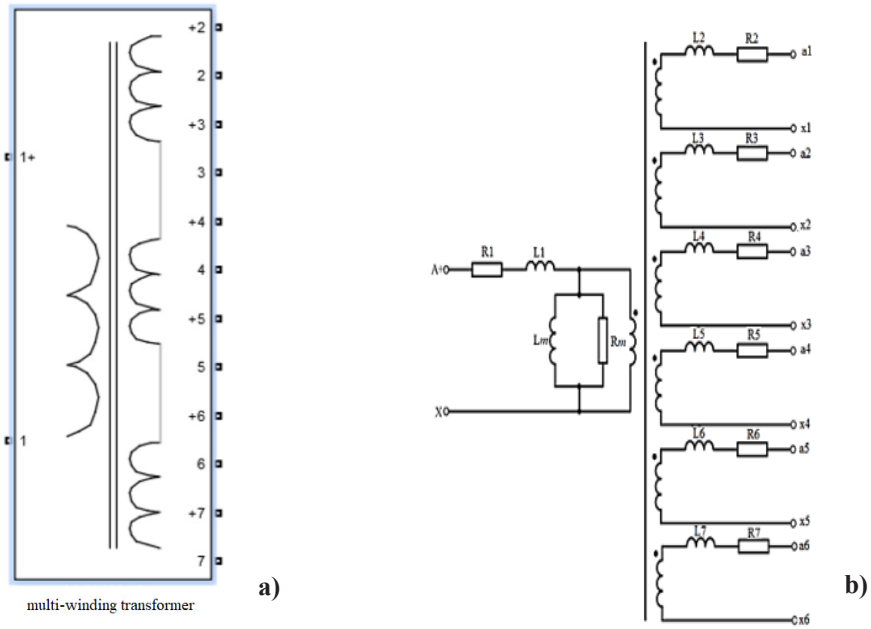

Figure 2. *Pictogram (a) and circuit design of the model multiwinding transformer of an electric locomotive (b) in the Simulink library*

The parameters of the computer model of the traction transformer JQFP-10160/25, determined by the calculation method based on the passport data of the transformer, as well as idle and short circuit modes, are shown in Table 1.

Table 1.

Design parameters and main electrical parameters of the transformer JQFP-10160/25

Parameters and data	Designation	Value
Winding short circuit impedance, Ohm	Z_k	36.47
short circuit losses, kW	ΔP_k	155,5
The active resistance of the windings, reduced to the primary	r_k	1.38
Inductive reactance due to stray magnetic fluxes, reduced to the primary winding transformer, Ohm	X_k	36.37
Inductive resistance of the primary winding, Ohm	$X_{1\sigma}$	18.19
Inductive resistance of the secondary (traction) winding a1-x1, ... a6-x6, Ohm	$X_{2\sigma}$	0.37
Leakage inductance of the primary winding, H	$L_{1\sigma}$	0.058
Leakage inductance of the secondary winding of the transformer, H	$L_{2\sigma}$	0.00118
Leakage inductance of the primary winding, H	r_1	0,69
Leakage inductance of the secondary winding of the transformer, H	r_2	0.014
Primary winding resistance, Ohm	Z_m	6950
Secondary winding resistance, Ohm	R_m	8060
Total resistance of the magnetic circuit, Ohm	X_m	13900
Active resistance of the magnetic circuit, Ohm	L_m	44
Active component of no-load current transformer, A	I_mA	3,1
Magnetizing current of the magnetic circuit of the transformer, A	I_m	1.8

A block diagram of a computer model of a traction transformer is shown in Figure 3

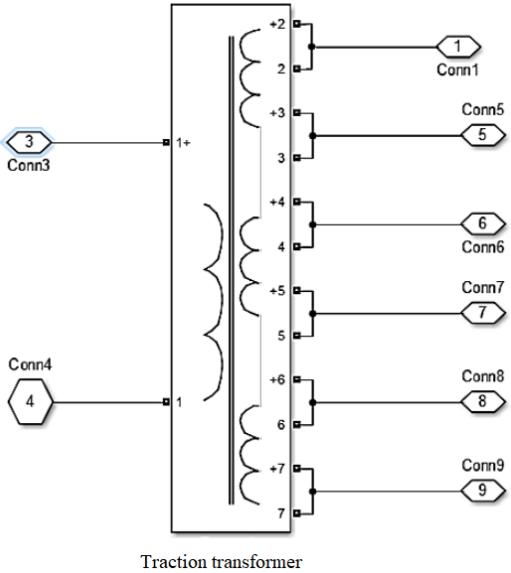

Figure 3. *Block diagram of JQFP-10160/25 traction transformer model of O'Z-ELR series AC electric locomotive*

Determination of the parameters of the traction transformer by the analytical method

Passport data of the JQFP-10160/25 traction transformer of the O'Z-ELR electric locomotive are given in Table 2.

Table 2.

Passport data of transformer JQFP-10160/25

Physical dimensions of the transformer	Parameter value
Power supply frequency, Hz	50
Rated power of the network winding, kVA	9000
Rated voltage of the network winding, kV	25
Rated current of the network winding, A	360
No-load current at a voltage of 25 kV,%	1,0
Rated voltage of traction windings a1-x1, ... a6-x6, V	1450
Transformation ratio	17,24

Rated current of traction windings a1-x1, ... a6-x6, A	965
Rated power of traction windings, kVA	1400×6
Short-circuit voltage (short-circuit windings a1-x1, ... a6-x6),%	49
Power loss of the nominal mode of the transformer, kW	243

$$Z_k = \frac{\bar{\bar{U}}_{1k} \cdot U_{1н} \cdot K_т}{I_{2н} \cdot n}$$

Short circuit impedance of the transformer, Ohm,

where $\bar{\bar{U}}_{1k}$ – the short circuit voltage, %;

$U_{1н}$ – rated voltage of the primary (mains) winding of the transformer,

$K_т$ – transformation ratio, $K_T = \frac{U_{1н}}{U_{2н}}$

n – the number of traction windings

$I_{2н}$ – rated current of the secondary (traction) winding of the transformer.

Short circuit loss power ΔPk spent on heating the transformer windings, kW,

$$\Delta P_k = r_k \frac{n^2 \cdot I_{2н}^2}{K_T^2}$$

where r_k – the active resistance of the transformer windings, reduced to the primary winding.

Losses in the steel of the transformer magnetic circuit in the nominal mode:

$$\Delta P_c = \Delta P_н - \Delta P_k$$

where $\Delta P_н$ - power losses in the nominal mode of the transformer.

The transformer operates with maximum efficiency at a load equal to ¾ of the nominal. In this case, the variable losses (in copper) are equal to the constant losses (in steel):

$$\Delta P_k \left(\frac{3}{4}\right)^2 = \Delta P_c$$

Hence the losses in copper for the transformer short circuit mode, kW:

$$\Delta P_k = \frac{\Delta P_н}{1+\left(\frac{4}{3}\right)^2}$$

Active resistance of the transformer windings, reduced to the primary winding, Ohm,

$$r_k = \frac{\Delta P_k \cdot 10^3}{n^2 \cdot I_{2н}^2} K_T^2$$

Inductive resistance of transformer windings due to stray magnetic fluxes, Ohm,

$$X_k = \sqrt{Z_k^2 - r_r^2}$$

The inductive resistance of the primary winding of the transformer, due to the magnetic leakage fluxes, is determined on the basis of bringing all the traction windings to one equivalent and assuming the equality of the magnetic leakage fluxes of the primary and secondary windings, Ohm:

$$X_{1\sigma} = \frac{1}{2} \cdot X_k$$

Inductive resistance of the equivalent secondary leakage winding, taking into account the accepted assumption, Ohm,

$$X_{2\sigma} = \frac{X_k}{2 \cdot K_T^2}$$

Leakage inductance of the primary (mains) winding, H,

$$L_{1\sigma} = \frac{X_{1\sigma}}{2 \cdot \pi \cdot f_c}$$

where f_c - the voltage frequency of the traction network, Hz.

Leakage inductance of each secondary (traction) winding of the transformer, (a1-x1…a6-x6), H

$$L_{2\sigma} = n \frac{X_{2\sigma}}{2 \cdot \pi \cdot f_c}$$

The active resistance of the primary (mains) winding of the transformer is determined based on the assumption of equality of losses in the primary and secondary windings: Ohm, $r_1 = \frac{r_k}{2}$

Active resistance of each secondary (traction) winding, (a1-x1,…a6-x6), Ohm,

$$r_2 = \frac{r_k}{2 \cdot K_T^2} \cdot n$$

Impedance of the magnetic circuit of the transformer, Ohm, $Z_m = \frac{U_{1н}}{I_{10}}$

where I_{10}- the no-load current of the transformer.

The active component of the no-load current of the transformer is determined on the basis of losses in the steel of the transformer, equal to the difference be-

tween total losses and short-circuit losses, A

$$I_{mA} = \frac{\Delta P_н - \Delta P_k}{U_{1н}}$$

Active resistance of the magnetic circuit for a T-shaped equivalent circuit and parallel connection of active and inductive resistances of the magnetic circuit, Ohm,

$$R_m = \frac{U_{1н}}{I_{mA}}$$

Magnetizing current of the magnetic circuit of the transformer, A,

$$I_m = \sqrt{I_0^2 - I_{mA}^2}$$

Inductive resistance of the magnetic circuit, Ohm, $X_m = \frac{U_{1н}}{I_m}$

Inductance of the magnetic circuit of the transformer, H, $L_m = \frac{X_m}{2 \cdot \pi \cdot f_c}$

The results of calculating the parameters of the windings of the JQFP-10160/25 traction transformer are systematized in Table 1.

Assessment of the adequacy of the computer model of the traction transformer

The adequacy of the computer model is evaluated based on the simulation of the idle mode and the short circuit mode of all traction windings.

The diagrams (Figure 4-5) show the results of the idling and short circuit test of the traction transformer.

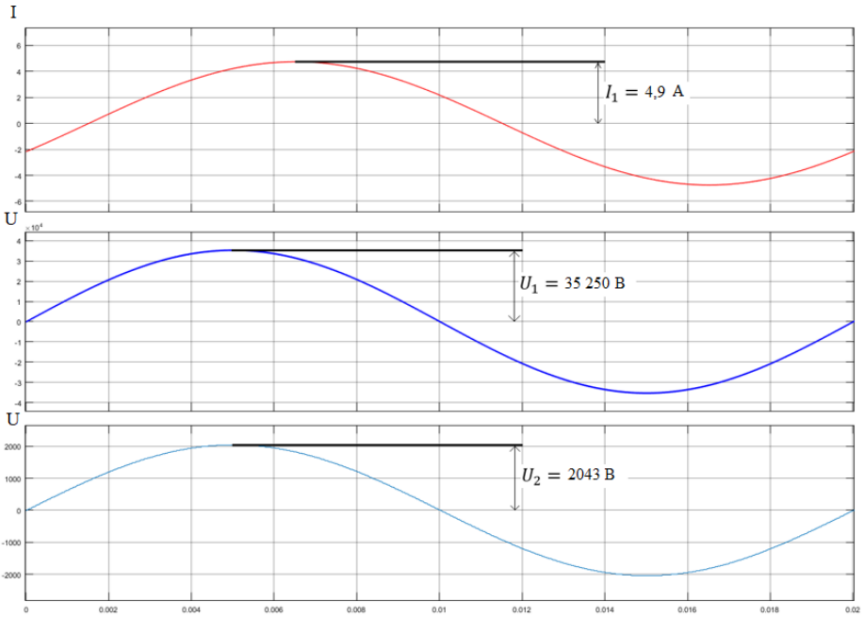

Figure 4. *Simulation of the idle traction experience transformer, U_1- voltage and I_1- current of the primary winding of the transformer at idle, U_2 - voltage of the traction winding*

Figures 3.7-3.8 show the amplitude values of the current and voltage of the transformer windings. When simulating the idling experience, the primary winding is fed rated voltage, the amplitude value of which is: $U_{1m} = 2500 \cdot \sqrt{2} = 35250\ V$ The amplitude value of the voltage of the traction winding of the computer model of the transformer in the idle mode is: U_{2m} = 2043 V

Relative error voltage of the traction winding of the computer model of the transformer: $\frac{U_{2н} \cdot \sqrt{2} - U_{2m}}{U_{2н} \cdot \sqrt{2}} \cdot 100 = \frac{1450 \cdot \sqrt{2} - 2043}{1450 \cdot \sqrt{2}} \cdot 100 \cong 0{,}1\%$

The amplitude value of the no-load current of the network winding of the computer model of the transformer: I_{10m}=4.9A

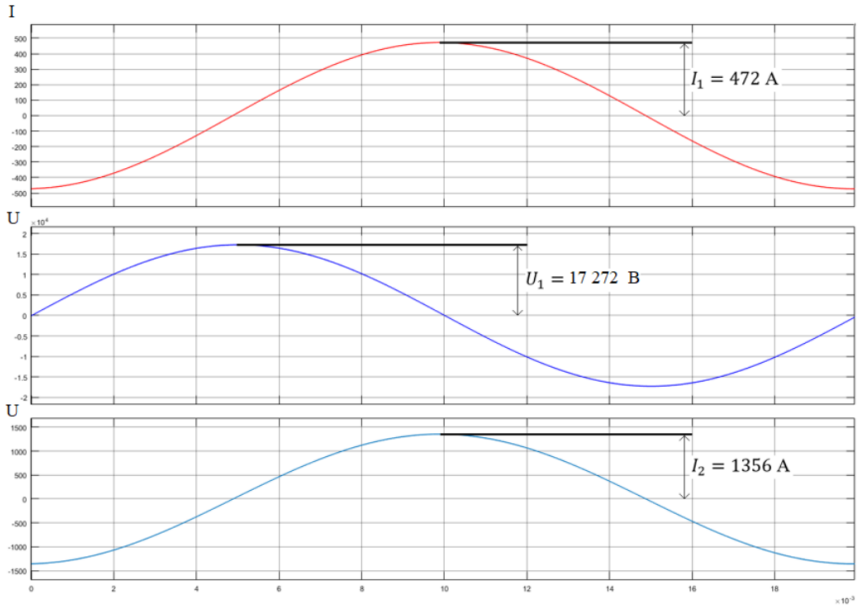

Figure 5. *Simulation of short circuit experience of a traction transformer, U_1 - voltage, I_1 - current of the primary winding and I_2 - current of the secondary winding of the transformer.*

Relative error of the no-load current of the primary winding of the computer model of the transformer:

$$\frac{0.01 \cdot I_{1н} \cdot \sqrt{2} - I_{10m}}{0.01 \cdot I_{1н} \cdot \sqrt{2}} \cdot 100 = \frac{0.01 \cdot 360 \cdot \sqrt{2} - 4.9}{0.01 \cdot 360 \cdot \sqrt{2}} \cdot 100 \cong 3.75\%$$

The magnetization characteristic of a typical computer model of the Multi-Winding Transformer is linear, without saturation, so the no-load current obtained in the computer model has a sinusoidal shape without distortion typical of the no-load current of a real transformer. When modeling the short circuit experience, the calculated voltage was applied to the primary winding, the amplitude value of which is:

$$U_{1кзm} = \frac{U_к}{100} \cdot U_{1н} \cdot \sqrt{2} = \frac{49}{100} \cdot 25000 \cdot \sqrt{2} = 17272 \text{ В}.$$

Hence $U_к$ - the short circuit voltage; $U_к$ =39%.

The amplitude value of the current of the network winding of the computer model of the transformer:

$$I_{1кз.m} = 472 \text{ A}.$$

Relative error of the current of the network winding of the computer model of the transformer:

$$\frac{nI_{2н}/K_т \cdot \sqrt{2} - I_{1кз.m}}{nI_{2н}/K_т \cdot \sqrt{2}} \cdot 100 = \frac{6 \cdot 965/17{,}24 \cdot \sqrt{2} - 472}{6 \cdot 965/17{,}24 \cdot \sqrt{2}} \cdot 100 \cong 0{,}4\%.$$

The amplitude value of the current of the traction winding of the computer model of the transformer in the short circuit mode: $I_{2кз.m}$=1356 A

Relative error of the current of the traction winding of the computer model of the transformer:

$$\frac{I_{2н} \cdot \sqrt{2} - I_{2кз.m}}{I_{2н} \cdot \sqrt{2}} \cdot 100 = \frac{965 \cdot \sqrt{2} - 1356}{965 \cdot \sqrt{2}} \cdot 100 \cong 0{,}35\%.$$

The obtained results of simulation of experiments of idling and short circuit of the traction transformer confirm the adequacy of the computer model to the real traction transformer. Therefore, we can assume that the calculated parameters of the traction transformer make it possible to reproduce electromagnetic processes in the traction drive of an AC electric locomotive of the O'Z-ELR series in traction and regenerative braking modes close to real ones.

References

1. *Bessonov A.A. Theoretical foundations of electrical engineering. Electrical circuits. M.: "High School". 1978. 516 p.*

2. *Nazirkhonov T. M., Yakushev A. Ya. Computer model of the traction transformer of the AC electric locomotive of the O'Z-ELR series / T. M. Nazirkhonov, A. Ya. Yakushev // Proceedings of the Petersburg University of Communications. – St. Petersburg: PGUPS, 2020. – V. 17. Issue. 3. – P. 416–427.*

3. *Potemkin V.G. Simulink: Environment for creating engineering applications / V.G. Potemkin. M.: Dialogue Mifi, 2003, 496p.*

DOI 10.34660/INF.2022.45.47.199

乌中电力机车电力电气设备
POWER ELECTRICAL EQUIPMENT OF UZBEK-CHINESE ELECTRIC LOCOMOTIVES

Buronov Firuz Yorkin ugli
Master's degree Student
Umarov Umidjon Xislatjon ugli
Master's degree Student
Volodin Anatoly Alexandrovich
Candidate of Technical Sciences, Associate Professor
Emperor Alexander I St. Petersburg State Transport University

抽象的。 文章介绍了乌中电力机车的电力电气设备。 分析了在电路中相互连接的异步牵引电机和 4q-S 转换器的显着特征和操作模式。

关键词：乌中电力机车，异步牵引电机，4q-S-转换器，半导体转换器。

Abstract. *The article deals with the power electrical equipment of the Uzbek-Chinese electric locomotives. The distinctive features and modes of operation of an asynchronous traction motor and a 4q-S-converter connected to each other in an electrical circuit are analyzed.*

Keywords: *Uzbek-Chinese electric locomotives, asynchronous traction motor, 4q-S-converter, semiconductor converters.*

Introduction

Uzbek-Chinese electric locomotives, which are made in China by order of "Uzbekiston Temir Yullari" JSC, with adaptation to the conditions of Uzbekistan, taking into account the climatic conditions of our region and its geographical features with complex mountainous terrain. Today, most of the locomotive fleet of Uzbekistan is made up of Chinese-made electric locomotives. Electric locomotives of the "O'zbekiston" series (since 2003), "O'Z-Y" (since 2009), "O'ZEL" (since 2013), "O'Z ELR" (since 2015), and a new generation of electric locomotives in Uzbekistan "2 O'Z ELR" and "2 O'Z UY" (since 2020) (Fig. 1).

Figure 1. *Electric locomotives of the "2 O'Z ELR" and "2 O'Z UY series" (Photo from railway.uz)*

Electrical part of electric locomotives.

The main feature of the electrical part of electric locomotives is the use of the method of electric drive of the variable-constant-variable type and three-phase asynchronous motors.

Asynchronous traction motors (ATM) are powered from the secondary windings of the transformer through four-quadrant (4q-S) converters that provide voltage, frequency regulation on traction motors (TEM) and power factor (Fig. 2). New electric locomotives differ from the old ones in that they use ATD and 4q-S converters. [2].

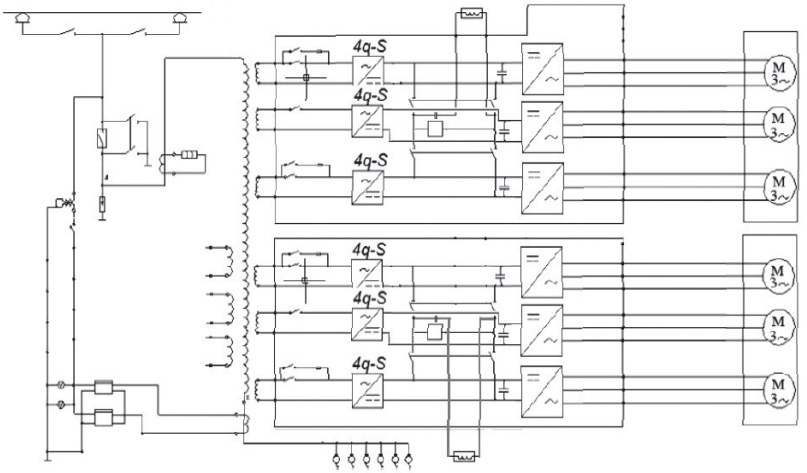

Figure 2. *Schematic diagram of an electric locomotive of the "O'Z-ELR" series*

Electric locomotives have two current collectors, which are connected through disconnectors. The power circuit is protected by the main switch. When performing work in the electrical part of the electric locomotive, a grounding disconnector should be used. In this case, other disconnectors must be switched off. Overvoltage protection is provided by a surge arrester; protection against overloads and short circuits - a current transformer, to the secondary winding of which a relay is connected. When this relay is activated, the main switch is turned off. The voltage of the contact network is supplied to the primary winding of the main transformer. This transformer has six secondary windings for powering 1M-6M traction motors through converters. [1]

Asynchronous traction motors

Traction motors of electric locomotives are a three-phase asynchronous electric machine with a squirrel-cage rotor with adjustable speed. Regulation is carried out by changing the value of the frequency of the supply voltage. An asynchronous machine is an alternating current machine, in which the rotor rotation speed is different from the field rotation speed. It uses the principle of the effect of a rotating magnetic field on a short-circuited coil. The magnetic system of an asynchronous machine consists of two steel cores: an outer annular fixed stator and an inner cylindrical rotating rotor. The machine has two windings, one of which - the primary winding of an induction motor which is placed in grooves on the inside of the stator core, and the other - the secondary winding which is placed in grooves on the outer surface of the rotor cylinder. To reduce eddy current losses, both of these cores are assembled from sheet electrical steel. Asynchronous trac-

tion motors can operate in traction and electric braking modes. The indicators of each mode of operation of an asynchronous traction motor (ATM), in contrast to collector machines, are determined by the law of traction motor control. In order to establish the most effective ATD control laws, it is necessary to consider the dependence of the torque on its parameters

$$M = \frac{m_1 p_1 U_1^2 r_2'/s}{9{,}81\omega_1\left[\left(r_1 + \frac{r_2'}{s}\right)^2 + (x_1 + x_2')^2\right]} \quad (1)$$

where m_1 and p_1 are, respectively, the number of phases and pairs of poles of the stator winding; U_1 – motor phase voltage; r_2' and x_2' – active and inductive resistances of the rotor reduced to the parameters of the stator circuit; $\omega = 2\pi f_1$ – angular frequency of rotation of the stator field; f_1 –stator current frequency; r_1 and x_1 active and inductive resistances of the stator winding, respectively; $s = \frac{(\omega_1 - \omega_2)}{\omega_1}$ relative slip of the rotor; $\omega = 2\pi f_{вр}/p_1$ angular frequency of rotation of the rotor. An analysis of equation (1) shows that the moment is characterized by three parameters: U_1, f_1 and f_2, and under conditions of electric traction they can vary over a wide range.

To facilitate the analysis of ATD operating modes, it is advisable to express the dependence of the electromagnetic torque through the stator magnetic flux, rotor current and absolute slip f_2:

$$M_э = \frac{m_1 p_1}{2\sqrt{2}}\ \omega_1 K_{об1} \Phi I_2' \cos\varphi_2\,; \quad (2)$$

$$M_э = \frac{p_1}{\sqrt{2}} \frac{\Phi^2 f_2 r_2}{[r_2^2 + (2\pi f_2 L_{2б})^2]}, \quad (3)$$

where ω_1 and $K_{об1}$ – respectively, the number of turns of the phase and the winding ratio of the stator winding; r_2 – unreduced resistance of the "cages" of the rotor; φ_2 – displacement angle between EMF vectors and rotor winding current: $\cos\varphi_2 = \frac{r_2}{\sqrt{r_2^2 + (2\pi f_2 L_{2б})^2}}$; $L_{2б}$ – inductance of the rotor bars from leakage fluxes.

For frequency-controlled asynchronous traction motors, the basic control law of M.P. Kostenko is known

$$\frac{U_1}{U_{1\,ном}} = \frac{f_1}{f_{1\,ном}} \sqrt{\frac{M}{M_{ном}}} = (f_1/f_{1\,ном})(\Phi/\Phi_{ном}), \quad (4)$$

where $U_{1ном}$ – is the nominal value of the phase voltage; M and $M_{ном}$ respectively, the current and nominal values of the moment; Φ and $Φ_{ном}$ – current and nominal values of the magnetic flux, respectively.

Considering that the speed of movement of the $v = 0{,}188\frac{D_к}{\mu}\frac{60f_1}{p_1}(1-s) \approx c_1 f_1$, and the traction force $F = \frac{2M}{D_к}\mu\eta_з = c_2 M$, where $D_К$ – the diameter of the driving wheel, m; μ – is the gear ratio of the traction reducer; $\eta_з$ – efficiency of the driving mechanism, we represent the expression (5) in the form

$$\frac{U_1}{U_{1\,ном}} = \frac{v}{v_{ном}}\sqrt{\frac{F}{F_{ном}}} \tag{5}$$

The rated values $v_{ном}$ and $F_{ном}$ correspond to the rated phase voltage and rated frequency $f_{1ном}$.

Semiconductor converters

On electric locomotives, converters with a pronounced DC link are mainly used to power the ATD, performing a two-stage conversion of electricity. In the traction mode, this is the rectification of the voltage taken from the secondary winding of the transformer, and its subsequent inversion into a three-phase one to power the ATD.

An autonomous voltage inverter (AVI) is used as a frequency converter and the number of phases to power the ATD on the rolling stock. AVI stabilize this voltage at a given level.

When using AVI, which performs the functions of not only converting the voltage frequency, but also regulating its magnitude due to modulation, on AC electric locomotives with ATD, a 4q-S converter is used as an input, stabilizing the voltage in the DC link (i.e. on AVI input).

4q-S converter

The primary winding of the transformer T is powered by an alternating current network with a voltage U_c. The secondary winding of the transformer through the inductor *L*c is connected to the four arms of the 4q-S converter, formed by IGBT transistors VT1-VT4 and diodes VD1-VD4. Resonant ($L_{ф1}$, $C_{ф1}$) and main ($C_ф$) filters connected in parallel with the load are connected to the output of the converter. (Fig. 3)

A feature of the 4q-S converter is that it is a step-up converter and for its normal operation, the voltage on the main filter capacitor ($C_ф$) must be greater than the voltage amplitude of the power source (in this case, the secondary winding of the transformer).

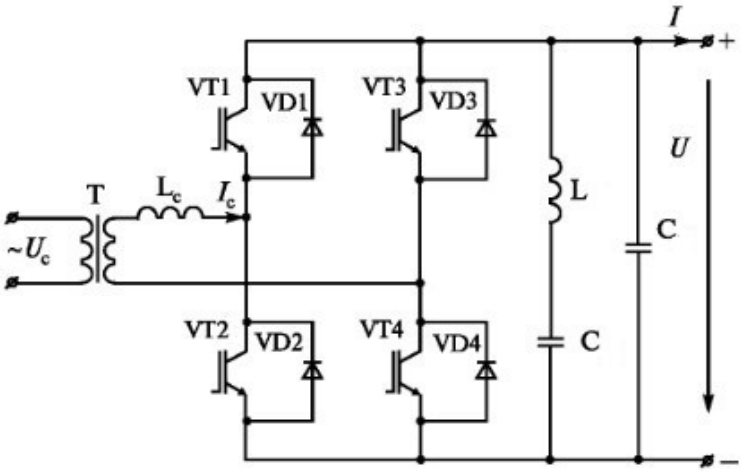

Figure 3. *Simplified circuit diagram of a 4q-S converter*

The 4q-S converter can be controlled either by direct regulation of the transformer secondary current (current corridor mode) or by sinusoidal pulse width modulation (PWM).

When using the current corridor mode, the mains current (I_c) is formed as a sinusoid with a specified phase shift relative to the supply voltage:

$$I_з(t) = I_{зmax} \sin(2\pi f_c t - \varphi_0) \quad (6)$$

Where $I_з$ – the set value of the mains current; $I_{зmax}$ – amplitude value of the given current; f_c – frequency of the supply network; φ_0 –phase shift between the given current and supply voltage.

The control of transistors VT1-VT4 is carried out as follows. The amplitude value of the mains current and the width of the current corridor $I_з$, are set (Fig. 4). At the beginning of the half-cycle, the supply voltage is insufficient to ensure the growth of the inductor current (I_c) with the intensity required to stay inside the current corridor. Therefore, the inductor charge (L_c) is carried out from the filter capacitor ($C_ф$) throughVT2, VT3 in the positive half-cycle and VT1, VT4 in the negative. When the current I_c increases to the upper limit of the corridor, the inductor is discharged to the power source through VT3, VD1 in positive and VT4, VD2 in negative half-cycles of the supply voltage. When the current drops to the lower limit of the corridor, the inductor is charged again, etc.

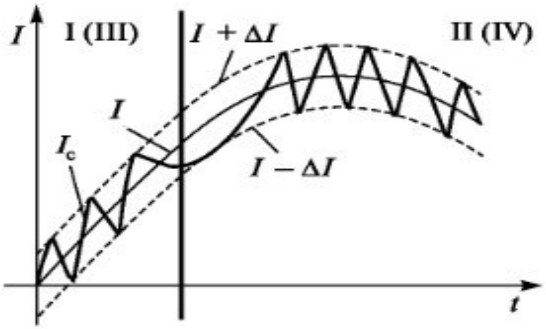

Figure 4. *Current corridor control 4q-S converter*

This mode corresponds to zones I and III (for positive and negative half-cycles) of the 4q-S-converter operation.

Conclusion

In Uzbekistan, the locomotive crews are very satisfied with the new equipment, as the new electric locomotives are fully computerized and, compared to previous generations of this equipment, are quite easy to operate. They are equipped with modern security and diagnostic systems. For example, if a hardware malfunction is detected along the way, then a corresponding message is displayed on the on-board computer monitor and ways to eliminate it are also indicated here. It is also noteworthy that modern technologies used in the presented locomotives, along with saving electricity, can also reduce fuel consumption. Currently, over 50 percent of the existing locomotives have been updated in the locomotive fleet of "Uzbekiston Temir Yulari" JSC.

References

1. Plaks A. V. Electric locomotive "Uzbekiston" / A. V. Plaks, D. O. Radzhibaev // Izv. Petersburg. University of Communications. – St. Petersburg: PGUPS, 2009. – No. 3. – P. 47–56.

2. Tursunov Kh. M. Modern electric locomotives for the railway of the Republic of Uzbekistan / Kh. M. Tursunov // Technical sciences – from theory to practice: collector of articles based on the VI Intern. scientific-practical. conferences. – Novosibirsk: SibAK, 2012. – P. 75–78.

3. Ovchinnikov A. N. High-speed and high-speed traffic on the railways of Uzbekistan / A. N. Ovchinnikov, A. F. Rasulov, Z. T. Fozilov // Way. – 2012. – No. 5. – P. 65–67.

4. Plaks A. V. Electric locomotive of the "O'zbekiston" series / A. V. Plaks, D. O. Radzhibaev, H. M. Tursunov // Bullet. VELNIII. – Novocherkassk: VELNIII, 2011. – No. 1. – P. 114–127.

5. Nazirkhonov T. M. Maintenance of traction converters in the electric transport of Uzbekistan / T. M. Nazirkhonov // X Intern. scientific-practical. conference "TRANS-MECH-ARTCHEM". – M.: MIIT, 2014. – P. 80–81.

6. Plaks A. V. New passenger electric locomotive of the "O'Z-Y" series / A. V. Plaks, D. O. Radzhibaev, H. M. Tursunov // Scientific problems of transport of Siberia and the Far East. – 2011. – No. 1. –P. 237–240.

7. Asynchronous traction drive of locomotives: textbook/ A. A. Andryushchenko, Yu.V. Babkov, A.A. Zarifyan and others; ed. A.A. Zarifyan a. – M.: FSBEI "Educational and methodological center for education in railway transport", 2013. - 413 p.

DOI 10.34660/INF.2022.57.96.200

城市和郊区铁路线的“智能”动车车辆概念
THE CONCEPT OF «SMART» MOTOR-CAR ROLLING STOCK FOR URBAN AND SUBURBAN RAILWAY LINES

Vikulov Ilya Pavlovich
Candidate of Technical Sciences, Associate Professor
Byltseva Vasilisa Dmitrievna
Alekseeva Margarita Alexandrovna
Emperor Alexander I St. Petersburg State Transport University

抽象的。 圣彼得堡地区和邻近地区的快速发展使得有必要加强现有的交通联系和基础设施。 在这些条件下，轻轨交通（LRT）成为城市和地区良好运转的首选方向之一。 为城市和郊区铁路引入“智能”动车组将解决许多问题，但同时，开发商需要考虑到这些设备的现代化要求。

关键词：有轨电车、机车车辆、铁路、数字化。

Abstract. *The rapid development of the districts of St. Petersburg and adjacent territories makes it necessary to strengthen the existing transport links and infrastructure. Under these conditions, light rail transport (LRT) becomes one of the preferred directions for the favorable functioning of the city and the region. The introduction of "smart" multiple unit rolling stock for urban and suburban railway lines will solve a number of many problems, but at the same time, developers need to take into account modern requirements for these pieces of equipment.*

Keywords: *tram-train, rolling stock, railway, digitalization.*

Table 1 shows a comparative analysis of the technical characteristics of a tram car and an electric train, showing the possibility of developing a universal tram-train rolling stock for urban and suburban lines [1,2].

Table 1.
Technical characteristics of the tram car and electric train

Main technical characteristics		
Wagon type	**AKSM-843 (BKM-843)**	**ES2G (Lastochka)**
Maximum speed, km/h	86	160
Seating places, people	66	368

Full capacity, persons	230	886
Weight, kg	47800	260000
Power of the traction system of engines, pcs×kW	4x105	366
Technical data of current collector		
Rated contact network voltage (DC), V	3000	600/750
Rated current, A	580	1000
Contact wire suspension height, not less than, mm	5700	5750
Skid height, mm	from 4100 to 6187,5	from 5500 to 6800
Maximum lift, mm	2300	2600
Overall size of the contact insert without and with protective whiskers, not less than, mm	1200 and 1600	1210 and 1700
Operating range, mm	400-2100	500-2500
Wheel set technical data		
Maximum static load on the wheelset, t	10	19
Weight, kg	538	1150
Bandage distance, mm	1474	1440
Diameter of worn and new wheels, mm	530-620	840-920
Track width, mm	1524±2	1520
Trolley technical data		
Car bogie base, mm	2400	1900 ± 2
Cart weight, kg	No more than 7200	4500 and 2766
Wheel type	Solid-rolled	Resilient
Difference between the diameters of the wheels of two wheelsets, mm, not more than	1	0,5
Brake type	Disc, electric	Disc, rail

The main problems in the implementation of a tram-train in suburban areas that require increased attention are the issues of interaction of wheel sets with the track infrastructure, a current collector with a contact wire, matching the parame-

ters of the traction drive with the parameters of external power sources, organizing the boarding and disembarking of passengers, compliance with traffic safety requirements, compliance with rolling stock digitalization standards. Next, ways to address these issues will be discussed.

The problem of fitting a tram-train into the dimensions of the rolling stock of railways. An analysis of the technical characteristics of rail rolling stock shows that a tram car is smaller than an electric train in terms of its main dimensions. Based on this, the tram car will be able to pass along the railway lines without obstacles [3,4] and in compliance with the requirements of the rolling stock gauge. The overall dimensions of the electric train and tram car are shown in Figure 1.

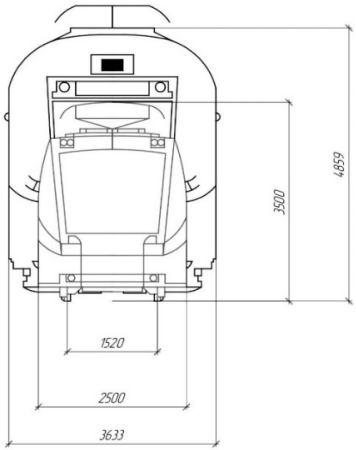

Figure 1. *Scheme of an electric train and a tram car*

The problem of interaction between the current collector and the contact network. The operating range of the height of the skid relative to the level of the rail head on the electric train is in the range of 5500-6800 mm. The working height range of the tram skid relative to the level of the rail head is 4100-6187.5 mm, therefore, from the point of view of the design of the tram-train, it is more expedient to use the tram current collector, since it is possible to compensate for the insufficient opening height of the current collector by using additional inserts in the current collector supports and the use of support insulators designed for the voltage of the railway contact network [5,6].

The problem of matching the voltage parameters of the contact network and the parameters of the traction drive. The presented circuit (Figure 2) provides the possibility of powering the tram-train both from the railway DC circuit with a

nominal voltage of 3000 V, and from the contact network of the tram with a voltage at the current collector of 550 V. The Qpm current type switch eliminates the possibility of simultaneously turning on the power supply from 550 and 3000 C. When powered from the railway contact network from the current collector T1 through the high-speed switch QF1, the linear contactor LK1, the output filter L and the diode VD3, it comes to an autonomous multi-cell high-frequency inverter AICH 1.1-1.6 through a step-up converter IP.

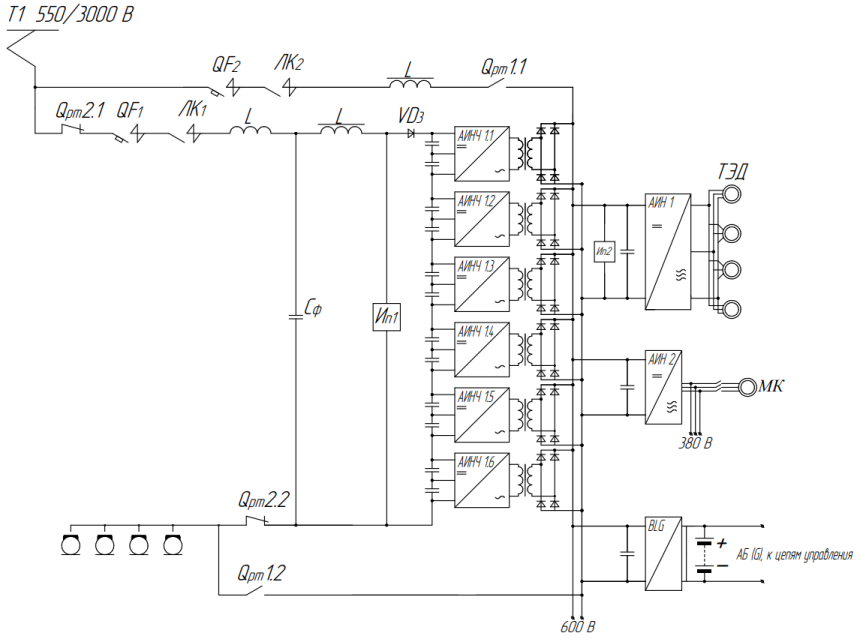

Figure 2. *Electrical diagram of the tram-train*

After conversion through an isolating isolation transformer and uncontrolled rectifiers, the rectified current is supplied to the intermediate bus with a voltage of 550 V, and from it to the AI1,2 inverters and the BLG battery charger. After entering the AIN1, the direct current is converted back into an alternating current to feed the asynchronous traction motors TM1-4 into the power circuit. Similarly, through AIN2, the motor-compressor and a three-phase circuit with a voltage of 380 V are powered. Through the BLG step-down boost converter, the battery is charged and the control circuits are powered. When the circuit is operated from a 550 V tram contact network, the current through the current collector, the QF2

quick-acting switch, the LK2 linear contactor and the output filter L goes directly to the 550 V bus, and from it AI1,2 and BLG. The remaining processes proceed in the same way as when working from a railway contact network.

The problem of interaction between the wheelset of a tram car and the track infrastructure of railways. The tram wheel is made structurally narrower than the railway wheel and has a smaller flange in height and width; for the possibility of safe passage of railway special parts, the wheels must be finalized. The wheelset of a BKM model tram car was taken as the basis for the design, to which a bandage made according to a new profile is mounted. Figure 3 shows a tram-train wheelset.

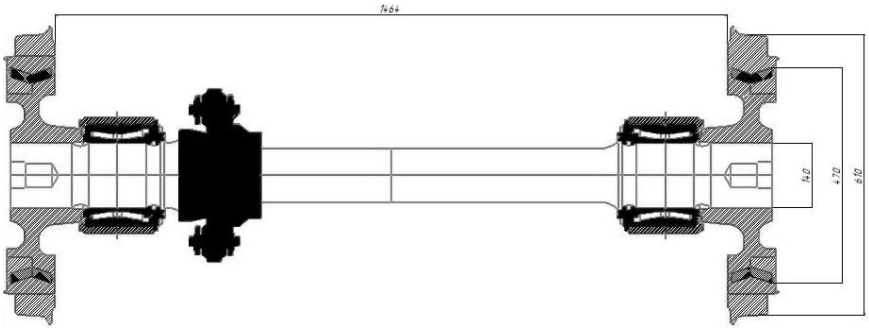

Figure 3. *Tram-train wheelset*

The problem of embarkation and disembarkation of passengers on railway lines. Modern tram systems use, as a rule, low platforms (300 mm), on railways, mainly high platforms are used (1100 from the top of the rail heads and 1920 from the edge of the platform to the axis of the track). The way out of this situation can be as follows: in continuation of the high platform, a low platform is built, connecting them with a ladder. Also, the tram-train can be equipped with retractable steps at the entrance doors to compensate for the difference in floor levels of vestibules and boarding platforms.

Currently, a “smart” concept of a tram-train is being developed, which will use digital technologies of "Russian Railways" OJSC and St. Petersburg State Unitary Enterprise "Gorelektrotrans". Tram cars use the GEO.RITM system - this is a special software for solving transport monitoring problems. Designed to track the location of the rolling stock, during operation it determines the values of additional parameters (current time, direction of movement, speed of movement, etc.).

Achieving the required level of digitalization can be achieved by improving and introducing sensors, “smart systems”, into new and already operated pieces of equipment. The tram-train system should bear the minimum economic and design

costs. These requirements will be met by the new MCS-007-003, created on the basis of MCS-007-002.

The microprocessor control and diagnostic system is designed to control power and auxiliary circuit devices and other devices. MPSU, based on information received from the control panel, as well as from devices and sensors, controls power converters and devices and provides:

- required operating modes of the equipment;
- interaction of individual wagons;
- interaction with security systems and digital technological radio communication;
- self-diagnostics and diagnostics of units, devices and electrical machines based on the information received from them;
- automatic control of auxiliary circuit equipment.

The main task of MCS-007-003 is predictive analytics, which monitors the technical condition of equipment and predicts failures with an indication of a specific locomotive node in real time and automatically detects violations of equipment operation modes. The design features of the system are that the MCS control system with the SIM function is integrated into the MCSD control system in the form of a module with a protective casing, shown in Figure 4.

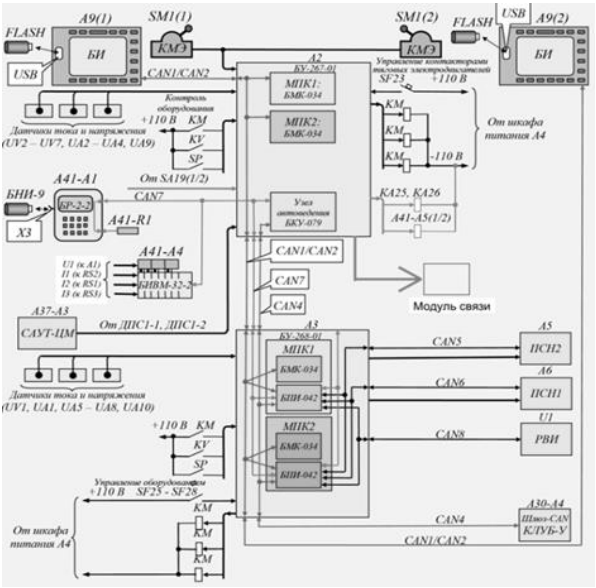

Figure 4. *Block diagram of MPSU-007-003*

The basic principle of operation of the MPSU is to transfer data from a satellite to a tram-train via GPRS systems via GLONASS / GPS channels using the corporate mobile network of "Russian Railways" OJSC and St. Petersburg State Unitary Enterprise "Gorelektrotrans", from rolling stock to a server, and then to external automated systems management. For software, you should use the existing application shown in Figure 5, integrated into Russian Railways - MCS Analyzer [7,8].

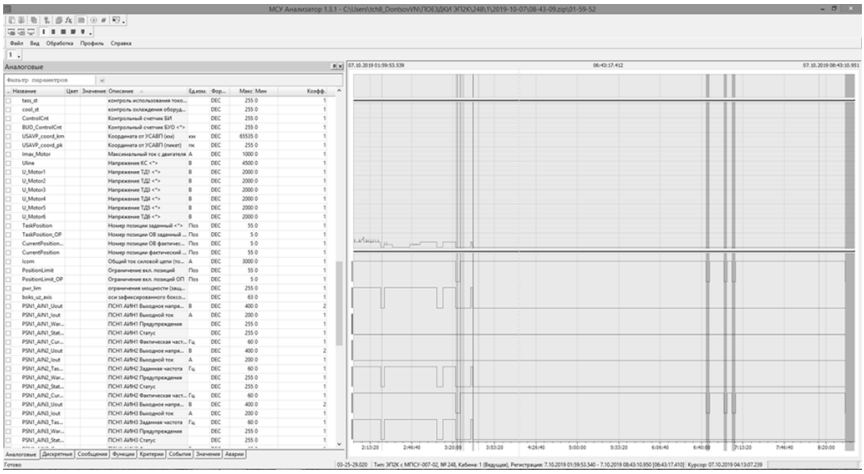

Figure 5. *Interface of the program MCS Analyzer*

This system will prevent emergency situations, such as an unscheduled stop of a tram-train en route, as well as ensure timely transmission of information about the need for repairs. The introduction of MCS-007-003 will bring the rolling stock to a new level of digitalization and simplify the work of maintenance personnel, thereby solving such problems as the large financial losses of "Russian Railways" OJSC and St. Petersburg State Unitary Enterprise "Gorelektrotrans", from unscheduled repairs and stops of the rolling stock en route.

The problem of compliance with traffic safety requirements. The tram-train must be equipped with a continuous automatic signaling system that transmits signal indications to the control panel of the rolling stock in order to increase the safety of its movement. The proposed design solutions will make it possible to successfully operate the tram-train both on urban rail transport lines and on mainline railway lines. The basis for the design of the tram-train should be a tram car of the BKM series. It is planned to use routes on the territory of the St. Petersburg agglomeration as a testing ground where it is possible to organize trial operation of a tram-train

References

1. Selezneva A.I., Gorbunova V.S. Problems of transport infrastructure in the planning of modern cities and ways to solve them. Magazine of Science and Education Perspectives. Issue No. 6. – 2013 – 195-199 p.

2. Prospects for the development of light rail transport in the cities of R.F. https://cyberleninka.ru/article/n/perspektivy-razvitiya-legkorelsovogo-transporta-v-gorodah-rf/viewer (date of access 08.04.2022).

3. Fedorov V.A., Kitayev S.V. Light rail transport in St. Petersburg. Transport of the Russian Federation. Magazine of science, practice, economics. – 2013 – 54-58 p.

4. Dudkin E.P., Chernyaeva V.A. Areas of effective use of urban rail transport and the possibility of their expansion. Transport of the Russian Federation. Magazine of science, practice, economics. – 2015 – 48-51 p.

5. Chernyaeva V.A., Levadnaya V.A. Analysis of design factors for urban transport systems. - Ufa: BGU. – 2013 – 284 p.

6. Kayonova G.A., Osyanina E.I., Shulga R.A. Young scientist. International Scientific Magazine No. 33 (323) / 2020. - Kazan: LLC "Young Scientist". – 2020 – 90 p.

7. Dzyuba, Yu.V., Pavlovsky A.A., Umansky V.I. Digital railroad. Technological level. – International electronic scientific magazine– 2018 – 208 – 2013 p.

8. Russian Railways, road to the future. https://18rzd.interfax.ru/ (date of access 23.05.2022).

DOI 10.34660/INF.2022.59.63.201

高速铁路的技术经济特点
THE TECHNICAL AND ECONOMIC CHARACTERISTICS OF HIGH-SPEED RAIL

Li Yiyuan
Master's degree Student
Shen Jieyi
Master's degree Student
Tsaplin Aleksey Evgenievich
Candidate of Technical Sciences, Associate Professor
Emperor Alexander I St. Petersburg State Transport University

摘要：随着社会经济的快速发展和区域间、城际联系的不断加强，普通铁路已难以满足时间短、运量大、交通舒适便捷的需求。　近年来，高铁脱颖而出，不仅带动了国家的经济效益，也促进了社会效益的发展。

Abstract. *With the rapid development of social economy and the continuous strengthening of inter-regional and inter-city connections, ordinary railways have been unable to meet the needs of short time, large transportation volume, and comfortable and convenient transportation. In recent years, high-speed rail has come to the fore, not only driving the economic benefits of the country, but also promoting the development of social benefits.*

Keywords: *high speed railway, economic benefits, social benefit*

The technical and economic characteristics of high-speed rail

1. High speed, high density

High-speed railways with operating speeds of 250 km/h and 300 km/h have clear advantages for medium and long distance transport.

For example, at a distance of about 1000 kilometers, high-speed rail and air transportation are compared, and after research, it turns out that their advantages are very obvious. In the future, the speed of trains on high-speed rail will be higher. In addition, high-speed rail can adopt high-density public transport mode with advanced communication signals and train control technology. The carrying capacity of high-speed railways is very high.

High-speed rail versus road and air

Motorway: The average annual one-way traffic capacity is about 95 million people.

Aviation: One-way capacity can reach 15 to 18 million people.

High-speed rail: Average annual one-way capacity will reach 47.45 million, with all reconnected trains, the number of passengers will reach 94.9 million, close to 100 million people.

Therefore, the carrying capacity of high-speed rail is very large.

2. Good comfort

The high-speed train has scientific and reasonable built-in, complete amenities, spacious and comfortable seats, good running performance, very stable performance, shock absorption, sound insulation, and very quiet inside the car. (Figure 1 and Figure 2)

Figure 1. *High-speed rail interior*

Figure 2. *High-speed rail interior*

The high-speed train runs smoothly and comfortably. It can provide an unrivaled personal space for aircraft and automobile operation, as well as meetings, entertainment, sightseeing and other environments.

The modern railway station and carriage facilities and high-speed rail equipment provide humanized services for passengers. They also have special access for the disabled, special toilets for the disabled, etc. to meet the diverse needs of different passengers.

3. Small footprint

High-speed railways take up less land resources. The practice of railway construction at home and abroad shows that high-speed railway can save construction land, and the effect is very obvious compared with the construction of airports and highways.

When France formulated the bill for the TVG Atlantic high-speed rail line (Paris-Le Mans), it proved that the land for building this 280-kilometer line is smaller than the land used for the construction of the Charles de Lego airport near Paris.

The European road network occupies 1.3% of the entire territory of Europe, while the railway network occupies only 0.03% of the land. Rail infrastructure occupies less land than road infrastructure.

To complete the equivalent turnover of the conversion of kilometers, the area

of roads is 3.7-13.6 times the area of railways. The capacity of a double-track railroad in the United States is equivalent to that of a 16-lane highway: the land required for a railroad is only 15m wide, while the land required for a road is 122m wide, more than 8 times that. railroad As a rule, high-speed rail occupies only 1/3 of the highway.

4. Low power consumption

The energy intensity of high-speed rail is relatively small, especially in the context of the shortage of oil resources, the size of energy consumption has also become a very important indicator for the rapid development of transportation methods.

Why can high-speed rail develop, which consumes much less energy than cars and planes.

This is stated in the report of the International Union of Railways:

Total emissions: Road transport accounts for 73% of European transport carbon emissions, aviation accounts for 13%, and rail transport accounts for only 2%.

Carbon emissions per capita: In terms of per capita energy consumption, high-speed rail is 17g carbon dioxide per kilometer, bus is 30g, car is 115g, and aviation is 153g.

Carbon emissions during construction: Construction in France of high-speed railways produces about 60 tons of carbon dioxide emissions per kilometer, while two-way six-lane motorways will generate 73 tons of carbon dioxide emissions.

Carbon emissions from vehicle manufacturing: high-speed trains will generate 0.8-1.0 CO2/pkm (carbon emission factor), which is much lower than the 20.9 CO2/pkm of cars and similar to the 0.5 CO2/pkm of aviation.

In general, whether building high-speed rail, building high-speed trains, or operating high-speed rail, high-speed rail has relatively low energy consumption and is an effective means of reducing global carbon emissions.

5. Little pollution

Data on air pollutant emissions from aircraft, cars and high-speed trains during a trip from Frankfurt to Hamburg in Germany (Table 1).

Table 1.

Comparison of data on emissions of pollutants into the atmosphere

	Airplane	**Automobile**	**high speed rail**
Sulfur dioxide (unit: g)	43.4	32	19.5
Hydroxide (unit: g)	268.3	223	17.2
Particulate matter (unit: g)	2.1	21.2	1
Carbon dioxide (unit: g)	77.1	86	19.2

At the same time, the noise pollution of high-speed railways is relatively low.

European statistics show that in Europe road transport is the main source of noise, affecting approximately 90 million people during the day and 50 million at night.

The railway affects about 12 million people during the day and only about 8 million at night.

In general, the environmental impact of high-speed rail is relatively small.

6. Good transport efficiency

The Japanese Tokaido Shinkansen was opened for seven years, and all costs (construction funds) were reimbursed, after 1985 its annual profit was 200 billion yen.

The annual net profit of ICE intercity high-speed trains in Germany is 1.07 billion marks.

The annual net profit of the French TGV reached 1.944 billion francs.

7. Safe and reliable, high level of punctuality

The work management system and the dispatching system of the high-speed railway use advanced equipment, which can ensure the orderly and normal operation of the railway throughout the entire process of organizing transportation, which can ensure the punctuality of the train.

On average, the Japanese Shinkansen is late by no more than 1 minute. The Spanish railway company has promised that the high-speed train from Madrid to Seville can be returned in full in just 5 minutes.

All high-speed railways are operated automatically and can operate around the clock unless extreme weather conditions such as earthquakes occur. According to the wind speed limit, if a windshield is installed, the train can travel 160 km/h even if the wind speed reaches 25-30 meters per second. Aircraft, airports and highways must be closed during bad weather such as thick fog, heavy rain and snow.

References

1. Qian Zhonghou. Introduction to high-speed railway [N]. 3rd edition. Beijing: China Railway Press, 2006

2. The role of Zhou Xiaowen high-speed railway in promoting the coordinated development of regional economy [J]. Railway Economic Research, 2010 (06)

3. Luo Wenzhi. Research on measures to improve the economic benefits of high-speed rail [J]. Modern Property, 2011. 10

DOI 10.34660/INF.2022.62.45.202

异步牵引电力机车的动态特性
DYNAMIC CHARACTERISTICS OF ASYNCHRONOUS TRACTION ELECTRIC LOCOMOTIVE

Liu Yanzhen
Undergraduate
Ivashchenko Valery Olegovich
Candidate of Technical Sciences, Associate Professor
Emperor Alexander I St. Petersburg State Transport University

抽象的。 本文主要是为了了解异步牵引电机，了解其设计和运行方式； 对异步牵引电动机特性的要求。

关键词：异步牵引电机，异步牵引电机特性，牵引特性。

Abstract. *This article is mainly for understanding the asynchronous traction motor, understanding its design and modes of operation; requirements for the characteristics of an asynchronous traction motor.*

Keywords: *asynchronous traction motor, characteristics of an asynchronous traction motor, traction characteristics.*

The structure and principle of operation of an asynchronous motor: The main components of an asynchronous motor are the stator and rotor, which are separated from each other by an air gap. Active work in the engine is performed by the windings and the core of the rotor.

The asynchrony of the engine is understood as the difference between the rotor speed and the frequency of rotation of the electromagnetic field.

The rotor is the moving part of the engine. The rotors of asynchronous electric motors are of two types: with squirrel-cage and phase rotors. These types differ from each other in the designs of the rotor winding.

Principle of operation: When an electric current is applied to the stator windings, a magnetic flux occurs. Since the phases are shifted relative to each other by 120 degrees, because of this, the flow in the windings rotates. If the rotor is short-circuited, then with such rotation, a current appears in the rotor, which creates an electromagnetic field. Interacting with each other, the magnetic fields of the rotor and stator cause the rotor of the electric motor to rotate. If the rotor is phase, then voltage is applied to the stator and rotor simultaneously, a magnetic

field appears in each mechanism, they interact with each other and rotate the rotor.

An asynchronous type electric motor is a universal mechanism and has several modes for the duration of operation:

Continuous;

Short-term;

Periodic;

Repeated-short-term;

Special.

Continuous mode is the main mode of operation of asynchronous devices, which is characterized by constant operation of the electric motor without shut-downs with a constant load. This mode of operation is the most common, used in industrial enterprises everywhere.

Short-term mode - works until a constant load is reached for a certain time (from 10 to 90 minutes), not having time to warm up as much as possible. After that it turns off. This mode is used when supplying working substances (water, oil, gas) and other situations.

Periodic mode - the duration of work has a certain value and is turned off at the end of the cycle of work. Operating mode start-work-stop. At the same time, it can turn off for a time during which it does not have time to cool down to external temperatures and turn on again.

Intermittent mode - the engine does not heat up to the maximum, but it does not have time to cool down to the external temperature. It is used in elevators, escalators and other devices.

Special mode - the duration and period of inclusion is arbitrary.

The electromechanical characteristics of traction motors determine the traction characteristics of the ERS, which largely reflect its traction properties and load conditions in operating modes. For any type of traction motors, traction characteristics must meet two requirements:

1.the number of characteristics should be such that, if possible, the entire traction area is covered, taking into account the restrictions;

2.the control system should provide the possibility of continuous operation at any point of the traction area.

With regard to asynchronous traction motors, two additional requirements should be introduced:

1.the specified traction characteristics must be provided under operating conditions without significant complication of the control system;

2.the control system must shape the traction characteristics in such a way as to ensure their rigidity during boxing, regardless of the shape of the characteristic in the traction mode.

Since the asynchronous traction drive has the ability to smoothly adjust the

voltage and frequency, the 1st requirement is easily met. There are no difficulties for fulfilling the 2nd requirement. The expediency of taking into account the 3rd requirement will be shown below.

The slope of the characteristics is not of great importance, which is important, for example, for DC traction motors. It is only necessary that the 4th requirement be met, i.e., the traction characteristic can be soft, like in sequential excitation engines, but it must become "hard" when the clutch is broken. This requirement can also be provided by means of regulation by delaying the increase in the frequency of the supply voltage when the load is dropped at the traction motor in the event of a clutch failure. In this case, there will be no reduction in the traction force of the electric locomotive.

Traction characteristics are the dependence of the traction force of an electric locomotive on speed:

These characteristics are built graphically from the electromechanical characteristic, which reflects the dependence of the wheel traction force on the current for each connection of the traction motors, both for full excitation and for all stages of excitation weakening. Therefore, the VL10 electric locomotive has 15 automatic characteristics that allow you to determine the traction force of the electric locomotive at any speed and at any connection.

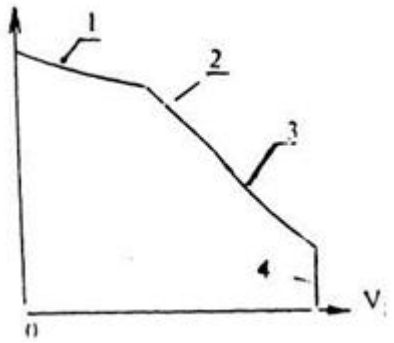

1. - linkage limitation. Beyond this limit, the traction force of the electric locomotive exceeds the traction force.

2. - current limit 600 A. Determines the maximum heating temperature of the windings of the traction motor and collector. Outside of this limit, the heating temperature exceeds the allowable temperature, so the following with large currents must be limited in time.

3. - restriction on the weakening of the excitation of the HVD on the P connection. The limitation is caused by the switching of traction motors. Beyond this limit, armature response increases and commutation deteriorates.

4. design speed limit 100 km/h. With a chassis designed for this speed, the design speed is determined by the fastening of the armature winding coils in the grooves of the core and the strength of the collector. The exception is the VL8 electric locomotive, in which the design speed is reduced to 80 km/h due to the design of the running gear.

References

1. Davydov, Yu.A. Traction electric machines: method. instructions for the implementation of the course project / Yu.A. Davydov. – Khabarovsk: DVGUPS Publishing House, 1999. – 24 P.

2. Katsman, M.M. Electrical machines / M.M. Katzman. – M.: High. school, 1990.

3. Alekseev, A.E. Traction electrical machines and converters / A.E. Alekseev. – L.: Energy, 1977.

DOI 10.34660/INF.2022.85.72.203

HXD2系列交流电力机车四象限牵引变流器（4QS）的高效控制
EFFICIENT CONTROL OF HXD2 SERIES AC ELECTRIC LOCOMOTIVE FOUR QUADRANT TRACTION CONVERTER (4QS)

Gao Qi
undergraduate
Vikulov Ilya Pavlovich
Candidate of Engineering Sciences, Associate Professor
Emperor Alexander I St. Petersburg State Transport University

抽象的。　本文分析了具有异步牵引驱动的电力机车电力电路的运行情况，描述了 HXD2 电力机车电力牵引变流器的电路，考虑了控制算法，开发了四象限变流器的仿真模型，并提出了 牵引变流器建模的结果。

关键词：电力机车HXD2，异步驱动，四象限变流器，计算机模型。

Abstract. *This article analyzes the operation of power electrical circuits of an electric locomotive with an asynchronous traction drive, describes the circuits of power traction converters of an HXD2 electric locomotive, considers control algorithms, develops a simulation model of a four-quadrant converter converter, and presents the results of modeling a traction converter.*

Keywords: *electric locomotive HXD2, asynchronous drive, four-quadrant converter, computer model.*

The object of the study is an AC electric locomotive HXD2 with a traction converter, which includes a four-quadrant input converter, an autonomous voltage inverter and asynchronous traction motors.

The electric locomotive is manufactured by Chinese companies CNR Datong Electric Locomotive Co., Ltd. together with the French company Alstom Transportation Co., Ltd. The traction power of freight locomotives with AC drive can reach 10000 kW. The results of scientific and technological achievements of Chinese manufacturers in the field of electric locomotive construction are implemented in this locomotive. The use of modern microprocessor control systems and traction converters on board an electric locomotive makes it possible to realize a wide range of traction power changes, high adhesion characteristics and power factor, reduce the harmonic composition of the electric locomotive current, as well as electromagnetic interference.

The general equipment layout of the HXD2 electric locomotive is shown in figure 1.

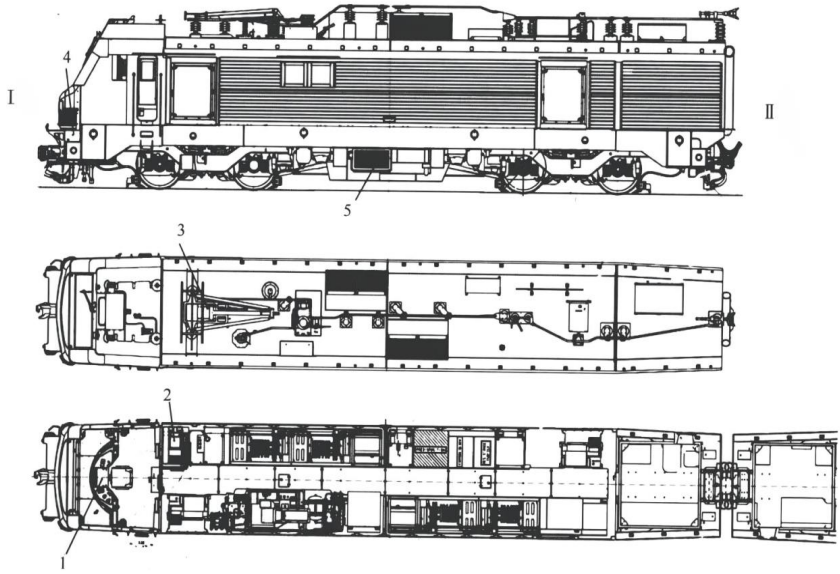

1 – Driver's cab equipment diagram; 2— Mechanical equipment; 3- Locomotive roof equipment; 4—Locomotive front equipment 5 — Location of equipment under the vehicle.

Figure 1. *General equipment layout drawing of electric locomotive HXD2*

Electric equipment of electric locomotive HXD2.

The traction converter consists of a four-quadrant converter, an intermediate DC link, filters, autonomous voltage inverters. The structure of the traction converter is shown in figure 2.

Figure 2. *Schematic diagram of the structure of the traction converter*

Power semiconductor converters are designed to control asynchronous traction motors and modes of movement of an electric locomotive with a train, by regulating traction and braking forces. The basis of the converters are modules of power transistors IGBT. A four-quadrant converter converts a single-phase alternating voltage of 2100 V into a direct voltage of the DC link at a level of 3775 V, then the voltage of the DC circuit is supplied to an autonomous voltage inverter, which generates a three-phase alternating voltage of 2945 V on a traction asynchronous motor. The normal operation of the four-quadrant converter is provided by the TCU. The connection scheme of an asynchronous traction motor involves powering one traction motor from one voltage inverter, which makes it possible to implement an axis-by-axis control system on an electric locomotive.

The technical parameters of the traction converter are given in table 1.

Table 1.

Traction converter parameters

Parameter	Meaning
Rated input voltage (AC)	2100V
Rated input current	987 A
Rated input frequency	50Hz
Intermediate voltage direct current (DC)	3775V
Maximum DC link voltage (DC)	4200V
Rated output voltage of voltage inverter (3AC)	2945V
Rated output current of voltage inverter	390 A
Maximum output current of voltage inverter	455 A
AC power module	233XHP, 233XHP - 1R
Inverter cooling method	Watercooling
Intermediate reference capacitor	3 x 1 mF
Secondary resonant capacitor	3x1. 33 mF
Secondary resonant capacitor current	399 A
Control voltage (DC)	110 V

The power circuit diagram of one HXD2 AC electric locomotive bogie is shown in Figure 3. The electrical circuit includes two four-quadrant converters (8 IGBT power modules), a DC link capacitor, two switching voltage regulators with a braking resistor (1 IGBT power module), filter capacitors and inductors, two three-phase two-level autonomous voltage inverters (6 IGBT power modules), two asynchronous traction motors and one auxiliary converter.

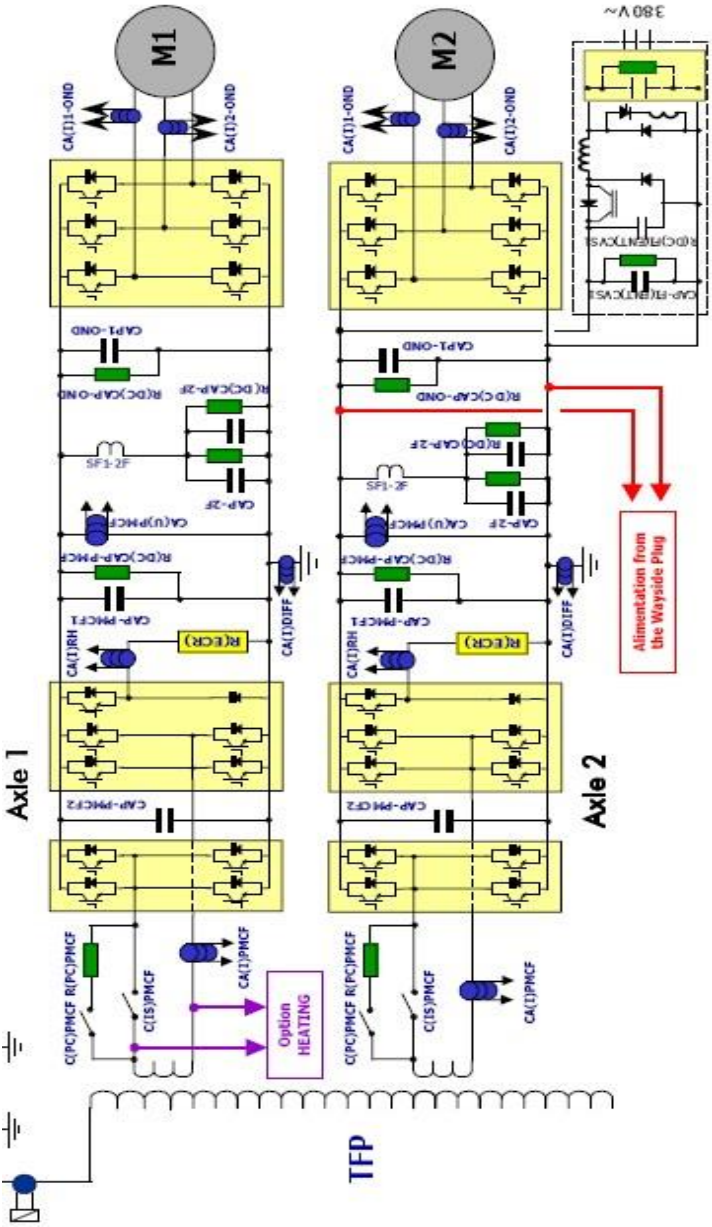

Figure 3. *Structural diagram of the electric traction drive system*

Four quadrant converter.

A four-quadrant rectifier can perform the function of rectifying and converting AC to DC (1, 3 quadrants). It can also implement an inverter function (quadrant 2 and 4) that converts DC power to AC power and feeds it back to the grid. At the same time, high short-circuit resistance can filter out the harmonic components of a certain frequency and improve the power quality of the power system.

The equivalent circuit diagram of a four-quadrant rectifier is shown in figure 4 (Upn — the primary voltage of the transformer,Uso — the voltage of the traction winding of the transformer, R_s — the resistance of the traction winding to direct current, L_s — the leakage inductance of the traction winding, U_{pmcf} — the modulation fundamental voltage, U_c — the rectified DC output voltage, I_s — the traction voltage (fundamental winding current).

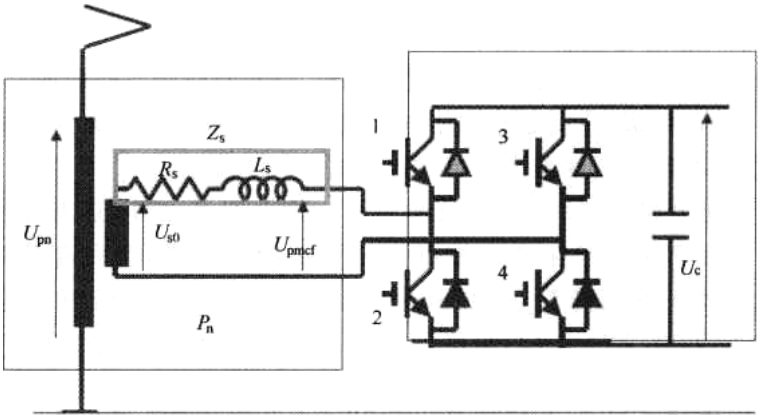

Figure 4. *Equivalent circuit diagram of a four-quadrant converter*

Simulation modeling of HXD2 AC electric locomotive traction converter

In order to find the optimal algorithms for the operation of the power electronic equipment control system, it is necessary to perform a series of experiments on a real object of study. However, the cost of experimental studies is relatively high, especially in high power traction systems, since the cost of equipment damage is very high. Therefore, computer simulation techniques are applied that can successfully reproduce the working state of the HXD2 AC locomotive traction converter system and realize continuous real-time control.

When building a simulation model for a four-quadrant converter of an HXD2 electric locomotive, it is necessary to analyze the converter under study, simplify its internal structure and form a model. The model is built using the Matlab/Sim-

ulink simulation software and the corresponding electrical library modules. The model of an electric locomotive, compiled in accordance with the power circuits of an electric locomo*tive,* is shown in figure 5.

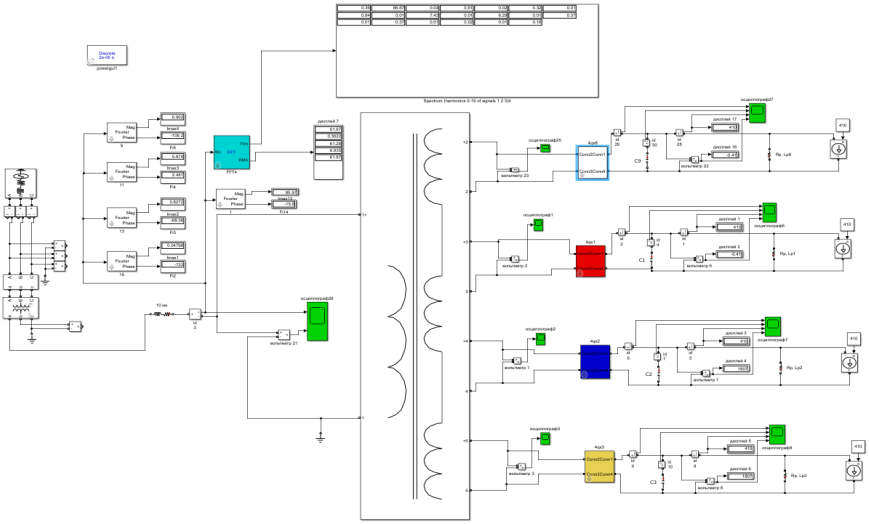

Figure 5. *4qs simulation model*

The model includes - a model of a traction substation, a model of a contact network, a model of an AC electric locomotive HXD2, blocks for analyzing currents and voltages in the electrical circuits of the converter.

HXD2 AC Electric Locomotive Traction Converter Simulation Process

Simulation circuit parameters: the voltage at the output of the transformer is set to 950 V, the inductance on the AC side is assumed to be 2 mH,v DC bus, the DC link capacitor has a capacitance of 12mF, the resonant inductance of the LC filter is assumed to be 0.27mH, the resonant capacitor is set to 9.3mF, the DC bus has a specified voltage of 1800V.

The simulation time is 0.6 s, the simulation algorithm is a discrete method for solving differential equations, and the simulation step size is 2e-5.

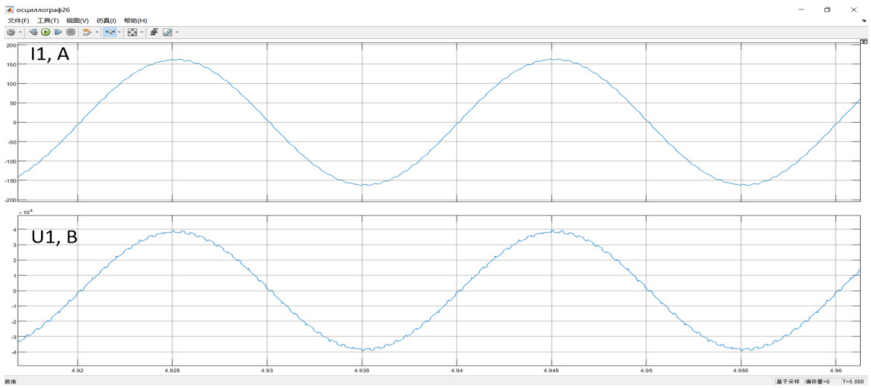

Figure 6. *Current and voltage in the primary winding of a traction transformer*

The DC link voltage as well as the currents of the IGBT power modules are shown in figure 7. It can be seen that the DC voltage is maintained at 1800±3 V under the control of the control loop.

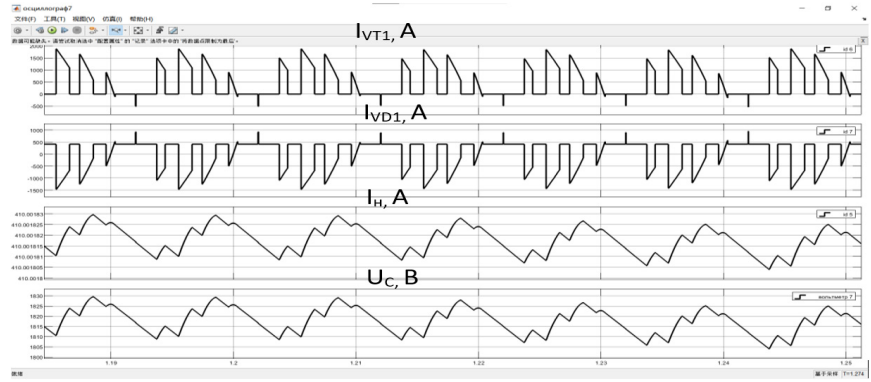

Figure 7. *Diagram of currents and voltages of a four-quadrant converter*

Conclusion

From the results, it can be seen that the voltage of the DC bus capacitor is stable at 1800V, the current on the AC side of the single-phase traction rectifier can follow the mains voltage well, and the power factor between voltage and current on the contact network side is almost one. The voltage of the capacitor on the DC side is maintained stable regardless of changes in the load current, which confirms the correctness of the proposed converter control strategy.

References

1. Zhang Shuguang. Electric locomotive HXD2 / China Railway Press, 2009 (HXD Type High Power AC Locomotive Technology Series)

2. Wu Xiaoyan. HXD2 Electric Locomotive Traction Converter Study, Southwest Jiaotong University, 2013.

3. Wu Lin. Simulation of the study of the traction converter. Southwestern Jiaotong University. 2010.

4. Wang Fuchen. Principle and Application of IGBT and Power Module Yongji New Speed Electric Motor Co., Ltd. 2012,8,18.

5. Zhang Jinfang. Principle and Application of IGBT and Power Module Yongji New Speed Electric Motor Co., Ltd. 2012,8.

6. Feng Xiaoyun, Wang Lijun, Ge Xinglai, Li Guanjun. Research and modeling of the control system for the traction drive of a high-speed electric train (J). Electric drive. 2008.

7. B.Laska. IGBT Development of traction converter (J). Converter technology and electric traction, 2004, V. 15:1-7.

8. Vikulov I.P., Nazirkhonov T.M., Yakushev A.Ya. Computer model of the traction transformer of the AC electric locomotive of the "O'Z-ELR" series. Proceedings of the Petersburg University of Communications. 2020. V. 17. № 3. P. 416-427.

9. Nazirkhonov T.M., Yakushev A.Ya., Vikulov I.P. Analysis of the spectral composition of the input current and voltage of a 4Q-S converter of an AC electric locomotive of the "O'Z-ELR" series using a computer simulation model

Bulletin of the results of scientific research. 2020. № 3. P. 41-63.

DOI 10.34660/INF.2022.78.76.204

无刷牵引电机在牵引机车车辆上的应用前景
PROSPECTS FOR THE USE OF BRUSHLESS TRACTION MOTORS ON TRACTION ROLLING STOCK

Huang Jingxuan
Undergraduate
Emperor Alexander I St. Petersburg State Transport University
Jing Chao
Undergraduate
Emperor Alexander I St. Petersburg State Transport University
Izvarin Mikhail Yulievich
Candidate of Technical Sciences, Associate Professor at the Department of "Electric traction", Federal State Educational Institution of Higher Education Emperor Alexander I St. Petersburg State Transport University

抽象的。 在越来越关注直流电机应用的今天，直流电机电源设计也备受业界关注。 在本文中，笔者将对直流电机电源的发展研究进行探讨，并提出相关建议供读者参考。

关键词：无刷电机，异步牵引电机，电机技术，电机设计

Abstract. *Today, with more and more focus on the application of DC motor, DC motor power supply design is also attracting much attention in the industry. In this article, the author will discuss the DC motor power supply development research and put forward related proposals for the reader's reference.*

Keywords: *Brushless motors, Asynchronous traction motors, motor technology, motor design*

1 Increasing power and traction

In accordance with the trends that have developed in recent years, the traction force of an electric locomotive when starting off should be 300-320 kN for a four-axle section, and the end of the hyperbolic section of the traction characteristic is in the region of speed 120-160 km/h for freight and 200-220 km/h for passenger locomotives and multi-unit electric trains. The continuous power of such an electric locomotive must be at least 6000 kW with the possibility of its short-term increase to 6400 kW. This does not mean that such power is typical for

all types of electric locomotives, but it is obvious that it will be higher than 1100-1500 kW per axle.

If until recently, the main traction motor of domestic manufacturers was a commutator, and foreign - asynchronous, then over the past 2 years, almost all the world's major manufacturers of EPS have also PMSM - traction motors based on permanent magnets. Such a significant advancement of this technology is associated with the creation of new alloys with an induction approaching 1.5 Tl. Will traction motors with permanent magnet excitation replace collector and asynchronous motors? The question is not entirely clear. The advantages are obvious - brushless motors have more power for the same volume and weight. Figure 1.1 shows the evolution of the traction drive of electric rolling stock, and table 1.1 shows the technical characteristics.

Figure 1.1. *Traction drive evolution*

Table 1.1.

actually achieved performance of various types of traction drive

traction motor type	direct current, URT-110(RF)	Asynchronous 1TB2216-0GB03 Electric train《Swallow》	With excitation from permanent magnets, series 1600 (Toshiba, Japan)	With permanent magnet excitation, TQ-600 (CSR, China)
Hourly power, kW	200	320	205	600
Weight, kg	2150	836	560	635
Speed rpm	1145	2200	N/A	4200
Geometric dimensions, mm	Height-800 Length-845 Width-1004	N/A	Length-600 Width-496	Height-697 Length-560 Width-654
Cooling type	Self-ventilated with axial fan	Self-ventilated with axial fan	Fully enclosed executive	Forced ventilation
Specific power, kW/kg	0.09	0.38	0.37	0.94
Efficiency	0.9	0.94	N/A	0.95

2 Structure of brushless DC motor

The brushless DC motor is mainly composed of two parts: one part is the motor body, and the other part is the encoder. An electronic switching circuit, composed of an electronic switch circuit, the principle of its structure is shown in figure 2.1.

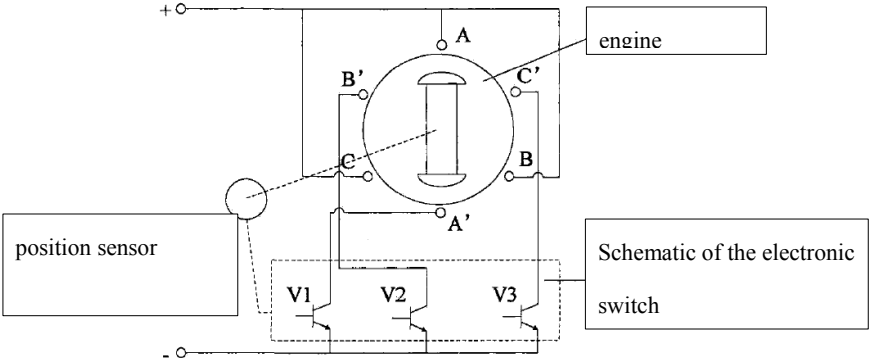

Figure 2.1. *Schematic diagram of the design of a brushless DC motor*

（1）Engine housing

The body of a brushless DC motor is mainly composed of a stator part fixed on the body and a rotor part that rotates with the rotor. The stator part includes a stator core fixed on the body and a stator winding embedded in the stator core. The three-phase stator winding is usually a lumped full-pitch winding; the rotor part includes permanent magnet steel connected to the rotating shaft through an annular or tiled structure, the rotating shaft and other auxiliary devices that can output mechanical torque, and between the rotor and the stator there is a gap Air gap, the magnetic field created by the rotor is evenly distributed in the air gap.

（2）Electronic switching switch

An electronic commutation switch cooperates with a position transmitter to control the conduction sequence of the motor windings. Electronic switching switches now use fully controlled power switches in combination with the switching control word generated by the encoder output after the conditioning circuit to control the conduction sequence of each stator winding for reliable operation of the engine.

（3）position sensor

The encoder plays an important role in the servo control system of the brushless DC motor, it detects the position of the motor rotor in real time and provides accurate switching torque for motor commutation. During motor operation, the encoder detects the position of the rotor relative to the stator winding and converts the rotor position signal into an electrical signal through a matching circuit to provide correct switching information for the inverter switching tube. The switching on and off of the inverter switching lamps is controlled by switching information so that the three-phase stator windings are switched in series. There are three main types of position sensors for brushless DC motors: photoelectric, electromagnetic and magnetic:

1）Photoelectric

This type of sensor is based on the principle of the photoelectric effect. The shade plate is evenly distributed with 120° electrical angle slots, and the number of slots is equal to the number of pole pairs of the rotor poles of the brushless DC motor. When a light source hits the phototransistor through the slits, the phototransistor outputs a "bright current", other phototransistors output a "dark current" because the light is blocked by the visor. The shading plate rotates with the rotor, and the phototransistor outputs a "light current" or "dark current" signal in turn. With the help of "signal of bright and dark current", the position of the magnetic pole of the rotor is obtained, the switching information is determined, and the three-phase windings of the motor are turned on in turn, to ensure the normal operation of the motor.

2）Electromagnetic

This type of sensor is made on the principle of electromagnetic effect, and there are three types of open transformer, ferromagnetic resonant circuit and proximity switch to detect rotor position information. The output signal of this type of sensor has a low signal-to-noise ratio, and the sensor itself is large, which is very inconvenient to use, the output signal of the sensor is variable, which cannot be directly used by the controller, and can only be used after correction and filtering.

3）Magnetic sensitive

This type of sensor is made using the principle that semiconductor elements are sensitive to magnetic fields, such as Hall effect elements or magnetoresistance elements. Common devices of this type of sensors include Hall elements, Hall integrated circuits, magnetically sensitive resistors and magnetically sensitive diodes, etc. The first two are made on the Hall effect and are collectively called Hall sensors. The rotor of the motor rotates, and several Hall elements are equidistantly distributed in the stator of the Hall sensor. The specific process of the Hall sensor determining the position of the rotor: During the operation of the motor, the rotor of the Hall sensor with permanent magnets outputs through a pair of magnetic poles a logic level corresponding to the state of the position of the rotor. The more, the more commutations are performed in one cycle. The logic level signal output by the Hall element is weak, and the accuracy is easily affected by the temperature to be handled by the conditioning circuit. This sensor is small in size and is mainly used in small and medium sized motors. The motor sensor of this system uses a Hall effect sensor.

The brushless DC motor controls the switching sequence of the inverter switching lamps by means of a position sensor output signal processed by the conditioning circuit, so that the three-phase stator windings are switched in turn, and the stator generates a jumping rotating magnetic field that drives the rotor. As the motor rotor rotates, the continuous encoder output changes the conduction state of the stator winding so that the motor rotates continuously. The schematic block diagram is shown in figure 2.2.

Figure 2.2. *Schematic block diagram of a brushless DC motor*

3 Basic Working Principle of Brushless DC Motor

According to the design characteristics of the brushless DC motor housing, we know that the rotor, which is composed of permanent magnet steel, generates a main magnetic field in the form of a trapezoidal wave, as shown in figure 3.1.

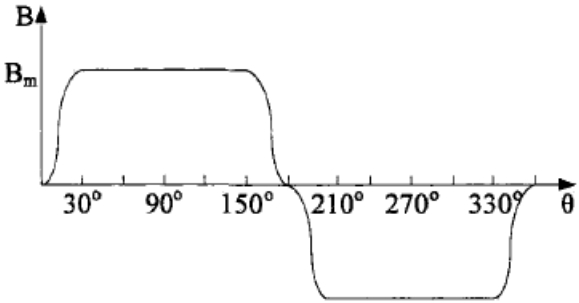

Figure 3.1. *Magnetic density diagram of the main magnetic field of the rotor of a brushless DC motor*

After the AC power is rectified and filtered, it turns into a DC source to supply power to the motor. Under normal conditions, the two phases of the three-phase windings are conductive, and the fixed magnetic field generated by the two-phase conductive windings has a certain angle with the magnetic field of the rotor, which causes the rotor to rotate; when the fixed magnetic field is parallel to the direction of the magnetic field of the rotor, the rotor cannot rotate, and the rotor cannot continue to rotate." In order for a brushless DC motor to rotate continuously, the fixed magnetic field generated by the conduction winding must have a certain angle with the magnetic field of the rotor, so the position sensor and the electronic commutation switch change the conductance of the stator winding into a sequence that can ensure that the stator winding creates a certain angle. There is always a certain angle between the magnetic field and the magnetic field of the rotor in direction.

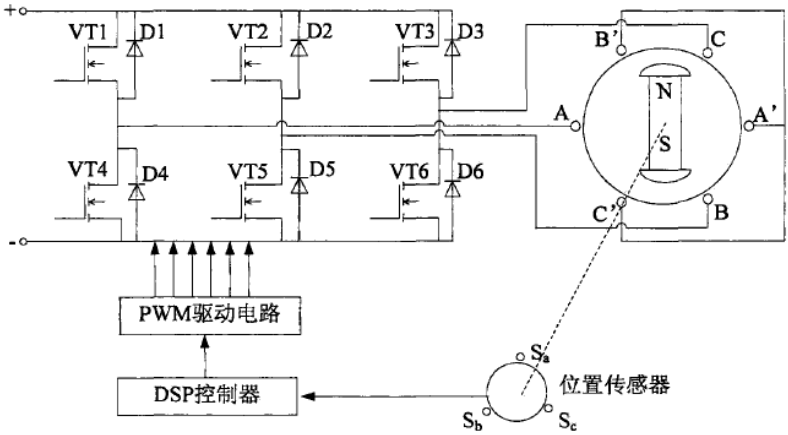

Figure 3.2. *Schematic diagram of a brushless DC motor control system*

The following is an example of a three-phase fully controlled star-connected bridge motor to illustrate the working principle of a brushless DC motor, as shown in figure 3.2. The conduction modes of the switching elements of the inverter in a three-phase fully controlled bridge type: two-two-wire and three-three-wire, two-two-wire is adopted in the article. The PMW control signal and the encoder signal control the switching tubes of the inverter, which are turned on and off in sequence so that the stator windings are energized or turned off with the switching tubes turning on and off in sequence. The current flowing in the conductive winding creates a magnetic field that interacts with the rotor, causing the rotor to rotate. As shown in figure 3.3.a, VT1 and VT5 are closed and current flows through the positive pole of the power supply - VT1 - winding A - winding B - VT5 - negative pole of the power supply The current carrying winding interacts with the magnetic field created by the rotor, causing the rotor to rotate counterclock-wise; when the rotor turns to an electrical angle of 60°, VT5 is off and VT6 is closed, as shown in figure 3.3.b, current flows through the positive pole of the power supply - VT1 - winding A - winding C - VT6 - negative current winding of the power supply and the magnetic field, the interaction created by the rotor causes the rotor to rotate counterclockwise, according to this law, the sequence of transistor conductivity: VT1, VT5-VT1, VT6-VT2, VT6-VT2, VT4-VT3, VT4-VT3, VT5-VT1, VT5 circulate so that the magnetic field, created by the current-carrying stator winding, also rotates with the conduction sequence of the switch tube. The magnetic field created by the stator windings jumps once for every 60° rotation of the electrical angle; the rotor interacts with the conductive windings so that the rotor also rotates with the rotation of the stator windings.

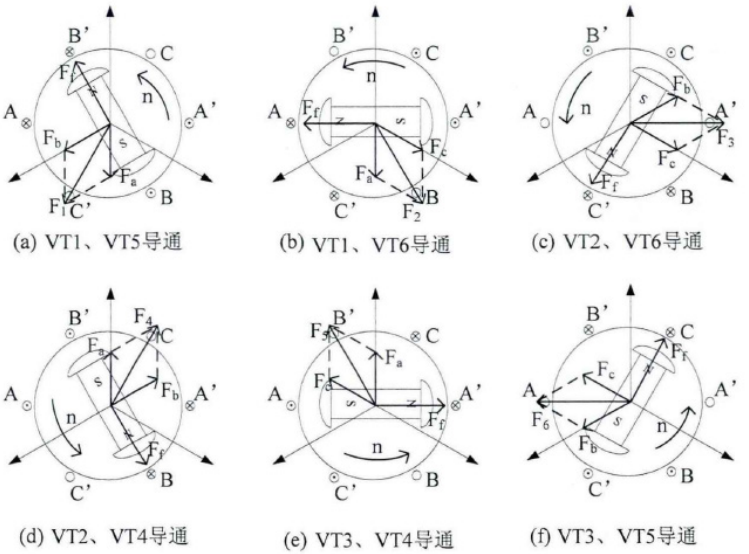

Figure 3.3. *Schematic diagram of the sequence of winding conductance, winding magnetic potential and rotor magnetic potential*

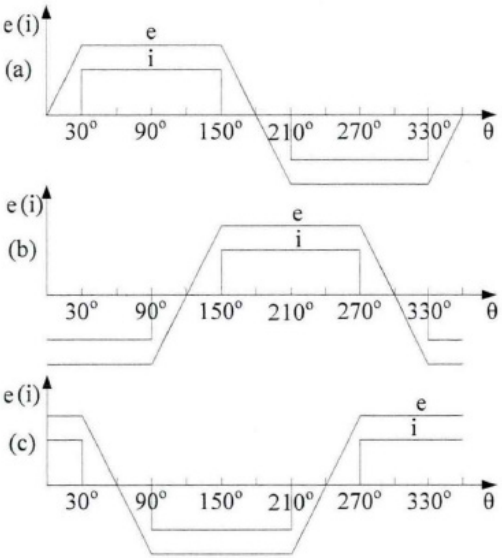

Figure 3.4. *Diagram of back EMF and phase current*

When the motor rotates, the main magnetic field cuts the stator winding, and the stator winding induces a reverse electromotive force with respect to the main magnetic field, and its shape matches the shape of the main magnetic field. For ease of analysis, the back EMF shape of the winding is simplified as a trapezoidal wave, and the width of the flat top is equal to the electrical angle of 120°, as shown in e in figure 1.8; phase current conduction range in the stator winding and the flat part of the back EMF common mode winding waveform are in phase completely match, as shown i in figure 3.4.

Conclusion

Advantages and disadvantages of brushless DC motors.

Low wear — The only physical interface between the rotating outside of the motor housing and the stationary windings inside are ball bearings, which means brushless DC motors wear out very slowly.

High speed — Brushless motors have much less friction than brushed DC motors, so they can run at higher speeds.

High Efficiency — Compared to other types of motors, brushless motors have very high operating efficiency, which means lower power consumption for the same output compared to brushed DC motors.

Very high control complexity — Brushless DC motors require specialized controllers and complex control algorithms to work properly.

High price — The cost of the motors themselves is not too high, but when the cost of the controller is added, the overall cost of using a brushless DC motor in a project becomes relatively high.

Need for specialized gears — In applications such as Dyson vacuum cleaners, brushless DC motors must be equipped with a gear to convert high speeds to the desired speed.

The development trend of traction motor*s is shown in Figure 3.5.*

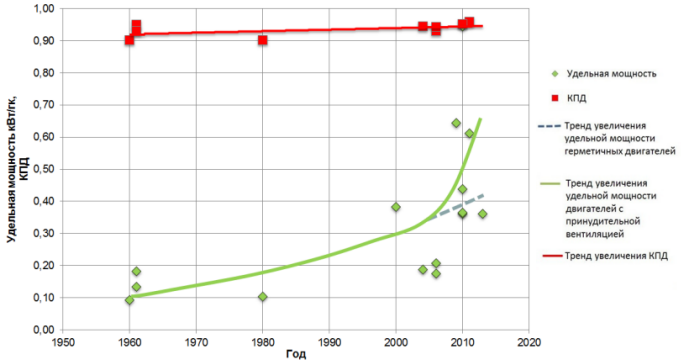

Figure. 3.5. *Development trend of traction motor performance*

References

1. Boyko E. P. Asynchronous general purpose motors E. P. Boiko, Yu. V. Gaintsev, Yu. M. Kovalev, et al.; edited by V. M. Petrov and A. E. Kravchik. M.: Energy, 1980.

2. Bulgakov A. A. Frequency control of asynchronous electric motors:A. A. Bulgakov. 2nd Edition: Science, 1966.

DOI 10.34660/INF.2022.23.12.205

交流电力机车网络控制系统
AC ELECTRIC LOCOMOTIVE NETWORK CONTROL SYSTEM

Zhang Chunyang
Master's degree Student
Xu Yiming
Master's degree Student
Chudokov Alexander Ivanovich
Candidate of Technical Sciences, Associate Professor
Emperor Alexander I St. Petersburg State Transport University

抽象的。 介绍了一种交流传动快速客运电力机车网络控制系统，给出了控制系统的结构，给出了关键部件的信息，描述了网络控制系统的主要功能。
关键词：客运电力机车，交流传动，网络控制系统，故障诊断

Abstract. *The network control system of an express passenger electric locomotive with an AC drive is described, the structure of the control system is given, information on key components is given, and the main functions of the network control system are described.*
Keywords: *passenger electric locomotive, AC drive, network control system, fault diagnostics*

The AC Drive Express Electric Passenger Locomotive is a 7200kW six-axle passenger electric locomotive designed to adapt to Chinese railway conditions. The single axle power is 1200 kW and the maximum working speed is 160 km/h. The network control system is a vehicle-mounted microcomputer network control system that monitors, controls and diagnoses the locomotive.

The control units in the locomotive communicate via the MVB bus and the MPU manages the bus to carry out the communication. The 6A system host and brake display (BDU) do not support MVB communication mode and are connected to the TCMS via RS485/RS422 bus. The reconnected locomotives are connected via the WTB bus, and the GW terminates the WTB data exchange to realize the reconnected locomotive operation.

The network topology of an AC-driven express passenger electric locomotive is shown in Figure 1. Each locomotive includes 2 Main Processing Units (MPUs),

2 MVB/WTB Gateways (GWs), 6 Traction Control Units (TCUs) and 2 Auxiliary Control Units (ACU), 3 Remote I/O Units (RIOM), 2 Driver Displays (DDU) and 1 MVB/HDLC Gateway (GW3), while also connected to Air Brake Control Unit (BCU), Train Power Unit (LG) , connecting the train protection system 6A.

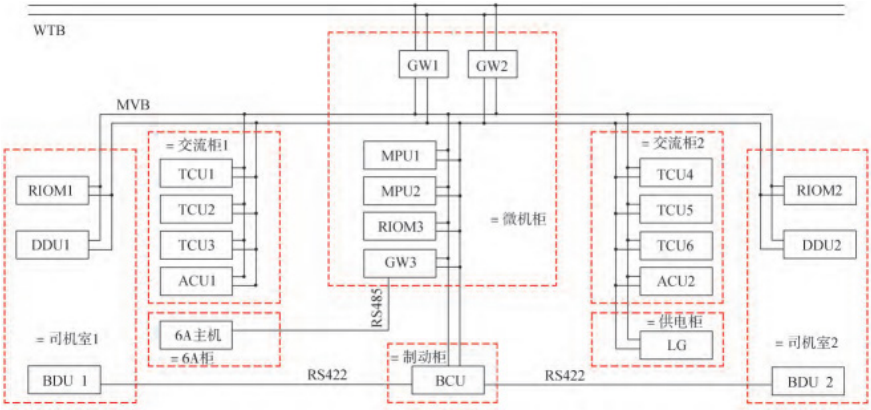

Figure 1. *Network topology of high-speed passenger electric locomotive with AC drive*

The MPU is installed in the micro cabinet of the mechanical room, and is the main component of TCMS, it not only realizes the MVB bus control function, but also realizes TCMS.

The central locomotive processing function completes the various logical locomotive control operations.

The MPU adopts chassis type structure, redundant design, and consists of two MPU1 and MPU2 with identical hardware. MPU1 and MPU2 are connected via the MVB bus. Under normal conditions, MPU1 is the master control device, and MPU2 is in a hot standby state. When MPU1 fails, MPU2 automatically takes over the work of the main control and does not affect normal operation. operation of the locomotive in the process of switching master-slave.

The MPU uses an x86 processor, an embedded VxWorks real-time operating system, and an IEC 61131 compliant graphical programming tool for engineering applications.

The GW is installed in a micro cabinet in the mechanical room to implement protocol conversion between WTB and MVB. GW is a high-level UIC gateway that complies with the IEC61375-1 standard and the UIC556 protocol. It can automatically perform train self-sorting of WTB equipment, automatically detect the direction of movement of locomotives, and realize reconnection management of

locomotives. It can also be used as four types of MVB bus equipment complete functions such as locomotive equipment status query, process data transmission, message data transmission, monitoring data transmission and bus control. GW uses 6U chassis structure and redundant design, which consists of 1 110V/24V power board, 1 24V/5V power board, and 2 CPU boards.

RIOM is installed under the operator's cab and in the micro cabinet of the mechanical room and is responsible for collecting the operator's operating instructions (such as the operation of the group of toggle switches and the operator's controller) and equipment status (such as feedback on the state of the pantograph, main switch, etc.), while at the same time, it controls the light indicators of the driver's console and executes control commands, as well as controls the corresponding relays, contactors and other actuating equipment.

RIOM uses a chassis structure that consists of chassis, backplane, 110V/5V power supply board, MVB/CAN gateway board, DI digital input board, DO digital output board, and AI analog input board. The structure and composition of RIOM1 and RIOM2 are completely identical. They are distinguished by dialing codes. They all use the 3U42TE chassis. RIOM3 uses the 3U84TE chassis. The number of DI boards, DO boards, and AI boards in a RIOM chassis can be configured according to the number of I/O points. The I/O board is a front socket, and the external interface is equipped with a 48-pin F-type connector. The RIOM communicates with the MPU via the MVB bus, and the boards (except for the power board) inside the RIOM communicate via the CAN bus.

The GW3 is installed in a micro cabinet in the mechanical room. GW3 is a module specially designed to realize communication between TCMS and 6A locomotive protection system, as well as perform MVB and HDLC protocol conversion function.

GW3 has modular design, 110V DC power supply, 2 MVB interfaces and 2 HDLC interfaces.

The DDU is installed on the operator's cab panel to implement human-computer interaction. Through the DDU, it is possible to perform locomotive characteristic parameter setting, locomotive status display and fault recording, query and download.

DDU uses a low power Intel Atom processor and a wide temperature 10.4" TFT LCD screen with two modes of human-computer interaction: full touch screen and buttons. Under normal conditions, the driver can perform convenient and fast driving operations through the full touch screen.

The network control system can realize more than 40 control functions at the level of train, locomotive and drive, mainly including reconnect control, traction/regenerative braking control, air-electric system/air-electric interlock combined control, over phase control, constant speed control, automatic end change control

and auxiliary converter control, etc.

Fast passenger electric locomotive with AC drive has 16 levels of traction and 16 levels of braking, all of which are geared and stepless, and different handle positions correspond to different traction / braking forces. The MPU converts the selected value of the horizontal position of the handle to the horizontal position and sends it to the TCU. When air and electricity are combined, it converts the percentage of electric braking force requested by the BCU into a horizontal handle position and sends traction/braking force.

The fast AC passenger electric locomotive has two braking control modes, air-electric combination and air-electric interlock, which can be selected on the display screen. In air-electric combined mode, electric braking takes precedence, and electric braking force takes the maximum value of electric braking force corresponding to the driver controller and automatic braking controller. In air-electric interlock mode, the auto brake controller only controls the air brake. As long as the driver controller is in the brake position, the air brake will be disengaged and the electric brake will be switched to drive.

The high-speed passenger electric locomotive with AC drive has the function of automatic terminal change. The automatic end changing function is mainly designed to reduce the workload of the driver and passengers when changing ends, at the same time, it can also prevent the deterioration of the roof insulation performance due to the influence of haze and the problem of draining from the roof during the manual process of changing and lowering the ends. When the locomotive is stationary, the brake cylinder pressure is greater than 90kPa, the pantograph is raised and the main switch is turned on, the driver only needs to press the automatic end change button and the power off button, and the double nose will be automatically raised, and the two main circuit breakers will be closed. After the driver re-activates any electric key in the cab, the corresponding main circuit breaker will be automatically turned off according to the activated cab, the corresponding pantograph will be lowered. If one pantograph is in the isolated state, after activating the automatic end change function, the isolated pantograph will continue to be isolated, and the other pantograph will always be in the raised state. Since the main circuit breaker does not open and the pantograph does not fall during the entire process of automatic end changing, the auxiliary system continues to work normally, which greatly improves the efficiency of end changing.

The TCMS high-speed passenger electric locomotive with AC drive is capable of diagnosing malfunctions of important components and the corresponding protection functions are triggered. After the diagnostic information is evaluated by the system, it is classified according to severity and displayed on the DDU on the driver's desktop. After a fault occurs, the system automatically saves the relevant operating data along with the fault and displays the cause of the fault and recom-

mendations for troubleshooting.

Fault diagnosis information can be downloaded via Ethernet or USB interface, which is convenient for locomotive maintenance personnel to conduct in-depth analysis of locomotive faults.

References

1. Yu Yue, Jiang Yueli Network control system for a powerful AC electric locomotive [J] // Electric traction and control, 2010 (3): 10-12.

2. Fu Ying, Li Xin, Hao Fengrong HXD3B AC Electric Locomotive Control System [J] Electric locomotives and urban rail vehicles, 2010 (2): 21-24.

3. Wang Xiaopeng HXD21000 AC Drive Electric Freight Locomotive Network Control System [J] Electric Traction and Control, 2015 (1): 1-4.

4. Wen Zhongjian, Cai Haixiang HXD1C High Power AC Electric Locomotive Network Control System [J] Electric locomotives and urban rail vehicles, 2011 (6): 11-14.

NOTES

科学出版物

上合组织国家的科学研究：协同和一体化

国际科学大会的材料

2022年5月28日，中国北京

编辑A.A.Siliverstova
校正A.I.尼古拉耶夫

2022年5月31日，中国北京
USL。沸点：98.7。 订单253.流通500份。

在编辑和出版中心印制
无限出版社